# INVESTIGATING THE ANTIVIRAL ACTIVITY OF THE INTERFERON-INDUCIBLE GTPASE MXA AGAINST INFLUENZA VIRUSES

**Lee Sherry**

**A Thesis Submitted for the Degree of PhD**
**at the**
**University of St Andrews**

**2015**

# Investigating the antiviral activity of the interferon-inducible GTPase MxA against influenza viruses

Lee Sherry

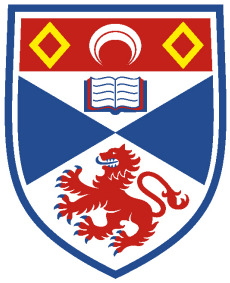

University of
St Andrews

This thesis is submitted in partial fulfilment for the degree of PhD
at the
University of St Andrews

September 2015

**DECLARATIONS**

I, **Lee Sherry**, hereby certify that this thesis (which is approximately 52,000 words) has been written by me, that it is the record of work carried out by me, and that it has not been submitted in any previous application for a higher degree.

Date ……..... Signature of candidate …….....

I was admitted as a research student in September 2011 as a candidate for the degree of **Doctor of Philosophy (PhD) in Molecular Virology**; the higher study for which this is a record and was carried out at the University of St. Andrews between 2012 and 2015.

Date ……..... Signature of candidate …….....

We hereby certify that the candidate has fulfilled the conditions of the Resolution and Regulations appropriate for the degree of Doctor of Philosophy at the University of St. Andrews, and that the candidate is qualified to submit this thesis in application for that degree.

Date ……..... Signature of supervisor …….....

**Dr. David Jackson**

In submitting this thesis to the University of St Andrews I understand that I am giving permission for it to be made available for use in accordance with the regulations of the University Library for the time being in force, subject to any copyright vested in the work not being affected thereby. I also understand that the title and the abstract will be published, and that a copy of the work may be made and supplied to any *bona fide* library or research worker, that my thesis will be electronically accessible for personal or research use unless exempt by award of an embargo as requested below, and that the library has the right to migrate my thesis into new electronic forms as required to ensure continued access to the thesis.

The following is an agreed request by candidate and the supervisors regarding the electronic publication of this thesis:

Access to printed copy and electronic publication of thesis through the University of St Andrews.

Date ……..... Signature of candidate …….....

Date ……..... Signature of supervisor …….....

**Dr. David Jackson**

**Acknowledgements**

Firstly I would like to thank everybody who has helped and supported me throughout my time in St Andrews. To anyone was has offered advice or reagents, it has been greatly appreciated.

I owe a huge amount of thanks to my supervisor, Dave, who not only took me on as a PhD student but allowed me to develop my own ideas whilst reigning me in when they got slightly too crazy. I appreciate all of the support I received throughout my PhD, particularly towards the end when I may have seemed slightly laid back. I would also like to thank Dave for not only understanding but also sharing in the importance of football-related chat in the lab as a welcome distraction from conflicting experimental results.

I would also like to thank Matt for the time we spent in the lab together, helping me with technical support and to develop my ideas, as well as creating the unique lab atmosphere that was the Jackson lab. I also want to say thank you to my friends from level 2, my PhD experience was made so much better by getting to experience it with you, even if I did take the mick out of each of you on a daily basis!

I also want to say a big thank you to Ola, who has been a big support to me throughout, even if I am a 'workaholic' and you 'hate my time courses with a passion'.

Finally I would like to say thank you to my Mum as well as my brother and sister, for their continued support throughout my academic career.

**Abstract**

The interferon (IFN) system forms an essential part of the innate immune response, up-regulating hundreds of IFN-stimulated genes (ISGs) in response to viral infection. A key protein in this response is the human myxovirus resistance protein MxA, an IFN-induced GTPase with broad-spectrum antiviral activity, capable of inhibiting many RNA and DNA viruses. One of the most studied antiviral effects of MxA is the inhibition of influenza A virus replication, yet the molecular mechanism of antiviral activity is still unknown. Influenza A viruses are inhibited by MxA at two distinct stages of viral replication; during viral entry and following primary transcription of viral mRNAs. The antiviral effects of MxA during viral entry are highly dependent on IFN, however activity exerted after primary transcription can occur in the absence of IFN. This study provides evidence that MxA exerts its antiviral activity at these two stages of viral replication through distinct mechanisms, and outlines a potential model of MxA antiviral activity following primary transcription. A potential third antiviral mechanism of MxA is proposed based on the findings that MxA is able to regulate cellular lipid metabolism, thereby potentially affecting virion composition. Mutational analysis of MxA highlights the significance of GTPase activity to the antiviral effects of MxA, while also demonstrating that natural single nucleotide polymorphisms in MxA have the potential to severely impair or prevent antiviral activity. Finally, this thesis shows for the first time that MxA exhibits antiviral activity against influenza B viruses. Overall this thesis provides new information illustrating how MxA provides potent antiviral activity against influenza viruses. Such information is vitally important as understanding the molecular basis of how proteins such as MxA function against many human pathogens is fundamentally important in our efforts to create better long-term treatment options for all viral diseases.

## Table of Contents

## List of Figures

## List of tables

## Abbreviations

| | |
|---|---|
| **% [v/v]** | Percentage concentration (volume per volume) |
| **% [w/v]** | Percentage concentration (weight per volume) |
| **°C** | Degrees Celsius (temperature). |
| **ΔG** | Gibbs Free Energy |
| **2', 5'-OAS** | 2', 5'- oligoadenylate synthetase |
| **aa** | Amino-acid |
| **ATP** | Adenosine triphosphate |
| **BSE** | Bundle Signaling Element |
| **CARD** | Caspase recruitment domain. |
| **CARDIF** | CARD adaptor inducing IFN-β |
| **cGAS** | Cyclic guanosine monophosphate–adenosine monophosphate (GMP-AMP) synthetase |
| **CH25H** | Cholesterol-25-Hydroxylase |
| **CL** | Cardiolipin |
| **CM** | Conditioned Media |
| **CPE** | Cytopathic effect. |
| **cRNA** | Complementary RNA |
| **CTD** | C-terminal domain |
| **DAPI** | 4', 6-diamidino-2-phenylindole |
| **DCs** | Dendritic cells |
| **DDX41** | DEAD box protein 41 |
| **DMEM** | Dulbecco's modified Eagle's medium. |
| **DMSO** | Dimethyl sulphoxide. |
| **dNTP** | Deoxyribonucleotide triphosphate. |
| **dsRNA** | Double-stranded RNA |
| **ED** | Effector Domain |
| **EDTA** | Ethylene diamine tetra-acetic acid. |
| **ER** | Endoplasmic Reticulum |
| **FACS** | Fluorescence Activtaed Cell Sorting |
| **FBS** | Foetal bovine serum |
| **GAS** | IFN-γ-activated site |
| **GBP** | Guanylate Binding Protein |
| **GED** | GTPase Effector Domain |
| **GFP** | Green fluorescent protein |
| **GTP** | Guanosine Triphosphate |
| **HA** | Hemagglutinin |
| **HCV** | Hepatitis C virus |

| | |
|---|---|
| **HIV** | Human immunodeficiency virus |
| **h.p.i** | Hours Post-infection |
| **HRP** | Horse-radish peroxidase |
| **HSV** | Herpes Simplex Virus |
| **IFITMs** | IFN-induced transmembrane proteins |
| **IFN** | Interferon |
| **IKK** | IκB kinase |
| **IL** | Interleukin |
| **IMP** | Importin Proteins |
| **IPS-1** | IFN-β promoter stimulator protein 1 |
| **IRF** | IFN regulatory factor |
| **IRG** | IFN regulated GTPase |
| **ISGF3** | Interferon-stimulated gene factor 3 |
| **ISGs** | IFN-stimulated genes |
| **ISRE** | IFN-stimulated response element |
| **IκB** | Inhibitor of NF-κB |
| **JAK** | Janus activated kinase |
| **JEV** | Japanese Encephalitis Virus |
| **kb** | Kilo-base |
| **kDa** | Kilo-Dalton |
| **LACV** | La Crosse Virus |
| **LGP2** | Laboratory of Genetics and Physiology 2 |
| **LPS** | Lipopolysaccharide |
| **M** | Molar concentration (moles per liter). |
| **M1** | Matrix protein-1 |
| **M2** | Matrix Protein-2 |
| **MAVS** | Mitochondrial antiviral-signalling protein |
| **MCMV** | Murine Cytomegalovirus |
| **MCS** | Multiple cloning site |
| **MDA-5** | Melanoma differentiation-associated gene-5 |
| **MHC** | Major histocompatibility complex |
| **min** | Minutes (time) |
| **MOI** | Multiplicity of infection |
| **mRNA** | Messenger RNA |
| **mRFP** | Monomeric Red Fluorescent Protein |
| **MS** | Multi-membranous Structure |
| **MS/MS** | Tandem Mass Spectrometry |

| | |
|---|---|
| **MW** | Molecular weight |
| **MyD88** | Myeloid differentiation factor 88 |
| **Mx** | Myxovirus Proteins |
| **NA** | Neuraminidase |
| **NDV** | Newcastle Disease Virus |
| **NEDD8** | Natural precursor cell expressed, developmentally down-regulated 8 |
| **NEMO** | NF-κB essential modulator |
| **NES** | Nuclear Export Signal |
| **NEP** | Nuclear Export Protein |
| **NF-κB** | Nuclear factor kappa B |
| **NLRs** | Nucleotide oligomerisation domain (NOD)-like receptors |
| **NLS** | Nuclear localisation signal |
| **NP** | Nucleoprotein |
| **NS1** | Non-structural protein 1 |
| **nt** | Nucleotides |
| **OASL** | 2'-5'-oligoadenylate synthetase-like |
| **ORF** | Open reading frame |
| **PA** | Polymerase Acidic protein |
| **PACT** | PKR activating protein |
| **PALM** | Photo-Activated Localisation Microscopy |
| **PAMPs** | Pathogen-associated molecular patterns |
| **PB1** | Polymerase Basic protein 1 |
| **PB2** | Polymerase Basic protein 2 |
| **PBS** | Phosphate-buffered saline |
| **PC** | Phosphatidylcholine |
| **PCR** | Polymerase chain reaction |
| **PE** | Phosphatidylethanolamine |
| **PEG** | Polyethylene glycol |
| **PFU** | Plaque forming units |
| **PI** | Phosphatidylinositol |
| **PI3K** | Phosphatidylinositol 3-kinase |
| **PIV5** | Parainfluenza virus 5 (formerly known as SV5; simian virus 5) |
| **PKR** | Double-stranded RNA activated protein kinase |
| **PRRs** | Pattern-recognition receptors |
| **PS** | Phosphatidylserine |
| **PVDF** | Polyvinylidene difluoride |
| **RBD** | RNA-Binding Domain |
| **RdRp** | RNA-dependent RNA polymerase |
| **RIG-I** | Retinoic acid-inducible gene I |
| **RIP1** | Receptor interacting protein 1 |

| | |
|---|---|
| **RLRs** | Retinoic acid-inducible gene I (RIG-I)-like receptors |
| **RNP** | Ribonucleoprotein complex. |
| **rpm** | Revolutions per minute |
| **RT** | Room temperature |
| **SARS** | Severe acute respiratory syndrome virus |
| **SD** | Standard deviation |
| **SDS** | Sodium dodecyl sulfate |
| **SDS-PAGE** | Sodium dodecyl sulphate polyacrylamide gel electrophoresis. |
| **SeV** | Sendai virus |
| **shRNA** | Small hairpin RNA |
| **SNP** | Single Nucleotide Polymorphism |
| **SOCS** | Suppressor of cytokine signalling |
| **ssRNA** | Single-stranded RNA |
| **STAT** | Signal transducers and activators of transcription |
| **STED** | Stimulated Emission Depletion |
| **TAK1** | TGF-β activating kinase 1 |
| **TAP** | Tandem Affinity Purification |
| **TBK1** | TRAF family member-associated NF kappa-B activator -(TANK)-binding kinase 1 |
| **TEM** | Transmission Electron Microscopy |
| **Th2** | Type 2 T-helper cells |
| **THOV** | Thogoto Virus |
| **TIRF** | Total Internal Reflection Fluorescence microscopy |
| **TLRs** | Toll-like receptors |
| **TNFα** | Tumor necrosis factor α |
| **TRAF3** | TNF-receptor associated factor 3 |
| **TRIF** | Toll-interleukin (IL)-1-resistannce (TIR) domain-containing adaptor inducing IFN-β |
| **TRIMs** | Tripartite motifs |
| **tRNA** | Transfer RNA |
| **Tyk2** | Tyrosine kinase 2 |
| **UTR** | Untranslated Region |
| **VISA** | Virus-induced signalling adapter |
| **VLIG** | Very Large Inducible GTPase |
| **vRNA** | Viral RNA |
| **VSV** | Vesicular Stomatitis Virus |
| **wMxA** | Wobble MxA |
| **WNV** | West Nile Virus |
| **wt** | Wild type |

| | |
|---|---|
| **x g** | Times g (gravity) |
| **µg** | Micrograms |
| **µl** | Microliters |

# Chapter 1 - Introduction

## 1.1 Introduction to Interferon

Viruses are incapable of self-replication without infecting a host organism. However, this is often not a symbiotic relationship as viral hijacking of host energy sources and metabolism can lead to cellular destruction, leading to tissue damage and even the death of the host organism. To combat this, the animal kingdom has evolved two specific mechanisms in the innate and adaptive immune systems.

The adaptive immune system is extremely specific and displays memory upon encountering a pathogen. This system has a large amount of 'cross-talk' with the innate immune system, which is capable of recruiting a large variety of adaptive immune cells through the production of cytokines and the presentation of antigens. However, this process requires additional time to become active when compared to the innate immune system and consequently can be seen as a secondary defence against viral infection. The primary defence is the innate immune system, which produces a non-specific but immediate response upon infection. Innate immunity consists of several different mechanisms including the complement system, the cellular response; particularly Natural Killer cells during viral infection, and the intracellular response; such as the interferon (IFN) response (Gerlier and Lyles 2011).

IFNs are secretory cytokines which are classified into 3 distinct groups; type I, II and III which each elicit their own antiviral effect (Randall and Goodbourn 2008). Type I IFNs were discovered in 1957 (Isaacs & Lindenmann, 1957) and consist of a large range of molecules with 13 distinct IFN-α genes in man and one IFN-β gene which are both induced directly as a reaction to viral infection. Other type I IFNs include –ω,

-κ, -ε and –δ, though the functions of these IFNs is less clear as they play other roles not related to the antiviral response, such as the regulation of maternal factors during pregnancy (Randall and Goodbourn 2008). Type III IFNs; -λ1, -λ2 and –λ3 are also induced in response to viral infection and appear to activate the same signaling pathways that are activated by IFN α/β genes (Uzé and Monneron 2007). Type II IFN refers only to IFN-γ which is induced by activated T cells or NK cells which have recognised an infected host cell (Goodbourn, Didcock, and Randall 2000). Type II IFN bears no structural resemblance to Type I IFN; however, they do have similar functions as they stimulate a number of the same genes (Goodbourn, Didcock, and Randall 2000).

### 1.1.2 IFN signaling

The IFN-α/β signaling cascade is activated through the hetero-dimeric IFN-α/β receptor, which appears to be expressed ubiquitously. Upon binding IFN-α/β the receptor transduces its signal through tyrosine kinases Tyk2 and Jak1. This leads to the activation of a multitude of downstream proteins culminating in the transcription of a large number of genes that lead to the overall antiviral state of the cell. This signaling cascade is described in more detail in Fig. 1.1 (Also comprehensively reviewed by S. Goodbourn et al. 2000.).

These genes are referred to as being IFN-stimulated genes (ISGs), however a subset of these can be induced in the absence of IFN, but by the presence of virus possibly offering some protection to primary infected cells. Although, it would appear that this non-IFN based response is far less effective, as IFN-α/β receptor knockout mice are

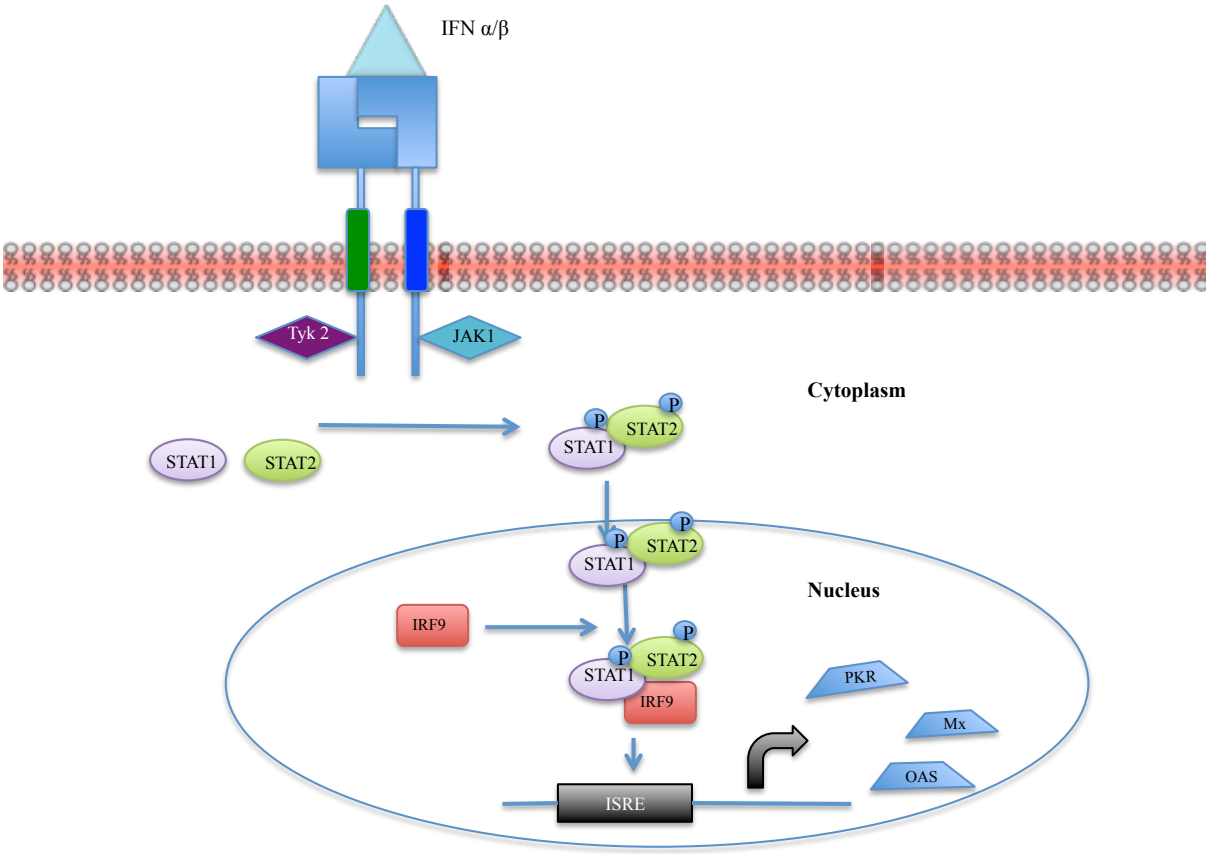


**Figure 1.1 IFN α/β signaling.** IFN α/β signaling is induced by IFN binding to the heterodimeric type I IFN receptor. IFN binding activates JAK1 and Tyk2, receptor associated Tyrosine kinases, which phosphorylate STAT1 and STAT2 that heterodimerise through SH2 domains. Following dimerization the STAT-1-STAT-2 complex translocates to the nucleus where it interacts with transcription factor IRF-9. This heterotrimer is known as ISGF3 that binds to the IFN-stimulated response element (ISRE) and initiates transcription of interferon stimulated genes (ISGs) such as protein kinase R (PKR), myxovirus resistance protein (Mx) and oligoadenylate synthetase (OAS). (Adapted from Randall & Goodbourn, 2008).

incredibly susceptible to virus infection, this could be two-pronged effect as IFN-α/β have crucial roles in the activation of adaptive immune responses therefore reducing the overall efficiency of the immune response. Type III IFNs bind to the hetero-dimeric receptor IL-28 which leads to a similar signal transduction and gene up-regulation seen in IFN-α/β but instead of ubiquitous expression appears to have limited tissue distribution (Meager et al. 2005; Zhou et al. 2007). The role of Type III IFN is still under investigation; however, early indications suggest that is not essential in the response against infection (Randall and Goodbourn 2008).

### 1.1.3 IFN Stimulated Genes

IFN signaling leads to the translation of a number of ISGs. Two such examples of these are Protein Kinase R (PKR) and 2'-5'-oligoadenylate synthetase (OAS). PKR is translated as an inactive monomer but dimerises into its active form upon binding viral double stranded RNA (dsRNA). Another activator of PKR is PACT (PKR activating protein) which is activated in turn by cellular stress (Ito, Yang, and May 1999; Patel et al. 2000). The activation of PKR can reduce the amount of viral protein produced through the phosphorylation of eIF2α. Phosphorylation of eIF2α can prevents eIF2α from being recycled, therefore stopping the initiation event in translation. Phosphorylated eIF2α can also lead to autophagy and has been implicated in the induction of apoptosis as well as cell cycle arrest; each having a negative effect on viral replication (Tallóczy et al. 2002).

OAS, like PKR, is also produced as an inactive monomer that requires dsRNA as a co-factor. Once activated OAS oligomerises ATP through 2'-5' phosphodiester linkages, these adenylate oligomers activate RNase L, an endonuclease which

degrades cellular and viral RNAs which generates 3'-monophosphates. Interestingly, OAS/RNase L has been shown to amplify the IFN response which is believed to be through interactions of the 3'-monophosphates with IFN signaling factors RIG-I and MDA-5 as removal of these limits the activation of IFN (Malathi et al. 2007).

### 1.2 Viral Induction of IFN

Viruses are capable of inducing the IFN response through several different mechanisms, as the host uses a variety of Pattern Recognition Receptor (PRR) proteins to recognise virus-specific nucleic acid sequences known as Pathogen Associated Molecular Patterns (PAMPs). Viruses induce IFN through a number of different mechanisms which can be divided into two different modes of activation; Toll-like Receptor (TLR)/Endosome dependent and TLR independent activation of IFN.

#### 1.2.1 TLR dependent IFN activation

Viruses can induce TLR-dependent pathways in several different ways. Firstly, TLRs either on the cell surface or internalisesd through endocytosis are capable of recognising dsRNA whether it is present in the extracellular medium or within an endosome leading to the induction of a robust IFN response. This had been clear since the 1960's, however in 2001 it was discovered that TLR-3 was the receptor which recognises dsRNA (Alexopoulou et al. 2001). TLR-3 has been shown to be important to the antiviral response in TLR-3 knockout mice which succumb to infection by Murine Cytomegalovirus (MCMV), yet show resistance to other viruses such as vesicular stomatitis virus (VSV) and reovirus, showing that although TLR-3 is

important to the IFN response it is not essential (Tabeta et al. 2004; Edelmann et al. 2004). TLR-3 signaling is described in Fig 1.2;

Viral single stranded RNA (ssRNA) is also capable of inducing IFN through the activation of endosomal TLR-7. TLR-7 is only expressed by a few cell types and most importantly in plasmacytoid Dendritic Cells, where it is exclusively expressed in the endosome, which can produce up to 50% of circulating IFN during a viral infection (Cao and Liu 2007). TLR-7 appears to have no sequence preference for ssRNA just several uridines in close proximity (Diebold et al. 2006). TLR-7 has been shown to recognise ssRNA from several different viruses such as HIV, Influenza and VSV (Diebold et al. 2004; Heil et al. 2004; Lund et al. 2004). TLR-7 signaling is described in Fig 1.3.

TLR-9 is the host factor responsible for the recognition of endosomal 'foreign' DNA which is distinguishable from host DNA as it is not methylated like host DNA. Similarly to TLR-3, TLR-9 is important to the innate immune response as TLR-9 deficient mice were again susceptible to MCMV due to the reduction in IFN production (Tabeta et al. 2004).

### 1.2.2 TLR Independent IFN activation

The cell is also capable of recognising viral PAMPs through TLR-independent mechanisms. One key mechanism is the recognition of intracellular viral RNA by RNA helicases. Three RNA helicases, RIG-I, MDA-5 and LGP2 have been shown to be important cytoplasmic proteins in the antiviral response.

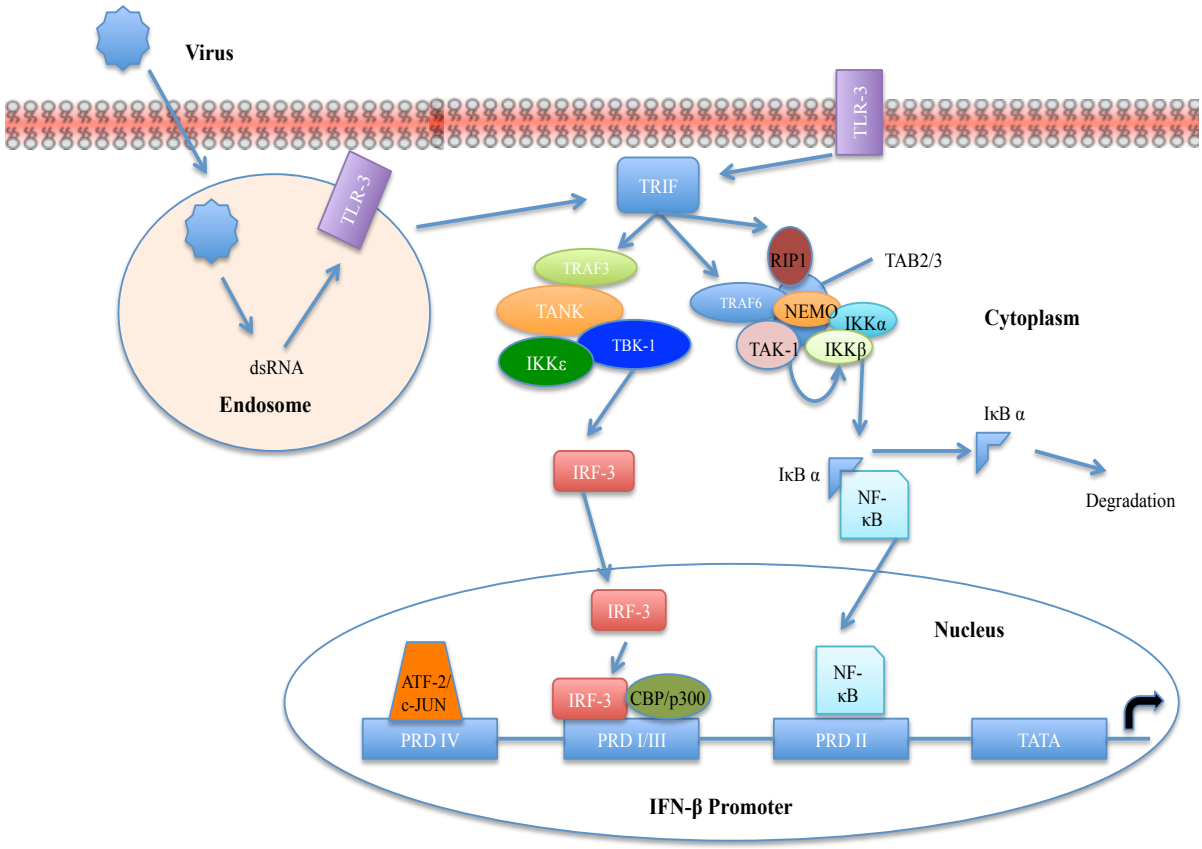


**Figure 1.2. TLR-3 signaling in response to dsRNA.** Double Stranded RNA (dsRNA) can be recognised either on the outside of the cell or inside endosomes through the uncoating of virus particles and presented to TLR-3. Once activated TLR-3 recruits scaffold adaptor protein TRIF, which recruits the components required for activation for either IRF-3 or NF-κB. IRF-3 activation is achieved through the recruitment of TRAF3, which can then bind TANK that can activate either IKKε or TBK-1. IKKε and TBK-1 are both capable of phosphorylating and activating IRF-3, which then translocates to the nucleus and assemble on the IFN-β promoter to stimulate transcription. NF-κB activation requires TRIF to recruit TRAF6 and RIP1 that in turn recruit the IKK complex and TAK1. TAK1 activates IKKβ through phosphorylation, which then phosphorylates IκB that then releases NF-κB to migrate to the nucleus to stimulate transcription of IFN-β mRNA (Adapted from Randall and Goodbourn, 2008).

RIG-I has been shown to recognise 5'- triphosphorylated dsRNA which are short in length as well as single stranded RNA which exhibits a 5'-triphosphate and base-paired ends such as defective interfering RNA and viral hairpins. This diversity of ligand demonstrates the wide variety of RNA viruses that are sensitive to detection by RIG-I. Mice deficient in RIG-I display increased susceptibility to a number of negative sense RNA viruses such as Newcastle disease virus (NDV), vesicular stomatitis virus (VSV) and sendai virus (Rodriguez, Bruns, and Horvath 2014).

Although MDA5 shares structural homology with RIG-I it has proved a lot more difficult to identify activating ligands for MDA5, which may be due to MDA5's relatively poor RNA binding activity when compared to RIG-I or LGP2 (Rodriguez, Bruns, and Horvath 2014). However, recently a number of studies have revealed potential RNA features and specific viral RNA regions that are recognised by MDA5. MDA5 activation was shown to be triggered by RNA that was longer than 2 kbp from sheared RNA populations or following enzymatic digestion (Kato et al. 2008). Also, MDA5-mediated signaling was shown to be preferentially activated by high-molecular-weight RNAs extracted from virus-infected cells (Pichlmair et al. 2009).

Mice deficient in MDA5 showed a greater susceptibility to certain positive-sense single-stranded RNA viruses, for example, poliovirus and encephalomyocarditis virus (EMCV) and murine norovirus (Kato et al. 2006; Gitlin et al. 2006; McCartney et al. 2008). However, a distinction between positive and negative-sense RNA virus recognition by MDA5 or RIG-I is oversimplified. For example, positive sense flaviviruses such as dengue virus and West Nile virus activate both RIG-I and MDA5 (Fredericksen et al. 2008; Loo et al. 2006). Similarly, the negative sense RNA virus

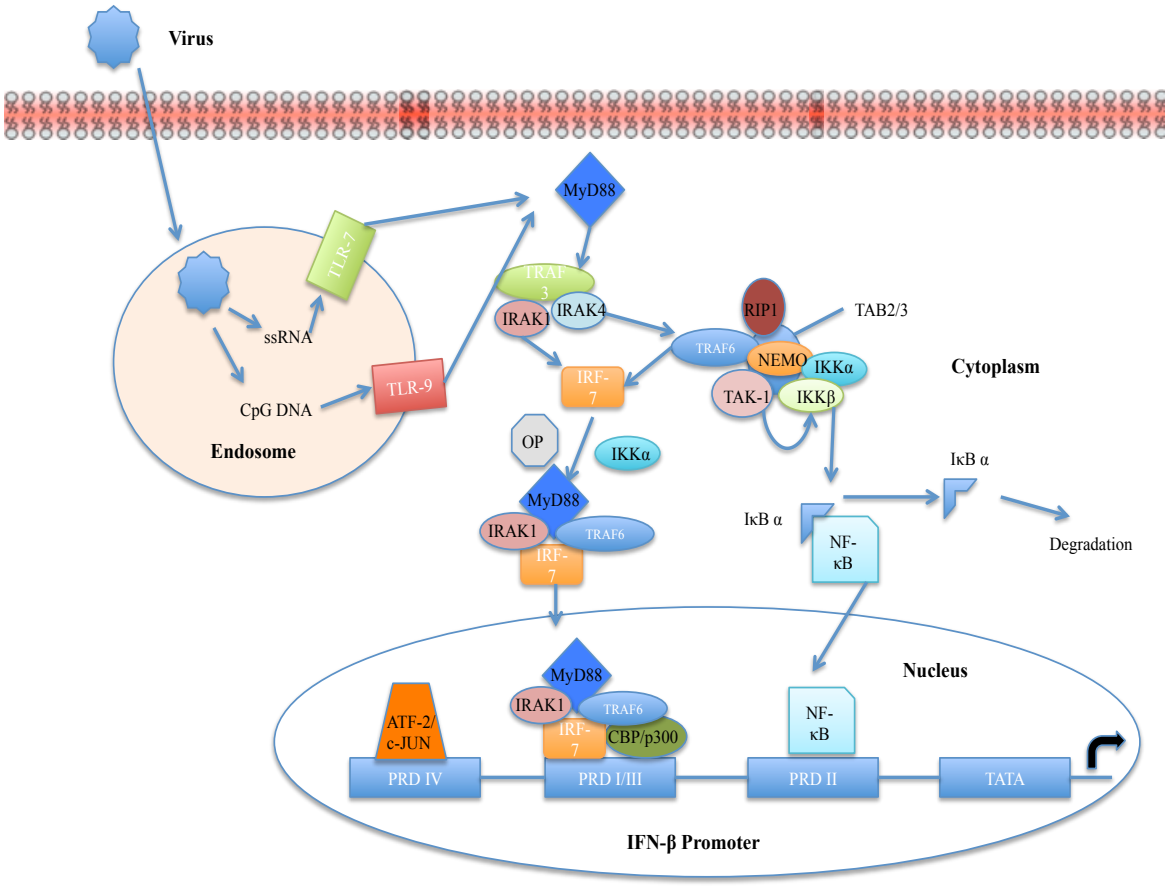


**Figure 1.3. TLR-7 and TLR-9 signaling.** In plasmacytoid dentritic cells, ssRNA or CpG DNA is presented to TLR-7 or -9 in endosomes either through endocytosis of nucleic acids, uncoating of viruses or the degradation of engulfed cells. Once activated TLR-7 and TLR-9 recruit the adaptor protein MyD88 that recruits IRAK1 and IRAK4, which recruits the signaling components required to activate IRF-7 or NF-κB. NF-κB activation is described in Fig. 1.2. IRF-7 activation requires the polyubiquitination of TRAF6, which leads to the phosphorylation of IRF-7 by IRAK1. A complex of IRF-7, MyD88, TRAF6 and IRAK1 then moves to the nucleus where it can promote transcription of IFN-β mRNA (Adapted from Randall and Goodbourn, 2008).

Sendai is believed to be recognized by RIG-I during early infection, yet MDA5 becomes more significant as the infection progresses *in vivo* (Gitlin et al. 2006; Yount et al. 2008). The activation of both RIG-I and MDA-5 form homodimers which can then allow for binding of adaptor protein CARDIF leading to downstream signal transduction, shown in Fig 1.4.

A third RNA helicase, LGP2, shares sequence conservation with the other RLRs however is lacking a Caspase Recruitment Domain (CARD) region entirely. LGP2 is expressed endogenously at low levels but accumulates rapidly in response to IFN or viral infection (Komuro and Horvath 2006). The exact role of LGP2 in antiviral immunity remains to be fully elucidated. Three mouse models that were knockout for LGP2 mice were reported with contrasting results (Satoh et al. 2010; Suthar et al. 2012; Venkataraman et al. 2007). This has lead to a recent model suggesting that LGP2 works as a biphasic switch where LGP2 acts as a concentration-dependent switch between the known MDA5-specific enhancement and a more universal RLR interference (Rodriguez, Bruns, and Horvath 2014).

Recent research has also focused on a number of newly identified cytoplasmic DNA sensors that lead to two known pro-inflammatory responses including AIM2, IFI16, DDX41 and cGAS (Bhat and Fitzgerald 2014). One response is mediated through AIM2, which is responsible for the maturation of pro-inflammatory cytokines via the recruitment of adaptor protein ASC allowing for the formation of the inflammasome (Hornung et al. 2009). Although the inflammasome is a major part of the immune response the second response is essential for innate immunity and the initial control of infection through the up-regulation of IFN (Atianand and Fitzgerald 2013). A key

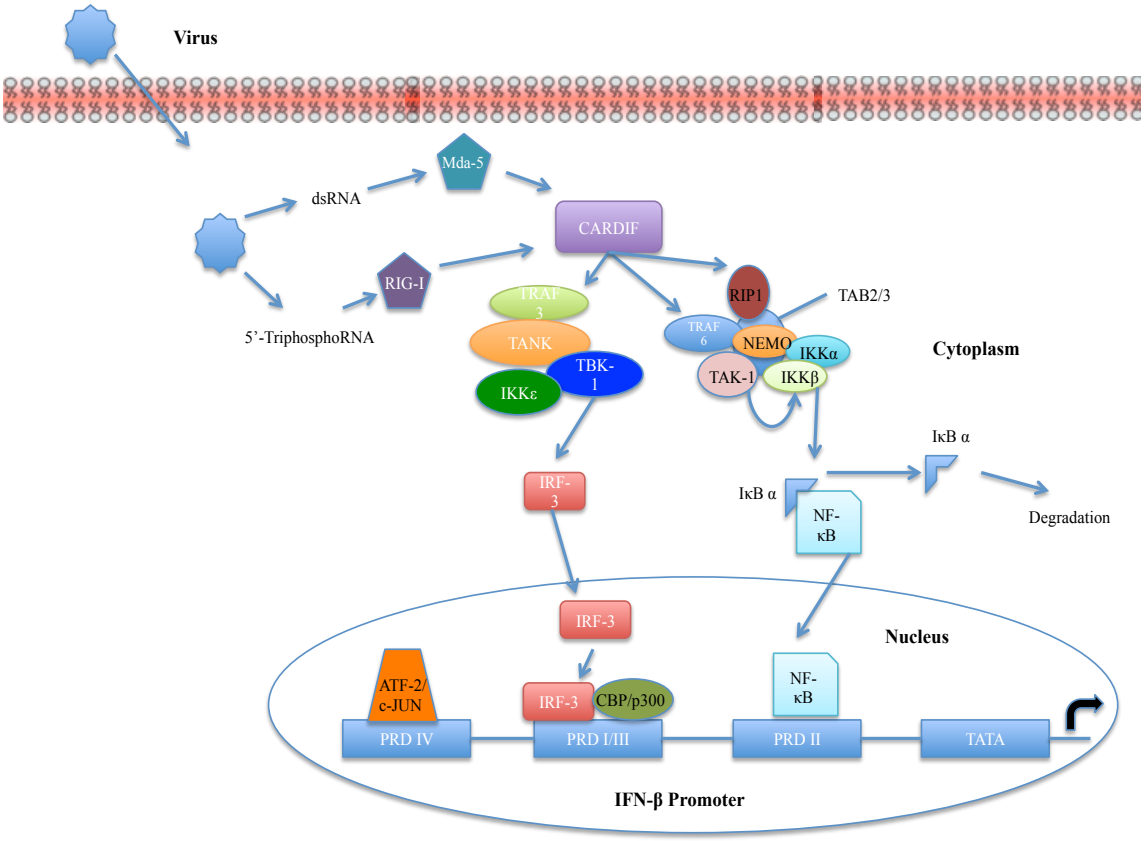


**Figure 1.4: MDA-5 and RIG-I signaling.** RNA helicases mda-5 and RIG-I are both activated by viral RNA, which is present in the cytoplasm through viral uncoating, transcription or replication. Both are activated by dsRNA, whereas ssRNA molecules with a 5' -triphosphate also activate RIG-I. Both contain an N-terminal CARD domain, which recruits the adaptor protein CARDIF. CARDIF acts as a scaffold for all the components necessary to activate either IRF-3 or NF-κB as described in Fig.1.2. This culminates in the transcription of IFN-β mRNA (Adapted from Randall and Goodbourn, 2008).

DNA sensor in this second response is cGAS, an OAS-1-like nucleotidyl transferase, which upon binding viral DNA, produces cyclic GMP-AMP (cGAMP) a cellular secondary messenger, which then activates STING in the endoplasmic reticulum leading to the downstream activation of IRF3 and the transcription of type I IFN (P. Gao et al. 2013; Ablasser et al. 2013).

However, cGAS does not only have antiviral activity against DNA viruses, as a recent study showed an underappreciated impact of cGAS on a wide range of RNA viruses, in particular showing the *in vivo* importance of cGAS against West Nile Virus (WNV) as cGAS knockout mice showed a significant increase in mortality when challenged with WNV compared with wild type mice (Schoggins et al. 2014)

It is also possible for viruses to induce IFN through their proteins as well as nucleic acids. For example, HIV gp120 has been shown to induce IFN-α/β and Human Cytomegalovirus and HSV-1 have been shown to activate IRF-3 complex formation without the translation of new protein (Capobianchi et al. 1992; Mossman et al. 2001; Preston, Harman, and Nicholl 2001). Expression of Measles virus nucleocapsid has also been shown to activate IRF-3 and induce IFN (tenOever et al. 2002) however, it is difficult to generalise this phenomenon as nucleocapsid proteins bind RNA and could therefore be presenting the RNA to the IFN signalling machinery (Randall and Goodbourn 2008).

### 1.2.3 Viral IFN antagonists

Viruses have developed several different mechanisms to evade the IFN response which can be split into 5 modes of action: i) interfere with host gene

transcription/translation; ii) limit the production of viral PAMPs to limit IFN production or by blocking IFN induction; iii) blocking IFN signalling; iv) inhibition of IFN-induced enzymes with antiviral activity; v) have an IFN resistant replication strategy (Randall and Goodbourn 2008).

One of the key mechanisms used by several viruses to circumvent IFN induction and signalling is the production of IFN antagonist proteins. For example, Hepatitis C Virus (HCV) produces the NS3/4a protein which targets and cleaves TRIF, an adaptor protein for TLR-3, and therefore blocksTLR-3 signalling and IFN induction (K. Li et al. 2005). Viruses can also inhibit the detection of PAMPs as shown by Parainfluenza Virus 5 (PIV-5) which produces the IFN antagonist protein V that inhibits MDA-5 activity, thereby blocking MDA-5 induced IFN production (Andrejeva et al. 2004). Viruses can also produce proteins which target IFN signalling as this can block the production of key antiviral proteins such as PKR, OAS, Mx and ISG15; for example PIV-5 V protein targets STAT-1 for degradation which can remove the cell from its antiviral state allowing PIV-5 to replicate efficiently (Carlos, Fearns, and Randall 2005) whereas Japanese Encephalitis Virus (JEV) NS5 protein appears to interfere directly with the IFN-α/β receptor by inhibiting Tyk2 activation, by activating protein tyrosine phosphatases (R.-J. Lin et al. 2004; R.-J. Lin et al. 2006). Fig 1.5 depicts the targets of some IFN antagonists.

Many viruses have evolved more than one mechanism to evade the IFN response as IFN antagonism is rarely, if ever, 100% efficient. This makes evolutionary sense as a virus may produce an antagonist which targets part of the IFN signalling pathway, however without inhibiting the induction of IFN, surrounding uninfected cells can

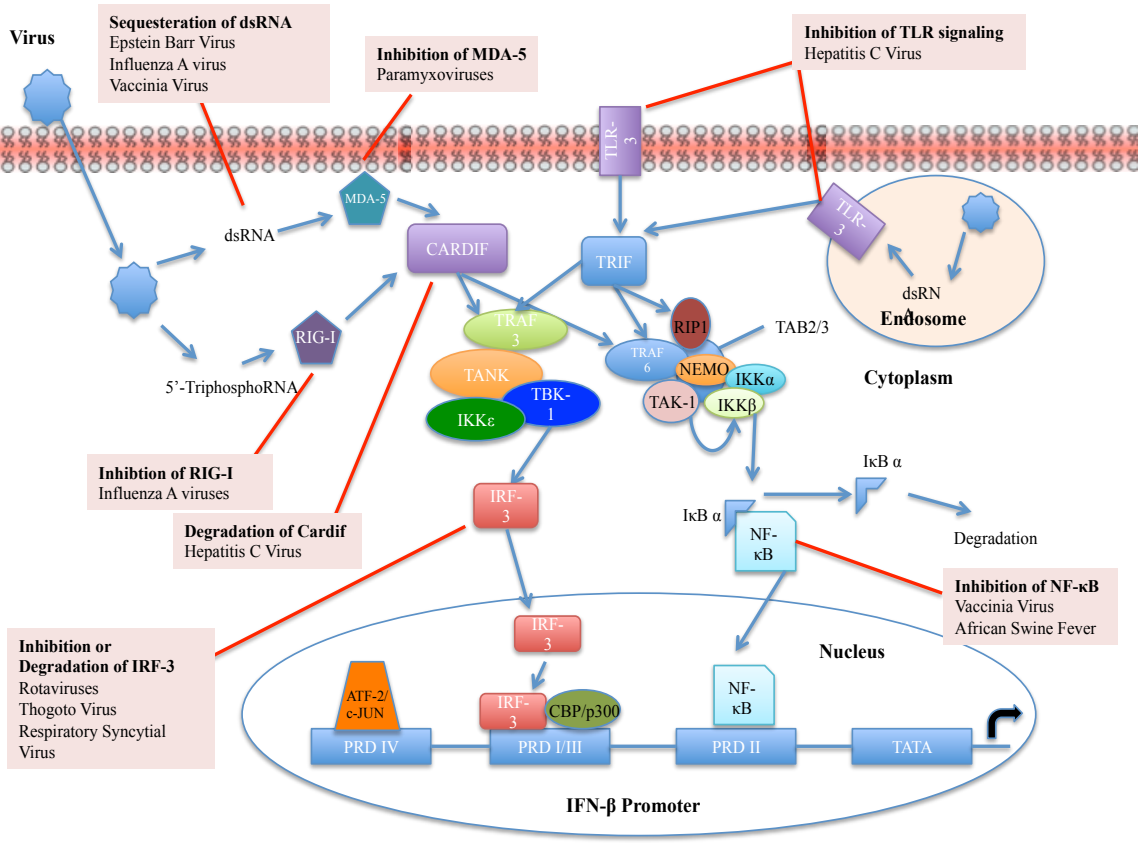


**Figure 1.5: Viral Antagonists that limit the production of IFN-α/β.** This represents IFN-β induction via both TLR-3 and RNA helicases, MDA-5 and RIG-I. The sites of viral antagonism are indicated within the signaling cascades.

induce an antiviral state which would stop the propagation of the virus and therefore decreasing replication effiency. One of the best described examples of a multifunctional IFN antagonist is the influenza A virus NS1 protein, which is capable of circumventing IFN responses through numerous mechanisms including but not limited to i) preventing host gene translation by inhibiting mRNA export; ii) blocking RIG-I mediated induction of IFN; iii) binding to dsRNA to render host PRRs such as OAS inactive; and iv) interacting with PKR and blocking its activity (Hale et al. 2008). However, it should be noted that many of the IFN antagonist multifunctional activities have been identified *in vitro* and require validating as biologically relevant in the context of a productive viral infection (Randall and Goodbourn 2008).

### 1.3 Introduction to influenza viruses

Influenza viruses are important human pathogens which annually result in approximiately 3-5 million severe infections requiring hospitilisation leading to 250,00 - 500,000 deaths (van de Sandt, Kreijtz, and Rimmelzwaan 2012). However, influenza viruses are not only a threat to human health but they also have huge economic implications as well as threatening global food security through infection of important live stock such as poultry, swine and equine species. Influenza viruses belong to the family *Orthomyxoviridae*, which are a group of viruses that have negative sense RNA genomes packaged in multiple single stranded segments. There are currently 6 defined genera within the *Orthomyxoviridae*: Influenzavirus A, Influenzavirus B, Influenzavirus C, Isavirus, Thogoto Virus and Quaranjavirus ("ICTV Virus Taxonomy 2014" 2015).

The 3 different types of influenza virus; A, B and C, differ in a number of ways. Firstly, while influenza A and B viruses possess 8 genome segments, influenza C viruses contain only 7. This is due to the fact that influenza C viruses only express a single surface glycoprotein capable of mediating both viral entry and release, whereas influenza A and B viruses express two separate proteins from two different genome segments, with each protein performing one of these functions. Another key distinction between the influenza viruses is their host specificity and pathogenicity. The natural host of influenza A viruses is wild aquatic birds but these viruses can also infect a wide range of different organisms including but not limited to livestock poultry, horses, pigs, cats, dogs, seals, ferrets and humans (Palese and Shaw, 2007).

Influenza A viruses contains only 1 species but can be subdivided based on their surface glycoproteins heamagglutinin (HA) and neuraminidase (NA). Following the recent discovery of influenza-like viruses in bats, there are currently 18 known subtypes of HA and 11 known subtypes of NA (Tong et al. 2012). Influenza A viruses can be highly pathogenic, capable of causing yearly epidemics, particularly from seasonal influenza A viruses such as H1N1 and H3N2 subtypes, due to an evolutionary process known as antigenic drift. This phenomenon is due to the high infidelity of the viral RNA dependent RNA polymerase (RdRp) introducing random mutations into each gene segment. Some of these mutations can offer increased viral fitness such as mutations which occur within the globular head region of HA, allowing the virus to avoid recognition by neutralising antibodies and it is these changes that requires the influenza vaccine to be updated annually (Smith et al. 2004).

Influenza B viruses primarily infects humans although both seals and ferrets have been seen to be susceptible to the virus. However unlike influenza A viruses, influenza B viruses consist of a single serotype that mutates 2-3 times slower than influenza A viruses coupled with the limited host range. Influenza C viruses are capable of infecting humans, dogs and pigs which can sometimes cause local epidemics, however these viruses are less common than influenza A and B viruses and normally only cause mild illness in children (Palese and Shaw, 2007).

### 1.3.1 Pandemic Potential of influenza A viruses

Influenza A viruses also have pandemic potential through their ability to infect a diverse range of host species and reassort their gene segments into a configuration capable of causing widespread infection in an immunologically naïve human population. This phenomenon is known as antigenic shift, where a novel HA is introduced to a human population through a reassortment event of gene segments when another host, often avian or swine, are infected by 2 or more influenza strains, which has then been capable of infecting humans. However, recent research has shown that reassortment is not a necessity for a virus to undergo a zoonotic event; only a small number of mutations were capable of producing an avian influenza virus, H5N1, which could directly transmit from animal reservoirs to humans (Herfst et al. 2012).

In recent years we have seen an increase in zoonotic influenza infections in humans. It is known that some influenza viruses are excellent donors of some genome segments such as H9N2, which has donated its internal gene complex to both H7N9 and H10N8 prior to human infection (Shanmuganatham et al. 2014). There have been

453 confirmed cases of H7N9 in humans since 2013, with a mortality rate of 38%, and represents one of a number of novel strains like H10N8 and H6N1 to cross the species barrier (Shi et al. 2013; T. Zhang et al. 2014). Examples of pandemic influenza outbreaks include the Asian flu of 1957 and the Hong Kong flu of 1968, which were caused by re-assorted H2N2 and H3N2 respectively. Also, the most infamous pandemic flu was the 1918 Spanish flu, a H1N1 that killed between 20 and 50 million people having a particular effect on young adults, making it unlike any other flu known before that time (van de Sandt, Kreijtz, and Rimmelzwaan 2012).

### 1.3.2 Virion structure

Influenza virus particles can vary greatly in size due to their pleomorphic nature; spherical particles are more uniform in size and have a diameter ranging between 80-100 nm whereas filamentous particles have been seen to stretch over 300 nm. The viral genome is enclosed within a lipid envelope as depicted in fig 1.6, which is taken from the host membrane punctuated with three transmembrane proteins; viral glycoproteins HA and NA along with the small integral membrane protein M2. Below the envelope is the matrix protein M1 encompassing the viral core made up of ribonucleoprotein (RNP) complexes consisting of each viral RNA segment encapsidated in nucleoprotein (NP) accompanied by the three proteins subunits of the RdRp (PB2, PB1 and PA), which are responsible for the transcription and replication of the viral genome (Palese and Shaw, 2007). Recent research by two groups using 3D electron microscopy reconstruction has finally revealed the structure of the RNP complexes in their native state showing a double-helical hairpin structure. At ~20 A resolution it shows that each RNP contains a single copy of the viral polymerase complex, viral RNA and NP forming the double helical structure with 5 or 6 pairs of

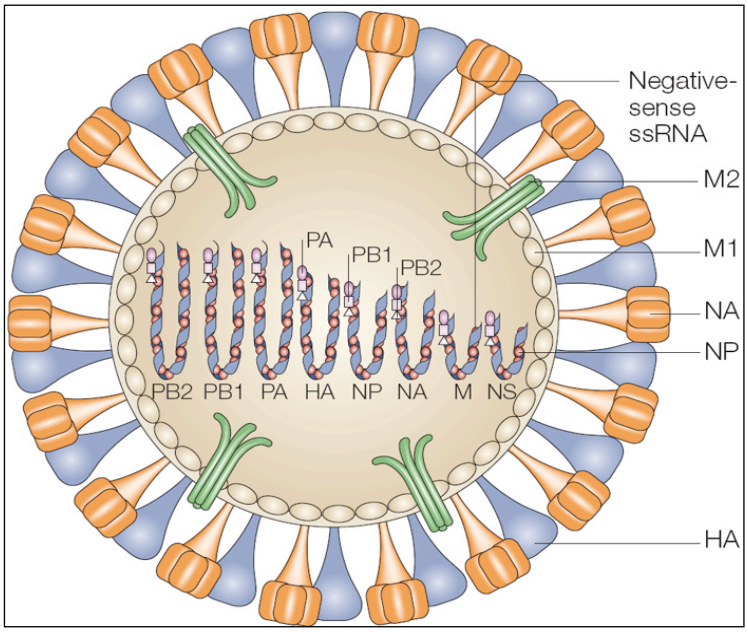


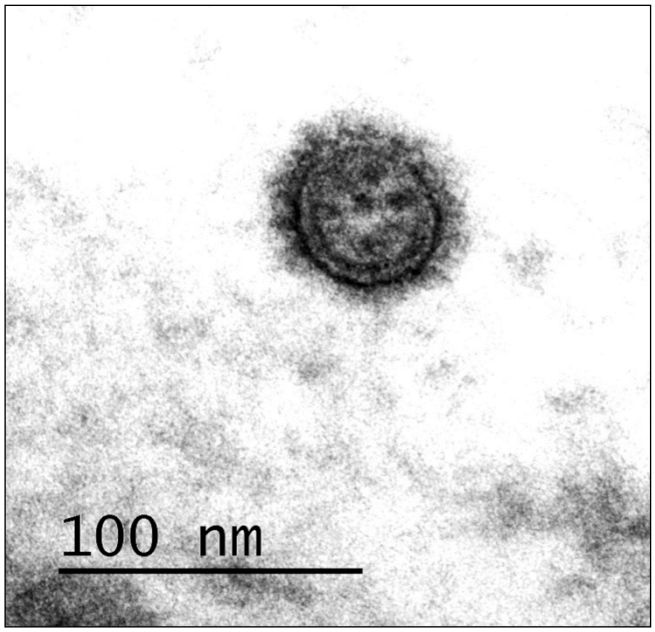


**Figure 1.6. Schematic and Electron micrograph of Influenza A virus**. The schematic shows the outer membrane envelope punctuated with the surface glycoproteins HA and NA along with the M2 ion channel protein. Inside the inner matrix layer each vRNA segment is encapsidated by NP, associated with one copy of the polymerase complex (consisting of three subunits; PB1, PB2, and PA) and folded in a double helical hairpin structure known as viral ribonucleoprotein complexes (vRNPs). NEP is also present within the virus particle but is not displayed in the schematic. The electron micrograph shows an influenza A/WSN/1933 (H1N1) virion at 40, 000x magnification, the spike-like projections are the surface glycoproteins and distinct RNA segments are clear inside the virion.

NP molecules per turn with an approximated 120-150 RNA nucleotides in each helical turn (Arranz et al. 2012; Moeller et al. 2012)

### 1.3.3 Viral Encoded Proteins

The influenza A virus genome is comprised of eight segments of negative sense RNA that together encode for 10 core proteins all of which are essential to all strains of influenza A virus for viral fitness (Palese and Shaw, 2007).

#### 1.3.3.1 Polymerase Proteins

The influenza virus encodes its own RNA-dependent RNA polymerase that is a complex of three proteins: polymerase basic protein 1 (PB1), polymerase basic protein 2 (PB2) and polymerase acidic protein (PA). Protein interaction studies have shown that PB1 binds to both PA and PB2, through its N- and C-terminal domains respectively (González, Zürcher, and Ortín 1996; MacDonald et al. 2012). A direct interaction between PA and PB2 was not elucidated until a bimolecular fluorescence complementation assay was used to study their interaction (Hemerka et al. 2009). Recently, high resolution atomic structure of the influenza polymerase complex has been solved showing that there are several intricate interactions between each subunit and not limited to the N-to-C terminal interactions which had previously been described (Sugiyama et al. 2009; Reich et al. 2014; Pflug et al. 2014).

**PB1**

PB1 contains the conserved characteristics associated with RNA-dependent RNA polymerases (Biswas and Nayak 1994). PB1 catalyses the sequential addition of

nucleotides during RNA chain elongation (Braam, Ulmanen, and Krug 1983). The active site for the polymerase activity is an S-D-D motif found at positions 444-446 (Biswas and Nayak 1994). PB1 is responsible for the initiation of transcription and replication through binding to the 5' and 3' terminal ends of both vRNA and cRNA respectively (González and Ortín 1999a; González and Ortín 1999b).

**PB2**

The PB2 protein plays an important role in the initiation of transcription by binding the cap on host pre-mRNA molecules (Ulmanen, Broni, and Krug 1981). The cap-binding ability of PB2 has been attributed to several different regions of PB2, however structural analysis of the cap-binding domain complexed with m7GTP showed that like other cap-binding proteins such as vaccinia virus VP39 and eIF4E, PB2 sandwiched the methylated base between two aromatic residues, H357 and F404 (Fechter et al. 2003). PB2 has also been shown to be involved in genome replication as some mutations within the N-terminal region of PB2 have been shown to affect replication but not transcription (Gastaminza et al. 2003). More recently PB2 has been shown to undergo a number of mutations which allows for host adaptation between avian and mammalian hosts (Neumann and Kawaoka 2015). Two of the most studied adaptation mutations are found at positions 627 and 701. It was shown that a glutamic acid at position 627, found in most avian lineages, restricted viral replication in mammalian hosts whereas a lysine at position 627 (encoded by most human influenza viruses), conferred efficient replication in the upper respiratory tract of mammals (Hatta et al. 2007). The PB2 D701N mutation is important for the ability of PB2 to bind to host nuclear import machinery, where an asparagine at position 701 increased the binding affinity of importin alpha in mammalian cells leading to an increase in

replicative machinery as well as promoting the nuclear import of incoming vRNPs in mammalian cells (Gabriel, Herwig, and Klenk 2008; Sediri et al. 2015).

**PA**

The PA protein also plays a critical role in the initiation of transcription; however, unlike PB2 it is required for cleaving capped pre-mRNAs rather than binding to them. Structural analysis has attributed the endonuclease activity required for cap-snatching to the N-terminal domain of PA, which is in agreement with previous mutational studies (Hara et al. 2006; Dias et al. 2009; Yuan et al. 2009). Not only does PA have a role in transcription but it has also been shown to be important for binding and regulating the synthesis of vRNA and cRNA (Hara et al. 2006; Huarte et al. 2003; Maier et al. 2008). Like PB2, PA has recently been shown to be important for host adaptation with a number of amino acids been shown to have an impact on the viruses ability to adapt to a mammalian host (Hu and Liu 2015). In fact, reassortment experiments that paired a human PA with an avian polymerase complex showed an increase in polymerase activity in vitro and a reduction in host restriction in mammalian cells (Mehle et al. 2012). The importance of PA to host adaptation was compounded further by in vivo experiments showing an increase in competent virus spread by avian H5N1 in guinea pigs when paired with a human PA segment (Y. Zhang et al. 2013).

#### 1.3.3.2 Nucleoprotein

Influenza nucleoprotein (NP) is an RNA binding protein essential for the transcription and replication of viral RNA as well as forming an integral part of vRNP and cRNP structures through its high affinity for RNA. Despite NP's affinity for RNA the

protein is indiscriminate about which RNA sequence it binds to (Yamanaka, Ishihama, and Nagata 1990). The crystal structure of NP has been solved for both H1N1 and H5N1 as a trimeric complex and showed that monomeric NP consisted of 3 main domains, a head domain, a body domain and a tail loop (Ye, Krug, and Tao 2006; Ng et al. 2008). NP is capable of undergoing homo-oligomerisation through the insertion of the tail loop into the middle domain of the adjacent NP monomer and recently this oligomerisation has been shown to be dependent on phosphorylation (W.-H. Chan et al. 2010; Mondal et al. 2015; Turrell et al. 2015) and to take place in a tail-loop first orientation independent of RNA binding (Turrell et al. 2013). Mutational analysis of both the RNA binding and oligomerisation domains of NP showed that both of these functions were required for the transcription of vRNA and that NP has an essential role as an elongation factor during viral transcription (W.-H. Chan et al. 2010; Turrell et al. 2013).

#### 1.3.3.3 Surface Glycoproteins

There are currently 18 subtypes of HA and 11 subtypes of NA have been identified, all of which have been found in the natural host of these viruses, water fowl, apart from the recently discovered H17N10 and H18N11 which were isolated from bats (Fouchier et al. 2005; Tong et al. 2012; Tong et al. 2013). The zoonotic potential of influenza viruses is dependent on the ability of the surface glycoproteins to allow for cell entry and egress following successful replication.

**HA**

The first step during viral infection is viral entry, which requires attachment of the virus to the host cell, a process mediated by the viral HA protein. HA is the most

abundant surface glycoprotein and is a type I integral membrane protein which undergoes a number of post-translational modifications such as glycosylation and acetylation of the cytoplasmic tail (de Graaf and Fouchier 2014). HA is initially translated and incorporated into virus particles as a single polypeptide, HA0, which is then cleaved extracellularly after virus release by host proteases to form two subunits HA1, which contains the receptor-binding domain of HA, and HA2, which contains the fusion subdomain. For attachment to the host cell HA targets sialylated glycan receptors on the cell surface and in 1983 it was shown that human and animal influenza viruses exhibited different preferences in the receptor specificity of HA (Rogers and Paulson 1983). Avian influenza viruses have a binding preference for sialic acid bound to galactose via an alpha 2,3 linkage, whereas human influenza viruses have a preference for alpha 2,6 linked sialic acid. However, viruses can easily evolve to change their receptor-binding specificity as it was recently shown that as few as 4 amino acid changes in an avian H5N1 HA was capable of switch specificity from alpha 2,3 to alpha 2,6, thereby allowing for successful airborne transmission of an avian virus among ferrets (Herfst et al. 2012).

The second major function of HA is low pH triggered fusion, which is required for the release of the viral genome. The low pH found in the endosome leads to a significant structural change in HA with the most prominent change in the position of the fusion peptide. Due to the hydrophobic characteristics of the fusion peptide the conformational change allows this peptide to bury itself in the endosomal membrane, thereby bringing the viral and endosomal membranes into close enough proximity for membrane fusion to occur. The presence of more than one HA trimer stimulates the production of a fusion pore, thereby connecting the viral interior with the host cell

cytoplasm and allowing the vRNP to exit the virus particle and enter the cytoplasm (Palese and Shaw 2007).

HA is also recognized by the adaptive immune system, which leads to the production of neutralizing antibodies raised against the numerous antigenic sites found on the globular head region of the HA1 domain. This helps to drive the evolution of the virus as due to the infidelity of the polymerase, a viral quasi-species is produced, with many of the mutant viruses containing mutations within the antigenic sites of HA1. Changes that allow the virus to go unnoticed by the immune system are termed 'escape mutants' which over time become fixed changes defining the antigenic drift of the virus (Smith et al. 2004).

**NA**

The NA protein is the second most abundant surface glycoprotein on influenza A virions and is a type II integral membrane protein which forms tetramers on the surface of the virion and infected cells (Eichelberger and Wan 2015). The native tetramer is required for enzyme activity and each monomer has a distinctive 6-bladed beta propeller (Russell et al. 2006). There is less NA than HA on the virion surface, however this is virus dependent. For example, in most viruses the ratio is ~ 5:1 HA to NA but the 2009 H1N1 pandemic virus had a ratio nearer to 2:1 (Getie-Kebtie et al. 2013).

NA has a number of essential roles throughout the virus life cycle. NA is a sialidase which cleaves glycosidic linkage between the sialic (N-acetylneuraminic) acid and an adjacent galactose residue (Shtyrya, Mochalova, and Bovin 2009). NA

enables incoming virions to access respiratory tract epithelial cells by destroying decoy receptors present on mucins (Matrosovich et al. 2004). However, it is unlikely that this receptor-destroying activity prevents HA from binding and infecting epithelial cells due to the increased ratio of HA:NA and because also NA appears to be segregated from HA on the virus surface (Calder et al. 2010). NA is essential for the release of nascent virus particles as shown by experiments in which reduced enzymatic activity of NA led to a reduction in viral plaque size due to inefficient cell-to-cell spread (Kilbourne et al. 1968). NA also removes sialic acids from its own glycoproteins, which is thought to prevent aggregation of nascent virions at the cell surface and may explain the relationship between NA activity and transmissibility as free, non-aggregated virions are more likely to have improved transmission in aerosol droplets that are inhaled into the lower respiratory tract (Lakdawala et al. 2011; Yen et al. 2011).

#### 1.3.3.4 Matrix Proteins

**M1**

Matrix protein 1 (M1) is the most abundant protein in the virion, oligomersing to form a protein layer just below the lipid bilayer, separating the inner core components from the membrane glycoproteins. M1 is believed to interact with the cytoplasmic tails of the surface glycoproteins and play a role in the organization of the outer membrane proteins. M1 is also known to play a number of important roles in the virus replication cycle. M1 is known to interact with both RNP and NEP/NS2 and is indispensible for the nuclear export of vRNPs (Sakaguchi et al. 2003). M1 has also been shown to be essential and sufficient to produce virus-like particles, as well as being shown to play an important role in the pleomorphic nature of influenza viruses thus providing

evidence for its critical role in viral egress (Latham and Galarza 2001; Gómez-Puertas et al. 2000; Martyna and Rossman 2014).

**M2**

The M2 protein of influenza A viruses is a type III integral membrane protein which forms a tetramer in its native state. M2 consists of 3 protein domains a short ecto-domain, a transmembrane domain and an endodomain with palmitate and phosphate modification (Shuck, Lamb, and Pinto 2000). The M2 protein has been shown to possess ion channel activity and plays a major role in viral entry. M2 conducts protons from the acidified endosomes into the interior of the virus leading to the dissociation of vRNPs from the rest of the viral components, therefore completing the uncoating process (Takeda et al. 2002).

This ion channel activity has also been suggested to play a role in the stabilization of HAs from premature low pH transitions in the trans-Golgi network. However, this secondary function is particularly important in the case of avian HA proteins H5 and H7, which have a multibasic cleavage site that can be cleaved by ubiquitous proteases and are consequently more susceptible to a premature low pH-induced conformational change (Ciampor et al. 1992). Another function attributed to the M2 protein is an Impact on the ratio of filamentous to spherical particles as well as evidence suggesting that M2 has a role in virion assembly through an interaction with nascent vRNPs at the cell (Roberts, Lamb, and Compans 1998; Hughey et al. 1995; Schroeder et al. 2005). M2 has also been shown to play a role in virus particle release through a highly conserved helix located within the M2 cytoplasmic tail mediates

a cholesterol-dependent alteration in membrane curvature mediating the final steps of influenza viruses release (Rossman et al. 2010).

### 1.3.3.5 Non-Structural proteins

**Non-Structural Protein 1**

The non-structural protein 1 (NS1) is the most abundantly expressed of any influenza virus protein, which at first was believed to not be present within the influenza virion (Krug and García-Sastre 2013). However, due to advances in technique sensitivity NS1 was found to be present in the virion, although the role played by NS1 in the virion is still to be elucidated (Edward C. Hutchinson et al. 2014). The NS1 protein varies in length between different virus strains but all NS1 proteins carry similar features. They consist of an N-terminal RNA Binding Domain (RBD) and a C-terminal Effector Domain (ED) and are capable of producing homo-dimers through the RBD (Chien et al. 1997). NS1 is a multi-functional protein capable of a number of different effector functions. Influenza A NS1 protein is capable of inhibiting the interferon response at a number of different stages during the host response to viral infection (see section 1.6). NS1 has also been shown to regulate both viral RNA synthesis as well as protein expression and other pro-viral functions such as the control of the cellular apoptotic response (Ayllon and García-Sastre 2015).

NS1 was initially thought to be a predominantly nuclear protein but it has since been shown that the cellular distribution of NS1 can change throughout infection suggesting a temporal regulation, potentially mediated through protein-protein interactions and post-translational modifications such as phosphorylation or coupling

with ubiquitin like proteins such as SUMO or ISG15 (C. Zhao et al. 2010; Hsiang, Zhou, and Krug 2012; Santos et al. 2013).

**Nuclear Export Protein**

In addition to NS1, vRNA segment 8 produces a second mRNA via a splicing reaction, which encodes for a 121 amino acid protein known as Nuclear Export Protein or Non-structural protein 2 (NS2) (Lamb and Lai 1980). The protein was initially designated as NS2 until it was shown to be present in virions at very low levels, suggesting a potential interaction with M1 (Richardson and Akkina 1991; Yasuda et al. 1993). Following the discovery of the function of NS2, where the protein was found to be responsible for exporting newly synthesized vRNPs out of the host cell nucleus ensuring their availability for packaging into nascent virions NS2 was renamed NEP (O'Neill, Talon, and Palese 1998).

Recently NEP has been suggested to have more than one function during the influenza virus replication cycle. It has been determined that NEP contributes to the viral budding process through interaction with a cellular ATPase, F1Fo ATPase, by recruiting F1Fo ATPase to the plasma membrane (Gorai et al. 2012). Additionally, NEP is capable of regulating the accumulation of viral RNA species, suggesting that NEP is able to promote the switch from viral transcription to replication for the production of genomic vRNPs (Robb et al. 2009; Mänz et al. 2012). Furthermore, there is substantial evidence that indicates mutations within NEP capable of increasing viral RNA replication offer a significant replicative benefit during mammalian adaptation of avian influenza virus (Mänz et al. 2012).

### 1.3.3.6 Accessory Proteins

Influenza A virus was believed to express 10 proteins from the 8 viral genome segments, however since 2001 a number of accessory proteins have been identified or theorized to be expressed by influenza A viruses (Vasin et al. 2014). Owing to the small size of the influenza genome, influenza has evolved a number of mechanisms for the expression of multiple proteins from a single gene segment, including alternative splicing of viral mRNAs as seen in segment 7 and segment 8. Other non-canonical mechanisms of translation employed by influenza A virus include non-AUG initiation, re-initiation, leaky ribosomal scanning as well as ribosomal frame-shifting (Firth and Brierley 2012; Yewdell and Ince 2012).

The eleventh influenza A protein was found to be encoded on segment 2, with an alternative open reading frame leading to the expression of PB1-F2 (W. Chen et al. 2001). Since this discovery, another 6 accessory proteins have been found to be expressed by influenza A virus as well as a hypothetical protein expressed from segment 8. These proteins and known functions are summarized in table 1.1.

## 1.4 Virus replication cycle

The viral replication cycle is a complex series of events, which can be divided into a number of different parts, each of which are integral for successful replication. The replication cycle of influenza A virus is summarized in fig 1.7.

### 1.4.1 Attachment and Entry

The first step in viral infection requires the attachment of HA to sialic acid present on the cell surface (Palese and Shaw, 2007). However a number of other host factors

| Protein | Segment | Function | Reference |
|---|---|---|---|
| PB1-F2 | 2 | Pro-apoptotic and pro-inflammatory effects<br>Regulation of immune response | (W. Chen et al. 2001; Krumbholz et al. 2011; Dudek et al. 2011) |
| PB1-N40 | 2 | Regulates viral replication | (Wise et al. 2009) |
| PA-N155 | 3 | Potential role in replication | (Muramoto et al. 2013) |
| PA-N182 | 3 | Potential role in replication | (Muramoto et al. 2013) |
| PA-X | 3 | Modulates host response and viral virulence | (Jagger et al. 2012) |
| M42 | 7 | Can functionally replace M2 | (Wise et al. 2012) |
| NS3 | 8 | Potentially related to host adaptation in mice | (Selman et al. 2012) |
| NS4 | 8 | Hypothetical Translation from the negative sense ORF. Function Unknown | (Clifford, Twigg, and Upton 2009) |

**Table 1.1. Influenza Accessory proteins and known functions.**

have been implicated in viral attachment such as Annexin V and in the case of macrophages and dendritic cells, C-type lectins, suggesting that additional co-receptors may be required for viral attachment (R. T. Huang, Lichtenberg, and Rick 1996; Londrigan et al. 2011).

Early imaging studies showed that influenza A virus was taken up via receptor-mediated endocytosis and that virus internalization could take place via clathrin-dependent and clathrin-independent mechanisms (Matlin et al. 1981). Influenza A viruses are also capable of being internalized via caveolin-dependent pathways but viral entry has also been shown to take place independently of both clathrin and caveolin (Sieczkarski and Whittaker 2002). In 2011, a fourth mechanism of viral entry became apparent as influenza A viruses were shown to utilize macropinocytosis as an alternative pathway for internalization (de Vries et al. 2011). Further research has shown that the mechanism of uptake is likely to be cell-type dependent but can also be determined by the pleomorphic nature of the virus as filamentous particles have been shown to be more likely to be taken up by macropinocytosis (De Conto et al. 2011; Rossman, Leser, and Lamb 2012). Following internalization the virus particle undergoes endosomal trafficking from localizing to early endosomes before moving toward late endosomes in the perinuclear region where due to changes in endosomal pH the virus is able to undergo fusion for the release of the viral genome (Edinger, Pohl, and Stertz 2014).

### 1.4.2 Fusion

Following internalization, the viral and endosomal membranes fuse in order to allow the genome to be released into the cytoplasm. During endocytic trafficking the

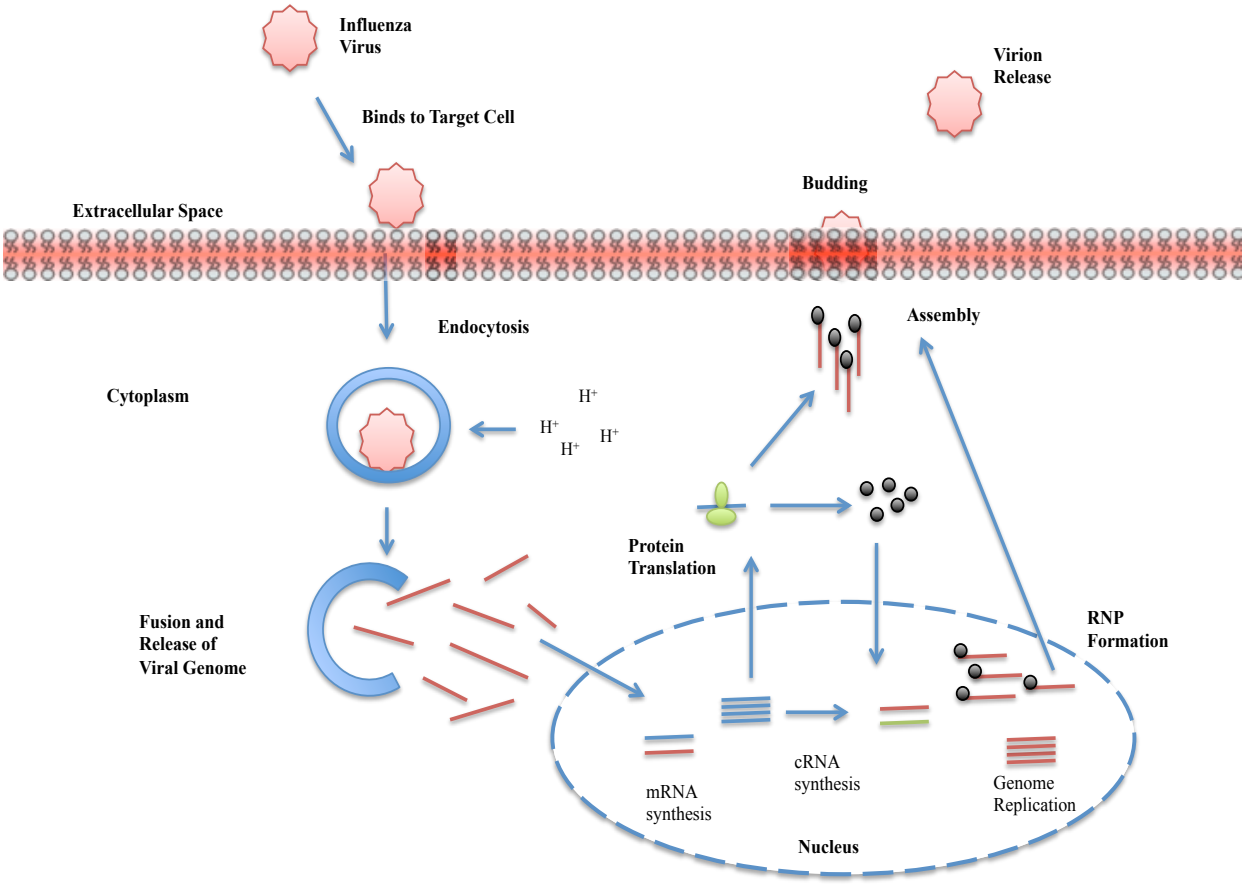


**Figure 1.7. Schematic of Influenza A virus Replication.** The virus binds to the target cell through HA which leads to the virus being endocytosed by the host cell. During the late stage of endocytosis the low pH causes a conformational change in HA allowing the viral and endosomal membranes to fuse, leading to the opening of a pore and the release of the viral genome to the cytoplasm. The viral genome is then imported into the nucleus where primary transcription of mRNA occurs, which is then translated in the cytoplasm. NP is then shuttled back into the nucleus, which triggers the switch to what is called secondary transcription producing cRNA as a template for genome replication. Once enough protein and genome has been made RNP complexes form and are transported to the plasma membrane for virion assembly. Virions are then released by the enzymatic action of NA. (Red = vRNA, Blue = mRNA and Green = cRNA)

endosomes undergo a step-wise acidification process as protons are pumped into the endosomal lumen (Pérez and Carrasco 1994). For Fusion to occur HA first needs to be cleaved from from $HA_0$, which assemble as trimers, into $HA_1$ and $HA_2$ by a trypsin-like serine endoprotease. After cleavage, the two disulfide-bonded protein domains produce the mature form of the protein subunits as a prerequisite for the conformational change necessary for fusion (Taubenberger 1998). The acidic environment leads to the final conformational change which inserts the fusion peptide into the endosomal membrane where the concerted structural changes of several HA molecules fuses the membranes and creates the fusion pore, allowing for the release of vRNPs (Palese and Shaw, 2007).

### 1.4.3 Uncoating and nuclear import

Uncoating is the process through which vRNPs are released into the cytoplasm and is dependent on both M2 and M1 (Edinger, Pohl, and Stertz 2014). M1 has been demonstrated to interact with vRNPs through its middle domain interacting with NP (Noton et al. 2007). This interaction as well as the interaction of M1 with the viral membrane needs to be released. This is mediated through the action of M2 which pumps protons from the surrounding endosome into the virion, lowering the pH causing the detachment of vRNPs from M1 and allowing for the genome to be released into the cytoplasm (Zhirnov 1990). Although, which host factors were required for uncoating to take place in unknown, a recent publication shows that an E3 ubiquitin ligase, Itch, is necessary for efficient uncoating (Su et al. 2013).

Once vRNPs are dissociated from M1 and released into the cytoplasm the vRNPs are then dependent on host factors for their transport into the nucleus for transcription and

replication. The vRNPs are translocated to the nucleus using the classical importin-alpha-importin-beta1 (IMPα-IMPβ1) dependent nuclear import pathway (Eisfeld, Neumann, and Kawaoka 2015). Nuclear import of vRNPs is determined by the presence of nuclear localization signals (NLS) present in NP which following the recently solved structures has been shown to be surface exposed making it available for interaction (Arranz et al. 2012; Moeller et al. 2012). This non-canonical NLS sequence at the beginning of NP binds to IMPα isoforms 1 and 5 and has been shown to be essential for the nuclear import of vRNPs (Cros, García-Sastre, and Palese 2005). NP has also been shown to bind to IMPα3 and IMPα7 although these are yet to be fully characterised (Gabriel et al. 2011). Additional studies have also shown that vRNPs only associate with the nuclear pore complex in the presence of IMPα and IMPβ and that transport into the nucleus also required RAN-GTPase (O'Neill et al. 1995). More recently an inhibitor of the IMPβ-RAN GTPase interaction was shown to inhibit the translocation of vRNPs into the nucleus (Chou et al. 2013), therefore providing more evidence that vRNP transport is dependent on this host process.

### 1.4.4 Transcription

Once the genome has translocated to the nucleus its primary role is to produce viral mRNA for the synthesis of new viral proteins (Mark et al. 1979). This process is termed primary transcription and uses m7G capped pre-mRNAs as a primer for mRNA synthesis, which are 'cap-snatched' by the viral polymerase proteins (Plotch, Bouloy, and Krug 1979). Transcription of influenza mRNA is initiated using a prime and realign mechanism which produces a methylated cap structure which is followed by a 10-13 nt host-derived sequence prior to viral specific sequence. This causes the

viral mRNAs to be longer than the full-length genomes at the 5' end (Deng, Vreede, and Brownlee 2006). The polymerase then uses the vRNA as a template producing a poly-A tail by reiterative stuttering at the poly-U sequence of 5-7 U residues conserved at the 5' end of vRNA which causes the viral mRNAs to be shorter in length than the viral genome (Poon et al. 1999). Following the production of the viral mRNA, it is then exported from the nucleus for translation by cellular ribosomes where newly synthesized PB1, PB2, PA and NP are all transported back to the nucleus for the synthesis of de novo vRNPs (Eisfeld, Neumann, and Kawaoka 2015). A number of host factors are involved in primary transcription including the RNA polymerase II (Pol II) complex and SFPQ. It is assumed that the viral polymerase complex interacts with actively transcribing Pol II to obtain cellular mRNA caps via cap-snatching (Engelhardt, Smith, and Fodor 2005). Although, Pol II degradation is promoted by PB2 and PA proteins, which has been associated with increased pathogenicity in mice (Llompart, Nieto, and Rodriguez-Frandsen 2014). Another host factor involved in primary transcription is a multifunctional splicing factor, SFPQ, which associates with several vRNP components promoting the polyadenylation of viral mRNA transcripts (Landeras-Bueno et al. 2011). Viral mRNA synthesis peaks between 2-6 hours post infection, followed by a sharp decline, thought to be due to a limited number of host caps available due to host shut-off or the degradation of Pol II induced by infection (Vreede et al. 2010).

### 1.4.5 Genome Replication

The replication of the viral RNA genome occurs in two different stages. During the first stage genomic vRNA is used as a template to produce complimentary RNA (cRNA). This is followed by the second stage where the cRNA is replicated into

vRNA. The mechanisms of initiation and termination of cRNA synthesis is different to those used for the production of mRNA as cRNA is a full-length copy of the vRNA and therefore does not have a 5' cap structure or a 3' poly(A) tail. The production of genomic RNA does not require a RNA primer due to the 5’ triphosphates at 5’ ends of both vRNA and cRNA (Fodor 2013; Vreede, Gifford, and Brownlee 2008).

Nascent NP and Polymerase proteins are required to protect genomic RNA from degradation. The recent observation that NP acts as an elongation factor during replication suggests that it is likely that the core reason that viral protein synthesis is required prior to genome replication is to provide newly synthesized trans-acting RNA polymerase. This can then be used to produce the cRNA and newly synthesized NP to stabilize elongation of full-length genome replication products whilst encapsidating de novo RNA (Fodor 2013; Turrell et al. 2013). It has also been proposed that NEP is involved in the regulation of viral RNA synthesis. NEP has been shown to regulate the balance been transcription and replication in vivo, increasing the amount of vRNA whilst reducing the levels of mRNA (Robb et al. 2009).

### 1.4.6 vRNP export

Newly synthesized vRNPs need to be transported from the nucleus to the cytoplasm for incorporation into nascent virions. Influenza viruses use the CRM-1-dependent Nuclear Export pathway to transport the viral genome into the cytoplasm (Eisfeld, Neumann, and Kawaoka 2015). NP is the only known part of the vRNP that has a Nuclear Export Signal (NES), however, without the presence of M1 or NEP vRNPs remain in the nucleus, showing that these two proteins are essential for vRNP export (Martin and Helenius 1991; Bui et al. 2000). M1 and vRNPs have been shown to

interact and this interaction is required to promote the export of vRNPs but M1 has not been shown to interact directly with CRM-1 and is therefore more likely to be an intermediary protein between vRNPs and the CRM-1 interacting partner (Sakaguchi et al. 2003).

NEP has been shown to interact directly with CRM-1 through two NES sequences, which when mutated through reverse genetics can have a severe impact on viral fitness and growth kinetics through its effect on nuclear export of vRNPs (Neumann, Hughes, and Kawaoka 2000; S. Huang et al. 2013). Although NEP has never been shown to directly interact with vRNPs, it can interact directly with M1 suggesting a model for vRNP nuclear export whereby vRNPs are bound to M1 which in turn bind to NEP in complex with CRM-1 allowing for nuclear export (Akarsu et al. 2003; Shimizu et al. 2011).

### 1.4.7 Trafficking to the Plasma Membrane

Following export from the nucleus, the vRNPs need to be transported through the cytoplasm to the plasma membrane for the assembly of nascent virions. After nuclear export vRNPs are found to localise to the microtubule organization centre (MTOC) (Momose et al. 2007; Amorim et al. 2011) and live cell imaging has shown that fluorescently tagged vRNPs move along microtubules towards the plasma membrane (Momose et al. 2011). This was supported by evidence that cells treated with microtubule depolymerisation compounds were found to produce less virus and have a different localization pattern for trafficking vRNPs (Momose et al. 2007). Membrane bound vesicles are a common microtubule cargo in mammalian cells and both vRNA and vRNPs have been seen to co-localise with Rab11-positive recycling

endosomes (Chou et al. 2013; Amorim et al. 2011; Momose et al. 2011). Following transport to the plasma membrane it appears that the vRNPs transfer from Rab11-positive endosomes to the plasma membrane suggesting a specific mechanism for this transfer, as suggested by the lack of Rab11 found in influenza A virions (Eisfeld et al. 2011; Shaw et al. 2008).

### 1.4.8 Packaging

The exact mechanism of vRNP packaging is also not fully understood, but two different models were suggested, random packaging and selective packaging (Palese and Shaw, 2007). However, with an increasing amount of evidence for selective packaging, it is now generally accepted that selective packaging is the mechanism through which influenza A viruses package their RNA genomes (Gerber et al. 2014). All vRNA segments have been shown to have segment specific packaging signals located at the 5' and 3' coding regions (Eisfeld, Neumann, and Kawaoka 2015). However, recent research has shown that internal vRNA sequences appear to be important for the efficient packaging of all 8 influenza genome segments through the production of vRNA-vRNA interactions, yet these sequences appear to be strain specific (Essere et al. 2013; Gavazzi et al. 2013).

Recent research into vRNP trafficking has provided an insight into the potential mechanism of sequence-specific selective packaging. Chou et al, recently showed that different vRNPs travel together toward the plasma membrane on Rab11-positive vesicles, suggesting a platform through which selective packaging of vRNA segments can take place (Chou et al. 2013). This hypothesis has garnered some support as a recent publication has showed, using a four-color FISH assay to visualize all eight

vRNA segments, that although vRNAs are not exported all together, they are also not exported individually. This suggests that viral RNA subcomplexes can further assemble whilst trafficking to plasma membrane via dynamic colocalization events using Rab11a-containing recycling endosomes as a platform (Lakdawala et al. 2014).

### 1.4.9 Virus Assembly

As the infection progresses, the plasma membrane becomes enriched with viral proteins, which leads to the budding of nascent virions around vRNPs. The viral glycoproteins HA and NA are concentrated to lipid raft microdomains. Although, the M2 protein also localizes to the plasma membrane it instead accumulates on the boundaries of lipid rafts. It has been suggested that M2 is required for the recruitment of vRNPs at the budding site via a direct interaction with M1 via its cytoplasmic tail (McCown and Pekosz 2005; B. J. Chen et al. 2008).

Although the precise mechanism of virus budding is unknown it has been suggested that vRNPs may facilitate budding via interactions with M1. Upon binding vRNPs M1 may undergo a conformational change that drives polymerization and therefore capsid formation. An alternative hypothesis suggests that binding to vRNPs reduces the extent to which M1 can alter membrane curvature, therefore allowing capsid formation to be initiated by HA and NA. However, evidence to support these models is currently lacking (Rossman and Lamb 2011). M2 has been shown to play a role in virus particle release through a cytoplasmic tail which has been shown to mediate a cholesterol-dependent alteration in membrane curvature mediating the final steps of influenza viruses release (Rossman et al. 2010). Following virion formation the virion may still be bound to the plasma membrane due to

the HA binding to sialic acid on the cell-surface. NA is then able to play a final role in virus release by cleaving sialic acid off the cell surface, preventing the HA-receptor interaction (Rossman and Lamb 2011). Interestingly, recent cryo-electron tomography experiments have shown NA to be concentrated at one location on nascent virions, which suggest the role of NA in facilitating the final release of nascent virions (Calder et al. 2010).

In addition to viral factors, a number of different host factors have been shown to be essential for budding include G-protein and kinase activity, as well as ATP, F1Fo-ATPase activity and actin filaments (Gorai et al. 2012). An interaction between M1 and an adaptor protein involved in recycling endosome trafficking, RACK1, has also been shown to be required for viral budding (Demirov et al. 2012).

### 1.5 Influenza and IFN

Influenza virus primarily targets the epithelial cells of the respiratory tract and can elicit the IFN response by PAMP activation of three main PRRs: TLRs, RIG-I and nucleotide oligomerization domain (NOD)-like receptor family pyrin domain containing 3 (NLRP3). TLRs are first to respond to influenza infection as TLR7 recognises ssRNA released by degraded RNPs from acidified endosomes whereas TLR3 will recognise dsRNA, likely to be in the form of pan-handle structures from incoming vRNPs (Diebold et al. 2004). TLR2 and TLR4 are also believed to detect influenza infection as these are localised to the cell surface allowing them to bind to the viral HA and NA proteins (Takeuchi and Akira 2009; Imai et al. 2008). NLRP3 is found in the NLRP3 inflammasome, which is also activated by dsRNA and leads to the activation of Caspase I allowing for the proteolytic maturation of IL-1β and IL-18

(Kanneganti et al. 2006). RIG-I can be activated by either dsRNA or 5'-triphosphate RNA and has been shown to induce IFN after binding newly synthesised, uncapped, viral RNA in the cytoplasm later on during infection (Hornung et al. 2006).

The activation of these PRRs leads the activation of the IFN-β promoter, which in turn leads to the production of IFN-β which then activates the IFN-signaling cascade through wither paracrine or autocrine signaling culminating in the transcription of over 300 ISGs allowing the host cells to establish an antiviral state (Randall and Goodbourn 2008). Some of these genes encode for antiviral proteins which are particularly important for the IFN response such as PKR, OAS and MxA but also ISG15, Viperin, Tetherin and IFITMs which have all been shown to play an important role in the IFN response to Influenza (van de Sandt, Kreijtz, and Rimmelzwaan 2012).

ISG15 has 2 domains, which exhibit structural homology similar to ubiquitin connected via a proline-containing linker. ISG15 has 2 main functions, it can be excreted from the cell and act as a cytokine or like ubiquitin can be conjugated to over 150 protein targets through an IFN inducible conjugation cascade including known antiviral proteins MxA and RIG-I (C. Zhao et al. 2005a; Lenschow et al. 2007). Mice which lack ISG15 have been shown to be more susceptible to infection by influenza A and B when compared to wildtype (wt) mice, and ISG15 has been shown to interact with the NS1 protein of A/Udorn/72 [H3N2] virus with two groups showing that ISGylation of NS1 impairs viral replication (Lenschow et al. 2007; C. Zhao et al. 2005a; Tang et al. 2010).

Viperin (Virus Inhibitory protein, endoplasmic reticulum-associated, IFN-inducible) is another ISG which can be induced by types I, II and III IFNs and has been implicated in the IFN response against influenza virus infection (Fitzgerald 2011). The expression of Viperin has been shown to alter plasma membrane fluidity by negatively affecting the formation of the lipid-raft micro-domains used by influenza for viral budding. Viperin has been shown to interact with and decrease the enzymatic activity of farnesyl di-phosphate synthase, which is integral to lipid raft formation, leading to inhibition of influenza virus release (Wang, Hinson, and Cresswell 2007).

Tetherin is a type II integral membrane protein localised to lipid rafts, which has been shown to restrict the release of some enveloped viruses such as HIV-1 (Watanabe, Leser, and Lamb 2011; Neil, Zang, and Bieniasz 2008). Although tetherin expression was shown not to reduce the infectious titre of released influenza viruses, it prevented the release of influenza virus-like particles (VLPs) into the media (Watanabe et al., 2011). Palese and colleagues, who looked at VLPs formed through NA expression from plasmid DNA, also observed this. They saw that VLP production could be inhibited by Tetherin but some NA subtypes were unaffected suggesting that NA may have a mechanism to combat the antiviral restriction factor Tetherin (Yondola et al. 2011).

IFITM (Interferon inducible Transmembrane protein) proteins were identified as being able to restrict early steps in the infection process of influenza A viruses and the flaviviruses, Dengue virus and West Nile virus (Brass et al. 2009). Humans have 5 IFITM genes, IFITM-1, -2, -3, -5 and -10 however, only IFITM-1,-2 and -3 are induced by IFN therefore suggesting an important role in antiviral activity (R. Jia et

al. 2012). IFITM proteins restrict viral infection by interfering with virus entry. When influenza A entry was monitored in IFITM-3 expressing cells by fluorescent microscopy, virion accumulation in IFITM3 positive membrane compartments was observed and indicated a failure to complete genome entry into the cytoplasm (Feeley et al. 2011). Following on from these *in vitro* studies, Everitt et al., (2011) used a knock out mouse model and found that IFITM-3 was essential for defending against influenza A infection with mice showing viral pneumonia when challenged with a low pathogenicity strain of influenza. These findings have also been shown to be relevant to human infection as a statistically significant number of patients hospitalized by H1N1/09 influenza were shown to have a single nucleotide polymorphism (SNP) that altered the splice acceptor site of the IFITM3 gene resulting in a protein that lacked the first 21 amino acids of the N-terminal region. This truncated version of IFITM3 was shown to have reduced influenza virus restriction and resulted in the relocalisation of IFITM3 from the endosomal compartment to the cell periphery. Therefore IFITM3, and in particular the N-terminal region, appears to have a crucial role in host defence against influenza infection by restricting virus entry (Everitt et al. 2012; R. Jia et al. 2012).

### 1.6 Influenza IFN evasion

With all these responses instigated by the host in response to infection influenza viruses have had to adopt several different ways to evade the IFN response in order to replicate and propagate infection. The biggest weapon influenza viruses have at their disposal is the NS1 protein, which is an antiviral antagonist protein capable of limiting IFN production. This has been shown through infections with modified viruses containing non-functional NS1 where the infected cells exhibit a much

stronger IFN response when compared to wild-type virus. The impact of NS1 is not limited to in vitro studies as defective NS1 viruses has been shown to have less virulence during mouse and swine studies (Falcón et al. 2005; García-Sastre et al. 1998). NS1 is capable of inhibiting RIG-I receptor signaling in several ways. Firstly NS1 limits the availability of its own PAMPs for RIG-I detection by forming a complex with RIG-I and what is thought to be a viral PAMP in dsRNA (Pichlmair et al. 2006; Mibayashi et al. 2007). Secondly NS1 prevents the oligomerization of TRIM25 by binding to the coiled-coil domain and therefore blocking TRIM25 – mediated ubquitination of RIG-I, which is essential for downstream signaling. Finally, another way in which NS1 is capable of blocking RIG-I signaling is by preventing the translocation of IFR-3, NF-κB and c-Jun/ATF2 transcription factors into the nucleus, therefore by inhibiting enhanceosome complex formation influenza NS1 is capable of blocking RIG-I mediated IFN-β gene transcription (Hale et al. 2008).

NS1 has also been reported to regulate host cell gene expression (Nemeroff et al. 1998). This is mainly through NS1 binding to the cleavage and polyadenylation specificity factor (CPSF30) complex and preventing it from processing the 3'ends of cellular pre-mRNAs into mature polyadenylated mRNAs. Without maturation these mRNAs are not exported out of the nucleus, which thereby halts subsequent cellular protein synthesis. As a subset of these mRNAs would encode IFNs, binding of NS1 to CPSF30 essentially prevents the synthesis of IFNs by preventing nuclear export of IFN-encoding genes. NS1 is also able to block the export of mRNA from the nucleus, possibly through binding components of the mRNA transport machinery (Satterly et al. 2007). This function may allow influenza to limit non-IFN related pathways which could prove beneficial to viral replication (Hale, Albrecht, and García-Sastre 2010).

NS1 is also known to directly block the function of both PKR and OAS. OAS binds to dsRNA and data suggests that the NS1 RNA binding domain out-competes OAS to bind to dsRNA thus blocking this antiviral strategy (Min and Krug 2006). The mechanism that NS1 uses to block PKR activation was initially thought to be similar to that of OAS, however, experiments using an RNA-binding defective NS1 was still capable of limiting PKR activation (S. Li et al. 2006). NS1 had also been shown to bind to PKR in a dsRNA dependent manner through residues 123-127 (S. Li et al. 2006; Min et al. 2007). Therefore, based on mapping studies it is hypothesised that NS1 binds to a linker region in PKR and prevents the conformational change from the auto-inhibition to the active conformation (S. Li et al. 2006; Hale et al. 2008).

However, NS1 is not the only protein that influenza utilizes to combat the IFN response. Both PB2 and PB1-F2 have been seen to limit IFN production through associating with MAVS, a protein found in the IFN induction cascade (Graef et al. 2010; Varga et al. 2011). Furthermore the viral polymerase complex of PB2, PB1 and PA have been shown to be involved in cap-snatching from host mRNAs and therefore can camouflage viral mRNAs as host mRNAs stopping host recognition whilst also reducing host cell gene expression including IFN (Sugiyama et al. 2009; Dias et al. 2009). Influenza viruses are also capable of inhibiting PKR in an NS1-independent fashion as influenza NP binds to the $p58^{IPK}$-hsp40 complex, thereby releasing $p58^{IPK}$, which inhibits PKR activity, therefore NP indirectly inhibits PKR (K. Sharma et al. 2011). The influenza virus NP protein encapsidates viral RNA which reduces the formation of dsRNA species and protects the RNA from recognition by cytoplasmic PRRs (van de Sandt, Kreijtz, and Rimmelzwaan 2012). Also, not only does influenza limit IFN production but it is also capable of inhibiting type I IFN receptor signaling

through the induction of SOCS (suppressor of cytokine signaling) proteins which act on JAK/STAT activation to inhibit IFN signaling (Pauli et al. 2008; Pothlichet, Chignard, and Si-Tahar 2008).

### 1.7 IFN inducible GTPases

The IFN-inducible GTPases are a superfamily of proteins that display inhibitory activities against a variety of microbial classes (Kim et al. 2012). Bioinformatic analysis has lead to the complete mapping of this superfamily in humans and mice but many other species have been annotated with IFN-inducible GTPases such as other primates, cows, dogs as well as lizards and birds, as seen in fig 1.8 (Kim et al. 2011; G. Li et al. 2009). There are currently 47 members in humans and mice which can be grouped in to 4 subfamilies based on paralogy and molecular mass; immunity-related GTPases (IRGs), guanylate binding proteins (GBPs), Myxoma (MX) resistance proteins and very large inducible GTPases (VLIGs/GVINs) (Kim et al. 2011; Martens and Howard 2006).

Crystal structures of several IFN-inducible GTPases reveal a globular N-terminal G domain followed by a C-terminal helical domain (Kim et al. 2012). This structure plus the biochemical similarities have lead to the GTPases being grouped together with the dynamin-like family of proteins including dynamins, mitofusin, atlastins and other dynamin-like proteins (Ferguson and De Camilli 2012). The IFN-inducible GTPases have a wide variety of functions including budding and fusion of transport vesicles, cytokinesis and organelle division. These GTPases have a low μM substrate affinity whilst exhibiting high rates of GTPase activity and are capable of oligomerising to

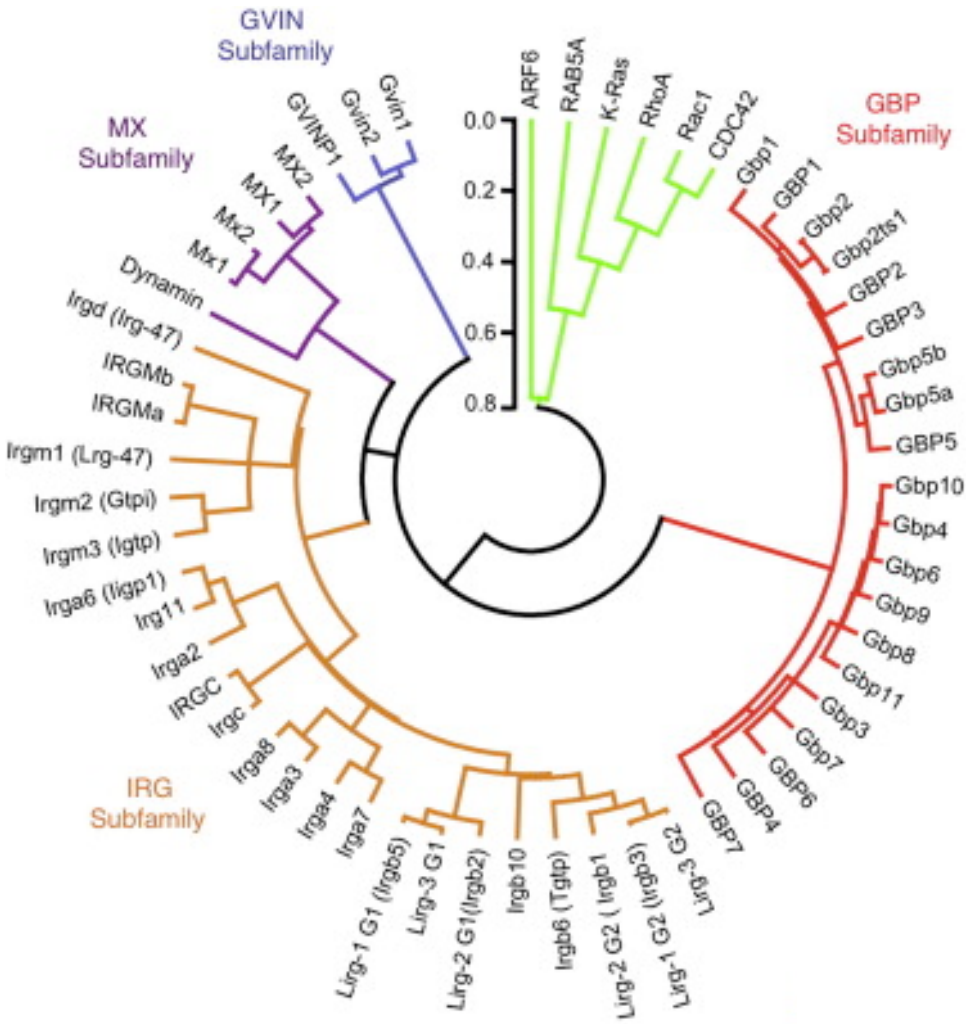


**Figure 1.8. IFN-inducible GTPase sub-families.** Phylogenetic tree depicting the 4 sub-families of IFN-inducible subfamilies: 21-47 kDa IRGs, 65-73 kDa GBPs, 72-82 kDa MX proteins and the 200-285 kDa GVINs. (Adapted from Kim et al, 2012).

form large complexes over 0.5 MDa in cells (Ferguson and De Camilli 2012). All IFN-inducible GTPases are transcribed in response to Type I, II or III IFN apart from the MX proteins which are only up-regulated by type I and III IFNs (Kim et al. 2011; Kresse et al. 2008). IFN-induced GTPases are some of the most up-regulated target genes during IFN signaling events, for example GBPs can account for up to 20% of the proteins induced by IFN-γ (Martens and Howard 2006). IFN-inducible GTPases are expressed by a large number of the mammalian cell lineages examined to date, which is in accordance with the wide-ranging distribution of IFN receptors (MacMicking 2012). Although, it should be noted that certain GBPs respond to TNF-α and IL-1β in murine macrophages and human endothelial cells, therefore furthering the number of ways the host can induce these GTPases (Degrandi et al. 2007; Tripal et al. 2007). This allows for a cell-autonomous defence to intracellular pathogens, protozoa and viruses in a wide range of cell types (Kim et al. 2012).

### 1.8 Mx Proteins

The Mx proteins were first discovered as a result of work performed by Jean Lindemann, who found that a particular inbred mouse strain was resistant to doses of influenza virus that proved to be fatal in ordinary laboratory mice (Lindemann, 1962). The research that followed on from this found that the resistance was caused by the *Mx1* gene, this lead to the screening of several inbred mice strains and perhaps surprisingly found that most of these strains were carrying non-functional Mx1 genes due to deletions and nonsense mutations (Reeves et al. 1988; Staeheli et al. 1988).

The Mx family of GTPases contains MxA and MxB in humans, with homologues found in mice referred to as Mx1 and Mx2. Both human Mx genes are found in close

proximity to each other at the distal end of chromosome 21 (21q22.3) which shares synteny with mouse chromosome 16 (Horisberger et al. 1988). The human MxA (76 kDa) and MxB (76/78 kDa) proteins are cytoplasmic proteins as is murine Mx2 yet murine Mx1 is found to localise in the nucleus, this difference in localisation has been suggested to allow each protein to target viruses in either the cytoplasm or nucleus respectively (Hug et al. 1988; O Haller et al. 1995). Human MxB appears to display a nuclear localisation-like sequence in its N-terminal extension and although it is thought to be a cytoplasmic protein it is localised to the cytoplasmic face of nuclear pores and has been suggested to play a role in regulating nucelocytoplasmic transport and cell-cycle progression (King, Raposo, and Lemmon 2004).

### 1.8.1 MxA

It is well documented that the production of MxA is tightly regulated by type I and III IFN signaling events and is one of the most highly inducible antiviral factors characterised to date (Holzinger et al. 2007). However, it has recently been shown that MxA is inducible through another pathway as an endogenous antimicrobial peptide, α-defensin, known to be expressed from polymorphonuclear leukocytes (PMNs) can induce MxA in periodontal tissue without the presence of IFN (Mahanonda et al. 2012).

MxA has a wide antiviral spectrum, with both RNA and DNA viruses known to be susceptible to its antiviral activity including orthomyxoviruses, asfaviruses, rhabdoviruses, togaviruses, hepadnaviruses and bunyaviruses (Sadler and Williams 2008). The antiviral specificities of Mx proteins appears to be reflected by the localization of the Mx protein within the cell (see Table 1.2), for example rodent Mx1

| Protein | Species | Intracellular localization | Antiviral specificity | References |
|---|---|---|---|---|
| huMxA | Human | Cytoplasm | Orthomyxoviruses, Bunyaviruses | (Georg Kochs, Haener, et al. 2002; Patzina, Haller, and Kochs 2014) |
| huMxB | Human | Nucleus/Cytoplasm | HIV-1 | (Z. Liu et al. 2013) |
| muMx1 | Mouse | Nucleus | Orthomyxoviruses | (T. Huang et al. 1992) |
| muMx2 | Mouse | Cytoplasm | Hantavirus, VSV | (Jin et al. 2001; Jin et al. 1999) |
| ratMx1 | Rat | Nucleus | Orthomyxoviruses | (Stertz et al. 2007) |
| ratMx2 | Rat | Cytoplasm | VSV, Bunyaviruses | (Stertz et al. 2007) |
| chMx | Chicken | Cytoplasm | Orthomyxoviruses, VSV | (Sasaki et al. 2013) |
| duMx | Duck | Nucleus/Cytoplasm | No antiviral activity | (Bazzigher, Schwarz, and Staeheli 1993) |
| asMx1 | Atlantic Salmon | Cytoplasm | Infectious Salmon AnaemiaVirus, Infectious Pancreatic necrosis virus | (Larsen, Røkenes, and Robertsen 2004; Jensen et al. 2002) |

**Table 1.2. Intracellular localization and antiviral spectrum of Mx proteins.** (Adapted from Haller, Stertz and Kochs. 2007)

is nuclear and therefore targets nuclear viruses such as influenza and THOV, whereas rodent Mx2 is cytoplasmic and has antiviral effect against cytoplasmic viruses such as LACV . Human MxA has been shown to inhibit clinically significant viruses such as coxsackie virus and Hepatitis B as well as all infectious genera of the bunyaviridae family (Andersson et al. 2004; Chieux et al. 2001; Gordien et al. 2001). However, the mechanism of action has been studied for several different viruses but is still unclear.

It is thought that MxA undergoes a physical interaction with viral nucleoproteins, which has been demonstrated by the co-sedimentation of THOV and LACV NP with MxA (G Kochs and Haller 1999). However, how this interaction takes place is still unknown and whether this translates for all viruses inhibited by MxA remains to be seen. The current hypothesis on how MxA implements its antiviral effect is that MxA accumulates as oligomers on membranes such as the endoplasmic reticulum which can recognise viral structures upon infection, which upon recognition recruits more MxA molecules to form co-polymers and therefore immobilise the virus for degradation (Sadler and Williams 2008; Otto Haller, Stertz, and Kochs 2007). However, this is speculation and is yet to be proven.

Mx proteins form a sub-family of dynamin-like GTPases (Otto Haller, Stertz, and Kochs 2007). Gao and colleagues recently presented a nucleotide-free atomic resolution structure of MxA showing an extended 3-domain structure characteristic of dynamin-like GTPases (S. Gao et al. 2011). As shown in fig 1.9, MxA is shown to have an N-terminal globular head region containing the catalytic GTPase (G) domain

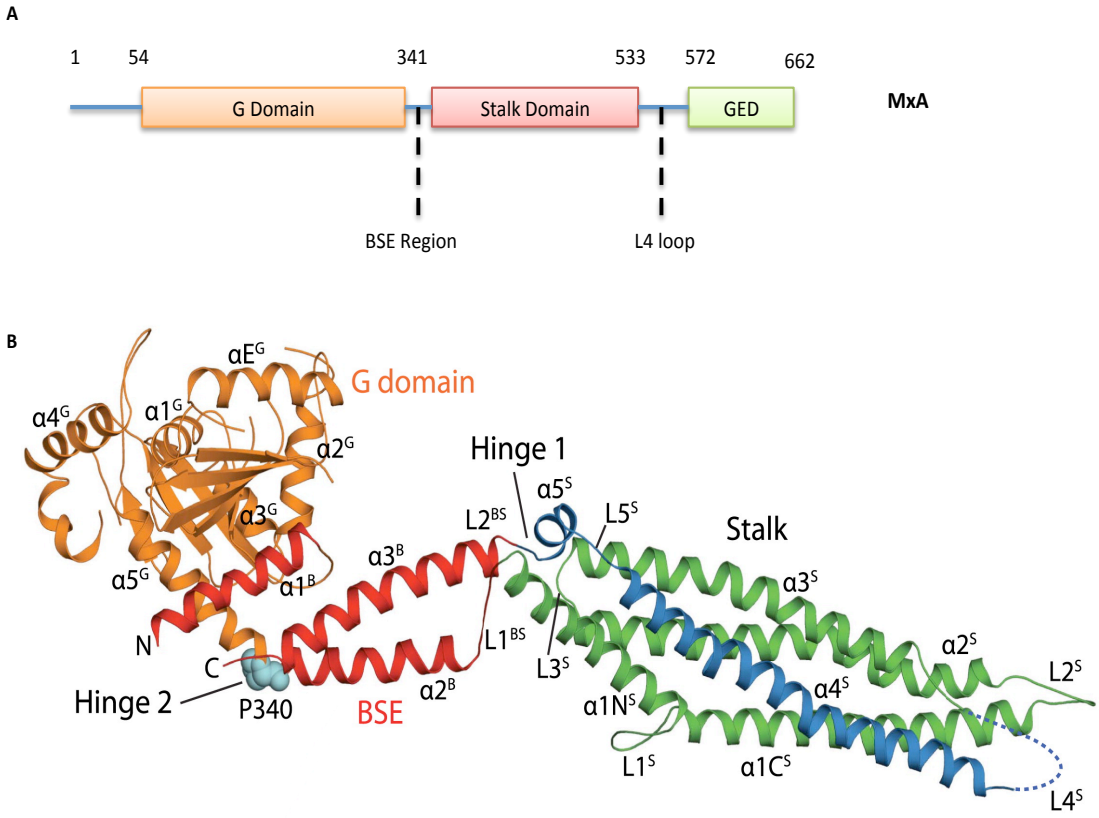


**C**

```
  1 MVVSEVDIAK ADPAAASHPL LLNGDATVAQ KNPGSVAENN LCSQYEEKVR PCIDLIDSLR
 61 ALGVEQDLAL PAIAVIGDQS SGKSSVLEAL SGVALPRGSG IVTRCPLVLK LKKLVNEDKW
121 RGKVSYQDYE IEISDASEVE KEINKAQNAI AGEGMGISHE LITLEISSRD VPDLTLIDLP
181 GITRVAVGNQ PADIGYKIKT LIKKYIQRQE TISLVVVPSN VDIATTEALS MAQEVDPEGD
241 RTIGILTKPD LVDKGTEDKV VDVVRNLVFH LKKGYMIVKC RGQQEIQDQL SLSEALQREK
301 IFFENHPYFR DLLEEGKATV PCLAEKLTSE LITHICKSLP LLENQIKETH QRITEELQKY
361 GVDIPEDENE KMFFLIDKIN AFNQDITALM QGEETVGEED IRLFTRLRHE FHKWSTIIEN
421 NFQEGHKILS RKIQKFENQY RGRELPGFVN YRTFETIVKQ QIKALEEPAV DMLHTVTDMV
481 RLAFTDVSIK NFEEFFNLHR TAKSKIEDIR AEQEREGEKL IRLHFQMEQI VYCQDQVYRG
541 ALQKVREKEL EEEKKKKSWD FGAFQSSSAT DSSMEEIFQH LMAYHQEASK RISSHIPLII
601 QFFMLQTYGQ QLQKAMLQLL QDKDTYSWLL KERSDTSDKR KFLKERLARL TQARRRLAQF
661 PG

54-341  = G Domain
366-533 = Stalk Domain
534-572 = L4 Loop
573-662 = GTPase Effector Domain
```

**Figure 1.9. Protein domains and structure of Human MxA**. **A**. Schematic representation of the domain structure of human MxA. **B.** Ribbon representation of an MxA monomer, the unresolved L4 loop is indicated by the dashed line. **C.** Amino Acid sequence of MxA with highlighted domains (Adapted form Gao et al. 2011)

followed by 3 helices which are known as the bundle signaling element (BSE) and the stalk region consisting of the middle domain leading into the C-terminal GTPase-effector domain (GED). Like other dynamin-like large GTPases, MxA is capable of self-assembly to form large homo-oligomers, which in vitro has been seen to produce ring-like and helical structures (Georg Kochs, Haener, et al. 2002; Accola et al. 2002). It appears that self-assembly of Mx proteins is critical to GTPase activity and protein stability as single amino acid change at position 612 in the GED from leucine to lysine led to a loss of self-assembly and GTPase activity. It should also be noted that MxA (L612K) was monomeric and degraded rapidly whereas wt MxA has a half-life of over 24 hours, suggesting that oligomerization also helps to prevent degradation and perhaps offers a storage from which active molecules can be recruited (Janzen, Kochs, and Haller 2000). A broad range of mutations across the BSE, stalk region, hinge region and GED have all been shown to have an effect on the antiviral activity of MxA as well as oligomerization and GTPase activity of MxA. However whether these mutations have affected individual functions of MxA or had large effects on the structural characteristics of MxA are unknown (Otto Haller et al. 2010; Sadler and Williams 2011).

The GTP binding domain has also been shown to be critical to the antiviral activity of MxA. Dick et al, (2015) set out to characterise a number of G domain mutants to ascertain the importance of GTP hydrolysis and G domain dimerization in MxA's antiviral function. Residues within the catalytic centre of the G domain were found to be essential for G domain dimerisation and although these mutants were able to precipitate the nucleocapsid of THOV, these mutants did not display antiviral activity

against influenza A virus, THOV or LACV due to the lack of GTPase activity (Dick et al. 2015b).

Another region that is thought to be important for antiviral activity is the L4 loop, which is an unstructured loop containing positively charged residues thought to be responsible for lipid binding as substitution of Lysine residues within the loop leads to a loss of lipid binding function without affecting oligomerization (von der Malsburg et al. 2011). In the model of oligomerization proposed by Gao et al., (2011) it was suggested that the L4 loop would be pointing towards the inside of the ring where it is capable of interacting with either viral structures or membrane structures such as the endoplasmic reticulum.

Mitchell and colleagues (2012) have studied the L4 loop from an evolutionary perspective to try and understand how MxA confers viral specificity across a wide range of viruses. They showed that the L4 loop has undergone significant positive selection and that a single amino acid change at position 561 in primate MxA was capable of altering the antiviral activity and specificity against both Thogoto Virus (THOV) and an avian influenza virus, suggesting that the L4 loop is a genetic determinant of MxA antiviral specificity (Mitchell et al. 2012). Following this, another position within the L4 loop has been shown to be important for the antiviral activity against both orthomyxoviruses and bunyaviruses. Mutations at position 561 or 562 abolished antiviral activity against both influenza and THOV, however this had no impact on the antiviral activity against LACV, yet a mutation at position 577 was shown to abolish antiviral activity against all 3 viruses leading to the suggestion that the proximal mutations in the L4 loop are specific to orthomyxoviruses whereas

the distal mutation at position 577 may have a conserved structural function (Patzina, Haller, and Kochs 2014).

### 1.8.2 MxB

Human MxB has two different isoforms, a long 78 kDa isoform and a shorter 76 kDa isoform. The 78 kDa isoform has a NLS sequence at the N-terminus of the protein, which appears to target the protein to nuclear pores. The translation of the shorter isoform starts from an alternative ATG at position 26 and is therefore lacking the NLS sequence and localised to the cytoplasm (Melén et al. 1996; King, Raposo, and Lemmon 2004).

Until recently, there was no known antiviral activity attributed to MxB despite being an IFN-inducible protein. MxB has since been shown to be a restriction factor for Human Immunodeficiency Virus (HIV-1), targeting the virus between reverse transcription and integration through an interaction with the viral capsid protein (Kane et al. 2013; Goujon et al. 2013; Z. Liu et al. 2013). Despite the large homology between MxA and MxB, the antiviral mechanism of MxB is highly distinct to that of MxA (X. Jia, Zhao, and Xiong 2015). It has been shown the long isoform is required for HIV-1 restriction and that this activity is independent of both oligomerisation and GTPase activity (Goujon et al. 2014; Fricke et al. 2014). The mechanism of action against HIV-1 is becoming clearer with the recent discovery that an RRR motif in the N-terminal end of MxB is required for binding of the viral capsid protein to MxB to exert its antiviral effect and not the nuclear localization determined by this region as previously thought (Schulte et al. 2015).

### 1.9 Influenza and MxA

MxA proteins have long been known for their ability to inhibit influenza viruses, however the mechanism of MxA's antiviral activity is not yet fully understood (Matzinger et al. 2013). Following cell entry, influenza imports vRNPs into the cell nucleus that leads to the activation of the viral RNA polymerases and the beginning of primary transcription. Murine Mx1 localises to the nucleus and blocks primary transcription likely through interacting with NP (Dittmann et al. 2008; Zimmermann et al. 2011). Human MxA is localised to the cytoplasm and therefore does not inhibit the primary transcription of influenza viruses like Mx1, instead human MxA is believed to inhibit a later stage in viral replication involved in genome amplification and secondary transcription. It has been suggested that MxA binds to newly translated NP and blocks it from entering into the nucleus to aid further rounds of transcription and genome replication (Zürcher, Pavlovic, and Staeheli 1992). Interestingly, a mutant form of MxA was produced to carry a foreign nuclear localization sequence, which resulted in re-localisation of MxA from the cytoplasm into the nucleus. This led to the MxA-mediated inhibition of influenza virus primary transcription, similar to that observed for murine Mx1 (Engelhardt et al. 2004; Zürcher, Pavlovic, and Staeheli 1992). This nuclear MxA variant was also shown to complex with NP whilst wt MxA was co-immunoprecipitated with NP, albeit under non-physiological cross-linking conditions (Turan et al. 2004). This suggested that these proteins both targeted the same viral protein or target structure (Dittmann et al. 2008).

It should also be noted that Mx1-mediated inhibition of influenza virus replication has been linked to the viral polymerase protein PB2. It was first shown that over-expression of the influenza polymerase complex could out-compete the inhibition by

Mx1 (T. Huang et al. 1992). This was followed by an experiment showing that it was the PB2 subunit, which could inhibit Mx1 when over-expressed (Stranden, Staeheli, and Pavlovic 1993). However, neither of these studies found a direct interaction suggesting that perhaps these two proteins are competing for a common target protein (Turan et al. 2004). Based on this observation Turan and colleagues looked at the possibility that MxA was interacting with the influenza virus polymerase complex, however they showed that PB2 over-expression only suppressed MxA to a small extent. The striking finding was the significant suppression of MxA inhibition by the over-expression of NP, showing that the antiviral effect of MxA against influenza virus is linked to NP through either direct or indirect interactions (Turan et al. 2004).

It has also been shown that subtypes and strains of influenza virus differ in their sensitivity to MxA inhibition. Dittmann et al., (2008) hypothesised that as the pathogenicity of different influenza virus strains can differ between hosts that it was possible that variation in their susceptibility to MxA inhibition could partially account for these differences in pathogenicity. They compared the sensitivity of various influenza strains to the antiviral effects of Mx1 and MxA and found some interesting differences. Firstly, it was clear that influenza viruses of avian origin were highly sensitive to Mx1 yet viruses from a human background were much less sensitive. Following re-assortments of components in a mini-replicon system it was clear that NP was the viral target structure for Mx1 as the exchange of other plasmids encoding for PB1, PB2 and PA did not show any significant change in Mx1 sensitivity. Interestingly, mini-replicon assays involving 1918 H1N1 ‘Spanish Flu’ was almost completely insensitive to inhibition by MxA, yet pathogenic avian strain H5N1 A/Vietnam/1203/04 replication was significantly inhibited by MxA. This suggested

that MxA is an important barrier blocking avian influenza viruses from infecting humans whilst also offering an insight of what may have contributed to the incredible virulence of 1918 "Spanish Flu" (Dittmann et al. 2008).

Evidence that influenza NP determined the sensitivity of a virus to Mx was strengthened further as Zimmermann and colleagues compared the 2009 pandemic strain H1N1 A/Hamburg/4/09 with the highly pathogenic avian H5N1 A/Thailand/1(KAN-1)/04 for their sensitivity to inhibition by MxA and Mx1. They found that both MxA and Mx1 significantly inhibited the H5N1 strain, whereas pandemic H1N1 was nearly insensitive and similarly to Dittmann et al., (2008) found upon substituting components of the viral polymerase that NP was the main target of MxA's antiviral effect. They also looked at this effect in vivo by producing re-assorted viruses containing the NP of H5N1 in a H1N1 background or vice versa. These viruses were then used to infect mice containing functional Mx1 and those mice infected with a virus containing the H5N1 NP survived, whereas those mice exposed to pandemic H1N1 NP succumbed to infection. This also suggested that NP is important to MxA sensitivity and also highlighted that human influenza viruses have evolved to encompass adaptive mutations to evade inhibition by MxA (Zimmermann et al. 2011).

Following on from this research, specific MxA resistant mutations have been identified in influenza NP (Mänz et al. 2013; Riegger et al. 2015). Manz et al, compared a recent MxA sensitive virus A/Thailand/1(KAN-1)/04 (H5N1) to the MxA resistant NP from pandemic H1N1 strains A/Brevig Mission/1/1918 (1918) and A/Hamburg/4/2009 and identified 5 key adaptive mutations which conferred for MxA

resistance at positions 16, 53, 100, 283 and 313. However, introducing these mutations into an MxA sensitive NP led to impaired viral growth in vitro (Mänz et al. 2013). Then the emergence of H7N9 in 2013 showed that this avian virus also encoded for a resistance mutation at position 52 which had been shown to compensate when other resistance mutations such as those at position 100, 183 and 313 were not present. The substitution of asparagine at position 52 for tyrosine led to the NP being more sensitive to MxA in a polymerase reconstitution assay, adding further weight to the hypothesis that MxA is a barrier to zoonotic transmission of avian influenza viruses (Riegger et al. 2015).

More recently, a study looking at how MxA expression affects influenza replication in IFN-treated primate cells has suggested that MxA may also have another mechanism to restrict influenza replication. Matzinger and colleagues looked to further previous work showing that MxA inhibits influenza A replication in mouse cells after primary transcription by determining the role of MxA in human influenza infection in primate cells. They found that pre-treating the cells with IFN before infection with human isolated viruses A/Memphis/7/01 and A/Wyoming/3/03 suppressed viral replication. Using siRNA to knockdown MxA expression in IFN treated cells released this suppression showing the importance of MxA to the control of influenza replication in primate cells. Following on from this, they used RT-PCR to look at the levels of influenza replication in naïve Vero cells and Vero cells which constitutively express MxA 8 hours after infection and found that the levels of all virus-specific RNA species were drastically suppressed, suggesting that MxA is capable of blocking influenza virus replication at a step prior to primary transcription (Matzinger et al. 2013).

Further evidence has confirmed that MxA exerts an antiviral effect prior to primary transcription. Xiao et al, (2013) showed that in the presence of IFN incoming viral genomes became trapped in the perinuclear region, unable to translocate to the nucleus for replication. They also went on to show that this block was dependent on MxA, although the over-expression of MxA was not enough to inhibit nuclear translocation, but also required pre-treatment with IFN, suggesting that an unknown IFN induced co-factor was also necessary for this antiviral effect of MxA (Xiao et al. 2013). However, how MxA exerts an antiviral effect so early during infection is still to be elucidated.

## 1.10 Aims of Thesis

It is well documented that the expression of MxA is tightly regulated by type I and III IFN signaling events and is one of the most highly inducible antiviral factors characterised to date (Holzinger et al. 2007). In fact MxA constitutes up to 1% of the total cytoplasmic proteins following induction via IFN (Horisberger 1992). MxA also has a wide antiviral spectrum, capable of targeting both RNA and DNA viruses (Sadler and Williams 2008). One of these targets is influenza viruses, yet the mechanism of antiviral activity against these viruses is still unknown.

MxA has been shown to inhibit influenza A viruses at two distinct stages of the viral replication cycle; during viral entry and following primary transcription of viral mRNAs. The antiviral effects of MxA during viral entry are highly dependent on IFN, however activity exerted after primary transcription can occur in the absence of IFN, suggesting two potentially different mechanisms of action. The aim of this thesis is to gain a better understanding of the functional characteristics required for MxA to exert its antiviral activity against influenza viruses at these two distinct stages of replication. Firstly this will be addressed using microscopy techniques to elucidate the nature of the IFN-dependent block in virus entry described by Xiao et al. (2013). Secondly mutational analysis will be used to determine the natural functions and characteristics of MxA responsible for antiviral activity in both the presence and absence of IFN. Finally this thesis will also investigate the impact of MxA against influenza B viruses and whether this strictly human pathogen harbours any natural resistance to the antiviral effect of MxA.

# Chapter 2 - Materials and Methods

## 2.1 Mammalian cell culture

### 2.1.1 Cell lines

Parental cell lines used in this study:

| Cell line | Origin |
|---|---|
| **293T** | Human embryonic kidney cells constitutively expressing Simian vacuolating virus (SV40) large T antigen. |
| **A549** | Human epithelial lung cells derived from a lung cell carcinoma. |
| **Calu-3** | Human epithelial lung cells derived from an adenocarcinoma (Kindly provided by Dr. J. Telford, University of St. Andrews). |
| **BEAS-2B** | Human epithelial bronchial cells transformed with an adenovirus 12-SV40 hybrid. (Kindly provided by Prof. R. E. Randall, University of St. Andrews) |
| **MDCK** | Madin-Darby canine epithelial kidney cells. |

The following cell lines were previously generated through lentiviral transduction and used in this study:

| Cell line | Origin |
|---|---|
| **A549/shMxA** | A549 cells which knock down the expression of IFN-induced GTPase, MxA (Kindly provided by Dr. D. Jackson) |
| **A549/MxA** | A549 cells which constitutively express the IFN-induced GTPase, MxA (Kindly provided by Dr. D. Jackson) |

The following cell lines were produced by lentivirus transduction for this study:

| Cell line | Origin |
|---|---|
| **A549/shMxA/wt wMxA** | A549/shMxA cells which constitutively overexpress wobble MxA (wMxA) wild-type |
| **A549/shMxA/R640A wMxA** | A549/shMxA cells which constitutively overexpress wMxA R640A mutant |
| **A549/shMxA/I376D wMxA** | A549/shMxA cells which constitutively overexpress wMxA I376D mutant |
| **A549/shMxA/T103A wMxA** | A549/shMxA cells which constitutively overexpress wMxA T103A mutant |
| **A549/shMxA/V268M wMxA** | A549/shMxA cells which constitutively overexpress wMxA V268M mutant |
| **A549/shMxA/G255E wMxA** | A549/shMxA cells which constitutively overexpress wMxA G255E mutant |
| **A549/shMxA/F561V wMxA** | A549/shMxA cells which constitutively overexpress wMxA F561V mutant |

| Cell line | Origin |
|---|---|
| **A549/shMxA/D478A wMxA** | A549/shMxA cells which constitutively overexpress wMxA D478A mutant |
| **A549/shMxA/KEKE wMxA** | A549/shMxA cells which constitutively overexpress wMxA KEKE mutant |
| **A549/shMxA/AKAK wMxA** | A549/shMxA cells which constitutively overexpress wMxA AKAK mutant |
| **MDCK/MxA** | MDCK cells which constitutively overexpress MxA |
| **A549/shMxA/GFP wMxA** | A549/shMxA cells which constitutively overexpress GFP-tagged wMxA |
| **A549/shMxA/GFP wMxA mRFP Rab 5** | A549/shMxA cells which constitutively overexpress GFP-tagged wMxA and mRFP-tagged Rab 5 |
| **A549/shMxA/GFP wMxA mRFP Rab7** | A549/shMxA cells which constitutively overexpress GFP-tagged wMxA and mRFP-tagged Rab 7 |
| **A549/GFP wMxA** | A549 cells which constitutively overexpress GFP-tagged wMxA |
| **A549/GFP wMxA mRFP Rab5** | A549 cells which constitutively overexpress GFP-tagged wMxA and mRFP-tagged Rab 5 |
| **A549/ GFP wMxA mRFP Rab7** | A549 cells which constitutively overexpress GFP-tagged wMxA and mRFP-tagged Rab 7 |

### 2.1.2 Cell maintenance

All cell lines were maintained in 25cm$^2$ or 75cm$^2$ flasks (Grenier) with Dulbecco's modified Eagle's medium (DMEM; Life Technologies) supplemented with 10% (v/v) heat inactivated foetal bovine serum (FBS; Life Technologies) and 500 units/mL Penicillin and Streptomycin (Life Technologies). Cells were incubated at 37 °C in a humidified incubator at 5% $CO_2$ and routinely passaged using trypsin/EDTA (Becton Dickinson Ltd.) at a frequency determined by the rate of cell growth.

### 2.1.3 Treatment of cells

#### 2.1.3.1 Interferon Treatment

Cells were treated using 1000 units/ml human recombinant interferon α-2a (IFNα-2a; Roferon; Roche Diagnostics) for at least 16 hours (unless stated otherwise) prior to viral infection.

#### 2.1.3.2 Transfection of plasmid DNA

Cells were transfected with plasmid DNA in suspension. Cells were detached using trypsin/EDTA and resuspended in antibiotic free DMEM/10% FBS and spun at 1000 rpm for 5 minutes. The supernatant was removed and cells were resuspended in an appropriate volume of antibiotic free DMEM/10% FBS before addition of plasmid DNA and transfection reagent FuGENE 6 (Promega) used following the manufacturer's instructions.

#### 2.1.3.3 Production of canine IFN from MDCK cells

To prepare conditioned media containing canine IFN, 100% confluent MDCK monolayers in 12-well plates were washed in PBS to remove any trace of serum. Cells were then inoculated at a high MOI of Sendai Virus in 300 µL serum-free DMEM and placed at 37 °C/5% $CO_2$ for 1 hour with gentle agitation at short intervals. Virus inoculum was removed, monolayers were washed with serum-free DMEM and 1 mL serum-free DMEM was added. Cells were then incubated at 37 °C/ 5% $CO_2$ for 18 hours. Supernatants were then harvested and cellular debris removed by centrifugation at 3000 rpm for 10 mins. Cleared supernatants were then filtered

through 0.45 μm membrane filters and aliquots were frozen at -80 °C. Prior to use, supernatants were UV-treated for 2 minutes to inactivate any live virus.

### 2.1.4 Generation of stable cell lines by lentiviral transduction

#### 2.1.4.1 Lentivirus production

HEK 293T cells were grown on 75 $cm^2$ flasks until approximately 70% confluent. Prior to transfection, antibiotics were removed from the media and cells were then transfected with 6 μg pCMVR8.91, 6 μg pVSVG and 10 μg of pdl plasmid containing the gene of interest using Lipofectamine 2000 (Invitrogen) following the manufacturer's instructions.

Lentivirus containing supernatant was harvested at 48 and 72 hours post transfection and cleared of cellular debris by centrifugation at 3000rpm for 10 minutes. The supernatant was then filtered through a 0.45 μm membrane filter and stored at -80 °C.

#### 2.1.4.2 Lentiviral transduction of mammalian cells

Parental cells were grown in 6-well plates (Grenier) until approximately 40% confluent. 1,5-dimethyl-1,5-diazaundecamethylene polymethobromide hexadimethrine bromide (Polybrene; Sigma Aldrich) was added to the lentivirus samples at a final concentration of 8 μg/ml and the target cells were transduced with the lentivirus supernatant (1.5 ml per well) for 2 hours before adding 1 mL DMEM/10% FBS and incubated for 48 hours.

Cells were then transferred to a 25 $cm^2$ tissue culture flask and cells expressing the transduced construct were selected using either puromycin (Melford) or blasticidin S (Melford) until control cells were dead. Cells were then passaged under selection with the exception of experimental procedures. The quality of each cell-line was assessed through Western Blot and Immunofluorescence analysis.

**2.1.4.3 Clonal selection**

Cells that showed heterogeneity in the expression of the protein of interest were then clonally selected to ensure a consistent level of expression by all cells. Cells that expressed green fluorescent protein (GFP) tagged MxA were sorted using Fluorescence activated Cell sorting (FACS), whereas cells that did not express a fluorescently tagged protein were sorted into 96 well plates so that only 1 cell was sorted per well, allowing for the growth of homogenous cell lines. The expression levels of selected colonies were assessed by immunofluorescence and immunoblotting as described below. FACS analysis was performed by Miss Claire Stewart.

## 2.2 Viruses and Viral Assays

### 2.2.1 Viruses used

**Influenza Viruses**

**rWSN**: Recombinant wild-type influenza A virus (A/WSN/33) generated and provided by Dr. D. Jackson (University of St Andrews).

**rUd**: Recombinant wild-type influenza A virus (A/Udorn/72) generated and provided by Dr. D. Jackson (University of St Andrews).

**rB/Yam**: Recombinant wild-type influenza B virus (B/Yamanashi/98) generated and provided by Dr. D. Jackson (University of St Andrews).

### 2.2.2 Virus infection

Virus preparations were diluted to an appropriate multiplicity of infection (MOI) in serum-free DMEM. The confluency and cell line used were dependent on the experimental design. Prior to infection cell monolayers were washed in Phosphate buffered Saline (PBS), (137 mM NaCl, 12 mM $Na_2HPO_4$, 2.7 mM KCl pH 7.4) to remove any trace of serum, virus dilutions were then added to the monolayer in an appropriate total volume for virus adsorption and incubated at 37 °C/5% $CO_2$ for one hour with gentle agitation at short intervals. The virus inoculum was then removed, and replaced with serum-free DMEM and incubated at 37 °C/5% $CO_2$ until the virus or cells were collected. The volumes used for virus infection were as follows: 300 µl for 12-well plate wells, 400 µl for 6-well plate wells, 1.5 mL for 25 $cm^2$ flasks 4 ml for 75 $cm^2$ flasks.

### 2.2.3 Virus stock preparation

To prepare influenza virus stocks, 100% confluent MDCK monolayers in 75 $cm^2$ flask were washed in PBS to remove any trace of serum. Cells were then inoculated at an MOI of approximately 0.001 in 4 mL serum-free DMEM and placed at 37 °C/5% $CO_2$ for 1 hour with gentle agitation at short intervals. Virus inoculum was removed, monolayers were washed with serum-free DMEM and 10 mL serum-free DMEM supplemented with 2.5μg/ml N-acetyl trypsin (NAT; Sigma) were added. Cells were then incubated at 37 °C/ 5% $CO_2$. Supernatants were harvested when 80-90% cytopathic effect (CPE) was observed (approximately 48-72 hours). Cell debris was removed by centrifugation at 3000 rpm for 10 mins. Cleared supernatants were then filtered through a 0.45 μm membrane filter and aliquots were frozen at -80 °C. Virus titers were determined by plaque assay as described below

### 2.2.4 Virus titration

Titration of influenza virus was carried out on confluent MDCK monolayers in 6-well plates. The procedure was carried out essentially as described elsewhere (Takeda et al., 2002). Virus titrations were carried out using 10-fold serial dilutions in serum-free DMEM, and then cells were washed in PBS in order to remove any traces of serum. Cells were inoculated with 400 μL of diluted virus preparation and incubated at 37 °C/5% $CO_2$ for 1 hour. The plates were gently agitated every 10 minutes to ensure even adsorption of the virus across the monolayers.

During this period, 2× overlay medium (13.4g DMEM, 3.7g $NaHCO_3$, 10mM HEPES pH 7.4, 1000 units/mL penicillin and streptomycin made up to 500 mL in distilled $H_2O$) supplemented with 2 μg/ml N-actetyl trypsin (NAT, Sigma) was incubated at

37°C. 2% agarose (NuSieve® GTG®) in water was melted in a microwave oven and placed in a 55°C water bath until required. After 1 hour, virus inoculum was removed and the 2× overlay medium and the 2% agarose were mixed in a 1:1 ratio, and 2 mL of this overlay mixture was added to each well. After the overlay had solidified, plates were inverted and incubated at 37°C with 5% CO2 until distinct plaques had formed (approximately 48 hours for influenza A virus, 72 hours for influenza B virus). Cells were fixed by adding 2 mL 5% formaldehyde/PBS on top of the agarose plugs for 1 hour at room temperature. Agarose plugs were then removed and washed with PBS, the monolayer was then stained with crystal violet (0.1% crystal violet, 8% formaldehyde, 20% methanol in PBS) to visualise the plaques or plaques were visualised by immunostaining as described below.

Virus titration using A549 cells were carried out as above until the removal of viral inoculum. Following the removal of viral inoculum the 2× overlay medium was mixed in a 1:1 ratio with 2% low-melting point agarose (Lonza SeaPlaque ® Agarose) and 2 mL of this overlay mixture was added to each well. After the overlay had solidified, plates were inverted and incubated at 37°C incubator with 5% CO2 for 5 days. Cells were fixed by adding 2 mL 5% formaldehyde/PBS on top of the agarose plugs for one hour at room temperature. Agarose plugs were then removed and washed with PBS, plaques were then visualised by immunostaining as described below.

### 2.2.5 Virus Yield Assay

To determine viral growth kinetics from individual experiments, confluent cell monolayers grown in 6-well plates were inoculated with virus at a MOI indicated for individual experiments. Following an adsorption period of 1 hour the inoculum was removed and 1.5 mL Serum Free DMEM supplemented 50 units/mL Penicillin and Streptomycin was added to each well. Cells were then incubated at 37 °C / 5% CO2 in a humidified incubator. Virus samples were harvested by removing the supernatant at various times post- infection and frozen at -80 °C. Virus titre was then determined by plaque assay on MDCK cells as described above.

### 2.2.6 Virus Input Assay

Cells were seeded into 12-well plates (nunc) containing coverslips 2 days before the experiment at a very low density aiming to be approximately 50% confluent for infection. After 24 hours, cells were treated with IFN (Roferon; Roche Diagnostics) for at least 16 hours before infection. Cells were washed in PBS to remove any trace of serum. Virus preparations were diluted to an appropriate MOI to allow detection of incoming virus particles via immunofluorescence without overloading the IFN system. Coverslips were placed on 12-well plate lids covered in parafilm and inoculated with 50 µL of diluted virus, covered and incubated for 30 minutes at 37 °C/5% $CO_2$. Coverslips were then washed in PBS followed by a citric acid wash (40mM Citric Acid, 10mM KCl and 135mM NaCl; pH 3.0) to remove any virus bound to the surface, followed by another wash in PBS. Cells were then placed back in 12-well plates with serum-free DMEM and cyclohexamide to block translation of any nascent protein. The cells were then incubated for 2-3 hours at 37 °C/5% $CO_2$.

Media was then removed from the wells and the cells fixed using 5% formaldehyde/PBS for 20 minutes before being replaced with PBS. Cells were then stored at 4 °C until analysis via immunofluorescence.

## 2.3 Molecular Biology

### 2.3.1 Polymerase Chain Reaction (PCR)

To amplify genes of interest PCR was carried out using polymerase enzymes either with proof-reading capability; PFU (Promega), Phusion (Thermo Scientific) and Q5 (New England Biolabs), or without proof-reading ability, Taq (Promega), depending on the purpose of the reaction. Reactions were performed to the manufacturer's instructions. Briefly, reactions were set up in a total volume of 30 or 50 μL containing enzyme buffer (at appropriate dilution), 200-300 μM of each dNTP, 3 Dimethyl Sulfoxide (DMSO; Thermo Scientific), between 10-50 ng of DNA template (dependent on polymerase used), gene specific forward and reverse primers at 1-1.5 μM (varied with polymerase used) and polymerase (unit definition depending on manufacturer) in sterile water.

Reactions were performed using thermocyclers with a general setting of initial denaturing step at 95-98 °C (varies with enzyme used), followed by 30 cycles of denaturing 95°C for 30 seconds, annealing 50-65 °C for 30 seconds and extension of DNA primer strands at 72 °C for as long as required for the polymerase to replicate the gene of interest, with a final extension step for 10 minutes at the same temperature.

### 2.3.2 Agarose Gel Electrophoresis

DNA samples were analysed by gel electrophoresis in gels of 1 – 1.5% (w/v) agarose (HydraGene) in TBE buffer (89 mM Tris, 89 mM Boric Acid and 2 mM EDTA) and ethidium bromide (1 μg/ml; Promega). Prior to loading of DNA samples, 6x-loading

buffer (Promega) was added to the samples at appropriate volume. Samples were resolved on agarose gels at 90 V in TBE buffer. For comparison, a DNA marker with known DNA size fragments (1 kb ladder; Promega) was loaded onto the gel. DNA was visualised on an ultra-violet transilluminator. If required DNA samples were excised from the gel and DNA was recovered using the GenElute Gel Extraction kit (Sigma Aldrich).

### 2.3.3 Restriction Enzyme Digestion

All restriction digests were carried out using enzymes from Promega and performed to the manufacturer's instructions. Typically, 3-4 μg of plasmid DNA or purified PCR product were digested in 20 reactions containing reaction buffer, 1 mg/ml acetylated BSA (Promega) and 5 units of the desired restriction enzyme were used per reaction at 37 °C for 3 hours. When a single enzyme was used for digestion of plasmid DNA to create cohesive ends for ligation, Calf intestinal Alkaline Phosphatase (CIAP, Promega) was added into reaction tube following digestion for 30 minutes to prevent vector self-ligation.

### 2.3.4 Ligation of DNA

DNA samples purified following restriction digest and gel purification were then used for ligation. Approximately 50 ng of vector backbone was mixed 1:3 (molar ratio) with insert, 1 μL of 10x T4 DNA ligase buffer and 0.2 μL T4 ligase (Thermo Scientific) was added to the mix and the total volume was adjusted to 10 μL in sterile water. The sample was incubated at room temperature for 30 minutes. The ligation mix was used to transform into competent *E. coli* DH5α cells as described below at a ratio of 1:10 (v/v).

### 2.3.5 Transformation of competent cells

Plasmid DNA was diluted to a suitable concentration and approximately 5 ng was added directly to 50 µL of thawed, *E. coli* DH5α chemically competent cells for plasmid propagation or *E. coli* Rosetta competent cells for protein expression. The plasmid-cell mix was incubated on ice for 30 min before being transferred to a 42 °C water bath for 45 seconds. Cells were then placed back on ice for 2 minutes, mixed with 250 µL SOC media (20 g bacto-tryptone, 5 g bacto-yeast extract, 0.5 g NaCl and 2.5 mL 1 M KCl adjusted to pH7.0 using NaOH to 1 L total volume followed by the addition of 20 mL 1 M glucose) and allowed to recover at 37 °C for 1 hour in a shaking incubator. Cells were then plated onto LB-agar plates supplemented with either ampicillin or kanamycin, plates inverted and incubated at 37 °C overnight. Individual colonies were picked for mini-cultures.

### 2.3.6 Preparation of plasmid DNA

For small-scale preparations of DNA, individual bacterial colonies were placed in 10 mL LB broth were supplemented with either ampicillin (50 µg/ml) or kanamycin (25 µg/ml) and incubated at 37 °C in a shaking incubator overnight. 5 mL of the bacterial culture was pelleted at 4000 rpm by centrifugation and plasmid DNA was extracted using the GenElute Plasmid Miniprep kit (Sigma Aldrich), according to the manufacturer's instructions. For large-scale DNA preparations 500 mL bacterial cultures in LB broth supplemented with either ampicillin or kanamycin were prepared and incubated at 37 °C in a shaking incubator overnight. The cells were pelleted by centrifugation and DNA was subsequently extracted using QIAfilter Plasmid Maxi kit (QIAGEN), according to the manufacturer's protocol. DNA concentration and quality

was assessed using a NanoDrop 1000 (LabTech) spectrophotometer. Plasmids were then sequenced at DNA Sequencing & Services, University of Dundee, to determine they were correct before use in experimentation.

## 2.4 Protein Analysis

### 2.4.1 SDS polyacrylamide gel electrophoresis

Protein samples were prepared for SDS-PAGE analysis in either 2x disruption buffer (4.2% (w/v) Sodium dodecyl sulphate, 2 M 2-Mercaptoethanol, 10 M Urea and bromophenol blue) and stored at -20 °C. The viscosity of the samples was reduced by sonication, then samples were heated to 100 °C for 5 minutes before loading onto the gel. Proteins were separated on 10, 12 or 15% polyacrylamide gels (30%:1; Sigma Aldrich?) at 180 V using Tris-Glycine running buffer (25 mM Tris and 190 mM glycine) until necessary separation was achieved. Gels were then either stained with Coomassie stain (0.5% (w/v) G250 Coomassie Blue (BDH Chemicals), 40% (v/v) methanol, 10% acetic acid) or the presence of specific proteins was determined through immunoblotting.

### 2.4.2 Immunoblotting

Following SDS PAGE, protein lysates were transferred to Polyvinylidene difluoride (PVDF; Millipore) membrane following membrane activation with 100% Methanol. Protein was transferred to the membrane by using the Trans-Blot Turbo Transfer System (Biorad) according to manufacturer's protocols. Following transfer, membranes were blocked for 1 hour (room temperature) in blocking buffer (5% (w/v) skimmed milk powder, in PBS). Then membranes were incubated for either 1 hour at room temperature or overnight at 4 °C with primary antibody diluted in 5% (w/v) skimmed milk powder, 0.1% (v/v) Tween 20 in PBS, the antibody was diluted according to the manufacturer's instructions. After incubation with primary antibody, membranes were washed several times with PBS-T (PBS, 0.1% (v/v) Tween 20) on a shaking platform. Membranes were then incubated with a IRDye 680/800-conjugated

secondary antibody (Licor), using a species raised against the primary antibody, in 5% (w/v) skimmed milk powder in PBS-T at room temperature for 1 hour followed by repeated washes in PBS-T. Probed proteins were subsequently detected using the Odyssey CLx Imaging System (Licor).

### 2.4.3 Immunofluorescence

Cells were grown on either 10 or 15 mm cover slips (Fisher Scientific). At the desired time cells were fixed using 5% (v/v) paraformaldehyde/PBS for 30 minutes followed by permeabilisation (10% (w/v) sucrose, 0.5% (v/v) Igepal, 0.5% (v/v) Triton X-100 in PBS) for 30 minutes. To block free aldehyde groups the cells were incubated with 100 mM glycine in PBS for 30 minutes before blocking non-specific binding sites with PBN, 1% BSA (Melford), 0.02% (w/v) sodium azide (Sigma Aldrich) in PBS for 1 hour. After the blocking steps, cells were incubated with primary antibody diluted in PBN for 1 hour, at a dilution recommended by the manufacturer. Coverslips were then washed with PBN before incubating the cells with Alexa Fluor (488 or 594, Life Technologies) conjugated antibody and 4', 6-diamidino-2-phenylindole (DAPI; 0.5 μg/ml; Sigma Aldrich) to stain nuclei for 1 hour. After washing unbound antibody with PBN coverslips were mounted onto glass slides with Fluoprep (Biomerieux) that was supplemented with 3% (v/v) 1,4-diazabicyclo[2.2.2]octane (DABCO; Sigma Aldrich). Images were taken using a Zeiss Axioplan 2, Deltavision or a Zeiss Pascal 500 confocal microscope**.**

### 2.4.4 Tandem Affinity Purification

293T cells transfected with 9 ug pcDNA TAP-empty, TAP-wMxA wt or TAP-wMxA T103A constructs were washed in PBS and removed from a 75 $cm^2$ flask using 10 mM EDTA in PBS. Cells were then resuspended in 250 µL TRIS-lysis buffer (50 mM TRIS-HCL pH 8.0, 100 mM NaCl, 25% (v/v) Glycerol, 0.5% (v/v) Igepal, Protease inhibitors (Roche)) and stored at -20 °C**.** Cell lysates were then thawed and sonicated to disrupt cellular membranes. Following sonication, cell lysates were centrifuged at 12, 000 rpm for 2 minutes. Then 20 µL of protein A beads were washed by inversion using IgG wash buffer (10 mM TRIS-HCL pH 8.0, 150 mM NaCl, 0.1% (v/v) Igepal, Protease inhibitors (Roche)) and centrifuged at 1, 000 rpm and the supernatant then removed. 200 µL of cell lysate was added to the protein A beads and made up to 1 mL with sterile water and NaCl to match the NaCl concentration in the IgG wash buffer. The beads were then incubated with the cell lysates rotating overnight at 4 °C**.** The samples were the centrifuged at 1, 000 rpm for 5 minutes, the supernatant carefully removed and replaced with 1 mL of ice-cold IgG wash buffer. The beads were washed a further 3 times before the samples are eluted using 100 mM acidified glycine (pH 3.0). Disruption buffer was then added to the eluate for analysis through SDS-PAGE, immunoblotting and Mass Spectrometry.

## 2.5 Miscellaneous Assays

### 2.5.1 Mini-Replicon (Luciferase)

293T cells in 12-well plates were transfected with 10 ng of pcDNA plasmids that express PB1, PB2, and PA, 100 ng of pcDNA-NP for A/Udorn/72, alongside 200 ng pCAGGS MxA or wobble MxA (wild type or mutants) plus 250 ng of pHH-ANSren, this plasmid expresses Renilla luciferase, which is flanked by the non-coding regions of the influenza A NS segment and used as a read-out for polymerase activity. These plasmids are transfected alongside 10 ng of pCMV-FF (which expresses firefly luciferase under the control of the cytomegalovirus [CMV] promoter used to normalize variations in transfection efficiency).

To analyse the luciferase activity of H5N1 A/KAN-1/2009 293T cells in 12-well plates were transfected with 10 ng of pCAGGS plasmids that express PB1, PB2, and PA, 100 ng of pCAGGS NP, alongside 200 ng pCAGGS MxA or wobble MxA (wild type or mutants) plus 250 ng of pHH-ANSren, and 10 ng of pCMV-FF.

For influenza B polymerase activity 293T cells in 12-well plates were transfected with 10 ng of pCI plasmids that express PB1, PB2, and PA, 100 ng of pCI NP for B/Pan/90, alongside 200 ng pCAGGS wobble MxA (wild type or mutants) plus 250 ng of pHH-BNSren, which is flanked by the non-coding regions of the influenza B NS segment and used as a read-out for polymerase activity, and 10 ng of pCMV-FF.

Twenty-four hours post-transfection, cells were lysed and firefly and renilla luciferase activities were measured using a dual-luciferase reporter assay (Promega). Results represent averages from three independent experiments ± SD.

### 2.5.2 Sample Preparation for Transmission Electron Microscopy

Following a virus input assay (described above) cells were fixed in 0.5% glutaraldehyde in PBS for 15 minutes before scraping the cells from the culture flask in a small volume of the fixative. The cells were then pelleted (16, 000 x g for 15 minutes) in an 1.5 ml Eppendorf tube, washed 3 times in 100 mM sodium cacodylate buffer (pH 7.2) followed by postfixation for 1.5 h in 1% osmium tetraoxide in 0.1 M sodium cacodylate reduced with 1.5% w/v potassium ferrocyanide to improve membrane contrast. Samples were subsequently washed 3 times with de-ionized MilliQ water and the cell pellet then underwent dehydration through a series of washes in increasing concentrations of ethanol (10 minutes per ethanol step), starting at 50% and finishing with 2 washes in 100% ethanol and 2 final washes in propylene oxide (15 minutes each). The propylene oxide was removed and replaced with an epoxy-propylene oxide mixture (1:1) and incubated, rotating overnight at room temperature. The pellet was then removed from the overnight incubation mix, blotted on filter paper and cut into smaller fragments prior to embedding in fresh epoxy resin. The embedded expoxy pellet was then baked at 65 °C for 24 hours or until the epoxy block had solidified. The embedded pellet was then mounted into an ultra-microtome (Reichert-Jung Ultracut) and a diamond knife is used to cut ultrathin sections (80 nm), which were collected onto pioloform-coated EM copper grids (Agar Scientific, Stansted, UK) for staining. To increase membrane contrast the sections were stained for 10 minutes using lead citrate (according to Reynolds, 1963), washed several times in MilliQ water, followed by staining with 3% w/v uranyl acetate for 5 minutes to increase protein contrast. The grids were subsequently washed several times in MilliQ water before air-drying. Sections were imaged using a JEOL 1200 EX transmission

electron microscope at 80kV and images taken with a Gatan Orius 200 digital camera (Gatan, Abingdon Oxon).

### 2.5.3 Lipid Extraction

Total lipids from various treated A549 cells were extracted based upon a slightly modified Bligh-Dyer method. Briefly, cells from confluent 25 $cm^2$ flasks were washed in PBS and suspended in 100 µL PBS and transferred to a glass tube, 375 µL of 1:2 (v/v) $CHCl_3$: MeOH added and vortexed. The samples were agitated vigorously for a further 10-15min. The samples were made biphasic by the addition of 125 µL of $CHCl_3$, vortexed, 125 ul of $H_2O$ added, vortexed again and centrifuged at 1000 g at RT for 5 min. The resultant lower phase lipid extract was transferred to a new tube, dried under nitrogen and stored at 4 °C, until analysis.

### 2.5.4 Electrospray-mass spectrometry analysis

Lipid extracts, were dissolved in 15 µL of choloroform:methanol (1:2) and 15 µL of acetonitrile:isopropanol:water (6:7:2) and analysed with a Absceix 4000 QTrap, a triple quadrupole mass spectrometer equipped with a nanoelectrospray source. Samples were delivered using a Nanomate interface in direct infusion mode (~125 nl/min). The lipid extracts were analysed in both positive and negative ion modes using a capillary voltage of 1.25 kV. MS/MS scanning (daughter, precursor and neutral loss scans) were performed using nitrogen as the collision gas with collision energies between 35-90 V. Each spectrum encompassed at least 50 repetitive scans. Tandem mass spectra (MS/MS) were obtained with collision energies between 35-90 V. Assignment of phospholipid and neutral lipid species was based upon a combination of survey, daughter, precursor and neutral loss scans. The identity of

phospholipid peaks was verified using the LIPID MAPS: Nature Lipidomics Gateway (www.lipidmaps.org).

## 2.6 Antibodies used

| Antibody | Species | Source | Dilution in Assay |
|---|---|---|---|
| **α-Actin** | Mouse | Sigma | 1:10000 (WB) |
| **α-Hong Kong/73** | Rabbit | Kind gift from by Prof. R. E. Randall, University of St. Andrews | 1:1000 (WB) |
| **α-Influenza A NP** | Mouse | Abcam | 1:200 (IF) |
| **α-Influenza B NP** | Mouse | Abcam | 1:200 (IF) |
| **α-MxA** | Rabbit | Santa Cruz | 1:50 (IF)<br>1:500 (WB) |
| **α-X-31** | Sheep | Diagnostics Scotland | 1:1000 (WB) |
| **IRDye® 800CW α-Mouse** | Goat | Licor | 1:20000 (WB) |
| **IRDye® 680RD α-Rabbit** | Goat | Licor | 1:20000 (WB) |
| **IRDye® 680RD α-Goat** | Donkey | Licor | 1:20000 (WB) |
| **Texas Red-conjugated α-Mouse** | Goat | Abcam | 1:200 (IF) |
| **Texas Red-conjugated α-Rabbit** | Goat | Abcam | 1:200 (IF) |
| **Alex Fluor® 488 α-Rabbit** | Goat | Life Technologies | 1:400 (IF) |

**Table 2.1Table of Antibodies**

## Chapter 3 – The impact of interferon and MxA on influenza virus infection

### 3. Introduction

The interferon response is the initial host barrier to viral infection, as described in section 1.1. The interactions between influenza A virus and components of the IFN response has been well studied, defining the multi-functional NS1 protein as the main IFN antagonist as well as roles for other viral proteins such as PB2, PB1-F2, and NP in regulating the host response to influenza virus infection. More recently a number of studies have been focusing on the impact of IFN on viral entry, and the impact this has on viruses that are entering cells already primed by IFN.

For example, cholesterol-25-hydroxylase (CH25H) is an ISG which was identified by two different groups to have antiviral activity in the early stages of infection (S.-Y. Liu et al. 2013; Blanc et al. 2013). CH25H is an enzyme that oxidises cholesterol to produce 25-hydroxycholesterol (25HC) a metabolite that has been shown to have an important role in lipid biosynthesis and metabolism as well as immunity (Wilkins and Gale 2013). Both groups identified this metabolite to have antiviral properties with Blanc et al, showing the impact of 25HC against murine cytomegalovirus (MCMV) as well as a range of other viruses including influenza A virus and herpes simplex virus 1 (HSV-1). It was suggested that the mechanism of action against MCMV was functional during DNA replication, differing from the impact on HSV-1, where 25HC inhibited viral entry (Blanc et al. 2013). This corroborated the results of Liu et al, who showed CH25H could have a broad-spectrum antiviral effect on a number of different enveloped viruses such as HSV-1, HIV-1, ebola virus and Rift Valley fever virus

among others, and provided evidence that 25HC inhibited virus infection through blocking viral fusion with host lipid membranes (S.-Y. Liu et al. 2013).

This section looks to investigate the effect of interferon on viral entry as well as the IFN-induced block of influenza genome translocation as described by Xiao et al. 2013, using electron microscopy. Secondly, this section explores the impact of the interferon stimulated GTPase MxA upon early influenza infection, both in the presence and absence of interferon. Lastly this section explores the influence of IFN treatment and MxA expression on the overall cellular lipid composition of human lung adenocarcinoma A549 cells.

### 3.1 Impact on virus entry

Previous work has shown that when cells are pre-treated with IFN, influenza virus is only capable of generating a productive infection in a subset of cells, dependent on the multiplicity of infection (MOI) (Xiao et al., 2013). At an MOI of 5, where all naïve cells were positive for viral antigen only 20% of cells pre-treated with IFN showed signs of a productive infection, and even when the MOI was increased to 50 the number of cells positive in the IFN-treated condition only reached 52%, indicating that the level of IFN-mediated protection was dependent on the amount of incoming virus particles and that influenza A virus was capable of overcoming the block through overwhelming the cellular response (Xiao et al. 2013). However, following the publication on the impact of ISG CH25H (S.-Y. Liu et al. 2013), and the broad-spectrum antiviral activity against enveloped virus offered another potential mechanism alongside the intracellular-acting ISGs such as IFITM3 and MxA(Feeley et al. 2011; Matzinger et al. 2013), for the low levels of influenza positive IFN treated cells as described by Xiao et al. (2013).

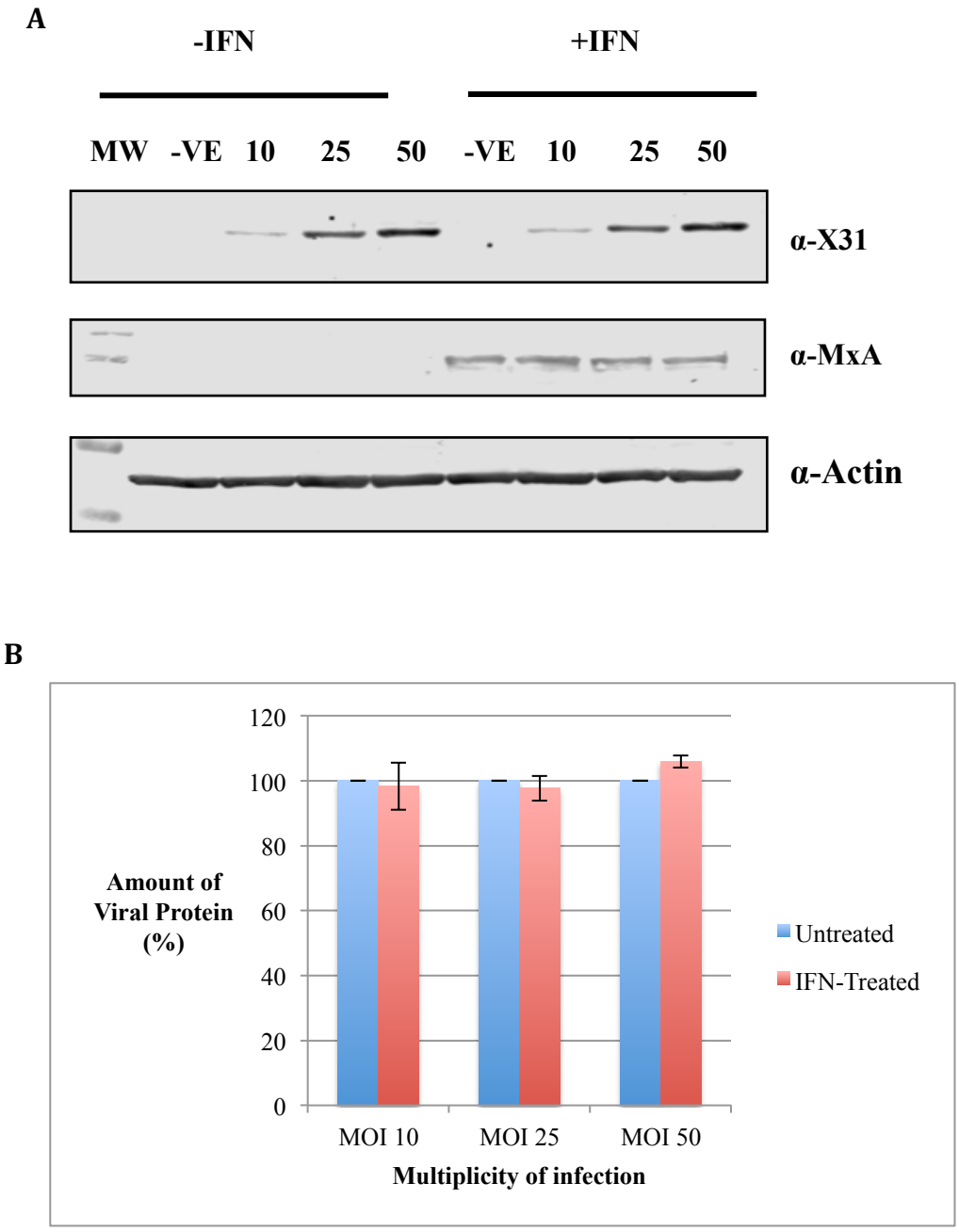


**Figure 3.1: Impact of IFN on Viral Entry. (A)** Immunoblot showing the level of virus endocytosed either in the absence or presence of IFN at increasing MOI following 1 h adsorption. Influenza NP was detected using a sheep anti-X31 antibody, MxA detection using a rabbit anti-MxA antibody acted as a control for induction of the IFN-induced antiviral state and actin was detected as a loading control. **(B)** Quantification of endocytosed viral protein normalised against actin levels. Results are shown as a percentage of viral protein in untreated A549 cells at each MOI and are the average of three independent experiments ± S.D.

The propensity for influenza virus entry in A549 cells with and without IFN pre-treatment was assed through quantitative western blot and plaque assay. A549 cells were either left untreated or pre-treated with 1000 units/mL IFN-α for 16 hours prior to infection. Cells were then infected with influenza A/Udorn/72 at a range of different MOIs for 1 hour, allowing for virus adsorption, with any excess virus removed using a citric acid wash. The cells were infected in the presence of cyclohexamide to ensure that any viral protein present was from input virus and not from early rounds of viral protein translation. Pre-treatment with IFN appeared to have no impact on the ability of influenza A virus to enter the cell. At MOIs of 10, 25 and 50 there is a negligible difference in the amount of viral antigen found in the cell whether they had been treated with IFN or not (Fig. 3.1). To further address whether IFN treatment prevented viral infection, A549 cells were either pre-treated with IFN or left untreated prior to infection with influenza A/Udorn/72 at an MOI 10. Following adsorption, the viral inoculum was removed from the cells, the concentration of virus remaining in the inoculum was determined by plaque assay and the titre was compared to that of the initial inoculum. In both IFN-treated and untreated conditions approximately 16% of the initial viral inoculum was not endocytosed by the A549 cells, suggesting that IFN pre-treatment has no impact on the initial stages of influenza virus entry (Fig. 3.2).

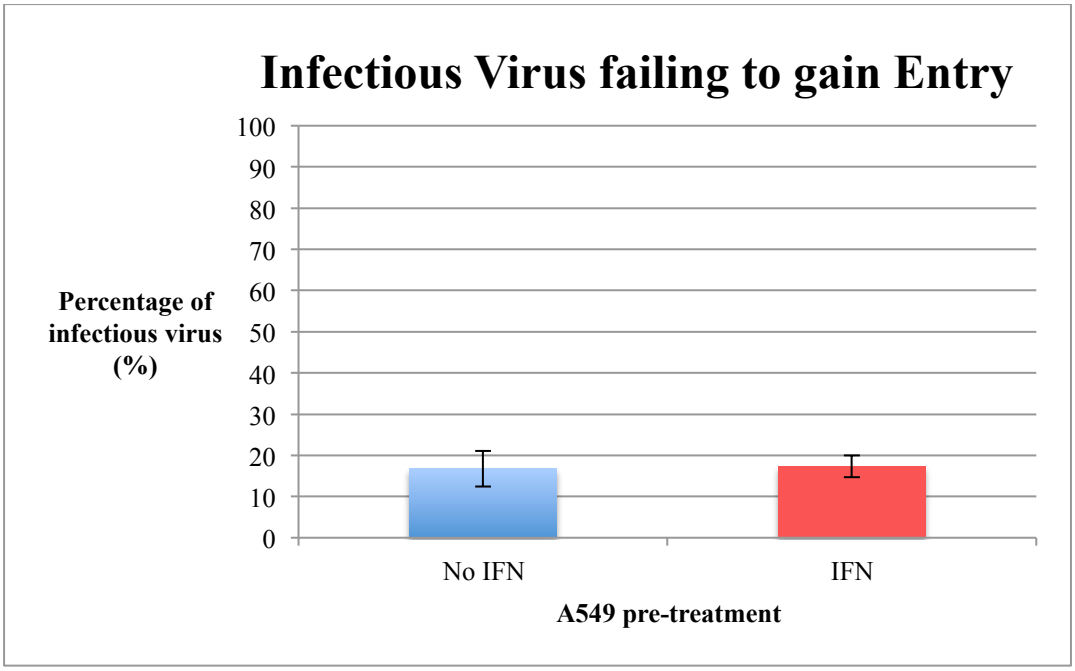


**Figure 3.2: Impact of IFN on Viral Entry.** A549 cells were either untreated or pre-treated with 1000 U/mL IFN-a for 16 h prior to infection with A/Udorn/72 at an MOI of 10. Following one hour adsorption, the viral inoculum was removed and the concentration of virus remaining in the inoculum was determined by plaque assay. The results show the concentration of infectious virus in the removed inoculum as a percentage of that used to infect the cells and represent the average of three independent experiments ± S.D.

### 3.2 Electron Microscopy analysis of the IFN-induced block in influenza genome nuclear translocation

The work of Xiao et al, (2013) showed that in cells pre-treated with IFN, influenza A virus genome was incapable of translocating to the nucleus, but instead was caught in the perinuclear region following endocytosis. They showed that this block was not only dependent on IFN but was also dependent on the presence of MxA (Xiao et al. 2013). To study this block in more detail it was first necessary to replicate this data using the viral input assay. An immunofluorescence-based infection assay in which a large MOI is used to infect cells in the presence of cycloheximide to inhibit any translation of mRNAs, thereby allowing one to visualise protein present in the input virions.

Figure 3.3 shows an example of an input assay using H1N1 influenza A/WSN/1933 (WSN). A549 cells were either untreated or pre-treated with 1000 units IFN for 16 hours prior to infection. The cells were then infected at a high MOI and incubated at 37°C for 3 hours, allowing sufficient time for the incoming viral genomes to translocate to the nucleus. In the untreated A549 cells there was a distinct nuclear staining for influenza NP. However, in the IFN treated cells, indicated by the cytoplasmic staining of MxA, the NP had a punctate pattern with the virus appearing to be stuck in the cytoplasm, often in the perinuclear region, corroborating with the results of Xiao et al, 2013.

Although it is clear that the incoming virus is blocked within the cytoplasm, it is not known at which stage during viral entry this block is taking place. In an attempt to get a clearer understanding of the IFN-mediated block on influenza nuclear translocation

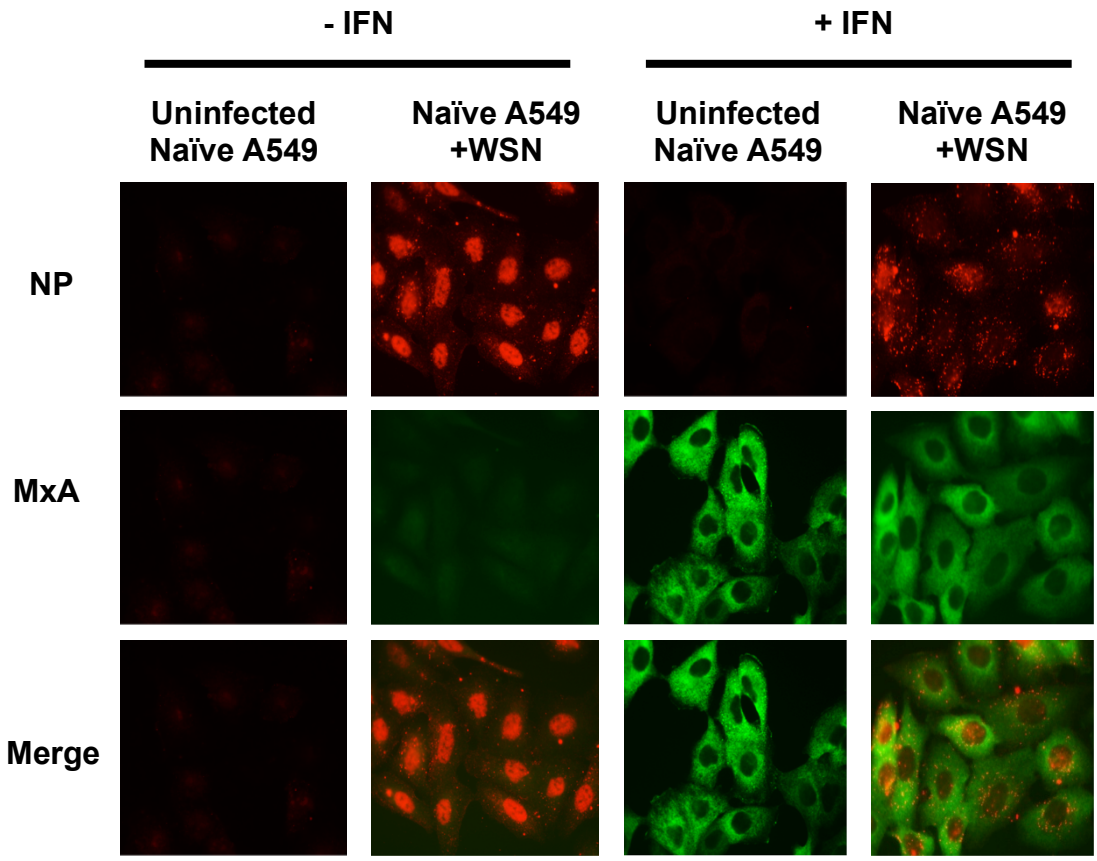


**Figure 3.3 Immunofluorescene of viral input assay.** Immunofluorescent staining of A549 cells 3 hours post-infection (h.p.i.) with WSN at an MOI of approximately 500 in the presence of cycloheximide. Interferon treatment was administered 16 hours prior to infection. Cells were fixed and probed with an α-influenza A NP monoclonal mouse antibody and an α-MxA polyclonal rabbit antibody then Texas red conjugated goat α-mouse and Alexa-488 conjugated goat α-rabbit. Red = NP, green = MxA.

the same assay was used but rather than use immunofluorescence the cells were processed for analysis by Transmission Electron Microscopy (TEM). As before, the same conditions as used in the immunofluorescence assay were used for analysis by TEM looking at infected and uninfected cells either in the absence or presence of IFN.

Figure 3.4 shows WSN-infected cells that have been pre-treated with IFN. The initial analysis showed that virus-infected, IFN treated cells appeared to have a large number of highly ordered, membranous structures located in the cytoplasm, often localizing to the perinuclear region. Panels A and B show two different micrographs at 4000x magnification containing these large multi-vesicular structures which are ranging between 300-1000 nm in diameter. Panels C and D show higher magnification cross-sections of these multi-membranous structures containing ultrastructure which could be indicative of a typical influenza virion when viewed under TEM, showing a clear lipid membrane and a fuzzy outer-layer, which would be indicative of the external glycoproteins. In both C and D the potential virion-like particle is located within a highly ordered membranous structure and after measuring the size of the particle in panel C it is approximately 100 nm in diameter, which fits with the biophysical characterisation of spherical influenza particles, which range between 80-150 nm in diameter. However, panel D has 2 potential virion structures, showing the same ultra-structure as seen in panel C, yet the size of the structures are much smaller in size. This could be because due to the nature of the cross-section, as the samples were sectioned into 80 nm slices and due to the random sampling the section could cut at any point through the 80-150 nm spherical virion. Therefore the size of the section we see may give a false representation as to the size of the 3D structure.

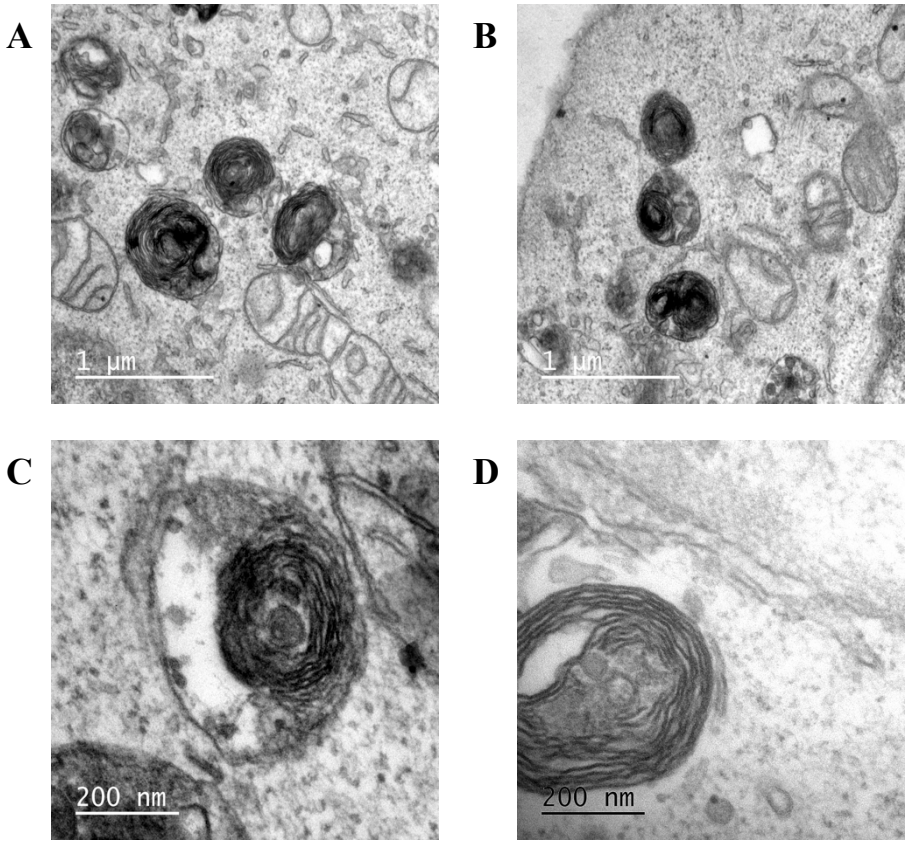


**Figure 3.4. Electron Micrograph of influenza WSN-infected cells post-IFN treatment.** IFN treated A549 cells were infected with WSN in an input assay as described above. After fixation the cells were sectioned under conventional EM conditions and stained using lead citrate and uranyl acetate. Panels A and B are at a magnification of 4000x. Panels C and D are at a magnification of 15000x. Panels A and B each show highly membranous structures in the perinuclear region in close proximity to mitochondria. Panels C and D are a higher magnification image of a multi-lamellar structure, potentially containing an influenza virion.

Following a review of the literature, it appears that these structures seen in Fig 3.4 are the cause of some controversy in the field, often being described as part of two different pathways, which culminate in degradation, by the lysosome. The structures fit the description of late endosomes becoming lysosomes or endolysomes, which typically exhibit multi-lamellar and multi-vesicular structures, typically found in the perinuclear region as well as fitting in the described size range of 250-1000 nm in diameter (Huotari and Helenius 2011). However, they also appear to fit the description of multi-lamellar autophagosomes, which are organelles that are induced to capture proteins, other damaged organelles and incoming pathogens producing multi-lamellar structures before fusing with the lysosome (Lai et al. 2007; Hernandez et al. 2003). Also, in each of these images it is interesting to note that these structures appear to be forming in close proximity to mitochondria, which also fits the criteria for autophagosomes (Hamasaki et al. 2013). Interestingly, autophagy has recently been shown to be involved in the degradation of Sindbis virus nucleocapsids, leading to suggestions that selective autophagy of incoming pathogens, such as viruses, is used as a defensive strategy by the host (Orvedahl et al. 2010; Dong and Levine 2013).

Figure 3.5 shows uninfected A549 cells that have been either untreated or pre-treated with IFN. The micrographs show that multi-lamellar structures observed in the WSN infected and IFN treated cells are also visible in the uninfected cells with and without IFN treatment. Similarly, as seen in the virus-infected cells, the multi-lamellar structures are also forming in the perinculear region in close proximity to mitochondria. It was not surprising to find that these structures are also present in both uninfected and untreated cells as it is likely to be a common cellular process

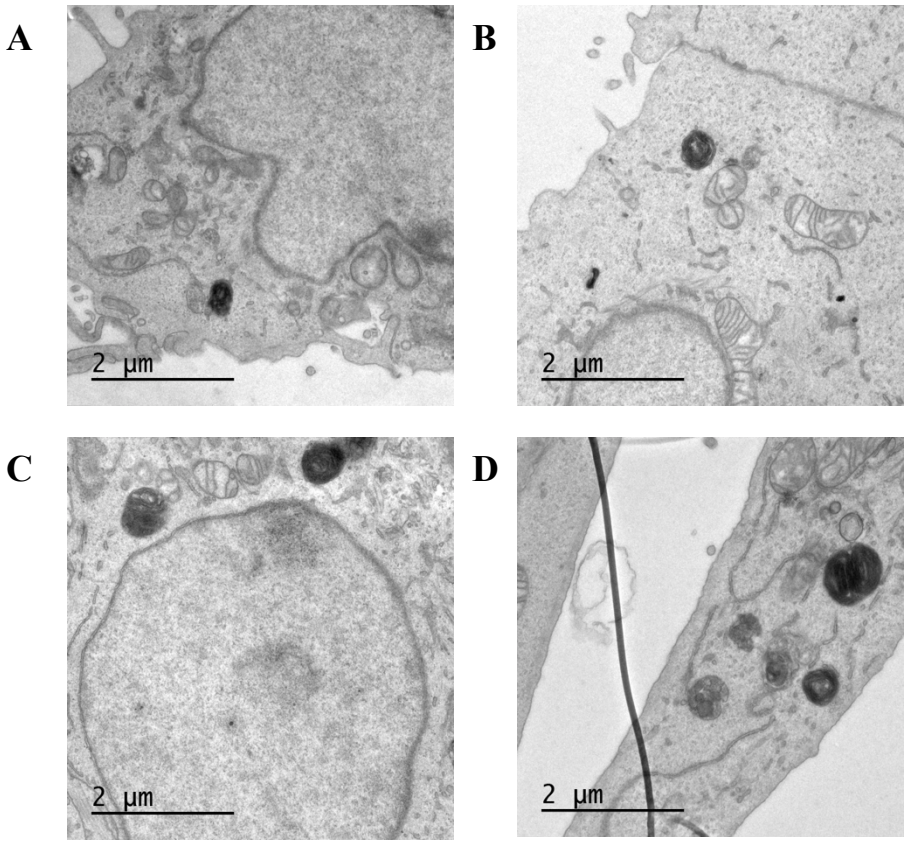


**Figure 3.5 Electron Micrograph of uninfected A549 cells.** Untreated or IFN-treated A549 cells were sectioned under conventional EM conditions and stained using lead citrate and uranyl acetate. All panels are at a magnification of 2000x. Panels A and B are untreated uninfected A549 cells whereas panels C and D have been pre-treated with 1000 U/mL IFN-a prior to sectioning. Each micrograph shows highly membranous structures similar to those seen in the virus-infected cells.

involved in either endocytosis or degradation. Interestingly, it appeared that these structures were more frequent in the WSN-infected cells and particularly in the presence of IFN treatment, however to confirm this observation these structures required quantification.

To determine the significance of these multi-membranous structures it was necessary to quantify the frequency at which they occur in each of the experimental conditions. However, due to the nature of these structures and other cellular organelles it is not possible to determine their number through standard counts. Equal numbers of different organelles can differ in size and this in turn can alter the number of times they can appear in 2D slices, as larger organelles will appear in more 2D slices than smaller organelles, leading to a misinterpretation of the frequency of each organelle. An example is shown in Fig. 3.6 A. as the schematic shows equal numbers of organelles which range in size, on the left a multi-vesicular body would be sectioned through 13 times, whereas the late endosome/lysosomal structure on the right would only be present in 6 sections despite there being equal numbers of organelles. Therefore to analyse these samples systematic uniform random (SUR) sampling was used for both its efficiency and lack of bias (Lucocq and Hacker 2013).

Following sample preparation, slices were appropriately stained and then viewed using TEM. Micrographs were taken in an SUR array, where 20 random images were taken per experimental condition at low-level magnification in order to maximize the amount of cytoplasm in each micrograph. Figure 3.6B shows an example of the SUR analysis that was performed on each micrograph. Initially a grid, which is larger than the micrograph, is placed over the micrograph at random and the number of times a

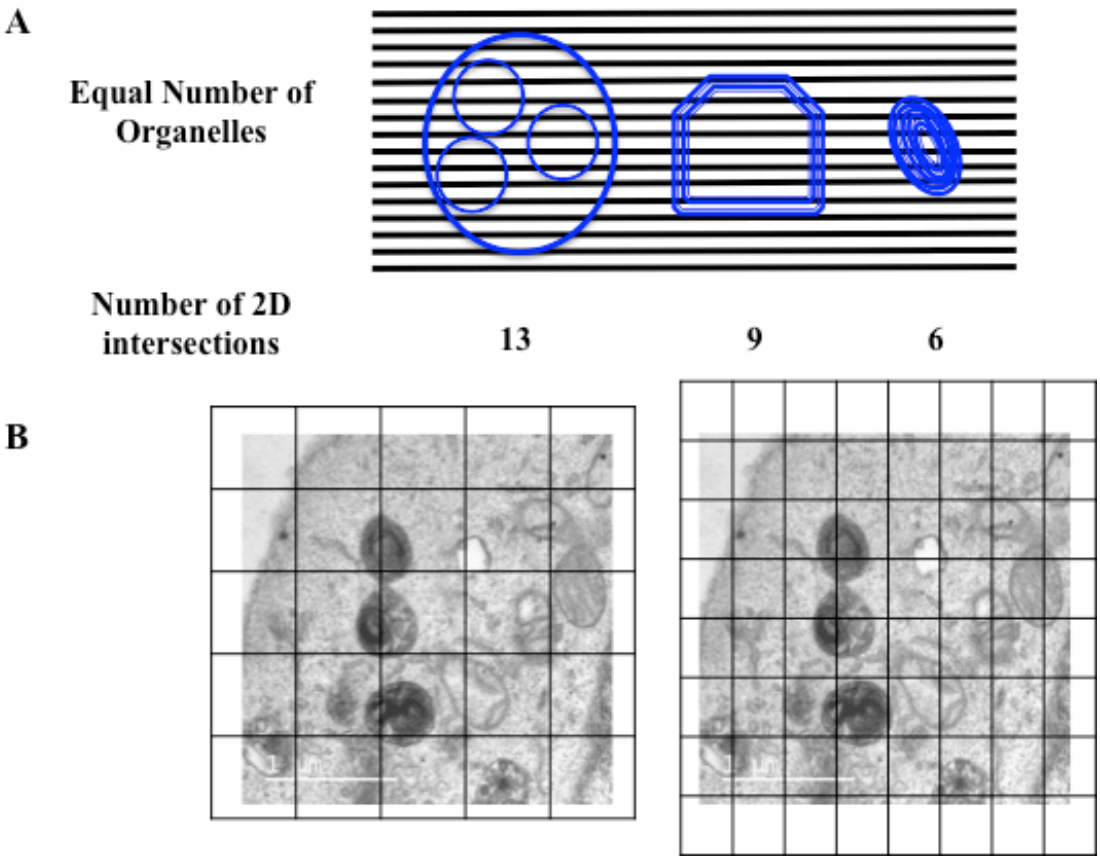


**Figure 3.6. Electron Micrograph Analysis. A.** The number of 2D intersections is influenced by the size of the organelle. The size of an organelle determines its chance of occurring in a section plane as illustrated by the 2D section planes (black horizontal lines). Although the numbers of each organelle in 3D are equal, the bias caused by sectioning would produce over twice as many profiles when the section planes intersect the largest organelle (in this case 13 section planes) compared with smallest organelle (6 section planes). **B.** Systematic uniform random (SUR) sampling allows the cell to be sectioned into a randomly placed and evenly spaced set of slices. Micrographs are taken at low magnification in an SUR array, covering a whole section profile (typically, these number 10–20). The magnification is selected to contain maximal areas of the cytoplasm but allow clear identification of ultrastructure profiles for subsequent image recording at high power. The grids are used for point counting on each of the micrographs to determine the ratio of cytoplasmic area to the structure of interest.

grid cross-section intersects the cytoplasm, a count is made. This is because the structures of interest can only be present within the cytoplasm. Then a second grid containing smaller squares is also placed over the micrograph at random and any time the grid cross-section intersects a multi-membranous structure (MS) it is counted. This then allows for a ratio of the amount of MS structures per cytoplasmic count, allowing for an unbiased comparison between experimental conditions.

Figure 3.7 shows the ratio of multi-membranous structures found in the cytoplasm of the different experimental conditions. Untreated, uninfected A549 cells had the lowest number of MS structures, with a MS:cytoplasm ratio of 0.001. Untreated, infected cells showed an increased MS:cytoplasm ratio of 0.0022. This increase was potentially due to incoming virions that were trafficked towards a degradation pathway or failed to fuse and release the viral genome for translocation to the nucleus.

Interestingly, pre-treatment of A549s with IFN led to a significant increase in the ratio of MS structures, giving a ratio of 0.0042, twice as many structures per cytoplasmic area than untreated, WSN-infected cells and a 4-fold increase on the uninfected, untreated cells, suggesting that these structures are induced by IFN treatment as an innate response to any incoming pathogens. This is further supported by the number of MS structures present in the IFN treated, WSN infected cells, as the ratio increases further to 0.01. This increase suggests that these structures, although naturally occurring at low levels within A549 cells, are induced by increased levels of endocytosis, as shown by the increase after WSN infection alone. It also shows that these structures are significantly induced by the pre-treatment with IFN as a potential host response to any incoming viruses and that infecting cells in a pre-existing

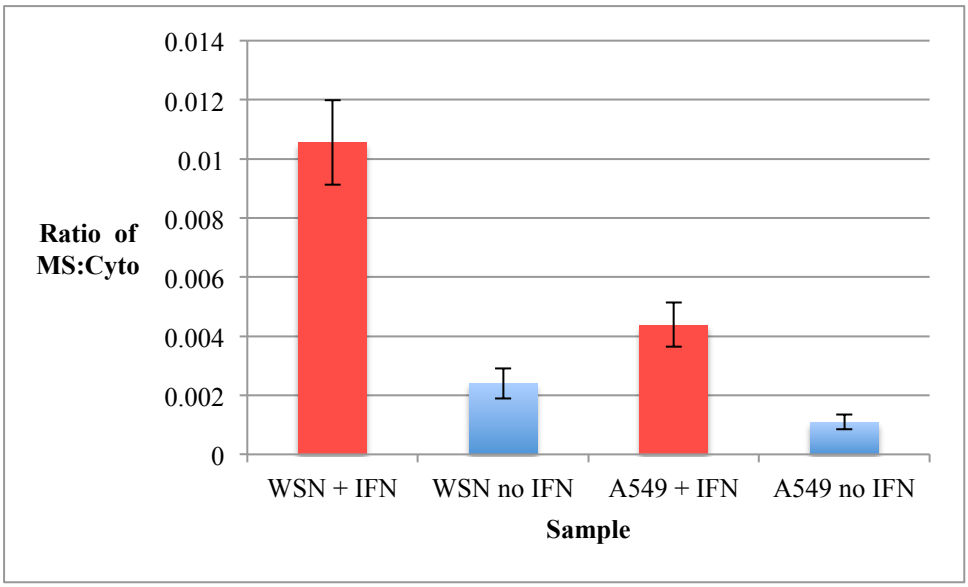


**Figure 3.7. Analysis of MS Ultrastructure.** A549 cells were either left untreated or treated with IFN for 16 hours prior to infection with WSN at an MOI of approximately 500 in a viral input assay. Cells were processed for EM analysis as described above. Systematic uniform random sampling was used to obtain 20 images at 2000x magnification per experimental condition. Micrographs were then analysed using grid cross-sections to determine the ratio of MS structures in the cytoplasm to the number of cytoplasmic counts. Results represent the average of three independent experiments ± S.D.

antiviral state with a high MOI of influenza virus can further induce the quantity of these structures present within the cytoplasm.

### 3.3 Does MxA inhibit influenza virus prior to primary transcription in the absence of IFN?

Previous work on the antiviral activity of MxA has shown that MxA can target two distinct steps of the virus replication cycle; i) over-expression of MxA alone has been shown to have an impact post-primary transcription, slowing the rate of viral RNA transcription and replication, and ii) Xiao et al. (2013) showed that in the presence of IFN, MxA is also capable of blocking the nuclear translocation of incoming viral genome. However, it has not been determined whether the over-expression of MxA in the absence of IFN treatment is capable of inhibiting the incoming viral genome from translocating to the nucleus. Previous studies have used a high MOI in the presence of cyclohexamide in order to visualise incoming viral genome without any genome replication. Using such a high MOI could over-power any antiviral effect exerted by MxA prior to primary transcription in the absence of IFN.

To address this A549-MxA cells, a cell line previously generated through lentivirus transduction to constitutively express MxA was infected with A/Udorn/72 at an MOI of 0.5 alongside naïve A549 cells and fixed 12 hours post infection. Following fixation the cells were immunostained for influenza NP as a marker for infected cells. The number of viral antigen positive cells was determined through taking 10 random images per condition at 20x magnification and then counted for the number of virus positive cells.

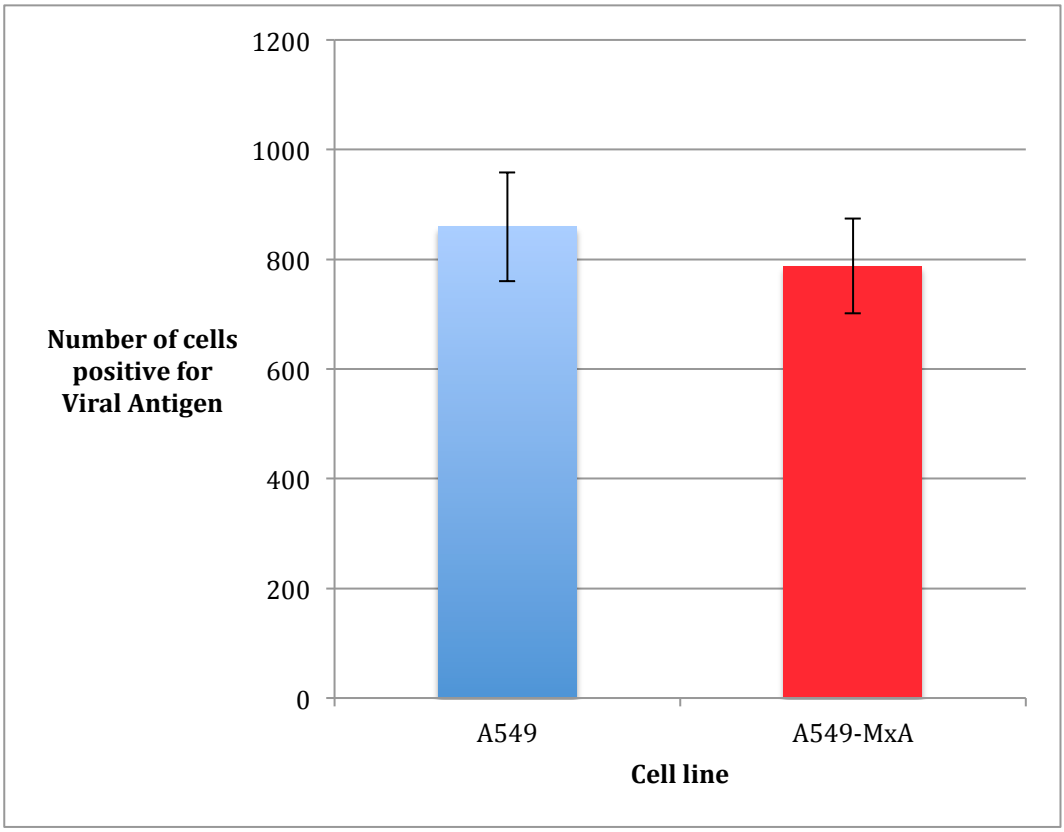


**Figure 3.8 Over-expression of MxA does not impact influenza nuclear import.** A549 and A549-MxA cells were infected with A/Udorn/72 at an MOI 0.5. Cells were fixed 12 h.p.i and immunostained for cell nuclei using DAPI and influenza NP. Systematic uniform random sampling was used to obtain 10 images per condition at 20x magnification. Cells that were positive for viral antigen were then counted using ImageJ cell counter. The results represent the average of three independent experiments ± S.D.

Figure 3.8 shows the impact of MxA on the number of influenza NP positive cells. The A549-MxA cells showed a small reduction in NP positive cells as naïve A549 cells had an average of 859.33 (+/- S.D 99.04) NP positive cells whereas the A549-MxA cells had an average of 787.66 (+/- S.D 86.40). However, there was no significant difference in the number of NP positive cells between naïve A549 cells and A549-MxA cells. This shows that in A549 cells that MxA over-expression does not appear to have a significant impact on the virus entering the nucleus and generating a productive infection and the small difference shown could be due to the effects the antiviral effects exhibited post-primary transcription. This result is also adds weight to the suggestion that MxA potentially has two separate antiviral mechanisms for inhibiting influenza virus, one which is IFN dependent and one which is independent of IFN.

### 3.5 The impact of MxA on viral protein expression

To determine the overall impact of MxA on influenza virus protein expression, naïve A549 cells, A549-MxA cells and A549-ΔMxA cells, a previously generated cell line which has been knocked down for endogenous MxA expression using an shRNA were infected with A/Udorn/72 virus at an MOI of 5. Cells had been either pre-treated with IFN (1000 U/mL) or left untreated for 16 hours prior to infection. Following infection cell lysates collected 8 h.p.i and assessed for the levels of viral NP via immunoblotting.

Figure 3.9A shows the effect of MxA on NP expression both with and without IFN pre-treatment. As expected MxA expression was not observed in either untreated naïve A549 cells or in A549-ΔMxA cells both in the presence and absence of IFN

treatment. Figure 3.9A clearly shows that in the absence of IFN the impact of MxA on NP expression is minimal, however in the presence of IFN there is a large decrease in the amount of NP being synthesized.

Figure 3.9B shows the levels of viral protein being produced firstly normalised to actin as the loading control and then normalised to naïve A549 cells without IFN treatment. In the absence of IFN there was only a 7% reduction in the amount of NP in A549-MxA cells when compared to naïve A549s, whereas NP levels in A549-ΔMxA increased by 11% compared naïve untreated cells.

However, in the presence of IFN there is a large impact on the amount of NP produced at 8 h.p.i. Using naïve, untreated A549 cells as 100% viral protein levels, IFN treated naïve A549 cells showed an 89% reduction in the amount of NP produced. A549-MxA cells showed a very similar reduction in the presence of IFN whereas the virus infection in A549-ΔMxA cells produced 52% the amount of NP as present in the untreated, naïve A549 cell control.

The amount of viral protein produced in the untreated cells demonstrates that without IFN treatment MxA appears to have little impact on the amount of viral protein produced, suggesting the only impact on virus replication is post-primary transcription, which is in line with the data seen in section 3.3. However, in the presence of IFN we see a huge reduction in the amount of NP being produced in both the naïve A549 cells and the A549-MxA cells as expected due to the large number of

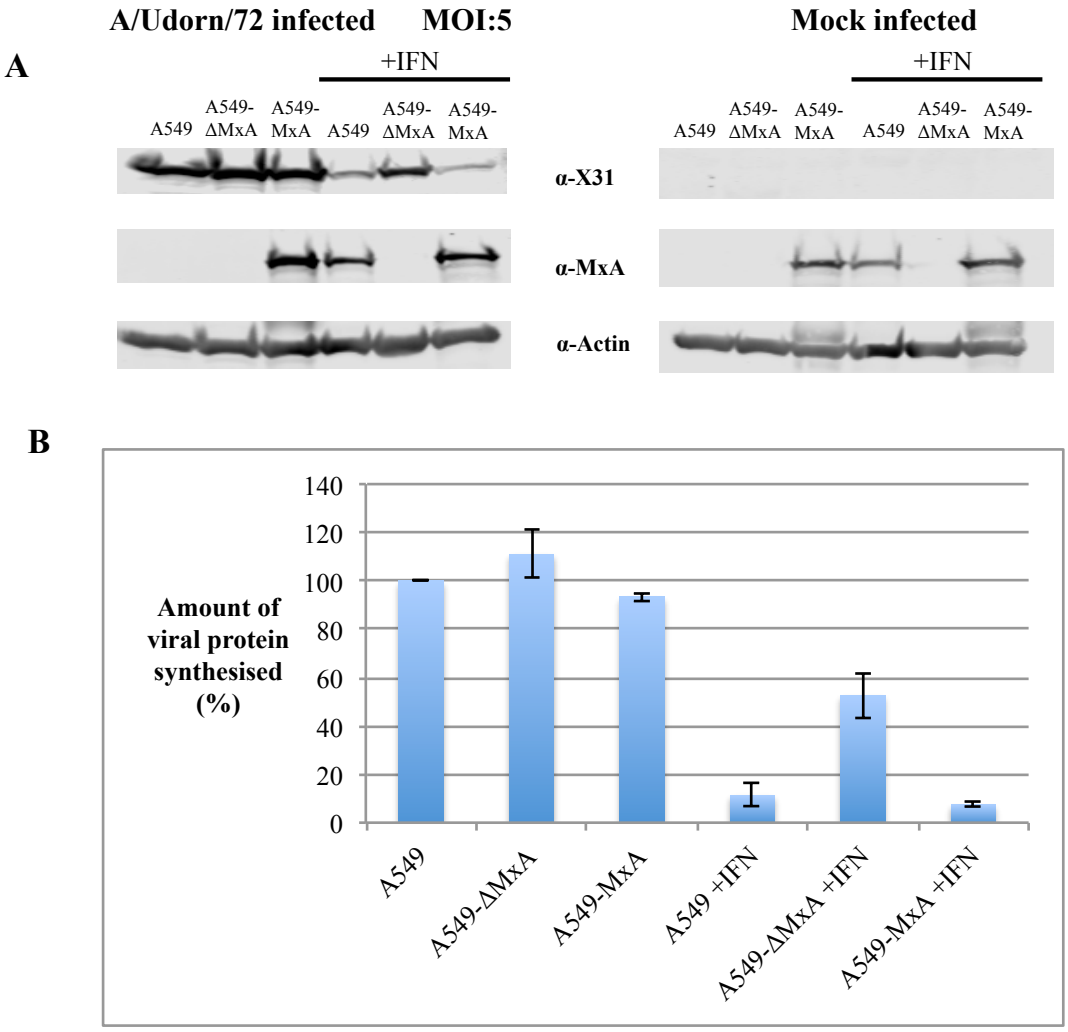


**Figure 3.9. The impact of MxA on influenza A virus protein expression. A.** Immunoblot showing the level of influenza NP expressed 8 h.p.i in A549, A549-ΔMxA and A549-MxA cells either in the absence or presence of IFN. Influenza NP was detected using a sheep anti-X31 antibody, MxA detection acted as a control for the presence of the IFN-induced antiviral state and actin levels were detected as a loading control. **B.** Quantification of NP synthesized 8 h.p.i firstly normalised to actin and then normalised to untreated A549 cells. The results represent the average of three independent experiments ± S.D.

antiviral proteins that are up regulated by IFN treatment. The over-expression of MxA only contributed an extra 4% reduction compared to naïve A549 cells in the presence of IFN. Interestingly, infected A549-ΔMxA cells produced 52% the amount of NP in the presence of IFN as untreated naïve A549 cells. This shows the importance of MxA to early influenza virus infection and the importance of MxA to the IFN response suggesting that approximately 40% of the reduction seen in naïve A549s in the presence of IFN is due to the expression of MxA.

### 3.5 The effect of MxA on viral titre

Although the results in section 3.4 gave a clear indication of the importance of MxA to the antiviral response it does not show the overall impact on the amount of virus produced during infection. To assess this naïve A549 cells, A549-MxA cells and A549-ΔMxA cells were infected with A/Udorn/72 virus at an MOI 0.001, supernatant samples were taken every 12 hours until 72 h.p.i and the infectious titre of each determined by viral plaque assay on MDCK cells.

At 12 h.p.i the amount of virus produced was relatively similar across the different cell lines, however by 24 h.p.i the viral titre was over half a log lower in the A549-MxA cells in comparison to the A549-ΔMxA cells and this level of attenuation continued for the remainder of the time course (Fig. 3.10A). Figures 3.10 B, C and D demonstrate the differences between the cell lines at 24, 36 and 48 h.p.i. respectively and clearly show the difference in the amount of virus produced. The amount of virus produced has been normalised to naïve A549 cells, which have been set as 100% virus production for a standard virus infection. At 24 h.p.i A549-ΔMxA cells produced an average of 60% more infectious virus particles than naïve A549 cells,

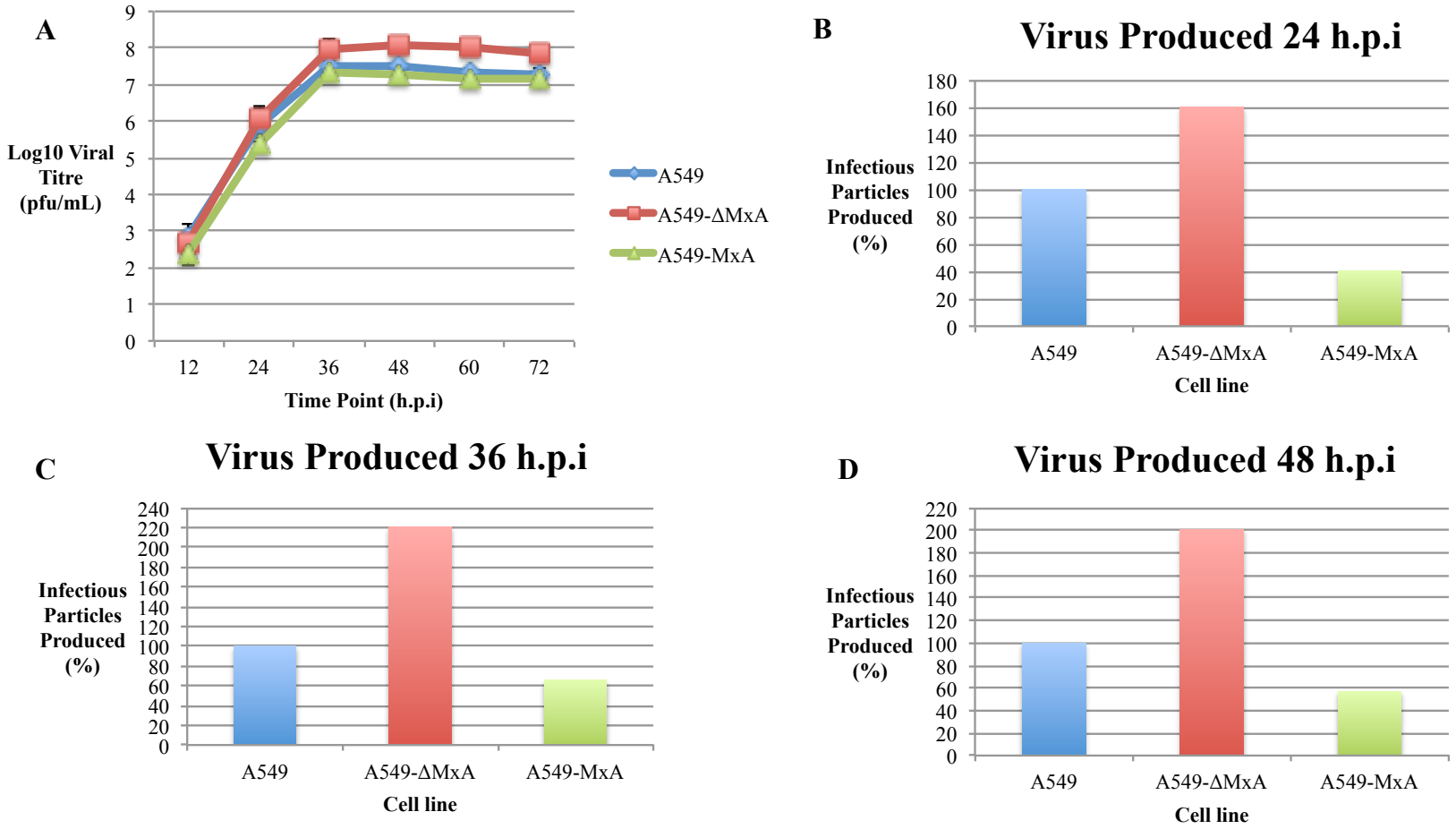


**Figure 3.10. Impact of MxA on influenza A Multistep infection. A.** A549, A549-ΔMxA and A549-MxA cells were infected at an MOI 0.001 using A/Udorn/72. Samples were taken every 12 hours post-infection and titred via plaque assay on MDCK cells. **B, C and D.** Show the percentage of virus produced normalised to naïve A549 cells as 100% virus production at 24, 36 and 48 h.p.i respectively

whereas the A549-MxA cells show a 60% reduction when compared to the naïve A549 cells. The infectious titre peaked at 36 h.p.i at which time the A549-ΔMxA cells had produced 120% more infectious virus particles than the naïve A549s with A549-

MxA cells producing only 66% the amount of infectious virus. A similar trend was observed at 48 h.p.i with 201% and 57% infectious virus particles produced from A549-ΔMxA and A549-MxA cells respectively.

These results clearly show the importance of MxA on influenza virus infection as the impact post-primary transcription is able to reduce the amount of virus produced by approximately 50% across the whole infection, whereas having cells incapable of producing MxA in response to virus infection showed an increased capacity to produce infectious virus particles.

However, the above analysis does not allow one to observe the impact that MxA is capable of having in the presence of IFN, which is the native cellular environment for MxA to be present. Therefore based on the previous results in section 3.4, where it was shown that MxA is hugely important to the antiviral response during early influenza infection, the three cell-lines which had either been untreated or pre-treated with IFN (1000 U/mL) were infected with A/Udorn/72 virus at an MOI of 5 in the absence of trypsin to observe the impact of MxA and IFN on a single viral replication cycle. Following inoculation, samples were collected every 3 hours until 15 h.pi and then a final read out at 24 h.p.i. Negligible levels of virus were present at 3 and 6 h.p.i as the single cycle of replication had not yet reached the point of virus release and following the virus inoculation the cells were washed with a citric acid wash to

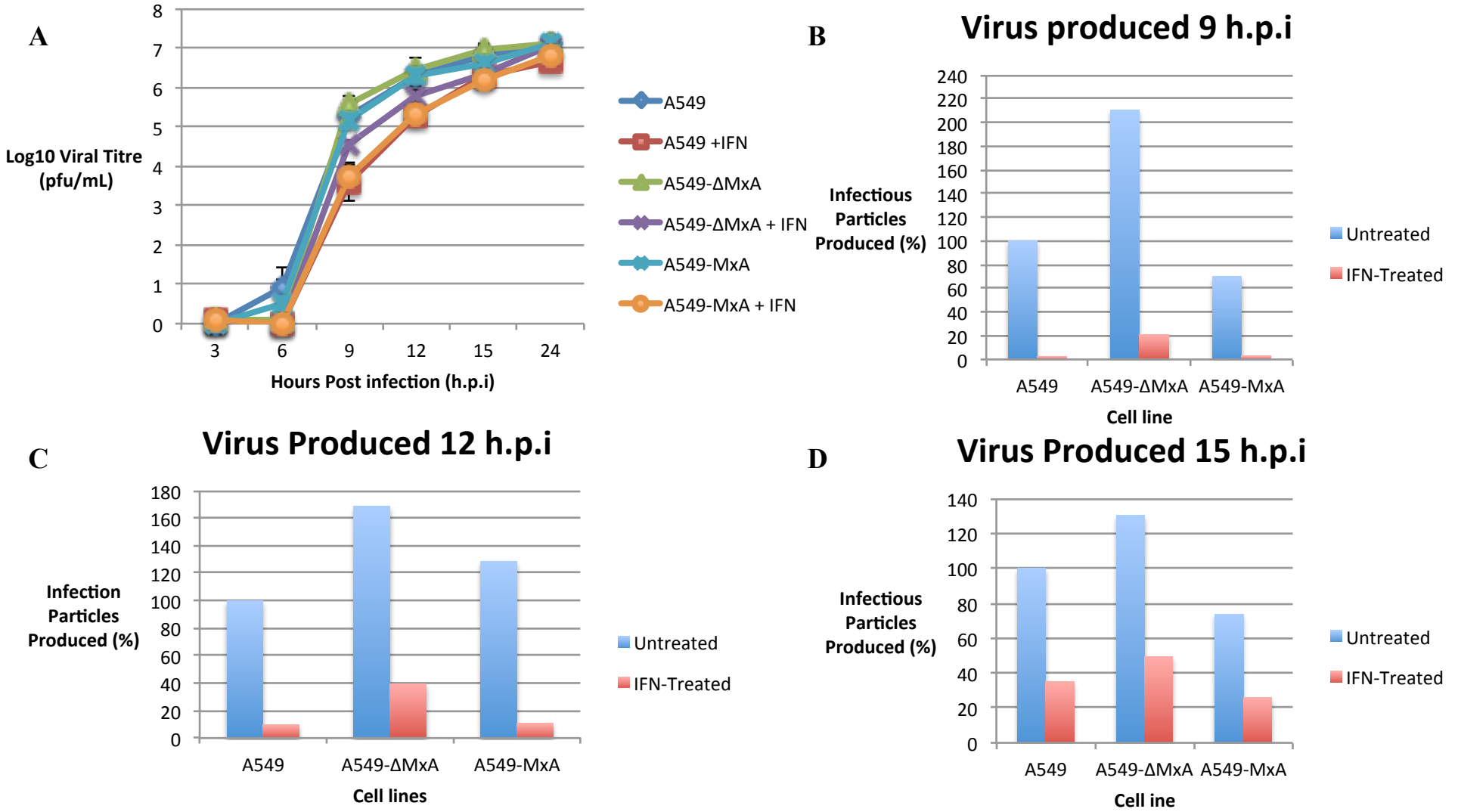


**Figure 3.11. Impact of MxA on influenza A single cycle infection. A.** A549, A549-ΔMxA and A549-MxA cells were either untreated or pre-treated with IFN-a 1000 U/mL for 16 hours prior to infection at an MOI 5 using A/Udorn/72. Samples were taken every 3 h.p.i until 15 hours and then at 24 h.p.i and titred via plaque assay on MDCK cells. **B, C and D.** Show the percentage of virus produced normalised to untreated naïve A549 cells as 100% virus production at 9, 12 and 15 h.p.i respectively

remove virus which had not been endocytosed (Fig 3.11A). Therefore the first time point at which virus was released was at 9 h.p.i. As seen in the multi-step growth curve (Fig. 3.10), there was a half-log difference between the amount of virus produced from A549-ΔMxA cells and the A549-MxA cells at 9 h.p.i. which slowly reduced over each time point suggesting that using a high MOI is capable of eventually surpassing the antiviral effect induced by the over-expression of MxA. Interestingly, at 9 h.p.i in the IFN-treated naïve A549 cells and A549-MxA cells there was a clear reduction in infectious viral titre of nearly 2 logs, whereas in the A549-ΔMxA cells the reduction in the presence of IFN at 9 h.p.i was only 1 log in comparison to untreated naïve A549 cells, again showing the importance of MxA on the early stages of influenza infection, particularly in the presence of IFN.

Figure 3.11B shows a graphical representation of viral titres released at 9 h.p.i normalised to untreated naive A549s as 100% virus production at each time point. In untreated cells there was approximately twice as many infectious virus particles produced by A549-ΔMxA cells compared to naïve cells, whereas in A549-MxA cells there was a 31% decrease in viral titre. In the presence of IFN it is clear that in the naïve A549 cells and the A549-MxA cells that IFN greatly reduced the amount of virus to 2.5% and 2.9% respectively, whereas the A549-ΔMxA cells produced approximately 20% the amount of virus of untreated naïve A549 cells. This supports the data shown in section 3.4 in which there was a large increase in the amount of NP protein translated in the IFN-treated A549-ΔMxA cells in comparison to IFN-treated naïve A549 cells and again shows the importance of MxA to the early stages of infection, particularly in the context of IFN.

This trend was continued at 12 h.p.i as Figure 3.11C shows a 60% increase in the amount of virus produced in A549-ΔMxA cells in untreated cells. At 15 h.p.i. this was reduced to a 30% increase on the amount of virus produced from naïve A549 cells whereas at 15 h.p.i the A549-MxA cells produce 73% the amount of virus as naïve A549 cells. This suggests that as the infection continues in the absence of IFN that the virus is able to reduce the impact of MxA over-expression and reduces the overall impact of not having endogenous MxA available.

In the IFN-treated cells there was a significant reduction in the amount of virus produced in all 3 cell lines at 12 h.p.i but again there was a significant difference in the amount of virus produced from the A549-ΔMxA cells in comparison to naïve A549 and A549-MxA cells. The level of virus production in the presence of IFN is 9.9% and 10.6% in these two cell lines respectively, however in A549-ΔMxA cells it was 40% that of untreated naïve cells. This trend continued at 15 h.p.i (Fig. 3.11D.) where A549 cells and A549-MxA cells produced 35% and 25% the amount of infectious particles compared to naïve untreated A549s yet the A549-ΔMxA cells produced 50%. This data not only shows that MxA has a large impact on the production of infectious influenza virus particles but also the importance of MxA to the early antiviral effects of IFN against influenza virus.

However, this data set also shows the capability of influenza virus to dismantle the host's pre-existing antiviral state as although the levels of virus produced at 9 h.p.i in the presence of IFN was in the order of 2 logs lower, producing only 2% the amount

of virus as the untreated control A549s, the percentage of virus produced from the IFN-treated cells increased steadily throughout the time course.

### 3.6 Influence of MxA on A549 Lipid profiles

A large amount of the work in the available literature regarding the IFN response and the ability of ISGs to inhibit viruses focuses on upregulated proteins and protein-protein interactions between ISGs and the viral proteins or blocking a specific part of the viral replication cycle to inhibit viral replication. However, a large part of the host defence lies in the cellular membranes, which are essential to both the host and enveloped viruses, but their role in the antiviral responses of the host is largely unknown. Briefly, mammalian cells consist of hundreds of different lipid species which can be grouped into three main classifications; glycerophospholipids, sphingolipids and sterols (Hermansson, Hokynar, and Somerharju 2011). The most abundant of which are glycerophospholipids, which can be catergorised based on their head group with the major classes as follows; phosphatidylcholines (PC), phosphatidylethanolamines (PE), phosphatidylinositols (PI) phosphatidylserines (PS) and cardiolipins (CL).

Lipids can be seen to exhibit three major biological functions within mammalian cells. Firstly, they are used to store energy, mainly in the form of steryl esters and triacylglycerols but also stored as fundamental building blocks for membrane biogenesis. The second major function is the formation of cellular membranes by polar lipids providing a barrier function to the outer environment as well as producing discrete organelles. The third function of lipids is to act as a chemical messenger during signal transduction. Lipid signaling can be bipartite in nature following the

degradation of amphipathic lipids as the hydrophobic portions can signal through membranes, whereas the polar portions are capable of transmitting signals through the cytoplasm (van Meer, Voelker, and Feigenson 2008).

MxA has been shown to bind to lipids and has been shown to shuttle between both the endoplasmic reticulum and the plasma membrane (von der Malsburg et al. 2011). Therefore removing endogenous MxA may have a significant impact on the lipid profile of the cell. To assess the overall impact of MxA on cellular lipid composition, the total cellular lipid contents of naïve A549 and A549-ΔMxA cells were extracted using the bligh-dyer method and analysed using electrospray-mass spectrometry. Interestingly, A549-ΔMxA cells showed a markedly different negative ion spectrum to naïve A549 cells (Fig. 3.12). The peaks corresponding to major lipid species present in each sample are labeled in Fig 3.12, which shows an increase in the abundance of a number of different lipid species in A549-ΔMxA cells compared to naive cells, such as PE 36:2, 38:4 and 40:4 and PG36:1. The results also show a reduction in levels of PS 34:2, 36:1 and 36:5 in comparison to naïve cells. These differences appear to show a clear impact of MxA on the lipid profile of A549 cells (Personal communication: Terry Smith). The increase in PE in A549-ΔMxA cells could potentially be advantageous for the virus as a recent study showed that for 4 different strains of influenza A virus the major lipid present in the virion was PE ranging from 48% up to 55% (Ivanova et al. 2015). This suggests that the virus requires a certain level of PE as it has been shown PE with suitable molecular geometry facilitate appropriate membrane fluidity and dynamics necessary for virus infection (R. B. Chan, Tanner, and Wenk 2010). The reduction in PS could also be of interest from the host's perspective, as PS is well known to be an important apoptotic

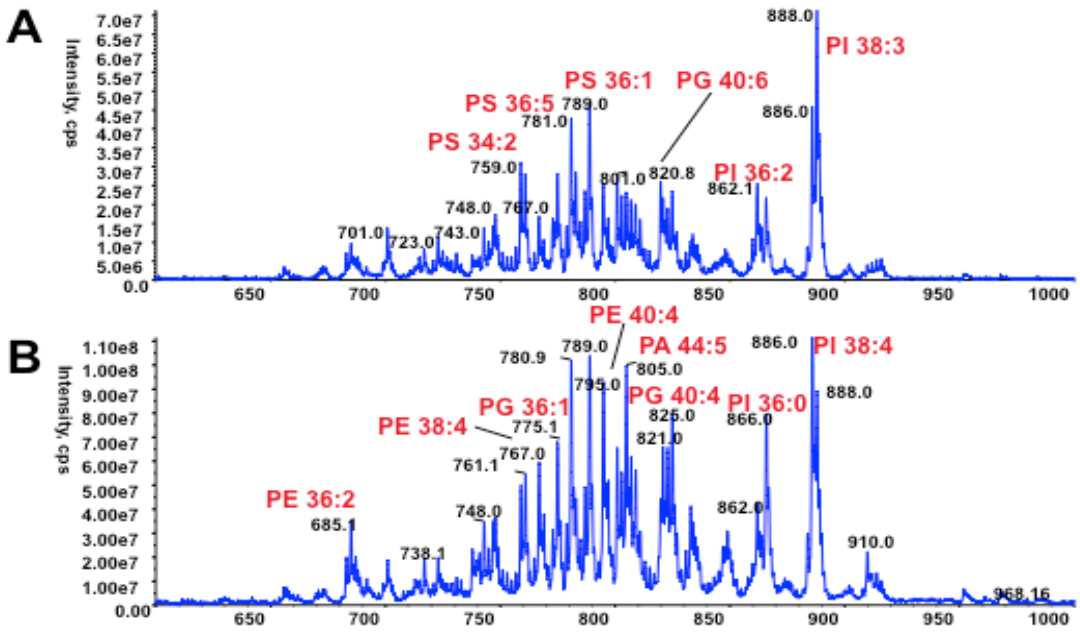


**Figure 3.12. Negative ion ES-MS lipidomic analysis of lipid extracts from naïve A549 and A549-ΔMxA cells.** Spectra show survey scans (600-1000m/z) of A) naïve A549 cells, B) A549-ΔMxA cells. The data is representative of 2 experiments.

marker, which is recognised by antigen presenting cells such as macrophages (Segawa et al. 2014). Therefore, MxA could have a role in regulating PS metabolism and trafficking, and potentially apoptosis. This profile suggests that MxA is potentially involved in lipid metabolism and is capable of altering the lipid profile of the cell. At first this result seems surprising, as MxA has only been reported to be expressed in response to IFN, whereas in this instance there is no IFN present within this system. However, although MxA transcription increases significantly following IFN treatment, transcriptomic data shows that small amounts of MxA are being transcribed at all times (Benitez et al. 2015). This coupled with the inherent stability of MxA within the cell suggests that there could be a small amount of MxA consistently expressed which could play a role in the either lipid metabolism or lipid trafficking within the cell

### 3.7 Discussion

Recent studies have indicated that ISGs can have an impact on the attachment and induction of endocytosis by enveloped viruses through the expression of CH25H (Blanc et al. 2013; S.-Y. Liu et al. 2013). To determine whether A549 cells were capable of inhibiting the initial entry of influenza A virus, A549 cells were pre-treated with IFN and then challenged with A/Udorn/73 at a range of different MOIs. The cells were then subjected to a citric acid wash to remove any virus particles that were bound to the cell surface but not endocytosed. The results clearly demonstrated that pre-treatment with IFN had no impact on the ability of influenza A virus to be endocytosed. Therefore it would appear that A549 cells do not express an ISG that is capable of inhibiting the initial entry of enveloped viruses. Consequently, any impact

of IFN-treatment on influenza virus replication in A549 cells is due to the intracellular ISG function.

Previously, it was shown that in the presence of IFN in A549 cells, incoming influenza virus genome was prevented from translocating to the nucleus and was found arrested in the perinuclear region (Xiao et al. 2013). Although it was clear that incoming virus was stuck in the cytoplasm and had been localised near to Rab-7, the nature of this block was still to be resolved. In this chapter the same viral input assay as described by Xiao et al. (2013) was used but analysed by transmission electron microscopy to try and further clarify where and how the incoming virus was blocked. The micrographs suggested a potential increase in multi-membranous ultrastructure in A549 cells after both IFN pre-treatment and virus infection, particularly at higher magnification where inside these structures there appeared to be structures possessing a double membrane and fuzzy glycoprotein outer-layer, not unlike the known influenza virion structure (Fig 3.4). However, the multi-membranous structures were also seen in other experimental conditions, although unsurprising as this is likely to be a normal cellular process potentially up-regulated in the presence of IFN, it meant that these structures required further quantification. This confirmed that these structures were much more abundant in A549 cells which had been pre-treated with IFN and infected with A/WSN/33 and in comparison to naïve untreated A549 cells, IFN treatment alone was capable of increasing the frequency of these structures. The identity of these structures is unknown, and is debated within the literature as to whether they represent late endosomes fusing with lysosomes, or whether they are in fact autophagic structures (Huotari and Helenius 2011; Hernandez et al. 2003; Lai et al. 2007).

It is well known that IFN-γ is capable of inducing autophagy, which in conjunction with constitutively expressed GTPases such as immunity-related GTPase M (Irgm) and IFN-γ inducible GTPases such as Irga6 produces a robust immune response against intracellular pathogens (Matsuzawa et al. 2012; P. Li et al. 2012; Z. Zhao et al. 2008). However, the induction of autophagy through IFN-β is a relatively new concept, as only recently has type I IFN been implicated in autophagy induction, shown to be dependent on both autophagy protein, atg7 and STAT-1 (Ambjørn et al. 2013). Importantly this was quickly followed by another research group showing that type I IFN induced autophagy in several different cell lines, including A549s, and was not a cell-line specific effect (Schmeisser et al. 2013). Further work will be required to determine whether the structures observed in Figure 3.4 are the product of lysosomal degradation or non-canonical autogphagy.

Xiao et al. (2013) also showed that this block was not only dependent on MxA but also dependent on IFN, as the over-expression of MxA was not enough to inhibit the translocation of viral genome to the nucleus but also required pre-treatment with IFN, suggesting a second antiviral activity of MxA after the initial observation of inhibiting influenza virus replication post-primary transcription (Zürcher, Pavlovic, and Staeheli 1992; Turan et al. 2004). This suggested that MxA was unable to block nuclear import of incoming influenza virus genome without the presence of IFN, however a caveat in their experimental approach was that in order for a detectable signal to be observed a very large MOI had to be used, which could have easily over-powered any antiviral effect produced by over-expressing MxA. This was addressed in this chapter by infecting A549 cells and A549-MxA cells at an MOI 0.5 and the levels of viral

antigen present were assessed. The data in Fig. 3.8 suggests that there was no significant difference in the number of cells displaying viral antigen and that the over-expression of MxA in A549 cells does not have an impact on influenza genome translocation. Therefore any differences observed in viral replication, such as the reduction in plaque number described by Xiao et al. (2013), in the absence of IFN were likely due to the antiviral effect induced by MxA following primary transcription. Although it did show that MxA was incapable of performing this block without IFN, it also suggested that there are two potentially different mechanisms to the antiviral activity exerted by MxA.

After determining the impact of MxA over-expression on the ability of influenza virus to establish a productive infection, it was necessary to determine the impact of MxA on virus replication as a whole in the presence of both over-expressed MxA and the lack of any endogenous MxA in A549 cells. The protein data shown in Fig.3.9 clearly showed that in the absence of IFN there was only a small difference in the levels of viral protein produced. However, the impact of IFN on virus protein and consequently virus production is highly significant as expected.

Interestingly, this data shows the importance of MxA to the early stages of virus infection particularly in the presence of IFN, as at 8 h.p.i, IFN-treated A549-ΔMxA cells produced 50% the amount of protein as untreated naïve A549 cells, which is a 40% increase over IFN-treated naïve A549s and A549-MxA cells. These results show the efficiency of the IFN response, as the over-expression of MxA coupled with IFN did not lead to a much greater reduction in viral protein produced. This is likely due to the large number of other ISG which are capable of producing an inhibitory effect

against influenza A virus, such as IFITM3, Viperin and ISG15 (Feeley et al. 2011; Wang, Hinson, and Cresswell 2007; C. Zhao et al. 2010).

However, the importance of MxA to the IFN response against influenza A virus is underlined by the large increase in viral protein produced without endogenous MxA. Therefore, if MxA has two separate mechanisms of antiviral function; one independent of IFN and one which is IFN-dependent. This data suggests that the IFN-dependent block of influenza A virus prior to primary transcription by MxA is more important to the host response than impact displayed following primary transcription in A549 cells.

MxA is known to reside at the endoplasmic reticulum (ER) and shuttle between the ER and plasma membrane whilst also being shown to be capable of binding to lipids and *in vitro* has been shown to be capable of tubulating liposomes mediated by a run of lysine residues in positions 554-557 (von der Malsburg et al. 2011). Based on this knowledge, it was hypothesised that MxA may have a role in lipid metabolism or shaping the lipid profile of the cell. This was investigated through whole cell lipid extraction and comparing the lipid profiles of naïve A549 cells and A549-ΔMxA cells to determine the impact of removing endogenous MxA.

Surprisingly, there was a clear difference in the overall lipid profiles of the two cell types. Differences were detected in the major glycerophospholipid head groups, in particular increased PE lipid peaks and reduced PS lipid peaks were observed, both of which could have an impact on virus infection. This is because lipids have intrinsic shapes that are dependent on the size of the head groups and acyl chain length and

saturation and these characteristics determine their side-by-side packing, and the curvature of the membrane (McMahon and Boucrot 2015). The change in lipid profile could offer an explanation for the increase in the viral titre produced from A549-ΔMxA cells. In the absence of IFN treatment, these cells should not be expressing levels of MxA, which could impact virus production. Therefore the levels of virus produced from cells that do not express endogenous MxA should be similar to naïve A549 cells. However, there is a large increase in the amount of infectious virus released from A549-ΔMxA cells (Fig. 3.11). This could be due to very small amounts of MxA that is constitutively expressed within the cell having an impact on lipid metabolism. Therefore completely removing MxA and subsequently increasing the cellular levels of PE, shown to be a key part of the viral lipid envelope by Ivanov et al. 2015, could lead to an increase in the levels of infectious virus produced. However, to determine the real impact of knocking out MxA on lipid levels an internal standard would be required to allow for quantification. Also, this analysis looks at the cellular lipid composition as a whole and does not differentiate between lipid localization as these changes could be taking place at any lipid bound organelle within the cell and not necessarily at the plasma membrane. To address this one would have to fractionate the cells and characterise the lipid levels in various cellular compartments, especially those found specifically in the plasma membrane. Changes in plasma membrane-associated lipids could then be correlated with effects on viral infectivity.

Despite these limitations, this data offers another potential role for MxA within the host cell and a third potential mechanism of antiviral activity, whereby MxA is capable of manipulating the cellular lipid metabolism so that progeny virions do not

incorporate the correct lipid composition required for optimal infectivity. Therefore although the virus particles would likely still be capable of binding to the host cell, they may not be able to undergo efficient fusion due to biophysical restrictions imposed by the altered curvature of the lipid membrane.

## Chapter 4 - Investigating the structural and functional characteristics of the antiviral activity of MxA

MxA is recognised as a key protein within the host antiviral response and can be defined through a number of major characteristics as not only is it a GTPase, it is also capable of binding to lipid membranes and homo-oligomerization which can lead to the production of huge ring-like structures *in vitro*, whilst existing primarily as a tetramer *in vivo* (Kochs et al. 2002 and Janzen et al. 2000). More recently canine Mx1 has been shown to play a role for apical transport of post-golgi vesicles, adding to the growing understanding of the number of functions performed by Mx proteins aside from their antiviral action (Hoff et al. 2014).

The previous section identified the importance of MxA to the interferon response during the early stages of influenza infection. To determine which of the aforementioned characteristics are essential to the antiviral activity of MxA against influenza virus a number of mutations previously described in the literature were introduced into MxA (Table 4.1). Each of the mutations were cloned into the MxA gene within the mammalian expression vector pCAGGS and lentivirus expression plasmid pdl-MCS-R' to be used in transient and stable protein expression systems respectively.

### 4.1 Characterisation of wobble MxA constructs

Previously it has been shown that the over-expression of MxA was not capable of inhibiting the translocation of incoming influenza genome to the nucleus (Xiao et al. 2013). This had been shown by silencing the expression of endogenous MxA using an

| Mutations | Function |
|---|---|
| **T103A** | Abolishes GTP binding and anti-viral activity but does form oligomers (Janzen , Kochs and Haller. 2000) |
| **G255E** | Human Biallelic polymorphism G255E is predicted to effect MxA structure (Duc et al. 2012) |
| **V268M** | Human Biallelic polymorphism V268M is not predicted to effect MxA structure (Duc et al. 2012) |
| **I376D** | Interface 1 mutant critical for oligomerization (Haller et al. 2010) |
| **D478A** | BSE stalk region, which oligomerised like WT but preferentially in dimer form. Can bind to La Crosse Virus NP and is active in an influenza A mini-replicon assay. (Gao et al. 2011) |
| **AKAK (554-557)** | Lipid binding mutant within the L4 loop shown to negate Mx lipid binding and liposome tubulation in vitro (van der Malsburg et a. 2011) |
| **KEKE (554-557)** | Lipid binding mutant within the L4 loop shown to negate Mx lipid binding and liposome tubulation in vitro (van der Malsburg et a. 2011) |
| **F561V** | Single amino acid change in L4 loop confers Thogoto virus antiviral specificity. F561V decreases its ability to restrict influenza A H5N1 replication. (Mitchell et al. 2012) |
| **F602D** | Interface 2 mutants that disrupts tetramer formation but produce monomers (Daumke et al. 2010) |
| **L612K** | Fails to form oligomers and has no detectable GTPase activity but still has antiviral activity in transiently transfected Vero cells against Thogoto Virus and Thogoto mini-replicon system. Rapidly degraded (Janzen, Kochs and Haller. 2000). |
| **R640A** | Does not oligomerise with or without the presence of [S]. Shown as a dimer. Does not sequester La Crosse V N nor does it inhibit H5N1 replication in a mini-replicon assay (Gao et al. 2011) |

**Table 4.1 MxA Mutations.**

shRNA targeting the MxA mRNA for degradation in A549 cells (A549-ΔMxA). Xiao et al. (2013), then re-introduced MxA into these cells using a codon-optimised version of the MxA gene (in which 3rd base synonymous changes were introduced) , which was no longer targeted by the shRNA and allowed constitutive expression of MxA within these cells. This provided a system in which the antiviral effects of overexpressed MxA could be monitored without the expression of endogenous MxA affecting the results. As the nucleotide sequence of the codon-optimised MxA gene had been "wobbled" (due to the redundancy of the genetic code) from its original sequence this will be referred to as wobble MxA (wMxA) from here on in. The nucleotide alignment is seen in Figure 4.1.

To determine the impact of the mutations introduced to MxA (Table 4.1) on its antiviral activity in the absence of endogenous MxA, the mutations of interest were also made in the wMxA background so that these mutant proteins could be introduced into the A549-ΔMxA cells. Prior to stable cell-line production the mutant MxA proteins were firstly characterised by determining their expression and localization in 293T cells by transient transfection. Figure 4.2 shows each of the constructs displayed cytoplasmic localization as expected. It is interesting to note that similar to wild-type MxA all but two of the mutant versions were distributed in areas of intense punctate expression. Although punctate staining of MxA is not typical of endogenous MxA expression induced through IFN, it is likely that the punctate phenotype observed in over-expression systems is due to the accumulation of larger quantities of protein being expressed leading to the formation of the higher molecular weight complexes postulated by Kochs et al. (2002). This hypothesis is supported by the phenotypes displayed by the MxA proteins containing mutations at position 602 and 612, which

```
ATGGTTGTTTCCGAAGTGGACATCGCAAAAGCTGATCCAGCTGCTGCATCCCACCCTCTA MxA
ATGGTGGTGTCTGAAGTCGATATTGCCAAGGCCGACCCCGCAGCCGCCAGCCATCCCCTC Wobble
***** ** ** ***** ** ** ** ** ** ** ** ** ** **   *** ** **
TTACTGAATGGAGATGCTACTGTGGCCCAGAAAAATCCAGGCTCGGTGGCCGAGAACAAC MxA
CTCCTCAACGGCGACGCCACCGTCGCTCAAAAGAACCCCGGAAGCGTCGCTGAAAATAAT Wobble
 * ** ** ** ** ** ** ** ** ** ** ** ** **    ** ** ** ** **
CTGTGCAGCCAGTATGAGGAGAAGGTGCGCCCCTGCATCGACCTCATTGACTCCCTGCGG MxA
CTCTGTTCCCAATACGAAGAAAAAGTCCGGCCTTGTATTGATCTGATCGATAGCCTCAGA Wobble
** **   *** ** ** ** ** ** ** ** ** ** ** ** ** ** **   ***  *
GCTCTAGGTGTGGAGCAGGACCTGGCCCTGCCAGCCATCGCCGTCATCGGGGACCAGAGC MxA
GCCCTGGGCGTCGAACAAGATCTCGCTCTCCCCGCTATTGCAGTGATTGGCGATCAATCC Wobble
** ** ** ** ** ** ** ** ** ** ** ** ** ** ** ** ** ** ** **   *
TCGGGCAAGAGCTCCGTGTTGGAGGCACTGTCAGGAGTTGCCCTTCCCAGAGGCAGCGGG MxA
AGCGGAAAATCTAGCGTCCTGGAAGCCCTCAGCGGCGTGGCTCTGCCTAGGGGATCCGGC Wobble
   ** **      ***  **** ** **    ** ** ** ** ** ** **   ***
ATCGTGACCAGATGCCCGCTGGTGCTGAAACTGAAGAAACTTGTGAACGAAGATAAGTGG MxA
ATTGTCACACGGTGTCCTCTCGTCCTCAAGCTCAAAAAGCTGGTCAATGAGGACAAATGG Wobble
** ** **  * ** ** ** ** ** ** ** ** ** ** ** ** ** ** ** ** ***
AGAGGCAAGGTCAGTTACCAGGACTACGAGATTGAGATTTCGGATGCTTCAGAGGTAGAA MxA
CGGGGAAAAGTGTCCTATCAAGATTATGAAATCGAAATCAGCGACGCCAGCGAAGTGGAG Wobble
 * ** ** **    ** ** ** ** ** ** ** **    ** **    ** ** **
AAGGAAATTAATAAAGCCCAGAATGCCATCGCCGGGGAAGGAATGGGAATCAGTCATGAG MxA
AAAGAGATCAACAAGGCTCAAAACGCTATTGCTGGCGAGGGCATGGGCATTTCTCACGAA Wobble
** ** ** ** ** ** ** ** ** ** ** ** ** ** ***** **   *** **
CTAATCACCCGTGAGATCAGCTCCCGAGATGTCCCGGATCTGACTCTAATAGACCTTCCT MxA
CTGATTACACTAGAAATTTCTAGCAGGGACGTGCCTGACCTCACCCTGATCGATCTGCCC Wobble
** ** ** *  ** **      * * ** ** ** ** ** ** ** ** ** ** **
GGCATAACCAGAGTGGCTGTGGGCAATCAGCCTGCTGACATTGGGTATAAGATCAAGACA MxA
GGAATCACACGGGTCGCCGTCGGAAACCAACCCGCCGATATCGGCTACAAAATTAAAACC Wobble
** ** **  * ** ** ** ** ** ** ** ** ** ** ** ** ** ** ** **
CTCATCAAGAAGTACATCCAGAGGCAGGAGACAATCAGCCTGGTGGTGGTCCCCAGTAAT MxA
CTGATTAAAAAATATATTCAACGGCAAGAAACCATCTCCCTCGTCGTCGTGCCTAGCAAC Wobble
** ** ** ** ** ** **  **** ** ** ***  *** ** ** ** ** ** **
GTGGACATTGCCACCACAGAGGCTCTCAGCATGGCCCAGGAGGTGGACCCCGAGGGAGAC MxA
GTCGATATCGCTACAACCGAAGCCCTGTCTATGGCTCAGGAAGTCGATCCTGAAGGCGAT Wobble
** ** ** ** ** ** ** ** **    ***** ***** ** ** ** ** ** **
AGGACCATCGGAATCTTGACGAAGCCTGATCTGGTGGACAAAGGAACTGAAGACAAGGTT MxA
CGCACAATTGGCATTCTGACCAAACCCGACCTCGTCGATAAGGGCACCGAGGATAAAGTG Wobble
 * ** ** ** **  **** ** ** ** ** ** ** ** ** ** ** ** ** **
GTGGACGTGGTGCGGAACCTCGTGTTCCACCTGAAGAAGGGTTACATGATTGTCAAGTGC MxA
GTCGATGTCGTCAGAAATCTGGTCTTTCATCTCAAAAAAGGCTATATGATCGTGAAATGT Wobble
** ** ** **  * ** ** ** ** ** ** ** ** ** ** ***** ** ** **
CGGGGCCAGCAGGAGATCCAGGACCAGCTGAGCCTGTCCGAAGCCCTGCAGAGAGAGAAG MxA
AGAGGACAGCAAGAAATTCAGGATCAGCTCTCTCTCAGCGAGGCTCTCCAGCGGGAAAAA Wobble
 * ** ***** ** ** ***** *****    **   *** ** ** *** * ** **
ATCTTCTTTGAGAACCACCCATATTTCAGGGATCTGCTGGAGGAAGGAAAGGCCACGGTT MxA
ATTTTTTTCGAAAATCATCCCTACTTTCGGGACCTCCTCGAAGAGGGGAAAGCTACCGTC Wobble
** ** ** ** ** ** ** ** **  **** ** ** ** ** ** ** ** ** **
CCCTGCCTGGCAGAAAAACTTACCAGCGAGCTCATCACACATATCTGTAAATCTCTGCCC MxA
CCTTGTCTCGCCGAGAAGCTGACATCTGAACTGATTACCCACATCTGCAAGAGCCTCCCT Wobble
** ** ** ** ** ** ** **    ** ** ** ** ** ***** **    ** **
CTGTTAGAAAATCAAATCAAGGAGACTCACCAGAGAATAACAGAGGAGCTACAAAAGTAT MxA
CTCCTGGAAAACCAGATTAAAGAAACCCATCAGAGGATCACCGAGGAACTGCAGAAATAC Wobble
**  * ***** ** ** ** ** ** ** ***** ** ** ***** ** ** ** **
GGTGTCGACATACCGGAAGACGAAAATGAAAAAATGTTCTTCCTGATAGATAAAATTAAT MxA
GGCGTGGATATCCCCGAGGATGAGAACGAGAAGATGTTTTTTCTCATCGACAAGATCAAC Wobble
** ** ** ** ** ** ** ** ** ** ** ***** ** ** ** ** ** ** **
GCCTTTAATCAGGACATCACTGCTCTCATGCAAGGAGAGGAAACTGTAGGGGAGGAAGAC MxA
GCTTTCAACCAGGATATTACCGCACTGATGCAGGGGGAAGAAACCGTGGGCGAAGAGGAT Wobble
** ** ** ***** ** ** ** ** ***** ** ** ***** ** ** ** ** **
ATTCGGCTGTTTACCAGACTCCGACACGAGTTCCACAAATGGAGTACAATAATTGAAAAC MxA
ATCAGACTCTTCACAAGGCTGAGGCATGAATTTCATAAGTGGAGCACCATCATCGAGAAT Wobble
**  * ** ** ** ** **  * ** ** ** ** ** ***** ** ** ** ** **
```

```
AATTTTCAAGAAGGCCATAAAATTTTGAGTAGAAAAATCCAGAAATTTGAAAATCAGTAT MxA
AACTTCCAGGAAGGACACAAGATCCTCAGCAGGAAGATTCAGAAGTTCGAGAACCAGTAC Wobble
** ** ** ***** ** ** **  * ** ** ** ** ***** ** ** ** *****
CGTGGTAGAGAGCTGCCAGGCTTTGTGAATTACAGGACATTTGAGACAATCGTGAAACAG MxA
AGAGGCAGAGAACTCCCCGGATTCGTCAACTACCGCACCTTCGAAACTATTGTCAAGCAG Wobble
 * ** ***** ** ** ** ** ** ** *** * ** ** ** ** ** ** ** **
CAAATCAAGGCACTGGAAGAGCCGGCTGTGGATATGCTACACACCGTGACGGATATGGTC MxA
CAGATTAAAGCCCTCGAGGAACCCGCCGTCGACATGCTGCATACAGTCACCGACATGGTC Wobble
** ** ** ** ** ** ** ** ** ** ** ** ***** ** ** ** ** ** ******
CGGCTTGCTTTCACAGATGTTTCGATAAAAAATTTTGAAGAGTTTTTTAACCTCCACAGA MxA
CGCCTGGCCTTTACCGACGTGTCCATCAAGAATTTCGAGGAATTCTTCAACCTGCACCGG Wobble
** ** ** ** ** ** ** ** ** ** ** ***** ** ** ** ** ***** *** *
ACCGCCAAGTCCAAAATTGAAGACATTAGAGCAGAACAAGAGAGAGAAGGTGAGAAGCTG MxA
ACAGCTAAAAGCAAGATCGAGGATATCCGGGCCGAGCAGGAAAGGGAGGGCGAAAAACTC Wobble
** ** **   *** ** ** ** **  * ** ** ** ** ** ** ** ** ** **
ATCCGCCTCCACTTCCAGATGGAACAGATTGTCTACTGCCAGGACCAGGTATACAGGGGT MxA
ATTAGACTGCATTTTCAGATGGAGCAAATCGTGTATTGTCAGGATCAAGTGTATAGAGGC Wobble
**  * ** ** ** ******** ** ** ** ** ** ***** ** ** ** ** **
GCATTGCAGAAGGTCAGAGAGAAGGAGCTGGAAGAAGAAAAGAAGAAGAAATCCTGGGAT MxA
GCCCTCCAGAAAGTGCGCGAAAAAGAACTCGAAGAGGAGAAAAAAAAAGAAGAGTTGGGAC Wobble
**  * ***** **  * ** ** ** ** ***** ** ** ** *****    *****
TTTGGGGCTTTCCAATCCAGCTCGGCAACAGACTCTTCCATGGAGGAGATCTTTCAGCAC MxA
TTTGGCGCCTTCCAGAGCAGCAGCGCCACCGACAGCAGCATGGAAGAAATTTTCCAGCAT Wobble
***** ** *****   ****   ** ** ***     ****** ** ** ** *****
CTGATGGCCTATCACCAGGAGGCCAGCAAGCGCATCTCCAGCCACATCCCTTTGATCATC MxA
CTCATGGCTTACCATCAGGAAGCATCTAAGAGAATCAGCTCCCATATTCCCCTGATTATT Wobble
** ***** ** ** ***** **    *** * ***  *  *** ** **  **** **
CAGTTCTTCATGCTCCAGACGTACGGCCAGCAGCTTCAGAAGGCCATGCTGCAGCTCCTG MxA
CAGTTTTTTATGCTGCAGACCTATGGACAGCAGCTGCAGAAAGCTATGCTCCAGCTGCTC Wobble
***** ** ***** ***** ** ** ******** ***** ** ***** ***** **
CAGGACAAGGACACCTACAGCTGGCTCCTGAAGGAGCGGAGCGACACCAGCGACAAGCGG MxA
CAGGATAAAGATACTTATTCTTGGCTCCTGAAAGAAAGATCCGATACATCTGATAAAAGA Wobble
***** ** ** ** **    ********** **  *   *** **    ** **  *
AAGTTCCTGAAGGAGCGGCTTGCACGGCTGACGCAGGCTCGGCGCCGGCTTGCCCAGTTC MxA
AAATTTCTCAAAGAGAGACTCGCCAGACTGACCCAGGCCAGAAGAAGGCTGGCTCAGTTT Wobble
** ** ** ** *** * ** **  * ***** *****  *  *  **** ** *****
CCCGGTTAA                                                     MxA
CCTGGCTGA                                                     Wobble
** ** * *
```

**Figure 4.1 Nucleotide alignment of endogenous and wobble MxA sequences.** Nucleotide sequences were aligned using the online sequence alignment tool Clustal Omega. Stars indicate bases that align.

encode for a phenylalanine to aspartate (F602D) and a leucine to lysine (L612K) respectively. Both of these mutations cause MxA to be expressed in a monomeric form incapable of forming oligomers, therefore suggesting that the punctate phenotype observed is likely due to higher molecular weight oligomer formation (Janzen, Kochs and Haller. 2000 and Daumke et al. 2010).

### 4.2 Impact of MxA mutations on influenza virus polymerase activity

Following the characterisation of wt and mutant wMxA protein expression, these constructs were then tested functionally in the influenza A virus mini-genome replication system. This system requires the expression of the influenza A virus polymerase subunits, PB2, PB1, PA and NP for successful replication of a negative-sense viral RNA template. The template in this assay was a renilla luciferase construct flanked by a conserved untranslated region (UTR) of the NS segment of influenza A virus. Transfected together this leads to the transcription and translation of renilla luciferase, the expression level of which can be directly correlated to the extent of polymerase activity. To control for the number of cells transfected a plasmid encoding firefly luciferase under the control of a CMV promoter was used to normalise the polymerase activity in a dual luciferase assay. As MxA is a cytoplasmic protein but the transcription of renilla mRNA in this assay occurs exclusively in the nucleus, the antiviral effects of MxA measured in this assay are solely due to its affect post primary transcription, likely through preventing newly synthesized NP from entering the nucleus to aid in transcription of the viral-like renilla vRNA gene.

Firstly, the wMxA constructs were assessed for antiviral activity using the H3N2 influenza A Udorn/1972 polymerase through transfection of the polymerase sub-units

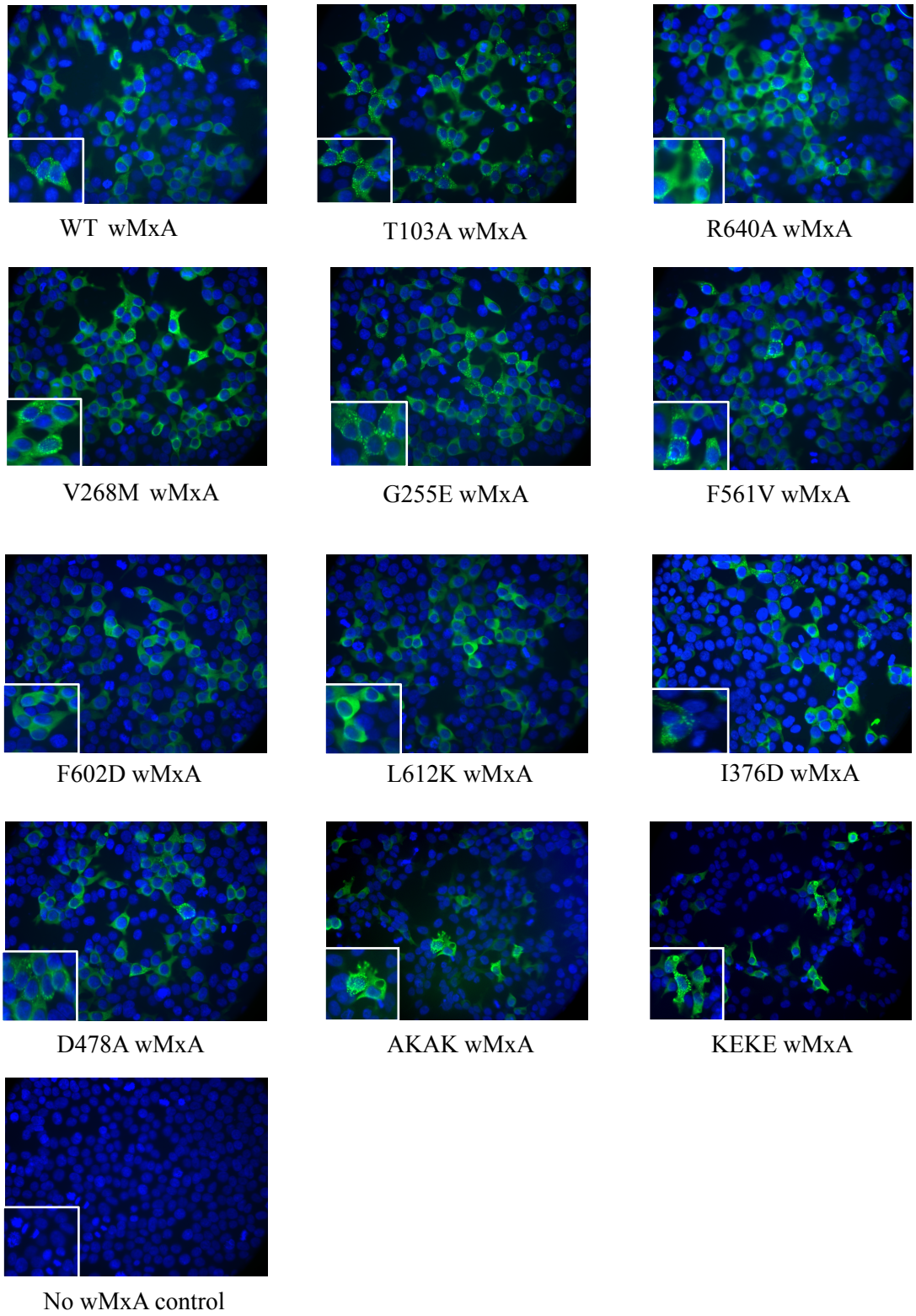


**Figure 4.2 Immunofluorescence of wMxA constructs.** Immunofluorescent staining of 293T cells 24h post-transfection with 500ng plasmid showing the expression phenotypes of wt and mutant wMxA proteins. 293T cells were first probed with an α-MxA polyclonal rabbit antibody then an Alexa-488 conjugated goat α-rabbit antibody. Nuclei were stained using DAPI. Green; α-MxA Blue; DAPI-stained nuclei.

and the two reporter genes. Following the dual luciferase assay the polymerase activity was normalised to the activity in the absence of wMxA to determine the level of antiviral activity exhibited by each of the mutant wMxA constructs.

As shown in Fig. 4.3 the expression of wt wMxA reduced the polymerase activity by approximately 60% overall. Although the T103A mutant was previously described to be an antiviral null mutant it displayed antiviral activity in this assay, although the level of activity was reduced in comparison to wt MxA. Two other mutants also showed similar levels of attenuation in antiviral activity as T103A as both lipid-binding mutants, AKAK and KEKE only reduced the polymerase activity by 30 and 35% respectively. Interestingly, MxA proteins containing the monomeric mutations, L612K and F602D, appeared to be just as effective as wt MxA in reducing H3N2 polymerase activity, suggesting that the ability of MxA to oligomerise is not required to produce the antiviral effect post-primary transcription.

The two dimeric mutants, R640A and D478A both appeared capable of inhibiting polymerase activity post-primary transcription, although the antiviral activity of the oligomerisation mutant I376D appears to be slightly more attenuated. Strikingly, these results show that the antiviral activity of one of the human polymorphisms, G255E, is similar to that of wt wMxA, whilst the activity of the other human polymorphism identified by Duc et al. (2012), V268M, was reduced in comparison to wt wMxA.

Avian influenza viruses have been shown to be more susceptible to the antiviral activity displayed by MxA (Zimmermann et al. 2011). Therefore to determine the

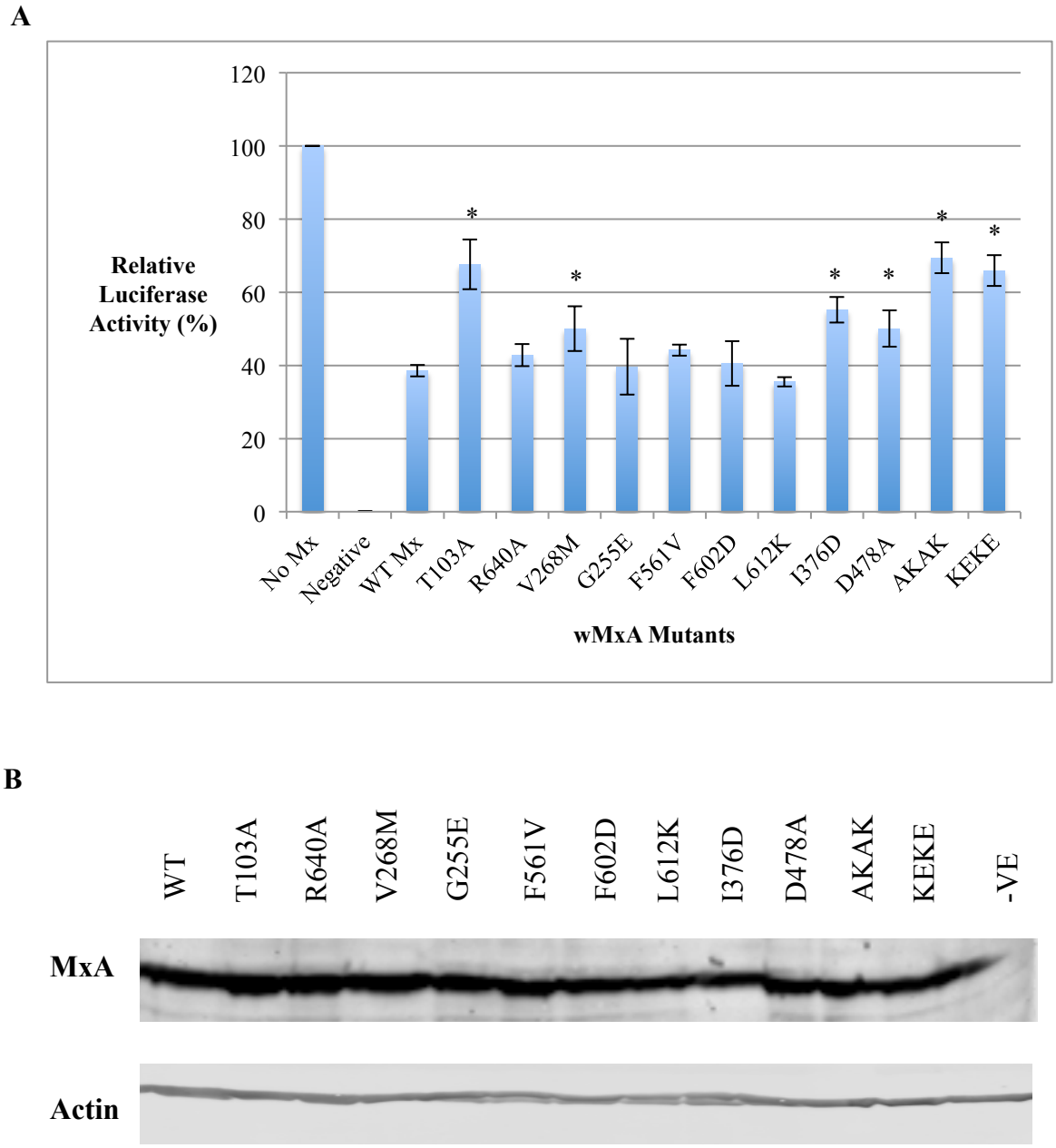


**Figure 4.3 The effects of MxA on A/Udorn/72 polymerase activity in a luciferase-based mini-genome assay. A.** 293T cells were transfected with plasmids expressing the polymerase subunits and NP of A/Udorn/72 virus (10 ng each), a renilla-encoding mini-genome plasmid (250 ng), a plasmid encoding firefly luciferase (10ng) and the various wMxA constructs (200 ng each). The relative luciferase activity was measured in a dual luciferase assay. Results are represented as a percentage of luciferase activity in the no MxA control and are the average of three independent experiments ± S.D. **B.** Immunoblot showing the level of wMxA expressed following 24h expression in 293T cells. MxA was detected through an α-Rabbit MxA antibody and actin levels were detected as a loading control. (* denotes p-value = <0.05 following students T-test)

impact of these mutations on the antiviral activity of MxA in the context of an avian polymerase, the dual luciferase assay was performed using the polymerase subunits from the A/Thailand/1(KAN-1)/04 (H5N1) virus (kindly provided by Martin Schwemmle, University of Freiburg).

It is clear from the data presented in Fig 4.4 that wt wMxA was much more potent in its antiviral effect when compared to the mutants wMxA constructs. The trend largely stays the same as that seen in the A/Udorn/72 polymerase assay, although the differences between wt wMxA and the other constructs were more prominent. A number of the results from the H5N1 polymerase assay are in line with previously published data, such as the reduced antiviral activity of F561V and D478A. Interestingly, human polymorphisms G255E and V268M as well as the monomeric mutants, F602D and L612K, all show reduced antiviral activity compared to wt wMxA, whereas in the previous assay these mutants were as active as wt wMxA. Despite a number of similarities, there are some differences with the current literature with both T103A and R640A exhibiting antiviral activity against influenza A viruses when previously they have been stated to have no antiviral effect (Janzen, Kochs, and Haller 2000; S. Gao et al. 2011).

**4.3 Influence of wobble RNA on MxA protein folding, localization and function**

One of the key differences observed was the impact of the antiviral-null mutant T103A, which although attenuated in comparison to wt wMxA, was not completely antiviral-null in the polymerase reconstitution assay using the polymerase and NP proteins of either A/Udorn/72 virus or an H5N1 virus. Interestingly a recent publication looking at the impact of G-domain mutations in MxA showed a

**A**

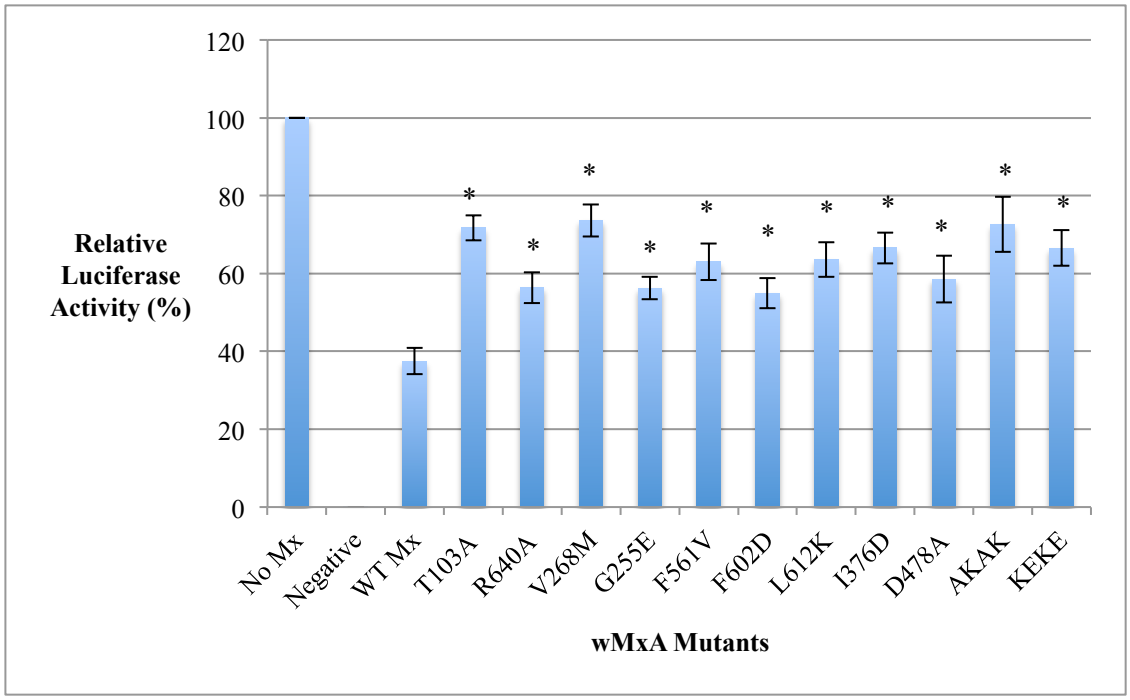


**B**

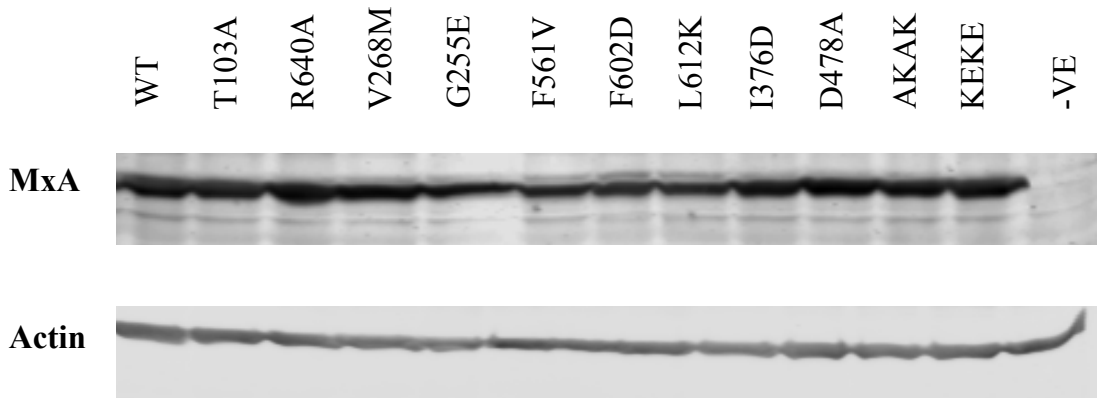


**Figure 4.4 The effects of MxA on A/Thailand/1(KAN-1)/04 (H5N1) virus polymerase activity in a luciferase-based mini-genome assay. A.** 293T cells were transfected with plasmids expressing the polymerase subunits and NP of A/Thailand/1(KAN-1)/04 (H5N1) virus (10 ng each), a renilla-encoding mini-genome plasmid (250 ng), a plasmid encoding firefly luciferase (10ng) and the various wMxA constructs (200 ng each). The relative luciferase activity was measured in a dual luciferase assay. Results are represented as a percentage of luciferase activity in the no MxA control and are the average of three independent experiments ± S.D. **B.** Immunoblot showing the level of MxA expressed following 24h expression in 293T cells. MxA was detected through an α-Rabbit MxA antibody and actin levels were detected as a loading control. (* denotes p-value = <0.05 following students T-test)

phenotypically different immunostaining pattern for T103A MxA than observed in section 4.1 for T103A wMxA (Dick et al. 2015a). Furthermore it was also shown that one of the antiviral-null human polymorphism mutations, G255E, showed a similar staining pattern to T103A MxA, again differing from what was observed for G255E wMxA.

Upon recognising these differences, the previously assessed mutations were then introduced to the wt MxA mRNA background and cloned into the mammalian expression vector pCAGGS to evaluate the phenotypic expression patterns of these mutations in both the wt mRNA background and the wobble mRNA background. 293T cells were transfected with each of the constructs and the distribution of MxA determined by immunofluorescence. Distribution of the wt MxA protein was similar to the wMxA constructs, as they displayed a distinct punctate phenotype associated with the over-expression of MxA with an otherwise diffuse cytoplasmic staining (Fig. 4.5). The distribution of MxA proteins containing other mutations was also similar in both mRNA backgrounds as seen for V268M, R640A, F561V and both lipid binding mutants AKAK and KEKE. Both the monomeric mutations F602D and L612K also show diffuse cytoplasmic staining with no punctate staining of MxA, indicating that the change in mRNA sequence did not impact the overall localization and functionality of these mutants.

However, there are some clear phenotypic differences in the appearance of a number of different mutants. Firstly, the antiviral-null mutant T103A showed a significantly altered expression pattern when expressed from the wt mRNA sequence when compared to the wobble mRNA sequence. MxA derived from the wt mRNA sequence

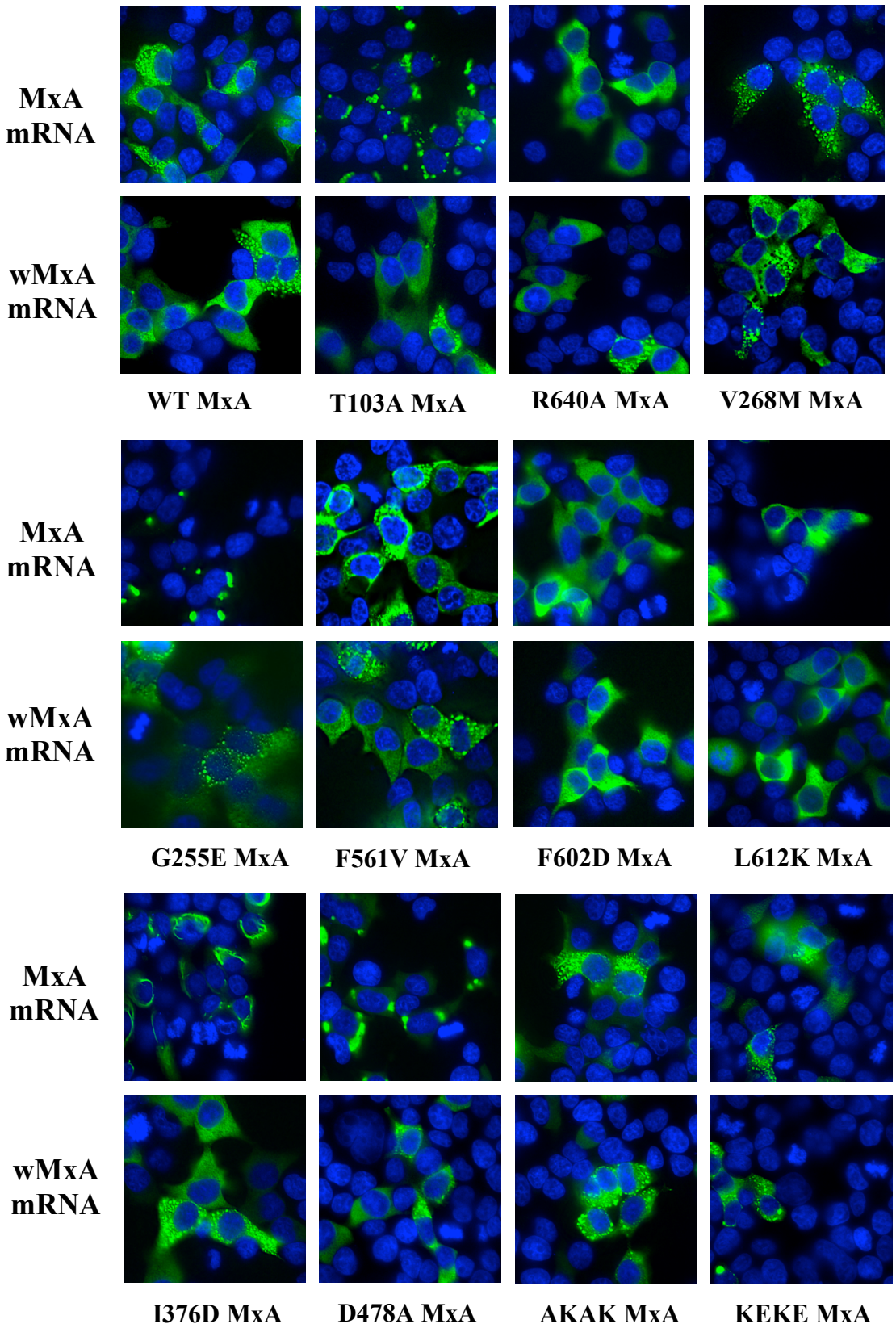


**Figure 4.5 Immunofluorescence comparison of MxA derived from wt MxA mRNA- and wMxA mRNA-expressing constructs.** 293T cells were transfected with 500ng plasmid to express MxA from either the endogenous mRNA background or the wobble mRNA background. 24 hours post-transfection cells were fixed and probed with an α-MxA polyclonal rabbit antibody followed by an Alexa-488 conjugated goat α-rabbit antibody. Nuclei were stained using DAPI. Green; α-MxA, Blue; DAPI-stained nuclei.

showed an aggregation pattern within the cytoplasm as described previously by Dick et al. (2015) whereas the MxA expression pattern from the wobble mRNA background shows a distinctly wt-like phenotype. This suggests that the mRNA sequence may play an important role in the overall protein expression pattern as these two proteins share the exact same amino acid sequence. A similar difference was observed between MxA proteins expressed from the wt-mRNA and wobble mRNA sequences contianing the human polymorphism G255E, with MxA derived from the wt mRNA sequence showing a clear punctate pattern, whereas that from the wobble mRNA demonstrated a wt-like expression pattern.

Two other mutants showed differing phenotypes when expressed from the different mRNA backgrounds. Both I376D and D478A present with a wt-like punctate over-expression phenotype from the wobble mRNA background. However, from the wt mRNA sequence these two mutants offer very different staining patterns. I376D was previously described to disrupt tetramer formation resulting in a predominantly dimeric form of MxA (S. Gao et al. 2010). However no immunofluorescence or antiviral functionality data was presented. The introduction of I376D into the wt mRNA background produced a striking phenotype suggestive of long oligomeric structures in the perinuclear region, which appears to be dependent on the level of MxA protein available as surrounding cells with less MxA expression appear to only have the beginnings of this structure whilst having a diffuse cytoplasmic background staining. D478A is a stalk mutant that has been shown to behave similarly to wild type *in vitro* and this mutant was shown to localise with LACV Nucleoprotein (N) (S. Gao et al. 2011). The expression phenotype seen in the wt mRNA background matches the previously published phenotype, however, this is not in the context of

LACV N, suggesting that this staining pattern is indicative of MxA localizing with another cellular organelle in the perinuclear region.

Following the identification of these differences in phenotype it was necessary to ascertain the impact of these mutations on the antiviral activity of MxA against influenza A virus post primary transcription. Figure 4.6 shows the comparison between the A/Thailand/1(KAN-1)/04 virus polymerase activity in the presence of the MxA mutants expressed from both the wt mRNA and wobble mRNA backgrounds. Both T103A and G255E show complete attenuation in the ability to produce an antiviral effect against influenza A virus when expressed from wt mRNA. This matches the data published by Dick et al. (2015) for both T103A and G255E, and is not surprising considering the aggregated phenotypes displayed by both of these mutants. Interestingly, the two other mutants that appear to display a non-wt like expression pattern after expression from wt MxA mRNA (D478A and I376D) do not appear to differ in antiviral activity regardless of the mRNA background, displaying inhibition at around the 50% and 60% mark for D478A and I376D respectively, which matches the antiviral activity previously stated for the D478A mutation (S. Gao et al. 2011). Although the change in mRNA background appears to have accounted for the majority of discrepancies between the data presented here and previously published data, R640A demonstrated a decent level of antiviral activity in both mRNA backgrounds, despite being previously described as antiviral null (S. Gao et al. 2011).

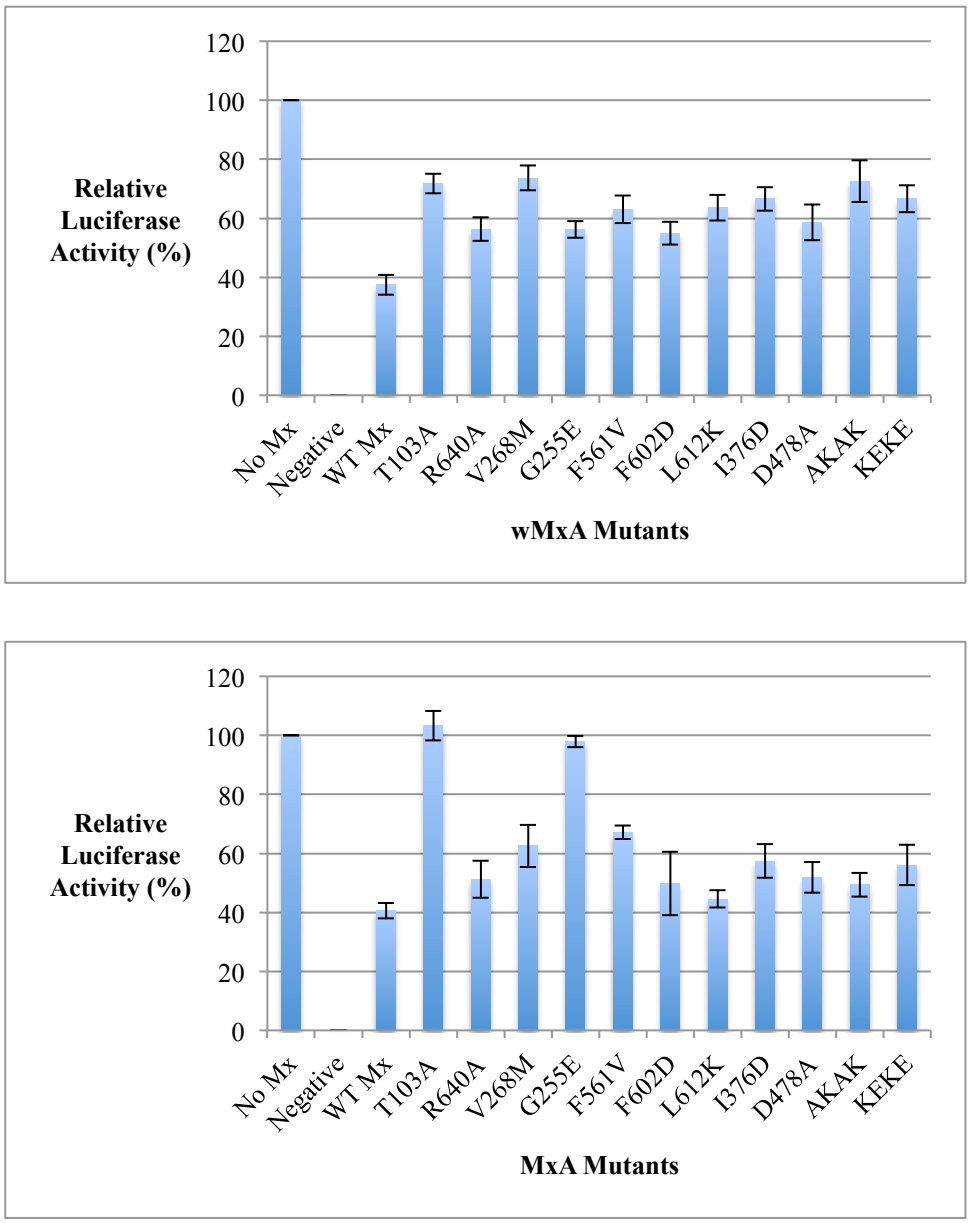


**Figure 4.6 Comparison between wMxA and MxA constructs in A/Thailand/1(Kan-1)/04 viral polymerase activity in a luciferase-based mini-genome assay.** 293T cells were transfected with plasmids expressing the polymerase subunits and NP of A/Thailand/1(KAN-1)/04 (H5N1) virus (10 ng each), a renilla-encoding mini-genome plasmid (250 ng), a plasmid encoding firefly luciferase (10ng) and the various MxA and wMxA constructs (200 ng each). The relative luciferase activity was measured in a dual luciferase assay. Results are represented as a percentage of luciferase activity in the no MxA control and are the average of three independent experiments ± S.D.

### 4.5 Identification of potential MxA interacting partners

MxA is believed to exert its antiviral effect by targeting and binding to influenza A virus NP (Dittmann et al. 2008). Although MxA has been shown to bind directly to THOV nucleocapsids as well as being shown to sequester LACV N protein, there has been no direct interaction shown between MxA and influenza A virus NP without the aid of cross-linking (G Kochs and Haller 1999; Georg Kochs, Janzen, et al. 2002; Turan et al. 2004). It is entirely plausible that NP-MxA interactions may be mediated by another viral or cellular protein. Furthermore the block in nuclear translocation of incoming influenza A virus vRNPs has been suggested to require an ISG co-factor (Xiao et al. 2013). Therefore it is possible that MxA may inhibit influenza virus via an indirect interaction. Despite MxA being able to perform a number of functions, there are a surprisingly low number of host proteins that have been shown to interact directly with MxA. To date the key interactors that have been identified include actin and tubulin, the cellular RNA helicases UAP56 and URH49, Fanconi anemia proteins, ISG15 and more recently, MxA has been shown to undergo SUMOylation (Horisberger 1992; Wisskirchen et al. 2011; Reuter et al. 2003; C. Zhao et al. 2005b; Brantis-de-Carvalho et al. 2015).

To identify potential interacting partners of MxA, wt wMxA and, following the discovery that wT103A is not completely antiviral null, but attenuated for antiviral activity against influenza A virus, T103A wMxA were cloned into expression vectors to allow expression with an N-terminal modified tandem affinity purification (TAP) tag. This modified TAP-tag no longer has a calmodulin-binding site, therefore allowing for purification in a single step using protein A. These two constructs were transfected into 293T cells alongside a third experimental vector which expressed the

modified TAP tag and linker sequence followed by a stop codon as a control for false positive hits. 48 hours post-transfection, the cells were lysed, the proteins of interest purified using IgG beads and separated by SDS-PAGE (Fig. 4.9 A) and confirmed by immunoblotting (Fig 4.9 B). The samples were then excised and prepared for mass spectrometry analysis by tandem mass spectrometry (MS/MS). The initial results were blasted against the MASCOT server before being analysed using the Scaffold4 software. Proteins were scored after a minimum of two peptides resulted in protein identification and due to large numbers of immunoglobulin domains being eluted, any protein identified as an immunoglobulin were excluded from the analysis.

The analysis resulted in the identification of 173 proteins (Fig 4.9 C) that include proteins involved in variety of cellular processes such as cytoskeleton proteins, molecular chaperones and helicases, mitochondrial and translation machinery, or proteins involved in trafficking between organelles such as the golgi, ER and the nucleus. Of the 173 identified proteins 77 of these were identified in all constructs, however, these were not excluded from analysis as although some of these also interacted with TAP tag alone, they were also previously identified interacting partners of MxA such as actin and tubulin (Horisberger 1992). Of all the identified proteins, none were specific to TAP-tag alone or T103A wMxA. The empty TAP construct also shared 6 proteins with only wt wMxA, whereas T103A wMxA shared 48 protein hits with wt wMxA, showing a large overlap in the proteins that both of these proteins bind to. Surprisingly, there appeared to be 42 proteins which were exclusively precipitated by wt wMxA. Although some of these may be partially explained by issues with detection thresholds.

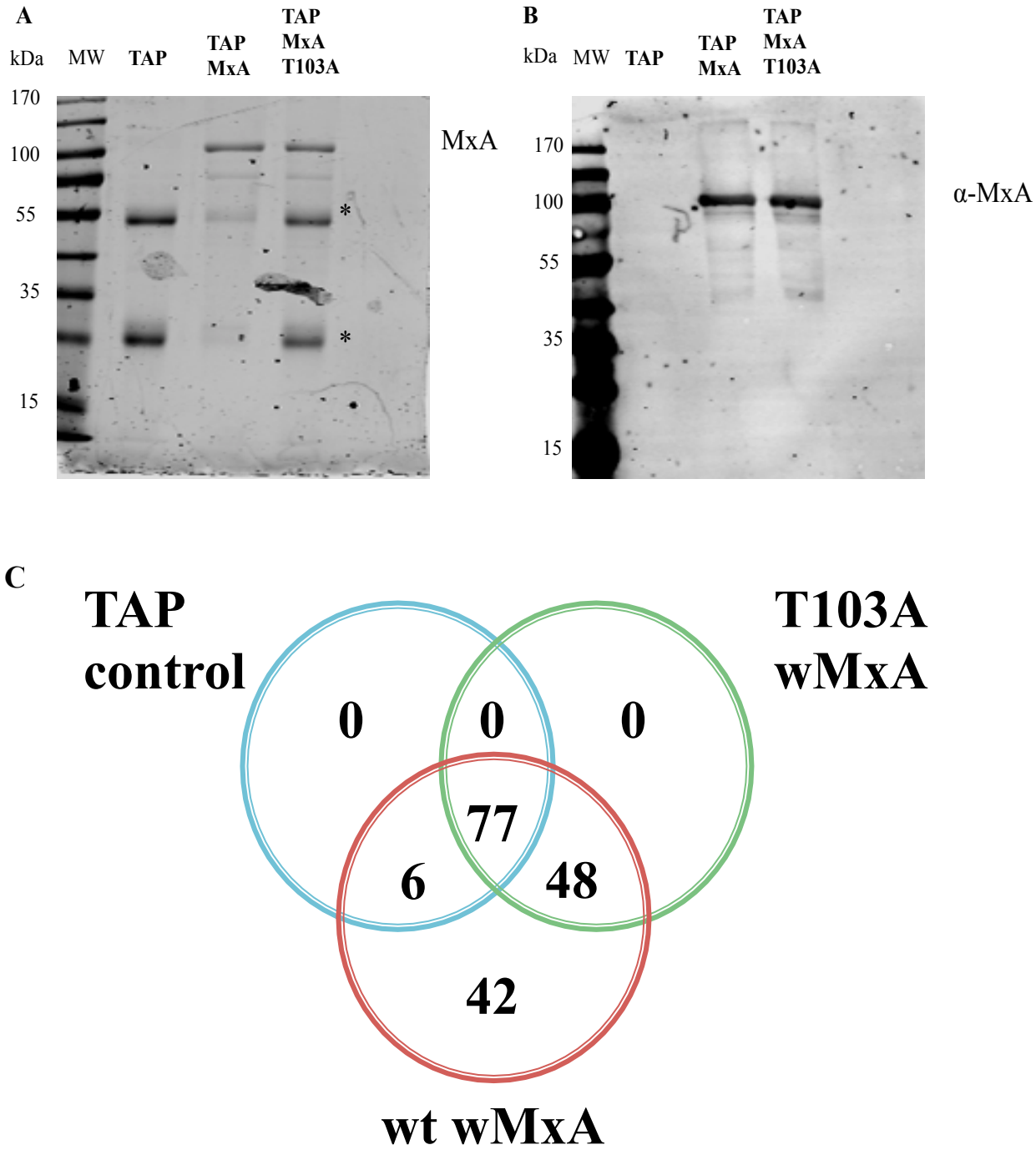


**Figure 4.7. Purification of potential MxA interacting partners.** TAP wt wMxA and TAP T103A wMxA were transfected into 293T cells alongside a TAP only control and cell lysates harvested 48 hours post-transfection. Following purification, protein lysates were analysed by SDS-PAGE via coomassie staining **(A)** and immunoblotting **(B).** MxA was detected using an anti-rabbit MxA antibody and then probed with a goat-anti-rabbit secondary antibody. **C**. Following MS/MS analysis of purified lysates, protein hits were further analysed using Scaffold 4 to determine the number of protein hits specific to MxA, T103A and the TAP control as depicted by the Venn diagram. *Denotes heavy and light antibody chains.

Table 4.3 shows a selected number of previously unidentified proteins that interact with MxA, and whether these proteins are identified as interacting with either wt wMxA or T103A wMxA. These proteins were selected for their potential relevance to the antiviral activity of MxA. This list predominantly features a large number of proteins that are directly related to nuclear import and protein trafficking. This is particularly interesting as both antiviral mechanisms proposed for MxA have an impact on the ability of influenza A virus to either traffic the genome or nascent NP into the nucleus. The interaction with Clathrin is interesting in relation to the IFN-dependent block described by Xiao et al. (2013) as this suggests that MxA is potentially interacting directly with the endocytic pathway, even in the absence of IFN. Also, MxA is shown to interact with a number of different coatomer subunits. Coatomer complexes are involved in the trafficking of membrane bound vesicles during endocytosis as well as for trafficking between the Golgi apparatus and the ER (L. P. Jackson 2014). This also suggests that MxA interacts with the endocytic machinery but also plays a role in transport between the Golgi and the ER, which is in agreement with localization of MxA (Accola et al. 2002).

| Protein | Function | Wt wMxA | T103A wMxA |
|---|---|---|---|
| **Clathrin** | Endocytosis | ✓ | ✓ |
| **Coatomer Subunits** | Endocytosis/Retrograde Transport | ✓ | ✓ |
| **Importin Subunit B-1** | Nuclear Import | ✓ | ✓ |
| **DDX39A** | RNA Helicase | ✓ | ✓ |
| **Hsp90** | Molecular Chaperone | ✓ | ✓ |
| **RANBP5** | Nuclear Import | ✓ | × |
| **Importin-4** | Nuclear Import | ✓ | × |
| **Importin-8** | Nuclear Import | ✓ | × |
| **Importin-9** | Nuclear Import | ✓ | × |
| **Nucleoporin (NUP 205)** | Nuclear Import | ✓ | × |
| **Alpha-Actinin 4** | Cytoskeleton | ✓ | × |

**Table 4.2 Selected interacting partners of MxA.** The MS/MS analysis identified 173 unique proteins that were precipitated by wt MxA. These proteins have been highlighted for their potential insight into the antiviral activity of MxA or known involved in the replication cycle of influenza A virus.

## 4.6 Discussion

Following a review of the literature a number of mutations in MxA previously shown to affect functions and characteristics of MxA were cloned into the wMxA gene within the pCAGGs mammalian expression vector to assess the affects of these mutations on the antiviral activity of MxA against a human-derived influenza virus polymerase (A/Udorn/72 virus), and an avian-derived influenza virus polymerase (A/Thailand/1(KAN-1)/04). A number of these mutants had been previously described in the literature and behaved similarly in the context of wMxA such as F561V and D478A. Whereas some of these had not been tested against influenza A but had displayed antiviral activity against THOV like L612K (Mitchell et al. 2012; S. Gao et al. 2011; Janzen, Kochs, and Haller 2000). However, a number of these mutations had not been previously characterised for antiviral activity such as I376D, F602D, the human polymorphisms G255E and V268M, as well as the lipid binding mutants AKAK and KEKE (Haller et al. 2010; Daumke et al. 2010; Duc et al. 2012; von der Malsburg et al. 2011). Interestingly the F602D mutant, in which MxA is monomeric, displayed a similar level of antiviral activity to wt MxA (Fig 4.3), which suggests that oligomerisation is not required for the antiviral activity of MxA post-primary transcription and agrees with the previous work shown for the other monomeric mutant, L612K, against THOV. Therefore it is not surprising that these two mutations show similar antiviral phenotypes. The two lipid binding mutants, AKAK and KEKE, showed a reduction in antiviral activity in comparison to wt MxA, but showed a similar level of activity to the L4 loop mutant F561V. It is plausible that the lipid-binding ability of MxA is involved in conferring its antiviral activity. However, the lipid-binding mutations occur close to the L4 loop. This flexible loop

has been shown to be highly important for antiviral activity against both orthomyxoviruses and bunyaviruses, therefore if these mutations impact the structure of the L4 loop this could also explain the reduction in antiviral activity (Mitchell et al. 2012; Patzina, Haller, and Kochs 2014).

Intriguingly, in the context of wMxA, both human polymorphisms, G255E and V268M, appeared to reduce the antiviral activity of MxA, but not to completely prevent this activity (Fig. 4.3 and 4.4). During these studies a paper was published in which the antiviral activity of these mutants was tested in the context of non-wobbled MxA and the authors showed the same reduction in antiviral activity conferred by the V268M mutation, however the G255E mutation completely abrogated antiviral activity (Dick et al. 2015a). The difference between the antiviral activity described in the wobble and non-wobble constructs was later determined to likely be due to differences in the coding RNA sequences. However, based on structural models described by Dick et al. (2015) these SNP mutations localise to the G interface and may influence dimer formation. Suggesting that when correctly folded these mutants may show diminished GTP hydrolysis alongside a reduced antiviral activity. Reductions in antiviral activity as a direct result of these and other SNPs in MxA could have significant implications for susceptibility of individuals to infection by influenza and many other viruses. Two SNPs found in the promoter region of MxA have been shown to be important for patient susceptibility for a number of different viruses including, SARS, enterovirus 71 and HCV (Hamano et al. 2005; X. Zhang et al. 2014; Shaker, Abdel-Rahim, and Bayoumi 2015). Therefore, it would be interesting and important to study whether such coding polymorphisms are present in

patients suffering from severe influenza infection as has been described recently for IFITM3 (Everitt et al. 2012).

It was previously reported that NP derived from avian influenza viruses is more susceptible to the antiviral effect of MxA post-primary transcription (Zimmermann et al. 2011) and NP residues conferring resistance/susceptibility to MxA have since been reported (Mänz et al. 2013). Based on these findings, the wMxA constructs were tested for their antiviral activity against in a mini-genome reporter assay using the viral polymerase derived from either A/Udorn/72 virus, a human virus that carries two of the key resistance mutations identified by Mänz et al. (2013), or A/Thailand/1(KAN-1)/04, an avian virus that is deemed to be Mx-sensitive. Interestingly, there did not appear to be a large difference in the susceptibility displayed between A/Udorn/72 and A/Thailand/1(KAN-1)/04 as both showed a 60% reduction in relative luciferase activity in comparison to samples lacking MxA (Figure 4.3 and 4.4). However, these experiments were transfection-based, the results of which are heavily influenced by the amount of plasmid that is transfected into the cells and the strength of the promoter from which the genes of interest are transcribed, particularly as it has been shown that increasing levels of NP is capable of outcompeting MxA and vice-versa (Zimmermann et al. 2011). A more appropriate read out to determine the impact of MxA sensitivity would be through viral infection in cell lines which constitutively express MxA, allowing the levels of viral protein to be determined via infection with equal number of infecting virus particles, rather than by plasmid promoter strength.

Following the recent publication from Dick et al. (2015), the mutants previously expressed in the wMxA background were cloned into a wt mRNA background and assessed for the impact on both phenotype and functionality in comparison to the wMxA constructs. Although a number of the constructs displayed a similar distribution to that observed for the wMxA versions, four constructs showed markedly different expression phenotypes (Fig. 4.5). Two of these mutants, T103A and G255E, were highly aggregated. This clarified the discrepancy between the inhibitory effect seen for the wMxA T103A, which had originally been described as an antiviral-null mutant using the wt mRNA background (Ponten et al. 1997). This loss in antiviral activity was attributed to the loss of GTPase activity as a result of the mutation, which was also suggested to be the reason for the punctate aggregation, as MxA is thought to require GTP-binding in order to oligomerise and localise to syntaxin-17, a marker for the smooth ER. Therefore, it was thought that MxA containing the T103A mutation is capable of binding to GTP but incapable of hydrolyzing it, leading to the formation of aggregates (Dick et al. 2015a). However, Fig. 4.5 shows that wMxA T103A does not show the same phenotype as that previously reported, showing a diffuse cytoplasmic staining akin to wt MxA as well as some punctate regions of higher molecular weight oligomers. Also, wMxA T103A is not completely antiviral-null (Fig. 4.6). Therefore the previously observed T103A phenotype is unlikely to be due to the protein sequence but should actually be attributed to the change in RNA sequence leading to protein aggregation.

The human polymorphism, G255E, was also characterised by Dick et al. (2015), and was determined to have no GTPase activity, like T103A. Similarly, G255E demonstrates the same phenotype, producing cytoplasmic aggregates with abolished

antiviral activity in the context of wt mRNA. Yet G255E wMxA not only exhibits a wt-like expression phenotype but also only shows minor attenuation in antiviral activity. A defining feature of both the T103A and G255E mutants is that they have been shown to have no GTPase activity in the context of wt mRNA, and therefore GTPase activity has been suggested to be integral to the antiviral activity of MxA. This has not yet been determined for the wMxA mutants but if these mutations do abolish GTPase activity then the antiviral activity seen for wMxA T103A and wMxA G255E suggests that although GTPase activity is important for MxA to fully exert its antiviral effect it may not be the whole story.

Interestingly, the other two mutants to exhibit different expression phenotypes were I376D and D478A, previously described as structural mutants which inhibited tetramer formation or encoded for a stalk interface mutant respectively (S. Gao et al. 2010; S. Gao et al. 2011). Although the previously published data did not show immunofluorescent data or antiviral activity for I376D, the differences in the expression phenotypes and antiviral activity in the different mRNA backgrounds is striking. Although, both I376D constructs show attenuation in comparison to wt MxA (Fig. 4.6), it appears that this mutant is still capable of exerting an antiviral effect post-primary transcription against influenza A virus.

MxA containing the D478A mutation was shown to behave similarly to wt MxA in a mini-replicon assay (Fig.4.6). Although, the distribution of the protein derived from the non-wobbled construct is similar to that seen by Gao et al, (2011), in this study it is not in the context of LACV N expression. This suggests that although D478A is capable of sequestering LACV N, however this mutation in the context of the wt

mRNA sequence is capable redistributing the localization of MxA, whereas the wMxA D478A construct offers a typical MxA staining pattern. This suggests that the staining pattern seen by Gao et al. (2011) is not due to the sequesteration of LACV N, but actually due to the change in mRNA sequence. The specific localization of these two mutants is unknown, although both appear to be perinuclear in appearance, the exact location may offer further evidence to determine what is required MxA to exert the full extent of its antiviral activity.

Intriguingly, for each mutant MxA, the amino acid sequence that is translated from both the wt and wobble mRNA constructs is identical, suggesting that the phenotype seen for these mutants may not be due to the individual mutation, but may be caused by changes to the mRNA sequence. It is possible that these changes in RNA sequence may have impacted the secondary structure of the RNA and therefore impacted interactions with RNA binding proteins and potentially altering the rate of translation. The impact of these mutations was assessed through the RNA secondary structure prediction software, mFold and is discussed further in the Appendix (A1).

Following the differences observed in antiviral activity between the wobble and non-wobble derived MxA proteins and the suggestion of a co-factor being necessary for MxA to exert it's IFN-dependent antiviral effect by Xiao et al, (2013), wt wMxA and the antiviral attenuated T103A wMxA were used in an attempt to identify potential interacting partners to offer an insight into the antiviral mechanism of MxA. As a marker for the successful purification of interacting partners, it was necessary to compare the protein hits with interacting partners that have been previously identified. A number of precipitated proteins had been identified previously by other studies

such as actin, tubulin, fanconi anemia proteins and HNRNP1 (Horisberger 1992; Reuter et al. 2003; Roy et al. 2014). This purification also identified one of the previously identified RNA helicases, URH49 (DDX39A) but not UAP56, which were previously shown to interact with MxA (Wisskirchen et al. 2011). This discrepancy could be down to a number of different reasons, for example, the method of precipitation and the buffers used to both lyse the cells and wash the beads are likely to be different between the different precipitation procedures, which could impact the proteins identified post-purification. Another reason for this difference is the threshold of detection and the amount of sample used for the MS/MS analysis, which could also influence the nature of the hits.

However, this analysis did also identify a large number of proteins that have not previously been reported to interact with MxA. Interestingly, a large number of these were involved with the nuclear import processes, as many importin proteins were identified as interacting with wt wMxA but not with T103A wMxA. A number of these proteins have also previously been shown to play a role during influenza A virus infection. Importin-β-1 is part of the classical nuclear import pathway, which is used by both vRNPs and monomeric NP as well as PB2 through direct interaction with importin-α, which then binds to Importin-β-1 before trafficking to the nuclear pore complex (E. C. Hutchinson and Fodor 2012; Strambio-De-Castillia, Niepel, and Rout 2010). Whereas PB1 and PA are imported to the nucleus using RANBP5, another protein identified as interacting with MxA, which is an importin-β-1 homologue which conducts nuclear import independently of importin-α (E. C. Hutchinson and Fodor 2012). Intriguingly, another protein suggested to be involved in the nuclear import of influenza polymerase proteins, Hsp90, suggested to import PB1-PB2 or

PB1-PA heterodimers directly into the nucleus, (Naito et al. 2007), was also identified as interacting with MxA. Alpha-actinin 4 was precipitated by wt wMxA. This protein has been shown to be important for efficient viral replication through directly interacting with NP and it has been suggested that this protein may have a role in the nuclear localization of NP (S. Sharma et al. 2014).

Taking all of this information together it seems there is a large degree of overlap between the proteins precipitated by MxA and those required by various components of influenza A viruses to gain entry into the nucleus. What is striking is the absence of some of these factors from T103A wMxA, a mutant that displays reduced antiviral activity compared to wt MxA. This reduced activity may be explained by a lack of GTPase activity, but could also be explained by the lack of interaction with an intermediate host factor required by MxA to block the nuclear import of NP. Although this requires further work, coupled with the inability to precipitate influenza NP with MxA without cross-linking conditions, this data opens the possibility for an alternative model of MxA antiviral action.

## Chapter 5 - Investigating the antiviral mechanism of MxA using constitutive expressing cell lines

In section 4 a number of mutations were inserted into MxA (Table 4.1) to determine which characteristics are essential to the antiviral activity against influenza A virus post-primary transcription. However, this analysis was done in the context of transient expression and did not determine the impact of each these mutations on the virus as a whole or in the context of IFN treatment, the native cellular environment for MxA.

Both the literature and the findings in section 3 show that MxA appears to have two distinct functions, one which is IFN-independent and one which is IFN-dependent (Xiao et al. 2013; Matzinger et al. 2013). Although it is clear that the block on nuclear translocation of the influenza virus genome during viral entry is dependent on both MxA and IFN, little is known about the specific details of this block. It has previously been shown that the viral genome localised near to, but not co-localised with Rab-7, a marker for late endosomes, but how and where MxA is recruited to incoming virus particles is still unknown (Xiao et al. 2013).

This section investigates the impact of the MxA mutations on the ability of MxA to exhibit an antiviral effect on influenza A virus in both context of IFN and viral infection. Secondly, this chapter addresses the localization of MxA and attempts to elucidate further aspects of MxA's ability to block the viral genome translocation to the nucleus prior to primary transcription.

## 5.1 Characterisation of cell lines

To achieve constitutive expression of the mutant wMxA constructs, A549-ΔMxA cells were transduced with lentiviruses encoding for the mutant of interest and selected for using puromycin; from here on in, all A549-ΔMxA cells expressing reintroduced wMxA will be referred to as A549-wMxA. A549-ΔMxA cells were used to create the wMxA-expressing cells such that the effects of the MxA mutations could be observed in the absence of endogenous MxA. The original transduction led to constitutive expressing cell lines that were heterogeneous in their expression levels. Therefore, to really assess the impact of these mutations it was necessary to select cells from a single colony to ensure for homogenous expression across the population, therefore allowing more certainty when assessing the effect these mutations have on the antiviral activity of MxA.

Fig. 5.1 shows the both the expression levels and cellular distribution of each of the A549-wMxA cell lines as determined by immunofluorescence. All wMxA cell lines showed diffuse cytoplasmic staining, similar to that observed in naïve A549s that have been pre-treated with IFN.

MxA expression was further tested by immunoblotting analysis (Fig. 5.2 A). Fig. 5.2 B shows the level of wMxA expression normalized to the levels of actin in each cell line compared to A549-MxA expression levels, which was set at 100%. It is clear that the level of expression wMxA expression is highly reduced in comparison to the A549-MxA cell line, with only A549-wR640A and A549-wD478A cells expressing over 20% the level of MxA seen in the A549-MxA cells. A549-wWT MxA only

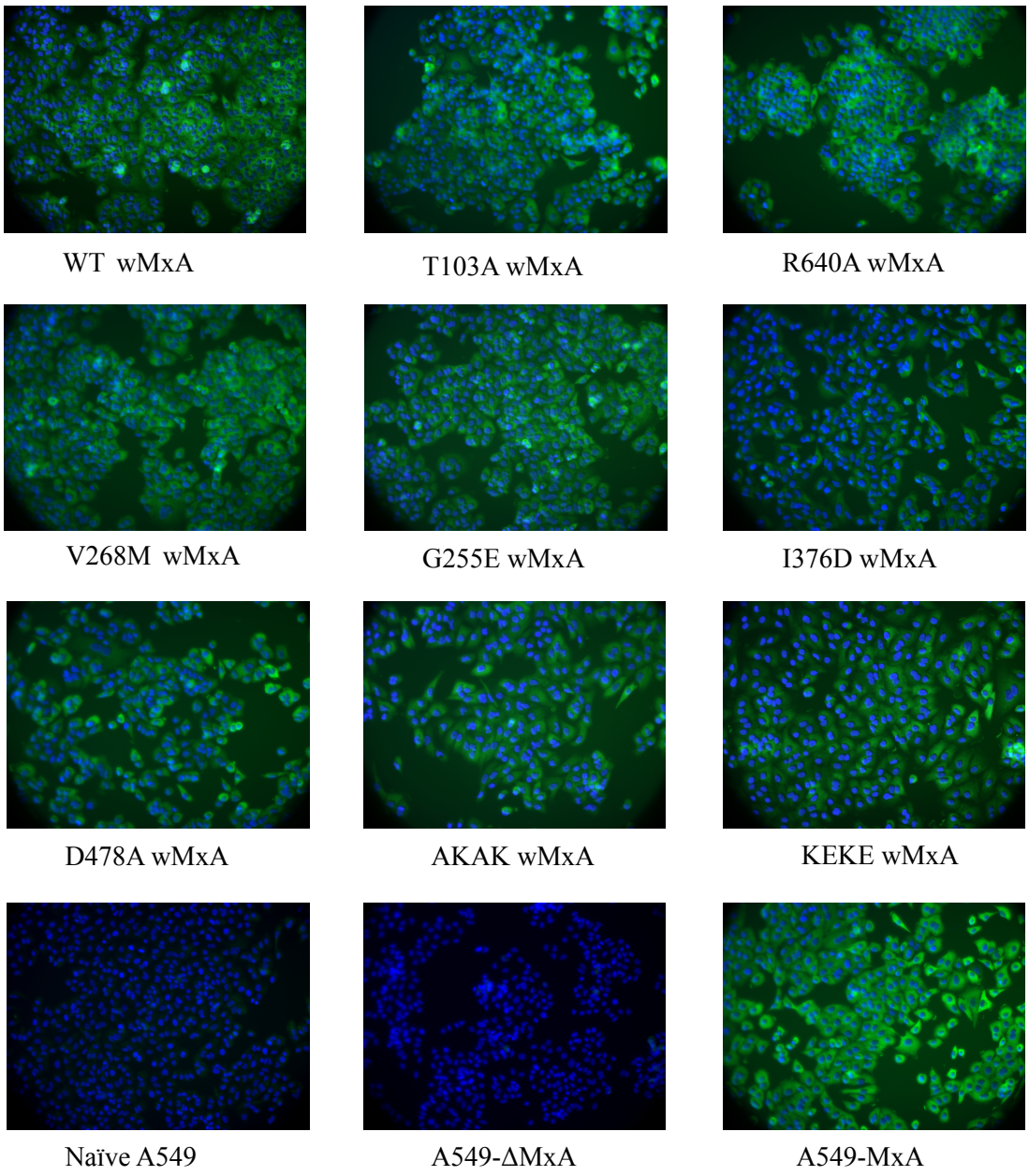


**Figure 5.1 Expression and cellular distribution of wMxA in A549-wMxA cell lines.** Clonally selected A549-wMxA cells were subjected to immunofluorescence analysis using a rabbit α-MxA polyclonal antibody and an Alexa-488 conjugated goat α-rabbit secondary antibody. Nuclei were stained using DAPI. Green; α-MxA Blue; DAPI-stained nuclei.

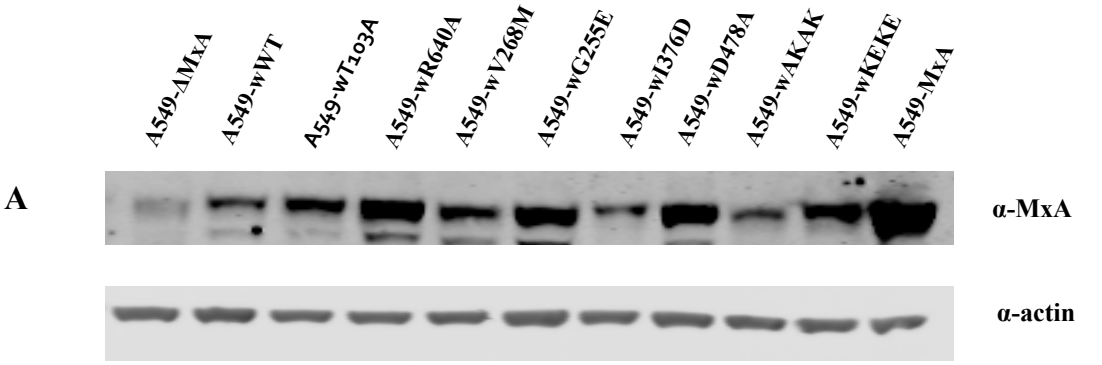


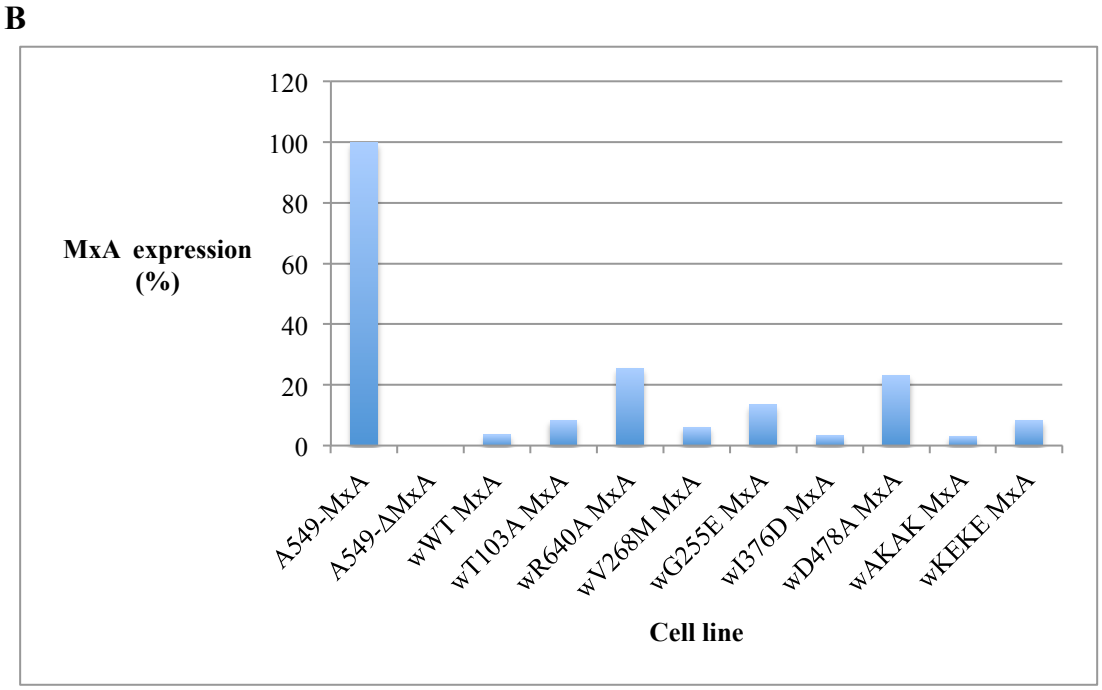


**Figure 5.2 MxA protein expression levels. A.** Immunoblot showing the MxA expression levels in the A549-wMxA cells in comparison to A549-MxA cells. MxA was detected using a rabbit anti-MxA antibody and actin was detected as a loading control **B.** Quantification of MxA expression levels, firstly normalised to actin, then to A549-MxA which was set as 100% MxA expression.

expressed to 3.5% the level seen in the A549-MxA cells, with similar levels produced in the A549-wI376D and A549-wAKAK cells. The A549-wV268M and A549-wKEKE expressed 6% and 8% respectively, whereas A549-wT103A and A549-wG255E expressed MxA at 8% and 13% the level expressed in A549-MxA cells. This is an important read-out when determining the importance of these mutations.

Unfortunately, it was not possible to create constitutively expressing cell lines for F561V, or the two monomeric mutants, F602D and L612K. In the case of F561V, despite several attempts at single colony selection, it was not possible to select a colony with good expression levels. Stability issues were caused by the monomeric mutations leading to declining levels of protein expression with each passage of the cells. This phenomenon has also been observed by another group (Personal communication: Jovan Pavlovic).

**5.2 Impact of MxA mutants on influenza A virus protein expression**

To determine the impact of wMxA on influenza A virus protein expression, A549-ΔMxA cells and the A549-wMxA mutant cells, were infected with A/Udorn/72 virus at an MOI of 5. Following infection cell lysates were collected 8 h.p.i and assessed for the levels of viral NP via immunoblotting. Figure 5.3 A shows that in the absence of IFN the impact of MxA on NP expression is minimal but does show some minor differences across the different A549-wMxA cell lines. Figure 5.3 B shows the levels of viral protein being produced firstly normalised to actin as the loading control and then normalised to the parental A549-ΔMxA cells. There was an approximate 10% reduction in the levels of influenza virus NP produced in the A549-wWT MxA cells

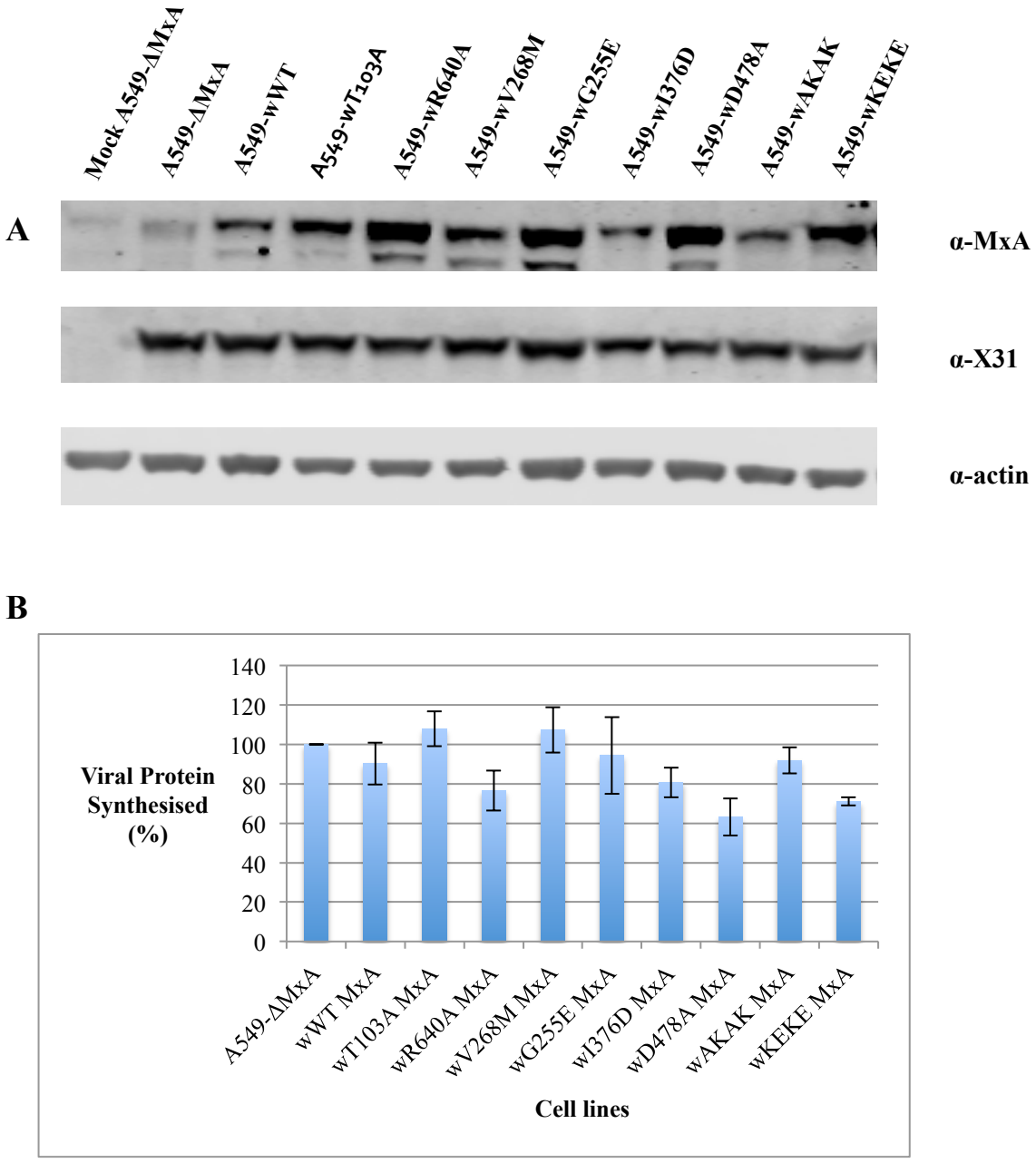


**Figure 5.3 Impact of wMxA on influenza A virus protein expression. A.** Immunoblot showing the level of influenza A virus NP expressed 8 h.p.i in either A549-Δ MxA or A549-wMxA cells. Influenza NP was detected using a sheep anti-X31 antibody, MxA was detected using a rabbit anti-MxA antibody and actin levels were detected as a loading control. **B.** Quantification of NP synthesized 8 h.p.i firstly normalised to actin and then normalised to NP levels in A549-Δ MxA. The results represent the average of three independent experiments ± S.D.

in comparison to A549-ΔMxA cells, with A549-wI376D also showing a similar level of inhibition. This coupled with the protein expression levels shown in Fig 5.2 indicates that only a small amount of MxA is required to have an impact on influenza A replication post-primary transcription (as the antiviral effect of MxA at this stage of viral replication is independent of IFN treatment). The expression of wT103A and the two human polymorphisms, wV268M and wG255E did not appear to reduced the level of NP produced, as levels were similar to those observed in cells lacking MxA (A549-ΔMxA cells). This suggests that GTPase activity is likely important to inhibit virus replication post-primary transcription and also that the two human polymorphisms are attenuated in their antiviral activity at this stage of infection. Interestingly, the two lipid-binding mutants displayed some antiviral activity with A549-wAKAK showing similar inhibition to A549-wWT and A549-wKEKE showing an increased reduction to 70% the level of NP produced in A549-ΔMxA cells. Also, the two cell lines that exhibit the highest level of MxA expression, A549-wR640A and A549-wD478A, showed an increased level of NP reduction, reducing the levels of expression by 24% and 37% respectively.

These results indicate that the over-expression of wMxA does indicate that a number of these mutations are still capable of impacting influenza A virus replication post-primary transcription. However, as shown in section 3.5 the impact of MxA on influenza virus protein expression is more prominent in the presence of IFN. Therefore, A549-ΔMxA cells and the A549-wMxA mutant cells were infected with A/Udorn/72 virus at an MOI of 5 following pre-treatment with IFN (1000 U/mL) 16 hours prior to infection. Following infection cell lysates were collected 8 h.p.i and assessed for the levels of influenza A virus NP via immunoblotting.

Figure 5.4 A shows the impact of each A549-wMxA mutant on NP production in the presence of IFN. As expected MxA expression was not observed in A549-ΔMxA cells. Differing levels of influenza NP expression in the presence of IFN were observed in the different A549-wMxA cell lines, suggesting that some of the introduced mutations are likely important to the antiviral activity exerted by MxA when the cell is in an antiviral state. Figure 5.4 B displays the levels of viral protein being produced normalised to actin as the loading control and then normalised to NP levels in the parental A549-ΔMxA cells. The A549-wWT MxA cells demonstrated a similar level of NP to that observed in the absence of IFN treatment (Fig 5.3 B). This was slightly surprising as MxA is such a key factor in the host antiviral response, however this may be due to the relatively low level of wWT MxA expression in these cells. A similar level of NP to that of wWT MxA-expressing cells was observed in A549-wG255E cells, which suggests in the presence of IFN, this polymorphism mutant is capable of inhibiting influenza A virus to a similar level as wt MxA. A similar level of NP was observed in A549-wI376D cells, which expresses MxA at a similar level to A549-wWT MxA and therefore suggests that this mutation is also capable of inhibiting influenza A virus in a similar way to wt MxA.

Interestingly, one of the lipid-binding mutants, A549-wAKAK, showed an increased level of inhibition, reducing influenza NP levels to 74% of A549-ΔMxA cells, suggesting that this mutation does not have an impact on the ability of MxA to inhibit influenza A virus, however, in comparison to the other lipid-binding mutant, A549-wKEKE, there is marked difference. A549-wKEKE cells expressed a similar level of NP to A549-ΔMxA cells, suggesting that this

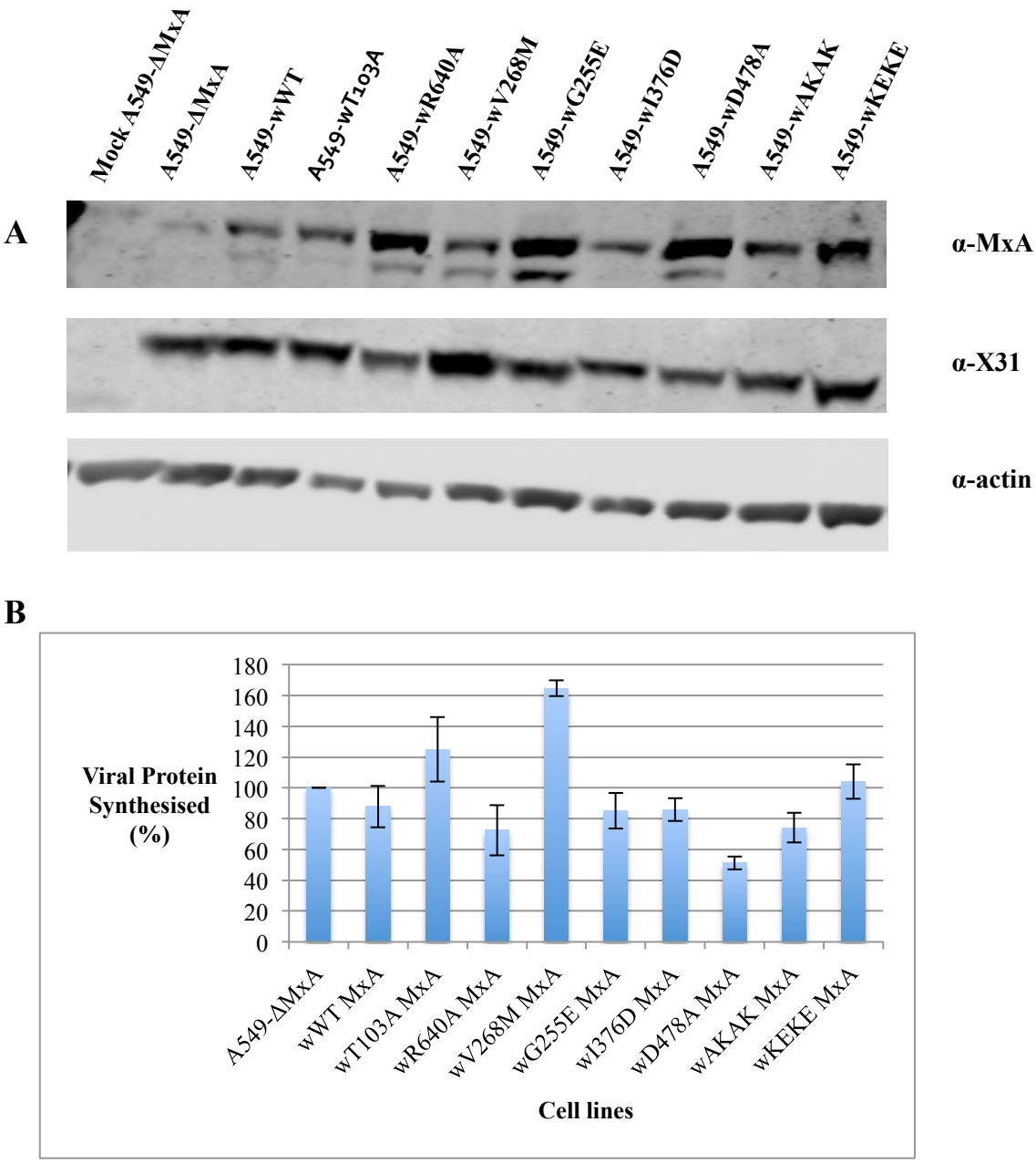


**Figure 5.4 Impact of wMxA on influenza A virus protein expression in the presence of IFN. A.** Immunoblot showing the level of influenza virus NP expressed 8 h.p.i in either A549-ΔMxA or A549-wMxA cells following 16 hours pre-treatment with IFN (1000 U/mL). NP was detected using a sheep anti-X31 antibody, MxA was detected using a rabbit anti-MxA antibody and actin levels were detected as a loading control. **B.** Quantification of NP synthesized 8 h.p.i firstly normalised to actin and then normalised to NP levels in A549-ΔMxA cells. The results represent the average of three independent experiments ± S.D.

lipid-binding mutant is potentially not capable of inducing the IFN-mediated block on influenza prior to primary transcription. It is also interesting to note that two other mutants, A549-wT103A and A549-wV268M, appear to show no increased reduction on influenza NP production, in fact both cell lines showed an increase in viral protein in comparison to A549-ΔMxA cells. This data suggests that MxA appears to require GTPase activity to fully exert the antiviral effect against influenza A virus in the context of IFN, whereas the human polymorphism V268M appears to be incapable of exerting the IFN-dependent antiviral function of MxA against influenza A virus. The two cell-lines that express the most MxA showed the largest reduction in influenza NP production, reducing the levels of protein by 28% in the A549-wR640A cells and by 49% in the A549-wD478A cells.

### 5.3 Influenza A virus replication analysis

Although the results in section 5.2 give a clear indication of the impact of these mutations on the ability of MxA to restrict viral protein production, it does not show the overall influence of these mutations on the amount of virus produced during infection. To assess this naïve A549, A549-MxA and A549-ΔMxA cells were infected alongside the A549-wMxA mutants with A/Udorn/72 virus at an MOI 5, supernatant samples were taken every 3 hours until 15 h.p.i and then at 24 h.p.i and the infectious titre of each determined by viral plaque assay on MDCK cells.

As seen previously in section 3.6 and Fig 3.11, the over-expression of MxA in the A549-MxA cells leads to a log-reduction in the number of infectious virions produced in comparison to A549-ΔMxA cells and an approximately 0.5 log-reduction in

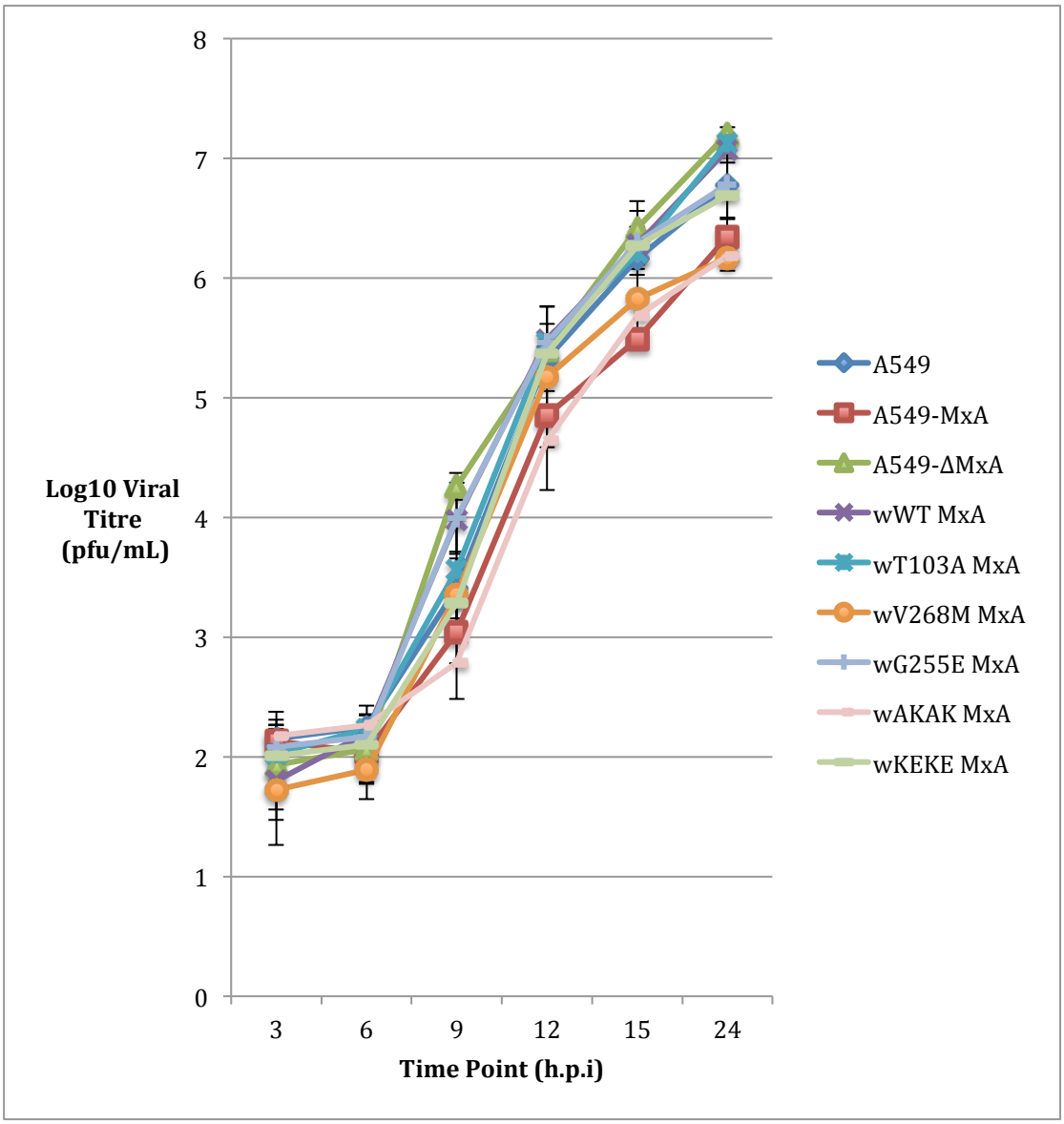


**Figure 5.5. Impact of wMxA on influenza A virus during a single cycle of replication. A.** Naïve A549, A549-MxA, A549-ΔMxA and the A549-wMxA cells were infected at an MOI 5 using A/Udorn/72. Samples were taken every 3 h.p.i until 15 hours and then at 24 h.p.i and infectivity determined by titration via plaque assay on MDCK cells.

comparison to naïve A549s (Fig. 5.5). Between 9 and 15 hours there does not appear to be a discernable difference in the number of infectious particles produced between the naïve A549 cells and the A549-wMxA cells for wt wMxA, wT103A, wG255E and wKEKE, suggesting that the over-expression levels in these cells may not be high enough to exhibit an impact on the level of infectious virions produced (Fig 5.5). These A549-wMxA cells did not show a large reduction in the number of virus particles produced compared to the parental A549-ΔMxA cells over the duration of the time course, with the largest difference being seen after the initial burst of virus production at 9 h.p.i. The human polymorphism cell line A549-wV268M, also showed similar levels of virus production as naïve A549 cells until the later time points. At 15 hours there was a minor reduction in infectious virus produced, although the range of plaques formed showed that this was not a significant reduction in plaque number, whereas at 24 h.p.i, the plaque number was similar to those produced by A549-MxA cells. Interestingly, one of the lipid-binding mutants, wAKAK, showed viral attenuation on a par with A549-MxA. This is somewhat surprising based on the differences in protein levels described in Fig 5.2, with these cell lines expressing less than 10% the amount of MxA expressed in the A549-MxA cells. Interestingly, this offers a similar insight as shown in Fig. 5.3 B, which suggests that the cell does not require a large amount of MxA to exhibit an antiviral effect post-primary transcription in the absence of IFN.

**5.4 Plaque reduction assays**

Although section 5.2 offers a clear indication of the inhibition offered by each of these mutations in both the presence and absence of IFN, it only determines the impact on protein expression at a high MOI during a single replication cycle.

Therefore, to see the impact of both these mutations through multiple replication cycles the A549-wMxA cells were assessed for the ability to inhibit the production of plaque-forming units in comparison to the parental A549-ΔMxA cells, naïve A549 cells and A549-MxA cells in the presence and absence of IFN. The cells were infected with 10-fold serial dilutions of A/Udorn/72 virus following either treatment with IFN (1000 U/mL) or no treatment for 16 hours prior to infection. Cells were then fixed 5 days post-infection and plaques visualised via immunostaining. Plaque number was then normalised to the number of plaques produced on the untreated A549-ΔMxA cells, which was set to 100%.

Fig. 5.6 shows the effect of each wMxA mutant on plaque number. In the absence of IFN, it is clear that the over-expression of the MxA mutants appeared to demonstrate an inhibitory effect on plaque number in comparison to the parental cell line A549-ΔMxA. However, in the various wMxA-expressing cells plaque number was approximately 50-60% the number observed in A549-ΔMxA cells, which is similar to the plaque number observed in naïve A549 cells. The A549-MxA cells showed a more dramatic impact on plaque number, reducing plaque number by approximately 75% in comparison to A549-ΔMxA cells. Surprisingly plaque number in the A549-wR640A cells was reduced by approximately 70% compared to A549-ΔMxA cells However this may be due to the increased levels of MxA expressed in this cell line in comparison to the others, as seen in Fig. 5.2.

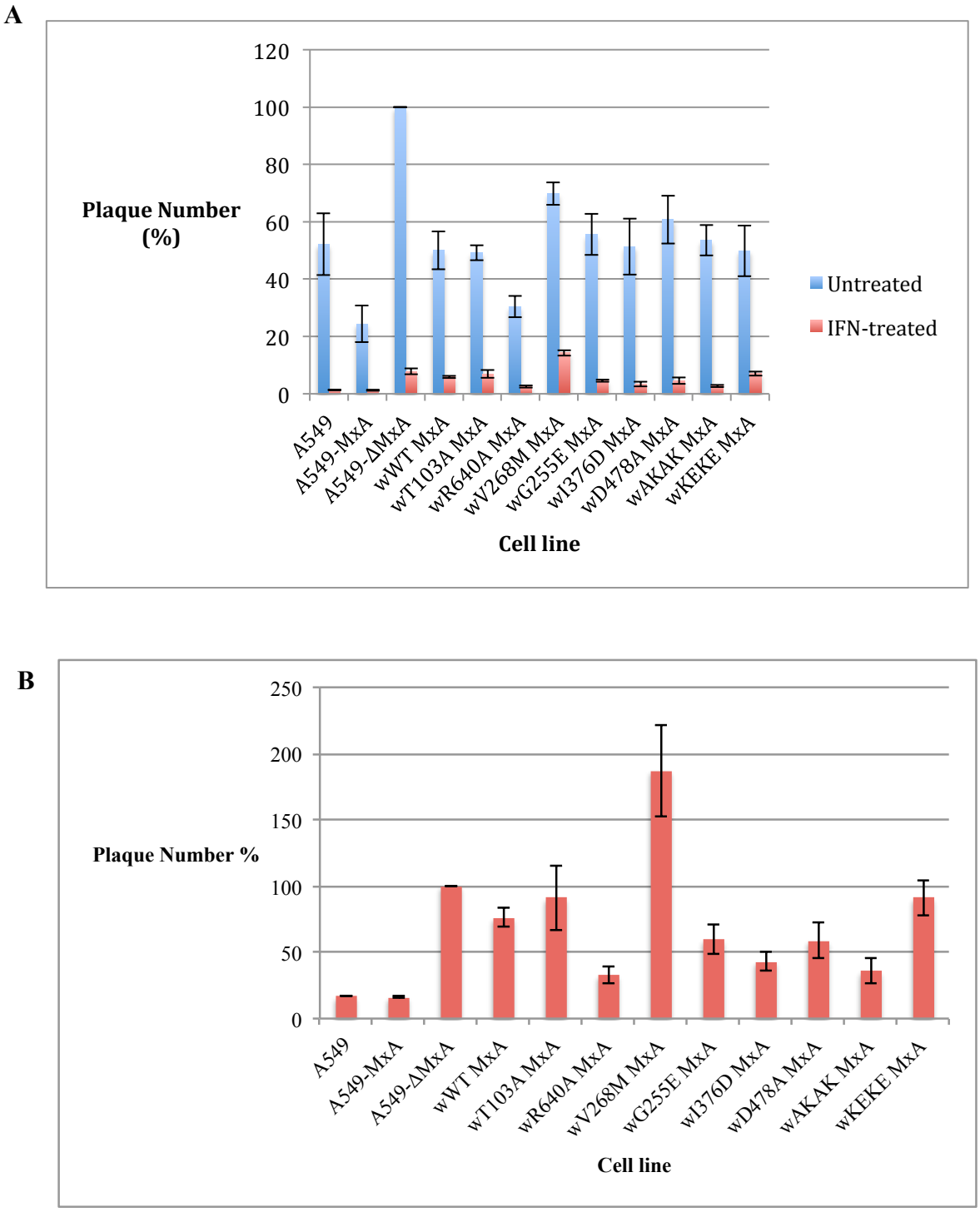


**Figure 5.6 Impact of wMxA on influenza A virus plaque development.** Naïve A549, A549-MxA, A549-ΔMxA and the A549-wMxA cells were either untreated or treated with IFN (1000 U/mL) 16 hours prior to inoculation with a serial ten-fold dilution series of influenza A/Udorn/72 in a viral plaque assay. Cells were fixed 5 days post-infection and plaque number was determined by immunostaining. Plaque number is expressed as a percentage of plaques observed on untreated A549-ΔMxA cells. Results are expressed as the average of three independent experiments ± S.D. **B.** Shows the same data for IFN-treated cells normalised to A549- ΔMxA cells in the presence of IFN.

In the presence of IFN (also shown in Fig. 5.6 B normalised to IFN-treated A549-ΔMxA cells), there were some more noticeable differences. It is clear from the reduction in plaque number that each cell line responded to treatment with IFN; however there were differing levels of plaque reduction between the various A549-wMxA cell lines. Both the naïve A549 cells and the A549-MxA cells reduced the plaque number to approximately 1.5% in the presence of IFN, whereas in the A549-ΔMxA cells plaque number was reduced to 8% in comparison to untreated A549-ΔMxA cells. Plaque number in the A549-wMxA wt, A549-wG255E and A549-wD478A cells was reduced to between 4-5%, which is an approximately 50% reduction in plaque number in comparison to IFN-treated A549-ΔMxA cells. It is interesting to note that three of the A549-wMxA cell lines reduced the plaque number to near A549-MxA levels, with the A549-wR640A, A549-wI376D and A549-wAKAK cells producing 2.5%, 3.3% and 2.7% the number of plaques observed on untreated A549-ΔMxA respectively.

Interestingly, A549-wT103A, A549-wV268M and A549-wKEKE, all showed similar patterns to that described in section 5.3, displaying similar plaque numbers, or in the case of A549-wV268M, an increase in the number of plaques in comparison to IFN-treated A549-ΔMxA cells. Both A549-wT103A and A549-wKEKE cells produced approximately 7% the number of plaques, suggesting a small additive effect for these two wMxA mutants in the presence of IFN in comparison to IFN-treated A549-ΔMxA cells. Whereas, A549-wV268M cells produced 14 % the number of plaques in comparison to IFN-treated A549-ΔMxA cells, a 6% increase on the number observed in A549-ΔMxA cells. Interestingly, these cells also showed a slightly higher number

of plaques in the untreated cells, showing only a 30% reduction in comparison to the other A549-wMxA mutants. The data therefore suggest that this human polymorphism may inhibit the IFN-dependent mechanism of MxA antiviral activity.

### 5.5 Investigating the antiviral activity of MxA using GFP MxA cell lines

MxA is known to localise closely to the ER membrane, being shown to co-localise with syntaxin-17 positive membranes (Dick et al. 2015; Accola et al. 2002). To see if these expression patterns were consistent across a range of different human lung cell lines, A549, BEAS-2B and Calu-3 cells were treated with IFN for 16 hours and then probed for MxA expression by immunofluorescence. Fig. 5.7 shows the expression patterns for MxA in each of the different cell lines. In both the A549 cells and BEAS-2B cells the MxA staining appeared more concentrated in the perinuclear region and also at the cell periphery around the plasma membrane. The perinuclear staining is likely to be MxA localizing to the ER and with MxA being known to shuttle between both the ER and the plasma membrane, the staining pattern was as expected (Accola et al. 2002). Calu-3 cells grow in clustered colonies rather than spread out like A549 or BEAS-2B cells, therefore it is more difficult to see this concentrated staining at the plasma membrane, but it is possible to determine increased staining in the perinuclear region.

This suggests that MxA is potentially capable of interacting with incoming virus particles from the moment the virus is endocytosed from the plasma membrane. Therefore in an attempt to determine where MxA is recruited to block incoming influenza virus particles, wt wMxA was tagged with GFP by cloning the gene into a lentivirus vector with an N-terminal GFP tag followed by a flexible linker to reduce

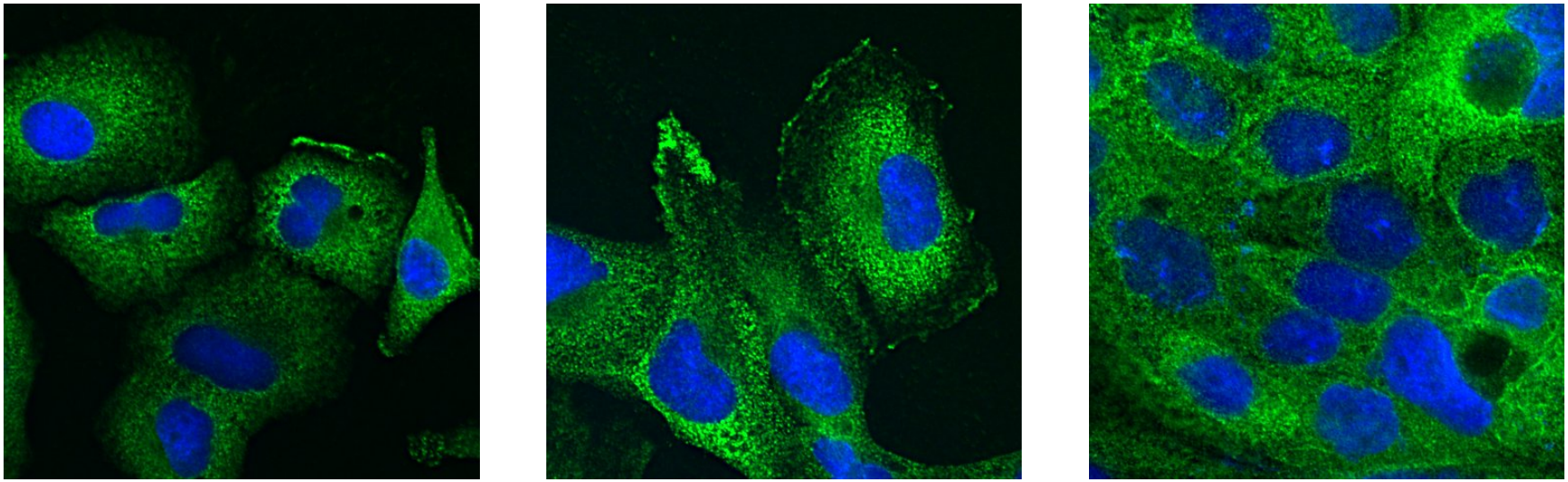


**Figure 5.7 MxA expression phenotypes in different human lung epithelial cells.** Immunofluorescent staining of A549, BEAS-2B and Calu-3 cells following treatment with IFN (1000U/mL) for 16 hours prior to fixation. Cells were first probed with an α-MxA polyclonal rabbit antibody then an Alexa-488 conjugated goat α-rabbit antibody. (Magnification 63x) Nuclei were stained using DAPI. Green; α-MxA Blue; DAPI-stained nuclei.

the likelihood of steric hindrance. The lentivirus was used to transduce both naïve A549 and A549-ΔMxA cells. Both of these cells offered heterogeneous populations of cells expressing different levels of GFP-MxA, therefore to maximize the expression levels, these cells underwent Fluorescence Activated Cell Sorting (FACS) to produce a population of cells with a good level of expression. Fig. 5.8 shows the expression pattern determined by immunofluorescence and the expression levels in both A549 GFP-wMxA and A549-ΔMxA-GFP-wMxA cells in the both the absence and presence of IFN via immunoblotting. There is a clear difference in the molecular weight between the GFP-wMxA and the endogenous MxA induced by IFN. Also, as expected the A549-ΔMxA-GFP-wMxA only show a band corresponding with GFP-wMxA even in the presence of IFN.

It had previously been noted within our lab that MxA is recruited into specific punctate spots within the cytoplasm in the event of infection with Pichinde virus, a member of the *Arenaviridae* family. Therefore to determine the functionality of GFP-wMxA, naïve A549 cells along with the two GFP-wMxA cell lines were infected with Pichinde virus at an MOI of 20, both in the presence and absence of IFN. The cells were fixed 48 h.p.i and immunostained for MxA. Fig. 5.9 shows that even in the absence of IFN, Pichinde virus is capable of inducing a large amount of MxA expression in naïve A549 cells and shows punctate cytoplasmic staining, suggesting that MxA is being recruited to potential sites of virus replication.

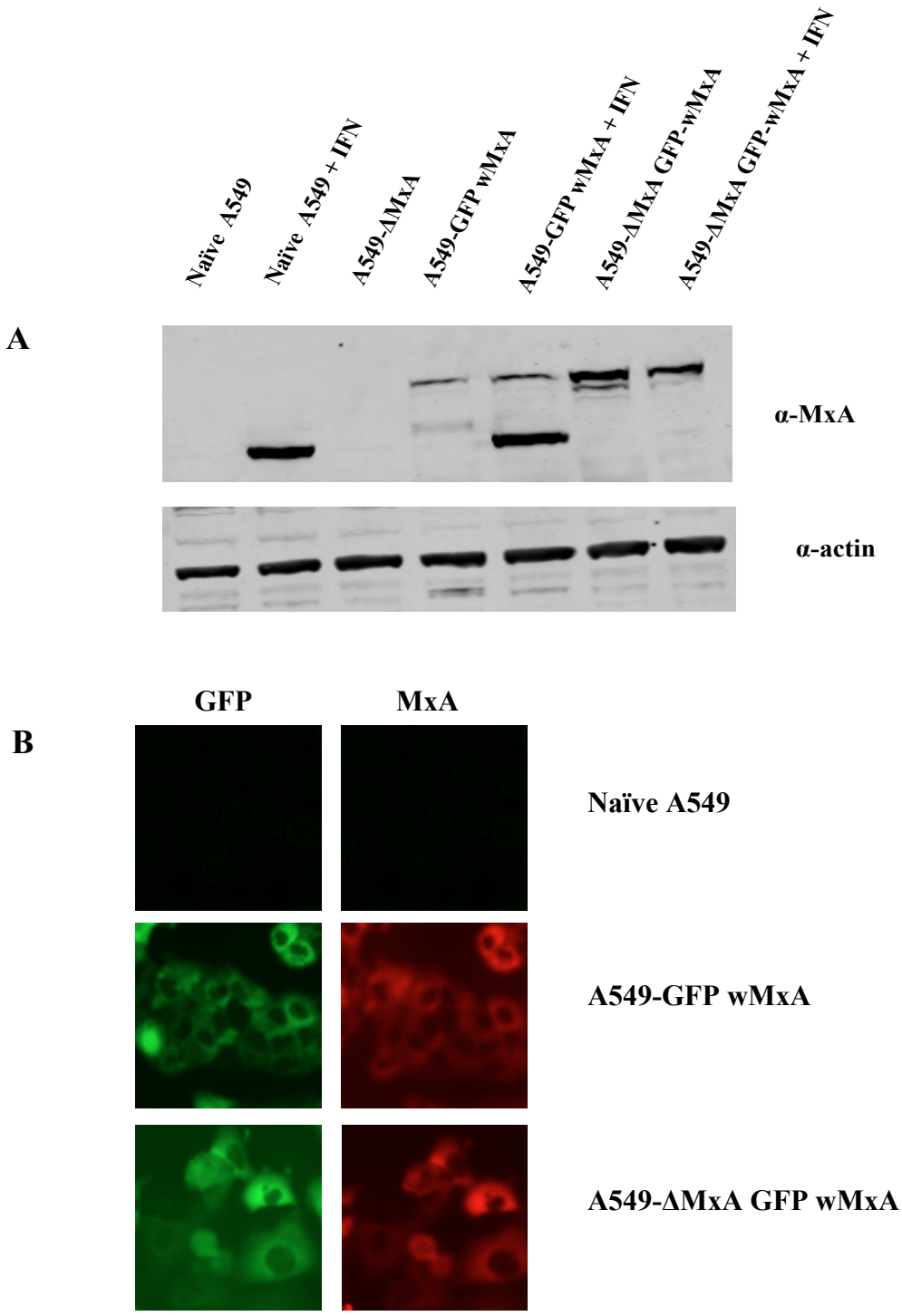


**Figure 5.8 Characterisation of GFP-wMxA expressing cell lines. A.** Immunoblot of FACS sorted A549 GFP-wMxA and A549-ΔMxA-GFP-wMxA cells in comparison to naïve A549 and A549-ΔMxA cells. Cells were untreated or treated with IFN (1000 U/mL) for 16 hours prior to sample collection. MxA was detected using a rabbit anti-MxA antibody and actin levels were detected as a loading control. **B.** Immunostaining of A549 GFP-wMxA and A549-ΔMxA-GFP-wMxA cells. Cells were first probed with a rabbit α-MxA polyclonal antibody then a Texas Red-conjugated goat α-rabbit secondary antibody. Green; GFP Red; α-MxA.

This is also the case in the A549 GFP-wMxA cell line as in both conditions, MxA was recruited to specific cytoplasmic regions, with both the GFP and MxA signals merging together, indicating that GFP-tagged wMxA was potentially functional. Interestingly, in the A549-ΔMxA-GFP-wMxA cells, there is no punctate staining visible with in the cytoplasm, despite the GFP fluorescence and MxA staining overlapping. Therefore it appears that for GFP-wMxA to be recruited to the punctate regions seen in the A549 GFP-wMxA cells the expression of endogenous MxA is required. This may indicate that either GFP-MxA is in fact non-functional or that multiple GFP-MxA molecules are not able to oligomerise without the presence of the non-tagged form and are therefore unable to be recruited to specific cytoplasmic areas upon Pichinde Virus infection.

To then determine where in the endocytic pathway MxA is recruited to the incoming virus particles, Rab 5, an early endosome marker, and Rab 7, a marker of the late endosome, were cloned into lentivirus vector with an N-terminal mRFP tag. These lentiviruses were then used to transduce the A549 GFP-wMxA cell line to create A549 GFP-wMxA/mRFP-Rab5 and A549 GFP-wMxA/mRFP-Rab7 cells. Fig. 5.10 shows the immunofluorescence characterization of the two cell lines. The mRFP-Rab 5 staining shows an overall more diffuse cytoplasmic staining, offering some increased expression around the perinuclear region. Whereas, the mRFP-Rab7 staining is more localised to the perinuclear region, likely reflecting the localization of late endosomes (Perez Bay, Schreiner, and Rodriguez-Boulan 2015). What is clear form these images, is that even in the absence of IFN and virus infection that there

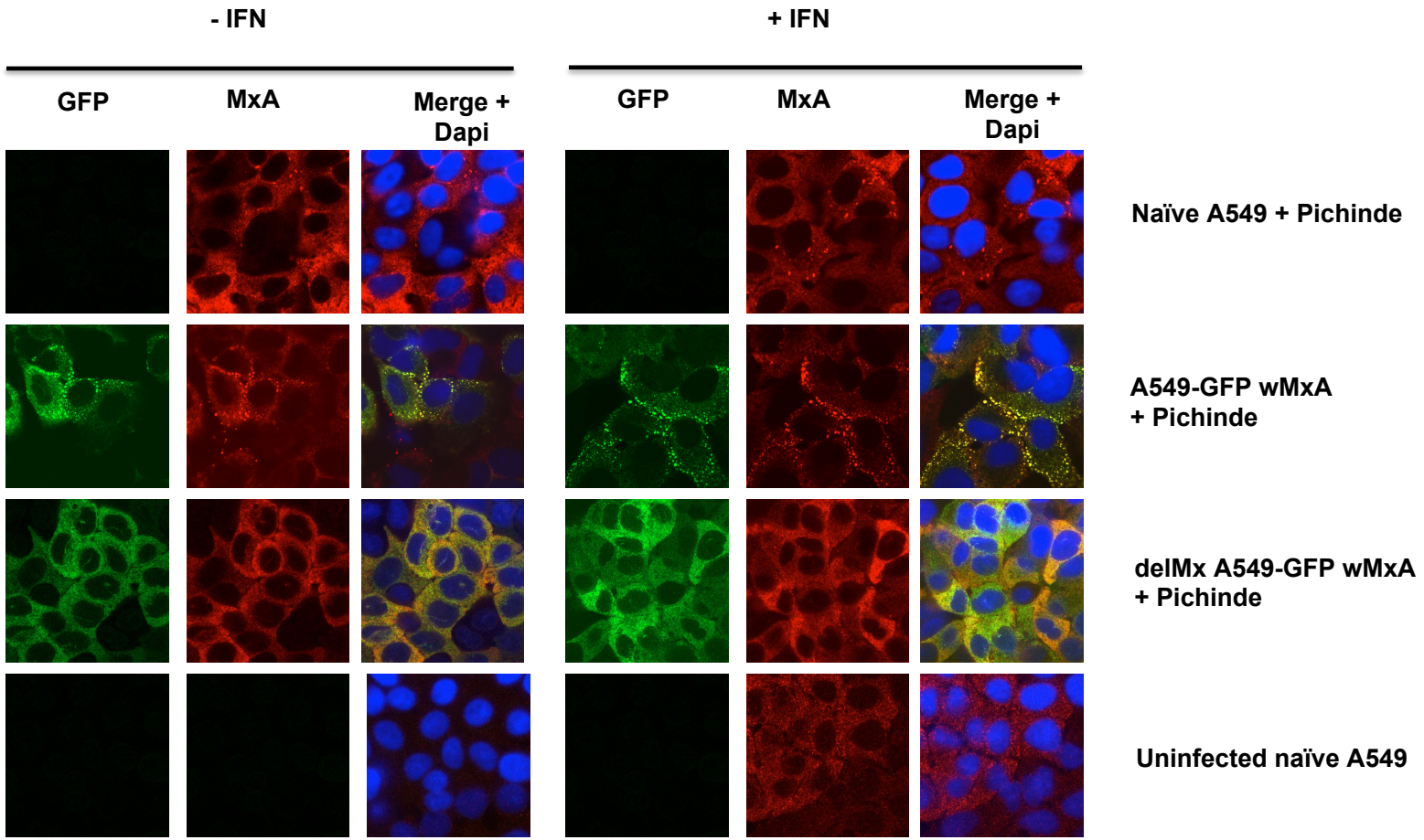


**Figure 5.9 Functional Characterisation of GFP-wMxA expressing cell lines.** Immunostaining of FACS sorted A549 GFP-wMxA and A549-ΔMxA-GFP-wMxA cells. Cells were either left untreated or treated with IFN (1000 U/mL) for 16 hours prior to infection with Pichinde virus at an MOI of 20. Cells were fixed 48 h.p.i and were first probed with an α-MxA polyclonal rabbit antibody then a Texas Red-conjugated goat α-rabbit antibody. Nuclei were stained using DAPI. Green; GFP Red; α-MxA Blue; DAPI-stained nuclei.

appears to be a reasonable level of overlap between GFP-wMxA staining and the two endosomal markers, mRFP-Rab5 and mRFP-Rab7. This is unsurprising following the identification of interacting partners shown to be involved in cellular trafficking seen in section 4.6. Yet, this localization is not seen in all cells, therefore it is difficult to determine whether this is a true co-localisation event.

The block exhibited on incoming influenza virus by MxA prior to primary transcription is known to be dependent on IFN (Xiao et al. 2013). Therefore, in an attempt to ascertain whether MxA is recruited to a specific step of endocytic trafficking, A549 GFP-wMxA/mRFP-Rab5 and A549 GFP-wMxA/mRFP-Rab7 cells were infected at a high MOI of A/WSN/33 following pre-treatment with 1000 U/mL IFN-α. The infection was fixed 1 h.p.i and analysed using confocal microscopy to determine the level of GFP-wMxA/mRFP-Rab co-localisation in comparison to mock-infected cells (Fig. 5.11). No co-localisation was observed after infection with influenza A virus, especially when considering the dramatic re-localisation demonstrated during Pichinde virus infection (Fig 5.9). These data are inconclusive in determining whether MxA is recruited to incoming endosomes and at what stage of the endocytic pathway this occurs and will therefore require further investigation.

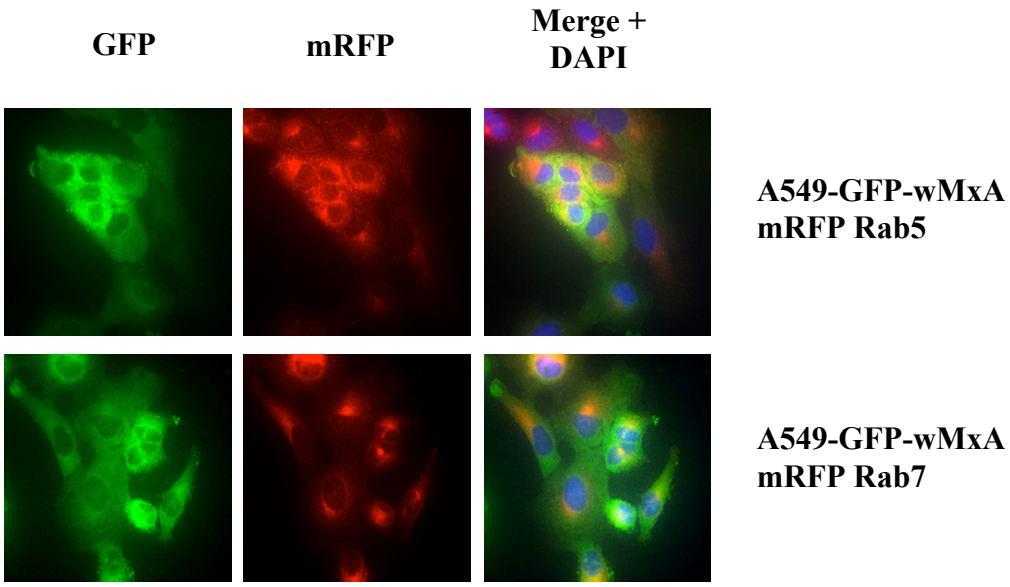


**Figure 5.10 Characterisation of A549 GFP-wMxA mRFP Rab-expressing cell lines.** Fluorescent images of A549 GFP-wMxA mRFP Rab 5 and A549 GFP-wMxA mRFP Rab 7 cells. Nuclei were stained using DAPI. Green; GFP-wMxA Red; mRFP-Rab Blue; Nuclei

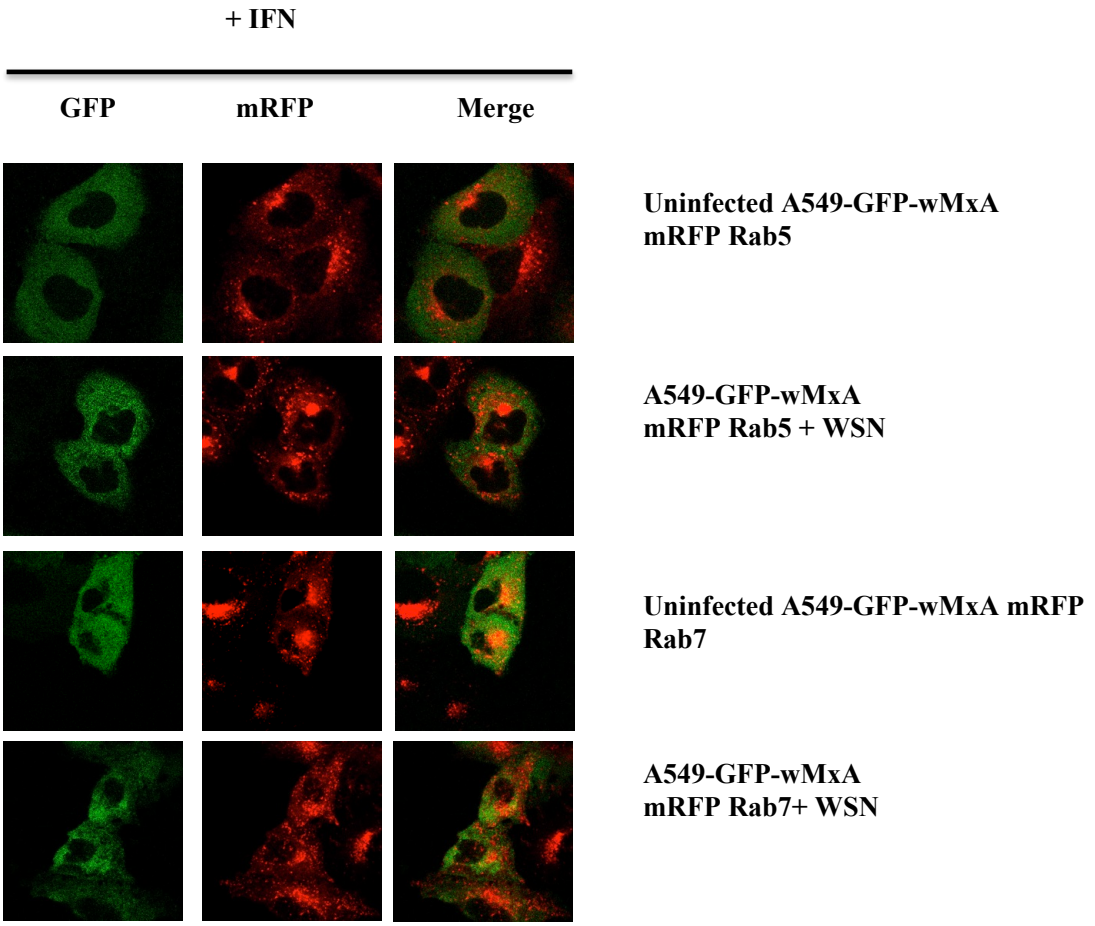


**Figure 5.11 Influenza input assay in A549 GFP-wMxA mRFP-Rab expressing cell lines.** Cells were either left untreated or treated with IFN (1000 U/mL) for 16 hours prior to infection with influenza A/WSN/33 virus at an MOI of approximately 500 in the presence of cycloheximide. Cells were fixed 1 h.p.i and analysed via confocal microscopy. Green; GFP-MxA Red; mRFP-Rab.

**5.6 Discussion**

The results in section 5.2 corroborate the previous results observed in Section 4.2 (Fig 4.4) where mutants T103A, V268M and G255E were shown to be attenuated in their ability to inhibit influenza A virus post-primary transcription in comparison to WT MxA. A549-wWT-MxA cells offered only a small level of attenuation in the absence of IFN, similar to the difference seen in section 3.5 (Fig 3.9). This was likely due to the low level of MxA expressed in A549-wWT-MxA cells compared to A549-MxA cells (Fig 5.2). However this does suggest that to exhibit an antiviral effect post-primary transcription, only a small amount of MxA seems to be required. Interestingly, some mutations seemed to show an enhanced reduction in the level of viral protein produced in comparison to A549-wWT-MxA cells. A549-wKEKE, A549-wR640A and A549-wI376D all displayed increased inhibition of influenza A virus in the absence of IFN, however each of these cell lines expresses MxA to a higher level than that seen for A549-wWT-MxA, and may offer an explanation as to the increased antiviral activity displayed here in the absence of IFN.

The ability of these mutations to inhibit influenza A virus protein synthesis in the presence of IFN was addressed in Fig 5.4. The data indicated that there appeared to be a similar reduction in viral protein levels in the A549-wWT MxA cells as that observed in the absence of IFN treatment (Fig 5.3 B) Again this is likely due to the low levels of wWT MxA being expressed, especially in comparison to the level of MxA which would be normally be induced following IFN treatment, where MxA can represent up to 1% of the cytoplasmic protein within the cell (Horisberger 1992). Therefore, as no endogenous MxA was present and the levels of WT-MxA were low (Fig 5.2), it is not surprising to see such a small impact of MxA in the presence of

IFN. A similar reduction in viral protein synthesis was observed in the human polymorphism A549-wG255E cells, which suggests in the presence of IFN this mutant was capable of inhibiting influenza A virus to a similar level as wt MxA. As this cell line expressed a higher level of MxA in comparison to the A549-wWT MxA cells, the data suggest that this mutant MxA protein may be slightly attenuated in its ability to inhibit influenza A virus prior to primary transcription. However, it cannot be ruled out that this difference could be due to the attenuation described post-primary transcription.

Interestingly, in the presence of IFN there appeared to be a difference in the impact of the two lipid-binding mutants. The A549-wAKAK cell line reduced influenza NP levels to 74% of A549-ΔMxA cells (Fig 5.4), suggesting that this mutation does not have an impact on the ability of MxA to inhibit influenza A virus. However, the other lipid-binding mutant, A549-wKEKE did not appear to have an impact on the level of reduction seen in the presence of IFN, suggesting that this lipid-binding mutant is potentially not capable of inducing the IFN-mediated block on influenza prior to primary transcription. This is surprising as both of these mutants have been previously described *in vitro* as having a diminished ability to bind to and tubulate liposomes (von der Malsburg et al. 2011), therefore it may be expected that they would behave similarly to each other in cell culture. However, neither of these mutants have been characterised in the context of mammalian cell culture, therefore it is possible that they have different binding capabilities under physiological conditions. Despite the fact that they have been characterised as lipid-binding mutants *in vitro*, perhaps only one of these, A549-wKEKE is truly diminished in its ability to bind to lipids within the cell. If this is the case, it suggests that the block induced prior to primary

transcription by MxA is potentially dependent on lipid binding, suggesting that MxA may interact directly with incoming viral endosomes.

Neither the A549-wT103A nor the A549-wV268M cell-lines showed an enhanced reduction in influenza NP production in comparison to A549-ΔMxA cells. This suggests that MxA may require GTPase activity to fully exert the antiviral effect against influenza A virus in the context of IFN, and the human polymorphism V268M may be incapable of exerting the IFN-dependent antiviral function of MxA against influenza A virus. This may be due to the reduced ability to hydrolyse GTP which has been previously described for V268M (Dick et al. 2015). If T103A has a reduced impact due to the lack of GTPase activity, then V268M may also be attenuated in its antiviral activity for a similar reason.

The results of the single cycle time course did not offer discernable differences between the different A549-wMxA cell lines, showing similar differences to that observed in Figure 5.3. This is likely due to the difference in MxA expression between the A549-MxA cells and the A549-wMxA cells. It is likely that the low levels of expression were not capable of producing a phenotypic difference for each mutant during a single cycle, high multiplicity infection. Unfortunately it was not possible to determine the impact that the R640A, I376D or D478A mutations as these cell lines had not been obtained at this point in the study.

To address the impact on these mutations in a multi-step, lower multiplicity infection as well as in the presence of IFN, these cell lines were subject to a plaque reduction assay. Interestingly, these results corroborate the results seen in section 5.2. In the

absence of IFN, the number of plaques was reduced in each cell line in comparison to A549-ΔMxA cells by approximately 40-50%, suggesting that even a small amount of MxA-expression is enough to exert an effect against influenza A virus post-primary transcription (Fig 5.6). Although this reduction is not as striking as observed in the A549-MxA cells, which offered a similar reduction to that seen in by Xiao et al. (2013). This suggests that although only a small amount of MxA is required for antiviral activity, that the impact is protein concentration dependent, as with increasing MxA increasing antiviral activity is observed, particularly post-primary transcription. This is in agreement with Riegger et al. (2015) who showed that increasing levels of MxA were even capable of reducing the polymerase activity of influenza A viruses containing MxA resistance mutations. This is further supported by the increased reduction observed in A549-wR640A cells (Fig 5.6), which expresses almost 8-fold more MxA in comparison to A549-wWT MxA cells (Fig 5.2).

The impact of these mutations in MxA is clearer in the presence of IFN. The number of plaques produced on the parental A549-ΔMxA cell line was reduced to 8% following IFN treatment in comparison to untreated cells (Fig 5.6). The expression of a number of the wMxA proteins reduced plaque number in comparison to the IFN-treated A549-ΔMxA cells suggesting that each of these mutations were capable of inhibiting influenza virus in an IFN-dependent manner. Plaque number in the A549-wWT MxA, A549-wG255E and A549-wD478A cells was reduced to 4-5%, which further highlights how only a small amount of MxA is required to exhibit an antiviral effect. It is interesting to note that both A549-wG255E and A549-wD478A cells expressed higher levels of MxA in comparison to A549-wWT-MxA cells, therefore

these mutants may actually confer for a slight attenuation in antiviral activity in the presence of IFN if similar levels of protein were expressed. Two of the A549-wMxA cell lines reduced the plaque number to near A549-MxA levels. Perhaps unsurprisingly, A549-wR640A was capable of this reduction, but this cell-line expressed MxA at a higher level that A549-wWT MxA and therefore suggests that this mutations has less impact on the IFN-dependent antiviral activity of MxA. Intriguingly, plaque number in A549-wI376D cells was also reduced in the presence of IFN. This is surprising as A549-wI376D cells expressed a similar level of MxA to the A549-wWT MxA cells. However, it is not possible to rule out that this is an impact of clonal selection and that by chance a cell-line that is less permissive to influenza A virus was selected.

As in section 5.3, the lipid-binding mutants showed differing abilities to reduce plaque numbers in the context of IFN. A549-wAKAK was capable of reducing plaque numbers to a greater level than A549-wWT MxA cells, suggesting that this mutation does not appear to prevent the antiviral activity exerted by MxA. Yet, A549-wKEKE showed similar numbers of plaques as the IFN-treated A549-ΔMxA, suggesting that the IFN-dependent mechanism of MxA is impacted by this mutation. Similarly to Fig 5.4, both A549-wT103A and A549-wV268M showed no increase in plaque reduction in comparison to IFN-treated A549-ΔMxA. Again this provides further evidence that these two mutations are important for the antiviral activity of MxA. Interestingly, A549-wV268M showed increased numbers of plaques in both the untreated and IFN-treated cells, therefore it is possible that the selected cells may be slightly more permissive to influenza A virus infection. Despite this, it is clear that they have responded to IFN due to the reduction in plaque number, therefore this suggests that

the human polymorphism V268M may be highly important in the response to influenza virus infection.

Although these cell lines do not express high levels of MxA, it is possible to determine some of the potential characteristics of MxA that are important for the IFN-dependent mechanism of antiviral activity against influenza A virus. The results in section 5.2 and 5.4 indicate that in the presence of IFN, MxA potentially requires both GTPase activity and lipid binding activity to fully exert its antiviral effect prior to primary transcription. The necessity of GTPase activity is supported through the attenuation observed in the cell-line expressing the V268M mutation, which has previously been shown to allow binding, but not hydrolysis of GTP (Dick et al. 2015). However, this could also be due to a potential interaction with another host-factor, as Xiao et al. (2013) suggested that MxA might interact with an unidentified IFN-inducible co-factor to exert its IFN-dependent antiviral effect. To understand this attenuation and to confirm the characteristics required for the IFN-dependent antiviral effect of MxA in more detail, further work is required.

The induction of MxA using IFN leads to a clear expression pattern, shown in Fig 5.7. Both A549 cells and BEAS-2B cells show concentrated MxA staining in the perinuclear region and also at the cell periphery around the plasma membrane. To assess where in the endocytic process MxA is recruited to exhibit its antiviral effect in the context of IFN two GFP-wMxA cell lines were created in the context of naïve A549 cells or A549-ΔMxA cells. The functionality of these cell lines was determined using Pichinde virus as seen in Fig. 5.9. The results showed that GFP wMxA requires the expression of endogenous MxA to allow recruitment to large punctate areas of

MxA staining, as in the context of the A549-ΔMxA-GFP-wMxA cells there was a lack of punctate staining. This suggests that the N-terminal tagging of MxA may have caused a structural change or sterically hindered the ability of GFP-MxA to be recruited to the sites of Pichinde infection, hence requiring the endogenous MxA to allow the GFP-wMxA recruitment observed in Fig 5.9. It is not clear whether this localization is due to MxA being recruited to sites of Pichinde virus replication or whether MxA is sequestering a specific viral protein. It has recently been observed that MxA is capable of sequestering the capsid protein of West Nile Virus into tubular cytoplasmic structures (Hoenen et al. 2014).

Experiments were performed to determine whether GFP-MxA was being recruited to a specific stage of the endocytic pathway during influenza virus infection (Fig. 5.11). Unfortunately the results were inconclusive and did not show any specific co-localisation events between the mRFP-labelled Rab proteins and the GFP-wMxA. This could be due to the difficulty in assessing fluorescently tagged proteins as due to the nature of microscopy, a single GFP-tagged protein can emit light as wide as 250 nm in diameter, when in reality the GFP protein itself is only 3 nm in size (Grove 2014). Therefore in a system where a large number of GFP-tagged MxA proteins are spread over a diffuse area such as the cytoplasm, rather than localizing closely to individual organelles, as seen with the mRFP-tagged Rab proteins, it can be difficult to determine where individual MxA proteins are localised. For example, in the context of Pichinde virus infection shown in Fig 5.9, there are only a few defined punctate areas per cell. This means that a relocalisation event is obvious to see as MxA is being recruited to a specific area. However, in the context of the viral input assay using influenza virus, an infection is taking place with a high MOI, therefore as

many as 500 influenza particles are being endocytosed per cell. Therefore any redistribution of MxA is likely to be spread over a large number of endocytic events, making it difficult to ascertain whether MxA is interacting directly with the incoming endosomes. Consequently, in order to determine whether MxA is being recruited to endosomes carrying incoming virus particles, more sensitive detection methods, such as single particle fluorescence microscopy, are required.

## Chapter 6 - The antiviral effect of MxA against influenza B virus

### 6. Introduction

There are 3 types of influenza viruses, all of which are capable of infecting humans. The most common of these are influenza A and B viruses, although similar, they have a number of unique features that set them apart. Influenza C virus is much less common and causes a milder disease in humans than both influenza A and B viruses. Although influenza A viruses are divided into subtypes based on the surface glycoproteins, HA and NA, influenza B viruses are not divided into subtypes but into 2 antigenically and genetically distinct lineages (Paul Glezen et al. 2013). These two lineages, B/Victoria/2/87–like (Victoria lineage) and B/Yamagata/16/88–like (Yamagata lineage), have circulated in humans worldwide since 1983 (Rota et al. 1990).

Unlike influenza A virus which has a diverse host range, influenza B virus has not been shown to have a natural reservoir in other animal species and although there has been several reports of influenza B virus isolation from seals, Osterhaus et al. (2000) showed that the virus was in fact identical to isolates from humans and has not undergone any host adaptation (Osterhaus et al. 2000). In a later study, it was shown that a number of seals had also been infected with an influenza B virus similar to B/Yamanashi/166/98, which is antigenically different from B/Seal/Netherlands/1/1999. This suggested a novel infection and offered evidence towards seals being another mammalian host for influenza B virus (Bodewes et al. 2013). More recently, it has been suggested that domestic pigs may also be a potential animal reservoir for influenza B virus as after infection with two viruses representative of the two distinct lineages of influenza B virus; B/Brisbane/60/2008

(Victoria lineage) and B/Yamagata/16/1988 (Yamagata lineage) pigs developed influenza-like symptoms and lung lesions. Pigs that were infected with B/Brisbane/60/2008 virus were also capable of successfully transmitting the virus to other animals. Therefore suggesting swine as another potential host of influenza B virus (Ran et al. 2015). It also been shown that influenza A and influenza B virus gene segments are not capable of reassortments. In fact, influenza B NP has been shown to inhibit the influenza A polymerase through competitively binding to the influenza A NP, therefore inhibiting replication (Jaru-ampornpan et al. 2014). Therefore, influenza B viruses do not have pandemic potential but are responsible for significant seasonal epidemics and has been shown to be the main circulating strain of influenza virus 1 in every 3 years (Y. P. Lin et al. 2004). Thus, influenza B virus still poses a significant threat to the human population.

Despite this, influenza B viruses are far less studied than influenza A virus with a number of assumptions suggesting that characteristics of influenza A viruses are likely to be true for influenza B virus. Although these viruses do share a number of characteristics, influenza B viruses harbour a number of unique differences.

For example, both viruses possess nucleotide sequences at the 3' and 5' end of each of the eight RNA segments which is completely conserved and following these common terminal sequences are further non-coding nucleotides which have been shown to be specific for each RNA segment (D. Jackson, Elderfield, and Barclay 2011). These regions are known as the untranslated regions (UTRs). Like influenza A viruses, the UTR regions of the influenza B virus genome are absolutely essential for replication (Barclay and Palese 1995). Although the function of the UTR regions

within the genome are unknown, there is a remarkable difference in the length of the 5′ non-coding regions of influenza B virus vRNA segments in comparison to those of influenza A viruses, with the influenza B virus UTRs being significantly longer (Stoeckle, Shaw, and Choppin 1987). It has been suggested that theses segment-specific regions could regulate gene expression or potentially be involved in the specific packaging of gene segments into nascent virions (D. Jackson, Elderfield, and Barclay 2011). Interestingly, a number of mutations introduced to the influenza B virus HA gene-specific non-coding regions at the 5′ end of the vRNA resulting in truncation, did not affect gene expression. However, a 67 nt deletion from this region could not be recovered into recombinant virus (Barclay and Palese 1995).

The influenza B virus genome also encodes for a specific protein, which is not present in influenza A virus, encoded on RNA segment 6 from an initiation codon just 4 nt upstream of the start of the NA ORF (Williams and Lamb 1986). This ORF produces a protein 100 amino acids in length known as NB. NB is a small hydrophobic type III integral membrane protein, which is completely conserved in all sequenced influenza B virus strains. Due to structural similarities it had previously been hypothesized that NB was the functional equivalent of the influenza A virus M2 ion channel protein. NB protein had also been shown to be incorporated in similar levels to M2 in nascent virus particles (Betakova, Nermut, and Hay 1996; Brassard, Leser, and Lamb 1996; Zebedee and Lamb 1988). However, NB was determined to not be essential for replication of influenza B viruses in MDCK cells via reverse genetics, as an NB-null mutant replicated as efficiently at wild-type (Hatta and Kawaoka 2003). Therefore NB was unlikely to be a true homologue of the influenza A virus M2 ion channel. Although this NB-null virus was shown to be attenuated in mice, suggesting that

although this protein may not be essential to replication in vitro, it may have a role in replication or pathogenesis in vivo. A protein encoded on the influenza B virus vRNA segment seven, the BM2 protein, was later shown to be the functional equivalent of the influenza A virus M2 ion channel protein (Paterson et al. 2003; Mould et al. 2003).

Recently the morphology of influenza B virions was investigated using cryo-electron microscopy and has shown some clear differences in virion morphology to that seen for influenza A viruses (Katz et al. 2014). Firstly Katz et al., (2014) assessed the number of glycoprotein projections per virion, and suggested that a typical 130 nm influenza B/Lee/40 virion may contain approximately 460 surface glycoproteins which is higher than the estimated 375 on a 120 nm influenza A virus particle (Harris et al. 2006). However, the most striking difference in this analysis was shown to be in the orientation of the vRNPs. Influenza A virions are best known to display a 7 + 1 configuration of the genome segments, yet the influenza B vRNPs do not share this configuration and appear to have a more twisted conformation of the RNPs suggesting a potential difference in genome packaging between influenza A and influenza B viruses (Harris et al. 2006; Noda et al. 2006; Katz et al. 2014).

Almost all research conducted into the antiviral activity of MxA against Orthomyxoviruses use either influenza A virus or Thogoto virus yet very little research has been done into the impact of MxA on influenza B viruses. Canine Mx1 has previously been shown to have no effect on influenza B virus replication as it was shown that the ability of the virus to replicate efficiently within MDCK cells was due to an inefficient IFN-induced antiviral response within MDCK cells (Frensing et al.

2011). Frensing et al. (2011) also showed that although canine Mx1 had no impact on influenza B virus replication, murine Mx1 was capable of inhibiting the virus in a mini-replicon assay. However, murine Mx1 localises to the nucleus unlike human MxA, which localises within the cytoplasm. Therefore this section investigates the impact of human MxA firstly on influenza B virus in mini-replicon assays and in the context of viral infection, secondly on the additive impact of IFN on the antiviral effect exhibited by MxA and finally, determining the ability of influenza B virus to overcome inhibition by MxA.

### 6.1 Effect of MxA on influenza B virus polymerase activity

In chapter 4 a number of wMxA constructs were tested for antiviral activity in influenza A virus mini-genome replication system. To build on the work of Frensing et al. (2011) and determine the antiviral impact of MxA on influenza B virus replication, mini-genome experiments were performed. In the influenza B virus version of this assay the renilla luciferase mini-genome template (used to quantify viral RNA replication) was flanked by the UTRs of the influenza B virus NS segment. 293T cells were transfected with the influenza B virus polymerase subunits (PB2, PB1 and PA; derived from B/Panama/90 virus) and NP alongside the wMxA constructs and the mini-genome construct. The transfection efficiency was determined through the transfection of a plasmid encoding firefly luciferase under the control of a CMV promoter. This was then used to normalise the polymerase activity in a dual luciferase assay. The polymerase activity was then normalised to the activity in the absence of wMxA to determine the level of antiviral activity exhibited by each of the mutant wMxA constructs.

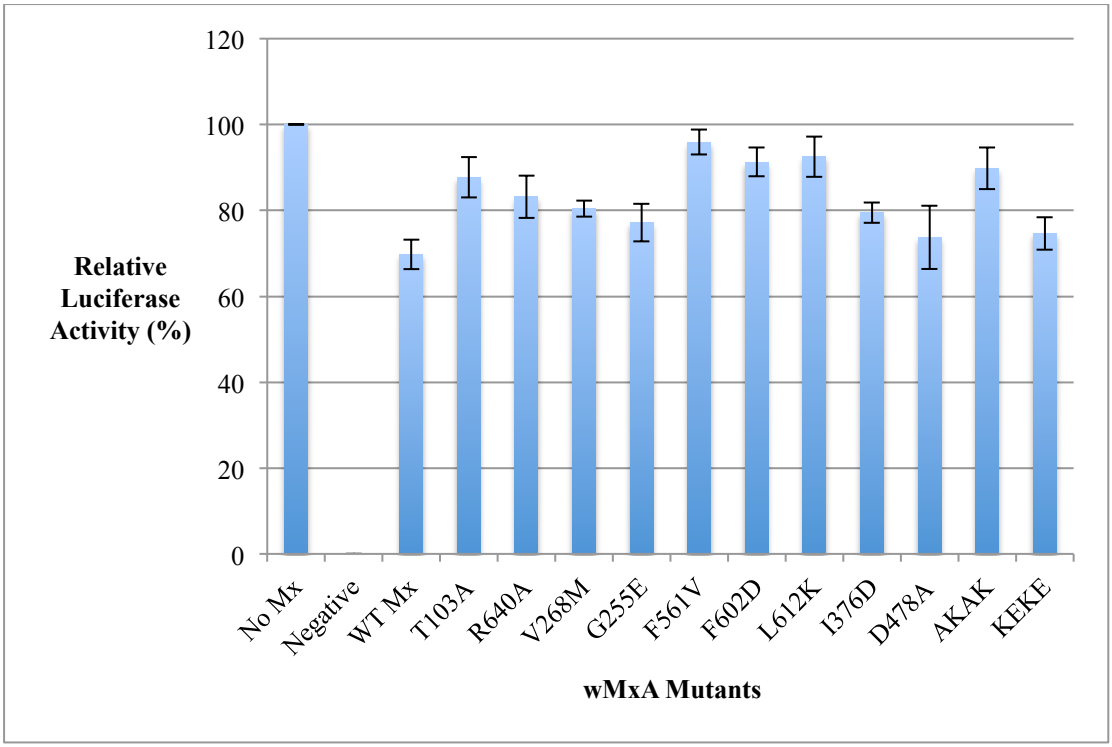


**Figure 6.1 Influenza B/Panama/90 Luciferase assay.** Relative Luciferase activity was measured and normalised to no the No MxA positive control following the transfection of expression plasmids encoding the viral polymerase subunits and NP (100ng) and the indicated wMxA construct (200ng). The polymerase activities are represented as a percentage of luciferase activity in the no MxA control and are the average of three independent experiments ± S.D.

Fig. 6.1 shows the impact of each of the wMxA mutations on the antiviral activity of MxA against influenza B virus. This clearly shows that MxA is capable of reducing the relative luciferase activity of influenza B polymerase, however the reduction is not as prominent as that seen in section 4.2 for influenza A viruses. Here wt wMxA only leads to a 30% reduction in the amount of luciferase activity in comparison to the no MxA control. All other mutants appear to be slight attenuated in comparison to wt MxA apart from D478A. Interestingly, T103A still has some antiviral activity but it appears that this affect is diminished in the influenza B polymerase assay, reducing activity by approximately 10% whereas in the influenza A assay T103A reduced polymerase activity by approximately 25% (Fig. 4.3). Also, it would appear that the monomeric mutations, L612K and F602D, are less active against influenza B averaging an 8% reduction along with the L4 loop F561V mutant which shows very little antiviral activity against influenza B virus. The human polymorphism proteins appear to show a similar pattern to that in the context of influenza A virus in that wMxA G255E has slightly more antiviral activity than V268M, yet both are capable of exerting an antiviral effect even if it is attenuated in comparison to wt MxA.

### 6.2 Expression of MxA leads to a reduction in plaque titre

To assess the impact of MxA on the virus as a whole, MDCK cells were transduced using a lentivirus expressing wt MxA for the constitutive expression of human MxA. Fig. 6.2 shows the expression levels of MxA in MDCKs through western blot and immunofluorescence analysis. The western blot shows a strong level of expression, which is supported by the immunofluorescence staining.

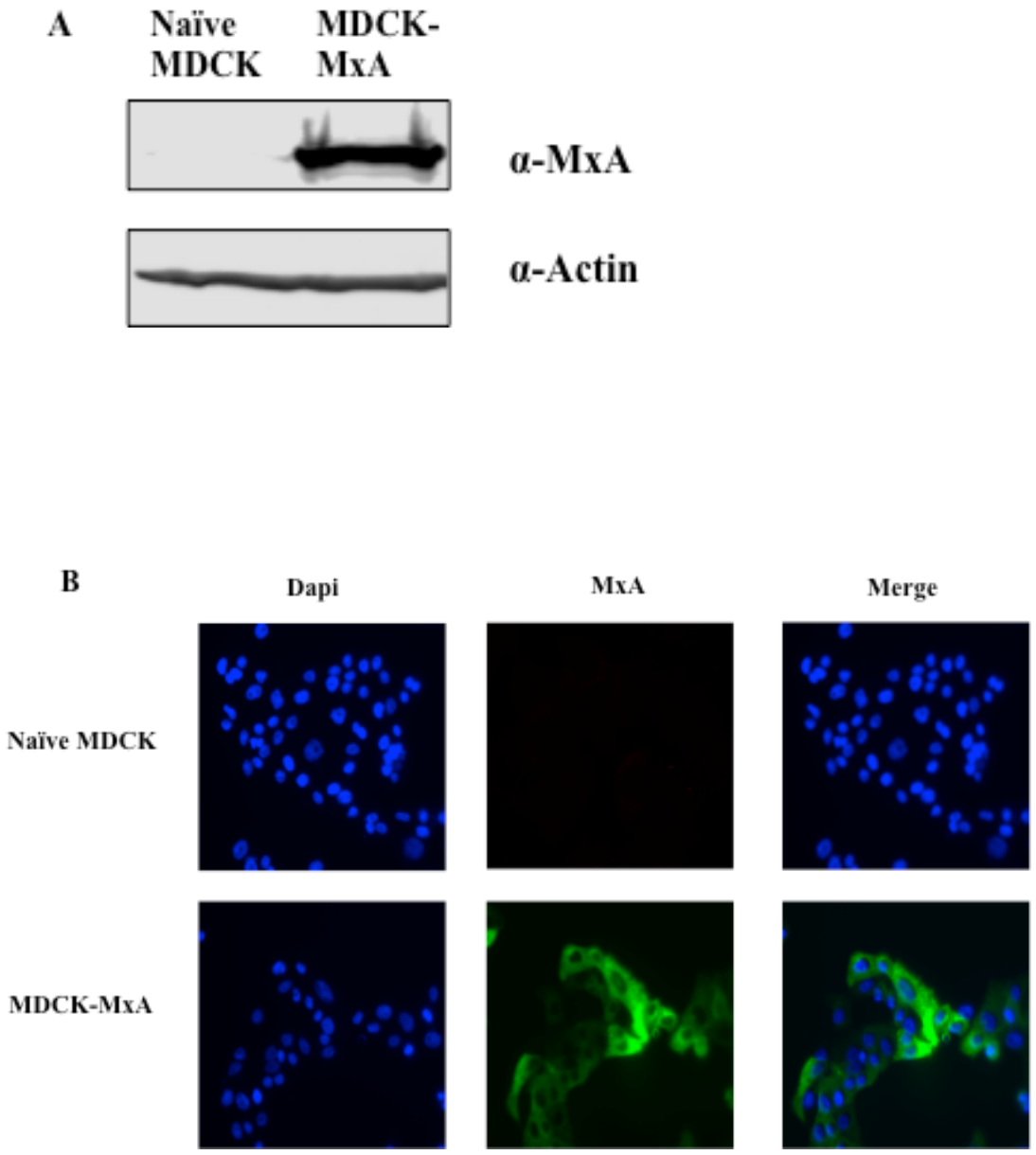


**Figure 6.2 Constitutive expression of human MxA in MDCK cells. A.** Immunoblot showing the expression of human MxA in MDCK cells. **B**. Immunostaining of naïve MDCK and MDCK-MxA cells. Cells were fixed and probed with an α-MxA polyclonal rabbit antibody then an Alexa-488 conjugated goat α-rabbit secondary antibody. Cell nuclei were stained with DAPI (blue).

MDCK cells are highly permissive to both influenza A and B viruses Therefore to determine the effect of human MxA on influenza viruses in MDCK cells, both influenza A/Udorn/1972 and influenza B/Yamanshi/1998 were assessed for the ability to produce plaque-forming units on both MDCK naïve cells and MDCK MxA cells. Fig 6.3 shows that human MxA reduces the ability of both influenza viruses to produce plaques on MDCK cells. In the case of influenza B virus, the over-expression of MxA leads to a 75% reduction in the number of plaques in comparison to naïve MDCK cells showing that MxA has a clear antiviral effect on influenza B virus. Surprisingly, it appears that the over-expression of MxA in MDCK cells has an even larger impact on the ability of influenza A virus to produce plaques, only producing 1.9% the number of plaques compared to the plaques produced on naïve MDCK cells. These results clearly highlight the ability of MxA to inhibit orthomyxoviruses, however they also highlight a clear difference in sensitivity to MxA in MDCK cells. Influenza A virus showed a much greater reduction in MDCK-MxA cells than previously observed in A549-MxA cells, where a 74% reduction in plaque number was reported, suggesting that the antiviral effect of MxA is also influenced by the cell line used for virus propagation (Xiao et al. 2013).

### 6.3 Does MxA inhibit influenza virus prior to primary transcription in MDCK cells in the absence of IFN

Section 3.4 attempted to address the impact of MxA over-expression on influenza virus prior to primary transcription in A549 cells. However, following the increased inhibitory effect of MxA in MDCK cells, the impact of MxA overexpression in the absence IFN treatment was addressed in MDCK cells. MDCK-MxA cells were infected with either influenza A/Udorn/72 or influenza B/Yamanshi/98 at an MOI of

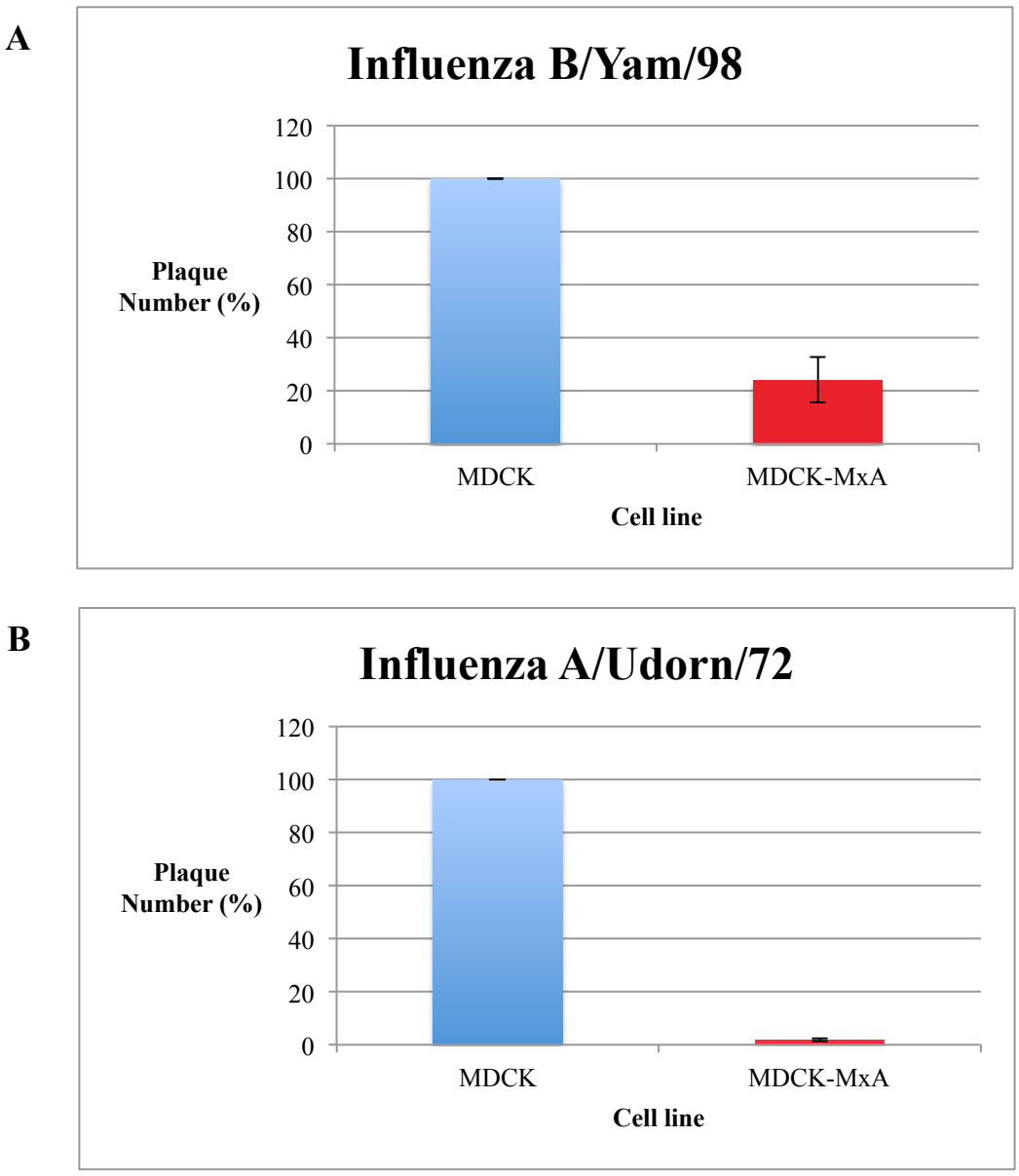


**Figure 6.3 Over-expression of MxA reduces plaque numbers of influenza viruses.** Naïve MDCK and MDCK-MxA cells were inoculated with a serial ten-fold dilution series of either (**A**) influenza B/Yam/98 or (B) influenza A/Udorn/72 in a viral plaque assay. The cells were stained using crystal violet after 72 and 48 hours respectively. Plaque number is expressed as a percentage of plaques observed on naïve MDCK cells. Results are expressed as the average of three independent experiments ± S.D

0.5 alongside naïve MDCK cells and fixed 12 hours post infection. Following fixation the cells were immunostained for influenza NP as a marker for infected cells. The average number of viral antigen positive cells was determined from 10 random images per condition at 20x magnification and the number of viral antigen positive MDCK cells was set to 100%. Fig. 6.4 A shows that the overexpression of MxA had very little impact on the number of influenza B virus infected cells, with MDCK-MxA cells averaging only a 4% reduction in the number of antigen-positive cells compared to naïve MDCKs. However, there was a much larger reduction in the number of influenza A virus NP positive cells (Fig 6.4 B). The over-expression of MxA in MDCK cells caused a 70% reduction in the number of influenza A virus NP positive cells. Although the influenza B virus data is reminiscent of the impact seen of influenza A virus in A549 cells (section 3.4), it appears that the over-expression of MxA had a much larger inhibitory effect on influenza A virus in MDCK cells, suggesting that perhaps in MDCK cells, MxA is capable of inhibiting the initial nuclear translocation of vRNPs without the presence of IFN. Although, it is not possible to rule out that this impact could be caused purely by the post-primary transcription antiviral effect being much stronger in MDCK cells than in A549 cells.

### 6.4 Impact of MxA on influenza B virus growth

Although the results in section 6.2 give a clear indication of the importance of MxA to the inhibition of influenza B virus, it does not show the overall impact of MxA on the amount of virus produced during infection. To assess this naïve MDCK cells and MDCK-MxA cells were infected with B/Yamanashi/98 virus at an MOI 0.001, supernatant samples were taken every 12 hours until 72 h.p.i and the infectious titre of

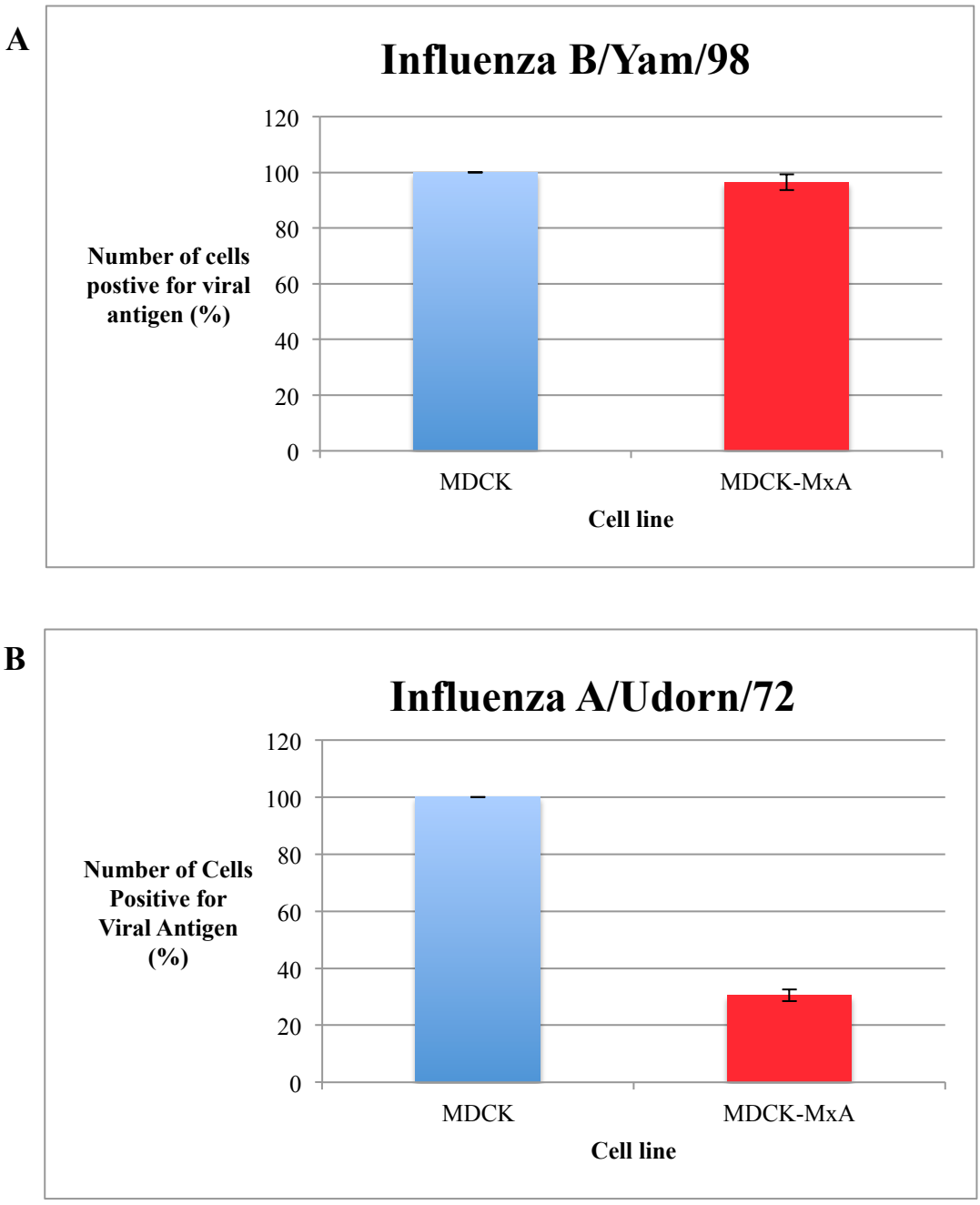


**Figure 6.4 Over-expression of MxA may impact nuclear import of influenza A virus but not influenza B virus in MDCK cells.** MDCK and MDCK-MxA cells were infected with (**A**) B/Yam/98 and **(B**) A/Udorn/72 at an MOI 0.5. Cells were fixed 12 h.p.i and immunostained for DAPI and influenza A or B virus NP. Systematic uniform random sampling was used to obtain 10 images per condition at 20x magnification. Cells that were positive for viral antigen were then counted using ImageJ cell counter. Results are expressed as a percentage of virus positive cells observed in naïve MDCK cells and are the average of three independent experiments ± S.D

each determined by viral plaque assay on MDCK cells. At 12 h.p.i the amount of virus produced was relatively similar across both cell lines, however by 24 h.p.i the viral titre was approximately a log lower in the MDCK-MxA cells in comparison to the naïve MDCK cells (Fig. 6.5). The viral titre peaked at 36 h.p.i in the naïve MDCK cells but this was delayed in the MDCK-MxA cells, which peaked 12 hours later at 48 h.p.i. The peak titre reached in the MDCK-MxA cells was also lower than that reached in the naïve MDCK cells, as the MDCK-naïve cells reached a peak of $5 \times 10^8$ pfu/mL whereas the MDCK naïve cells only reached $9.2 \times 10^7$ pfu/mL.

These results clearly show that MxA is an important antiviral protein that can exhibit an effect against influenza B virus infection as the over-expression of MxA alone is able to reduce the amount of virus produced by a log in the early stages of infection up until 36 h.p.i and by half a log in the latter stages of infection in MDCK cells, showing a similar trend to the antiviral effect demonstrated by MxA against influenza A virus in A549 cells.

As described earlier MxA has been shown to target two distinct steps of the virus replication cycle; one of which is independent of IFN, requiring only the over-expression of MxA and one that is IFN dependent. In previous chapters, A549 cells were pre-treated with IFN-α prior to infection to induce the antiviral state and promote the IFN dependent activity of MxA. However, despite being IFN-competent cells, MDCK cells do not respond well to universal IFN and therefore an alternative method of inducing an antiviral state in MDCK cells was required. It has been shown by Frensing et al. (2011) that through the production of conditioned media (C.M) it is possible to induce an IFN response. Therefore MDCK cells were infected at a high

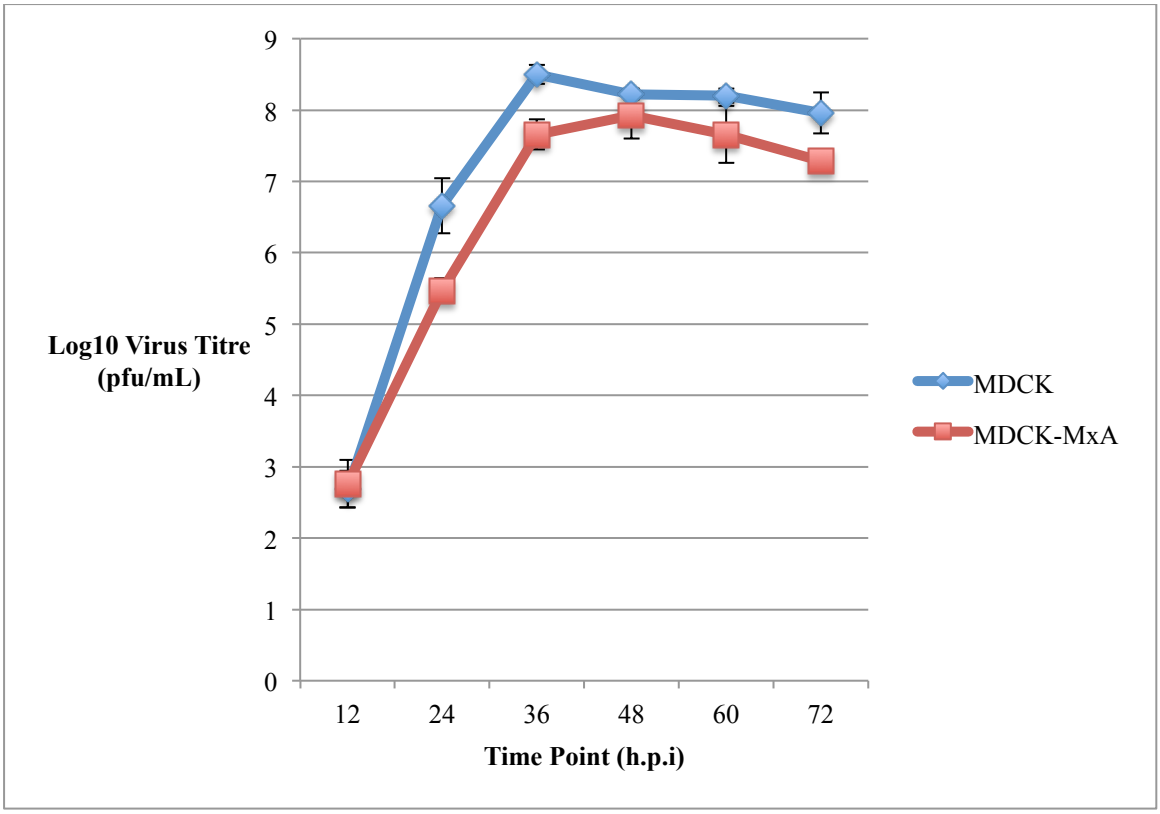


**Figure 6.5. The impact of MxA on influenza B virus multistep replication.** Naïve MDCK and MDCK-MxA cells were infected at an MOI 0.001 using B/Yam/98. Samples were taken every 12 hours post-infection and titred via plaque assay on MDCK cells. Results represent the average of three independent experiments ± SD.

MOI with Sendai virus, a high IFN inducing virus, to allow secretion of IFN into the supernatant. The supernatant was collected 18 h.p.i and stored at -80C. Prior to use the supernatants were UV-treated for 2 minutes to inactivate any virus and then placed onto fresh MDCK cells. The cells were lysed 16 hours post-treatment and assessed for the induction of canine Mx1 as a marker for IFN stimulation via immunoblotting. Fig. 6.6 A shows that pre-treatment of MDCK cells with C.M lead to the production of Mx1, suggesting that this method could be used to induce an antiviral state in MDCK cells to determine the impact of IFN on influenza B replication as well as any additive effect IFN treatment may have on MDCK-MxA cells.

To determine the impact of MxA on influenza B virus protein expression, naïve MDCK cells and MDCK-MxA cells were infected with B/Yamanashi/98 virus at an MOI of 5. Cells had been either pre-treated with UV-inactivated C.M or left untreated for 16 hours prior to infection. Following infection cell lysates were collected 8 h.p.i and assessed for the levels of viral NP via immunoblotting. Figure 6.6 B shows the impact of MxA on influenza B virus NP expression both with and without C.M pre-treatment. Naïve MDCK were negative for Mx1 expression but in conditioned-media treated cells there was a clear band showing the induction of Mx1 expression, indicating that these cells were in an antiviral state. Figure 6.6 B demonstrates that the over-expression of MxA alone had a negative impact on the levels of NP synthesized and this impact was amplified by pre-treatment with C.M. However, pre-treatment with C.M led to a large decrease in the amount of NP synthesized in both naïve MDCK and MDCK-MxA cells.

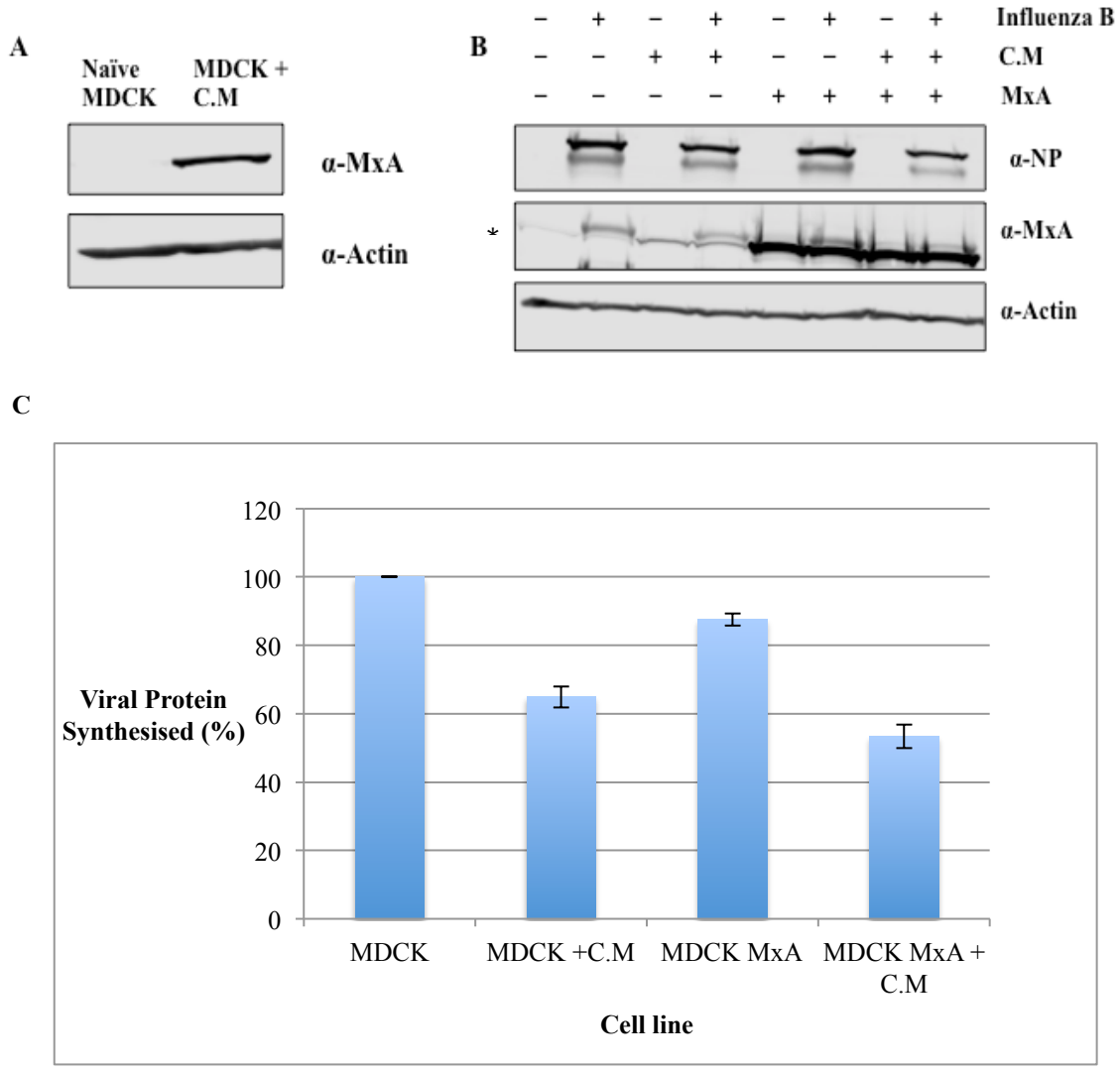


**Figure 6.6. The impact of MxA on influenza B virus protein expression. A.** Immunoblot showing that conditioned media is capable of inducing Mx1 expression in MDCK cells. **B.** Immunoblot showing the level of influenza B virus NP expressed 8 h.p.i in MDCK and MDCK-MxA cells either in the absence or presence of C.M. Influenza B virus NP was detected using a rabbit anti-B/Hong Kong/73 antibody, MxA detection acted as a control for the presence of the IFN-induced antiviral state and actin levels were detected as a loading control. **C.** Quantification of NP synthesized 8 h.p.i firstly normalised to actin and then normalised to untreated MDCK cells. The results represent the average of three independent experiments ± S.D. (* The higher band where there are doublets is due to a background influenza B band as both the anti-MxA and anti-B/Hong Kong/73 are rabbit antibodies)

The levels of influenza B virus NP were quantified and normalised firstly to actin as the loading control and then to naïve MDCK cells without treatment with C.M (Fig. 6.6 C). In the absence of IFN the over-expression of MxA caused a 13% reduction in NP levels in comparison to untreated naïve MDCK cells. Using C.M to prime the cells prior to infection had a larger impact on the levels of influenza B virus NP produced at 8 h.p.i. In comparison to naïve, untreated MDCK cells, C.M treated naïve MDCK cells showed a 36% reduction in the amount of NP produced. Pre-treatment with C.M has an additive effect on the impact MDCK-MxA cells, which demonstrated a very similar reduction in the presence of C.M reducing the amount of NP to 53% the amount of NP present in the untreated, naïve MDCK cell control.

The results from the untreated cells are very similar to the results observed in influenza A infected A549 cells in section 3.5. The quantity of viral protein produced in the untreated cells demonstrates that without IFN treatment MxA appears to have a slightly larger impact on the amount of viral protein produced for influenza B virus in MDCK cells in comparison to influenza A virus in A549 cells. Therefore suggesting the only impact on influenza B virus replication is post-primary transcription, but also that perhaps influenza B virus is potentially as susceptible to MxA in MDCK cells as influenza A/Udorn/72 virus is in A549 cells. However, in the presence of C.M a larger reduction in the amount of NP was produced in both the naïve MDCK cells and the MDCK-MxA cells likely due to the large number of antiviral proteins that are up-regulated by the induction of the antiviral state. The MDCK-MxA cells contributed an extra 11% reduction compared to naïve MDCK cells in the presence of C.M.

Interestingly, even with naïve MDCK cells in an antiviral-induced state, influenza B virus was capable of producing 64% the amount of viral protein compared to untreated, naïve MDCK cells 8.h.p.i. This reduction pales in comparison to the reduction observed in IFN-treated influenza A virus infected A549 cells, which showed a reduction of up to 90% in NP production (Fig 3.9). This highlights the species difference in the IFN response against orthomyxoviruses and how canine kidney cells lack an efficient innate immune response against influenza viruses, which corroborates with the previous work of Frensing et al. (2011). Even the over-expression of MxA did not lead to a more dramatic response in the presence of IFN, as the comparative differences between MDCK and MDCK-MxA cells in untreated and C.M-treated were 36% and 34% in MDCK and MDCK-MxA cells respectively. This suggests that perhaps the IFN response in MDCK cells does not lead to the up-regulation of a co-factor required for MxA to exhibit the IFN-dependent antiviral activity shown by Xiao et al. (2013) in A549 cells.

Although the previous results give a clear indication of the importance of MxA and IFN on influenza B virus infection, they do not show the overall impact on the amount of virus produced during infection. Therefore naive MDCK and MDCK-MxA cells were untreated or pre-treated with C.M for 16 hours prior to infection with B/Yamanshi/98 virus at an MOI of 5 in the absence of trypsin to observe the impact of MxA and IFN on a single viral replication cycle. Following inoculation, samples were collected every 3 hours until 15 h.pi and then a final sample collected at 24 h.p.i.

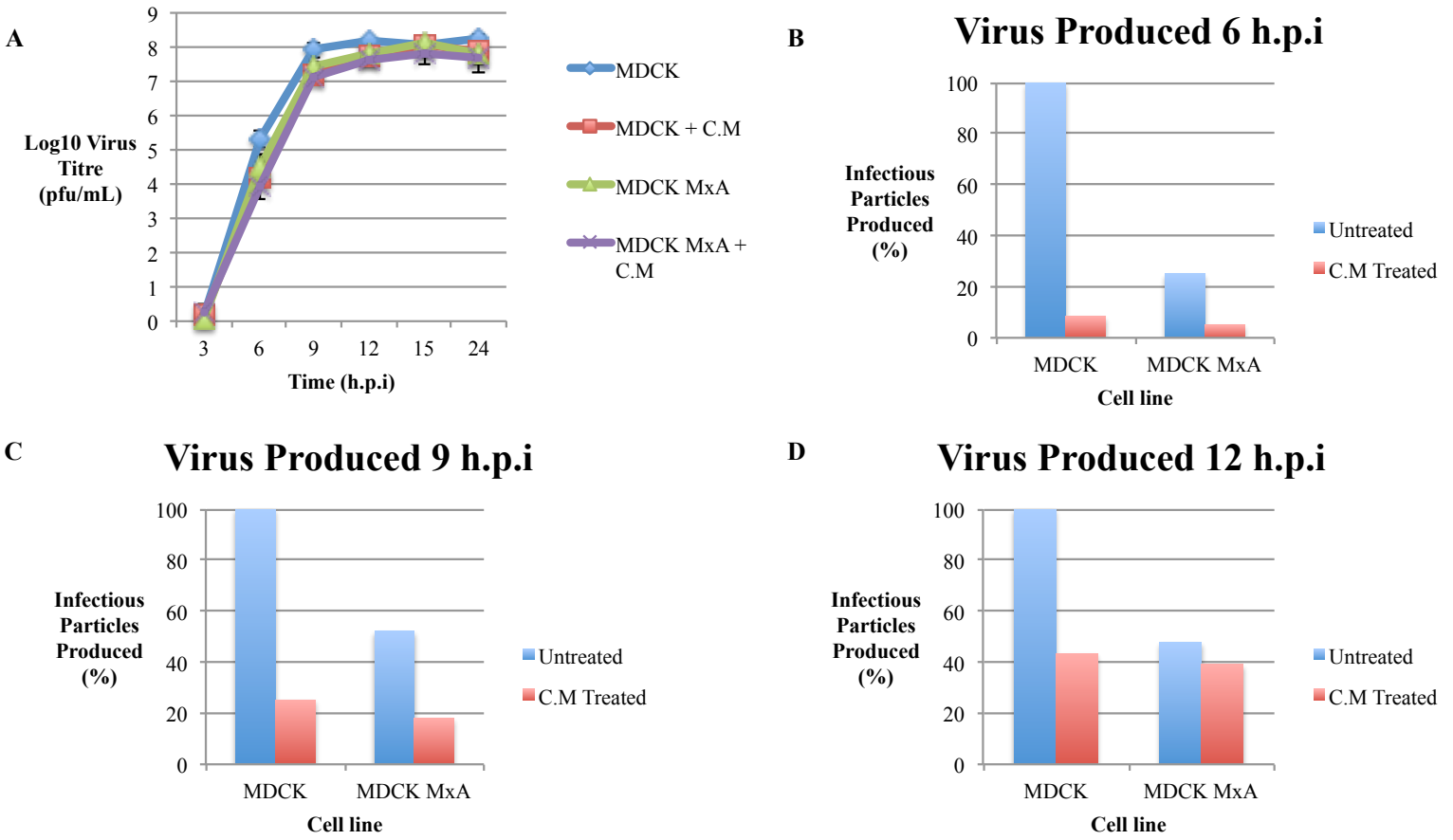


**Figure 6.7. Impact of MxA on a single cycle of influenza B virus replication. A.** MDCK and MDCK-MxA cells were either left untreated or pre-treated with C.M for 16 hours prior to infection at an MOI 5 using B/Yam/98. Samples were taken every 3 h.p.i until 15 h.p.i. with a final sample taken at 24 h.p.i. Virus titres were determined via plaque assay on MDCK cells. **B, C and D.** Show the percentage of virus produced normalised to untreated naïve MDCK cells as 100% virus production at 6, 9 and 12 h.p.i respectively

Negligible levels of virus were present at 3 h.p.i. as the single cycle of replication had not yet reached the point of virus release and following virus inoculation the cells were washed with a citric acid wash to remove virus which had not been endocytosed (Fig. 6.7 A). Therefore the first time point at which infectious virus was released was at 6 h.p.i. Similar to the data shown in the multi-step growth curve (Fig. 6.5), there was a 1-log difference between the amount of virus produced from naïve MDCK cells and the MDCK-MxA cells at 6 h.p.i. which then reduced to a 0.5 log reduction by 9 h.p.i. Similar to that trend seen in the multi-step growth curve, the over-expression of MxA caused influenza B virus to peak slightly later than in naïve MDCK cells with MDCK-MxA cells peaking at 15 h.p.i whereas naïve MDCK cells peaked at 12 h.p.i. It is also noticeable that the difference in titre between naïve MDCK and MDCK-MxA cells reduced over each time point suggesting that using a high MOI is capable of eventually surpassing the antiviral effect induced by the over-expression of MxA.

Interestingly, inducing an antiviral state in MDCK cells did not cause the same level of inhibition of infectious virus production for influenza B virus compared to that observed in section 3.5 for influenza A virus in A549 cells. Pre-treatment with C.M did lead to a clear reduction in infectious titre in both naïve MDCK and MDCK-MxA cells but only modest increase on the reduction seen by the over-expression of MxA. At 6 h.p.i in both cell-lines treated with C.M there was a reduction in infectious viral titre of approximately 1.2 and 1.4 logs (naïve and MxA-expressing cells respectively). This extent of inhibition slowly reduced to approximately 0.5 log by 12 h.p.i with infectious virus production peaking at approximately 15 h.p.i. Although, it is noticeable that C.M treatment did offer an additive effect to the antiviral activity of

MxA, as the viral titre from C.M treated MDCK-MxA cells never reached the same level as the untreated naïve MDCK cells.

Figure 6.7 B shows a graphical representation of viral titres released at 6 h.p.i normalised to untreated naive MDCK cells as 100% virus production at each time point. In untreated MDCK-MxA cells, the overexpression of MxA alone resulted in a 75% reduction in the amount of virus released at 6 h.p.i. The induction of IFN prior to infection greatly reduced the amount of virus produced from both naïve MDCK cells and MDCK-MxA cells to 8.5% and 5% respectively. This trend was continued at 9 h.p.i as Figure 6.7 C shows that the amount of infectious virus produced in untreated MDCK-MxA cells increased to 52% the amount of virus produced in naïve MDCK cells. However, at 12 h.p.i. the amount of infectious virus produced from MDCK-MxA cells in comparison to naïve MDCKs was similar at 47% (Fig 6.7 D). This suggests that, despite the clear impact of MxA on influenza B virus at early time points during infection, as the infection progressed in the absence of IFN the virus was able to reduce the impact of MxA overexpression.

In the C.M treated cells there was a large reduction in the amount of virus produced in both cell lines compared to untreated naïve MDCK cells. At 9 h.p.i, the amount of virus produced had increased to 25% and 18% of untreated naïve MDCK cells (C.M-treated naïve MDCK and MDCK-MxA cells respectively) (Fig. 6.7 C). This trend continued at 12 h.p.i (Fig. 6.7 D.) where C.M treated MDCK cells and MDCK-MxA cells produced 43% and 39% the amount of infectious particles. However at the later time points the C.M treated cells only showed a modest increase in inhibition in comparison to naïve untreated MDCK cells, which produced between 4% and 8%

more infectious virus in the MDCK and MDCK-MxA cells. This data, coupled with the protein production data highlights that MxA is clearly capable of inhibiting influenza B virus post-primary transcription but also highlights the inefficiency of the IFN response in MDCK cells against orthomyxoviruses as following 12 h.p.i the level of inhibition exhibited by C.M-treated cells is on a par with untreated cells which only overexpress MxA.

However, this data set also shows the capability of influenza B virus to dismantle the host's pre-existing antiviral state as although the level of virus produced at 6 h.p.i in the presence of IFN was only 8% the amount of virus in the untreated control MDCK cells, the percentage of virus produced from the C.M treated cells increased steadily throughout the time course.

### 6.5 Investigating influenza B virus MxA resistance

The current literature points towards the viral NP being the antiviral target of MxA, for orthomyxoviruses as well as other virus families such as bunyaviridae. Therefore, it is reasonable to assume that the NP of influenza B virus may also be the antiviral target of MxA. Specific amino acids in influenza A NP have been described to either cause susceptibility or resistance to MxA (Mänz et al. 2013). Mänz et al. (2013) identified a cluster of amino acids which conferred resistance at a number of positions, with a particular emphasis on positions 100, 283 and 313 and mapped these onto the A/HK/483/97 (H5N1) virus NP structure previously solved by Ng et al. (2008). A follow-up study also identified position 52 as having the potential to confer resistance to human MxA in influenza A NP (Riegger et al. 2015). The structure for influenza B NP has also been determined recently and used the A/HK/483/97 (H5N1)

NP structure for molecular replacement in order for it to be solved (Ng et al. 2012). Therefore to study whether influenza B virus NP encoded for amino acids that increased susceptibility to MxA, the structures for influenza A and influenza B NP were aligned and assessed for amino acid conservation at the positions highlighted by Mänz et al. (2013). The influenza B virus NP structure used for the structural alignment comes from B/Managua/2008 which only has 5 amino acid substitutions in comparison to B/Yamanshi/1998, none of which overlap with the residues of interest. The alignment is shown in Fig. 6.8 and the amino acid comparison is presented in table 6.1.

It is clear from the structural alignment that the NP of both influenza viruses is highly similar in structure as described by Ng et al. (2012), who suggest that the only major difference is the orientation of the tail loop, whereas the majority of other structural differences are in flexible surface loops. The table lists the key amino acid positions that have been previously suggested to determine resistance to the antiviral effect of MxA. Interestingly, the structural alignment shows that there is a mix of MxA sensitive amino acids and amino acids that confer resistance to MxA. For instance, aspartic acid is required to confer resistance at position 53 in influenza A NP, whereas the equivalent position in influenza B NP is E104, which has been shown to be present in MxA-sensitive avian NP. Furthermore, at positions 283 and 289, resistance is encoded by proline and tyrosine respectively whereas the corresponding amino acids in influenza B virus NP are K341 and F347 suggesting that influenza B virus NP may be susceptible to the antiviral effect of MxA.

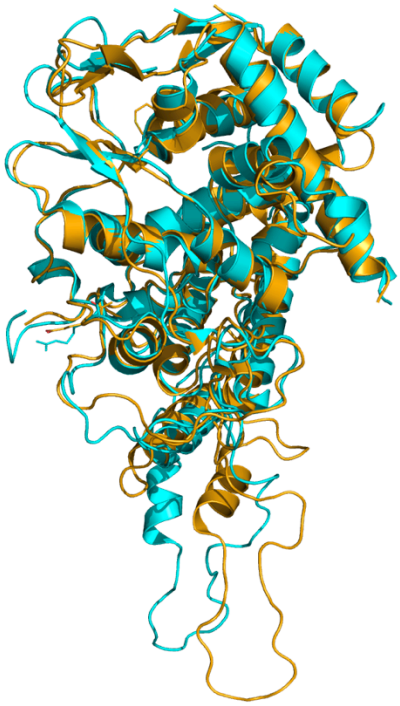

**Figure 6.8 Structural Alignment of influenza A and influenza B virus NP.** The NP of influenza B/Managua/2008 (PDB no. 3TJ0) was structurally aligned to A/HK/483/97 (PDB no. 2Q06) using Pymol. Influenza A NP = aqua and influenza B NP = gold.

| Amino Acid Position in influenza A | MxA Susceptibly Amino Acids | Resistance Mutation | Amino Acid and position in influenza B/Yam/98 |
|---|---|---|---|
| 16 | G | D (Not in structure) | N/A |
| 52 | Q | N | M103 |
| 53 | E | D | E104 |
| 100 | R | I/V | V158 |
| 283 | L | P | K341 |
| 289 | Y | Y | F347 |
| 313 | F | Y/V | V369 |

**Table 6.1 Structural Alignment of influenza A and influenza B virus NP.** This table lists the amino acids that confer for either MxA resistance or susceptibility for influenza A viruses are displayed against the structurally aligned amino acids of influenza B/Yamanshi/98 virus

However, two of the key amino acids suggested to confer resistance in influenza A NP by both Mänz et al. (2013) and Riegger et al. (2015) are present in the corresponding positions in influenza B NP. Both I/V100 and Y/V313 have been shown to increase MxA resistance in influenza A virus NP and influenza B virus NP encodes for V158 and V369 at the corresponding positions, suggesting that influenza B virus may well be resistant to the antiviral effect of MxA. Yet, it could also be difficult to determine the potential resistance markers within influenza B virus NP for MxA, as influenza B virus NP encodes a large N-terminal extension which did not offer any density in the crystal structure (Ng et al. 2012), therefore suggesting that this N-terminal extension is flexible and has the potential to mask parts of influenza B virus NP.

The structural alignment suggests that resistance to MxA may be found at different positions, as a number of positions identified by Mänz et al. (2013) are shown to have the same 'resistance' amino acids, yet influenza B virus is inhibited by MxA in both plaque reduction assays and viral growth curves (Fig 6.3 & Fig 6.5). To determine whether influenza B virus was capable of becoming resistant to the antiviral effect of MxA, B/Yamanshi/98 was serially passaged through MDCK-MxA expressing cells and assessed for resistance to MxA through plaque reduction assays in MDCK and MDCK-MxA cells. Figure 6.9 shows the percentage of plaque number on MDCK-MxA cells at each passage in comparison to naïve MDCK cells. At passage 0 (P0) the plaque number produced on MDCK-MxA cells was only 25% that of naïve MDCK cells and P1 showed a similar number of plaque number at 31%. Following P2 the number of plaques rose sharply to 61% and P3-P5 averaged consistently around the

65% mark in comparison to naïve MDCK cells. However, by P6 there was another sharp increase in the number of plaques as plaque number on the MDCK-MxA cells was equal to or greater than the plaques observed on naïve MDCK cells. Subsequent passages, P7, P8, and P9, averaged between 85 and 96% the number of plaques on MDCK-MxA cells in comparison to naïve MDCKs.

This data suggests that influenza B virus is capable of evolving to produce mutations causing resistance to the antiviral effect of MxA. To determine whether these mutations took place in influenza B virus NP, the viral RNA was extracted from P0 and P9 and used to produce cDNA for sequencing. Unfortunately the sequencing did not reveal any coding mutations to have taken place in NP, therefore the reason for the enhanced replication in MDCK-MxA cells is currently unknown. Sequencing of other gene segments may shed light on this enhanced replication.

**6.6 Discussion**

Frensing et al. (2011), showed that influenza B virus polymerase activity was sensitive to Mx1 expression, therefore this activity was assessed for sensitivity to human MxA and the panel of wMxA mutants described in section 4.2. These assays were performed using the same conditions and amounts of plasmids used to determine the impact of wMxA on A/Udorn/72 virus (Fig 4.3). The data suggests that although MxA is capable of producing an inhibitory effect against the influenza B virus polymerase, it is not as potent as against influenza A virus. This is possibly because influenza B virus is a predominantly human virus that may have evolved resistance to human MxA. Based on this data it appears that the L4 loop mutant is the most attenuated against influenza B virus. This is not surprising as this mutation substitutes

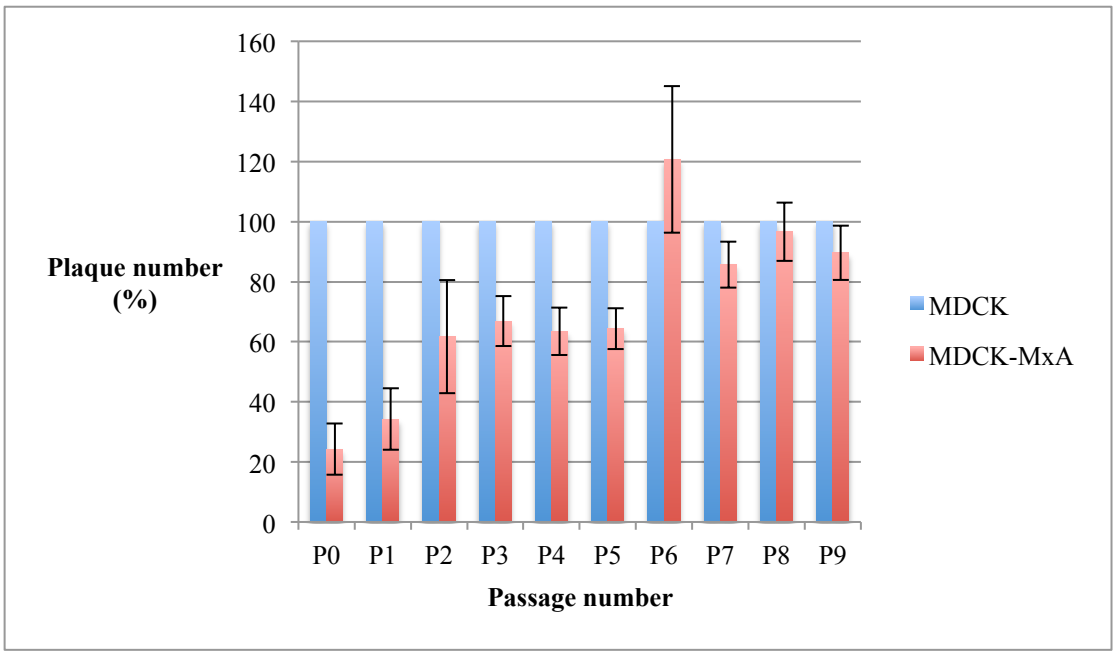


**Figure 6.9. Viral passage through MDCK-MxA cells.** MDCK-MxA cells were infected at an approximate MOI 0.001 using B/Yam/98 and viruses collected after observation of approximately 80-90% cytopathic effect. Samples were titrated via plaque assay on MDCK and MDCK-MxA cells. The cells were stained using crystal violet after 72 and 48 hours respectively. Plaque number is expressed as a percentage of plaques observed on naïve MDCK cells. Results are expressed as the average of three independent experiments ± S.D

the phenylalanine at position 561 for a valine which is present in the equivalent position in the MxA protein of macaques. This has previously been shown to be a key antiviral determinant for MxA against influenza A virus. Therefore as influenza B is a predominantly human virus, it is likely that this point mutation is going to have an increased impact on the antiviral activity of MxA against influenza B virus (Mitchell et al. 2012).

Interestingly, the T103A mutant is still capable of producing some antiviral effect, therefore suggesting that GTPase activity may not be entirely necessary for antiviral activity, but removing GTPase activity may lessen the antiviral effect of MxA as seen for influenza A virus in section 4.2. This data also indicates that the two monomeric mutants appear to be attenuated in antiviral activity against influenza B virus whereas this is not the case for influenza A, where both F602D and L612K appear to be only slightly attenuated, if at all, in comparison to wt wMxA. This suggests that perhaps the ability to oligomerise is more important for the antiviral activity against influenza B virus than it is against influenza A virus. However, with the reduced antiviral activity of MxA against influenza B virus in this assay, it makes it difficult to determine the importance of the wMxA mutations on the antiviral activity against influenza B virus and therefore further work is required to determine the structural and functional characteristics required for the antiviral activity of MxA against influenza B virus.

Interestingly, there was a large difference in the inhibitory affect of MxA on the ability of influenza A and influenza B viruses to produce plaques. The difference seen for influenza B virus was akin to that seen for influenza A virus in A549-MxA

expressing cells as demonstrated by Xiao et al. (2013). This suggests that the mechanism of antiviral activity is maybe similar to that seen in A549-MxA cells, where it is suggested that MxA inhibits the nuclear translocation of nascent NP post-primary transcription (Zürcher, Pavlovic, and Staeheli 1992; Dittmann et al. 2008). However, the impact of MxA on influenza A virus was much more prominent in MDCK cells than previously seen for A549 cells yet the 2 log reduction in plaque titre is similar to the reduction observed in murine 3T3 cells overexpressing human MxA (Pavlovic et al. 1990). A similar 2 log reduction was observed in the levels of influenza A virus genomic viral RNA in Vero cells overexpressing human MxA (Matzinger et al. 2013). Although genomic viral RNA is not the same read-out as viral titre, it is interesting to see the parallels in the scale of inhibition.

Following on from the differences in plaque reduction, it was also clear that MxA had a large impact on the early stages of influenza A virus replication in MDCK cells (Fig 6.4). As influenza B virus has already shown similar results in the plaque reduction assay (Fig 6.3) to influenza A virus in A549 cells, it comes as no surprise that there was a negligible difference in the number of cells which were positive for viral antigen in MDCK-MxA cells in comparison to naïve MDCKs as seen for influenza A virus in A549 and A549-MxA cells in section 3.4. However, there is a clear 3-fold reduction in the number of influenza A virus antigen positive cells in the presence of MxA. This data agrees with the plaque reduction data and suggests that perhaps MxA is exerting an antiviral effect prior to primary transcription. However, this can not be conclusively proven as if MxA has an increased impact post-primary transcription, by blocking nuclear translocation of nascent NP more efficiently, then MxA could be causing the increased inhibition through this mechanism instead. It is also interesting

to note that it has not been possible to observe a direct interaction between influenza A virus NP and MxA without the aid of cross-linking, whereas MxA has been shown to interact directly with other viral nucleoproteins such as THOV NP and LACV N (Turan et al. 2004; G Kochs and Haller 1999; Georg Kochs, Janzen, et al. 2002). Taken together, the differences in inhibition between human cells overexpressing MxA and cells from other hosts, coupled with the fact that an interaction between influenza A virus NP and MxA has only been observed via cross-linking, suggests that there may also be another host factor or factors involved in the antiviral activity of MxA.

Influenza B virus replication was reduced by a log in MDCK-MxA cells in early stages of both the single cycle and multi-cycle growth curves, reducing the peak titre that virus was able to reach in comparison to naïve MDCKs. This is the first time that human MxA has been shown to have an antiviral effect on influenza B virus, showing MxA to have antiviral effect against a number of the members of the orthomyxoviridae family, including influenza A virus, influenza C virus and Thogoto Virus (Marschall et al. 2000; Frese et al. 1995; Pavlovic et al. 1990). Although, this may be slightly surprising with influenza B virus being specific to humans it may have been possible for the virus to evolve intrinsic resistance to what is a key protein in the host antiviral response against orthomyxoviruses.

The initial impact of MxA on influenza B virus protein expression showed a minor reduction in NP synthesis which suggests that when MxA is overexpressed in the absence of IFN it is only capable of inhibiting influenza B virus post-primary transcription. However, it was shown that in the presence of IFN in A549 cells, MxA

was capable of producing another antiviral function, suggesting that another ISG may work as a co-factor for MxA to produce this effect (Xiao et al. 2013). To investigate whether MxA was also capable of inhibiting nuclear translocation of the influenza B virus genome in the presence of IFN, cells were pre-treated with C.M and assayed for protein levels. Although the C.M treatment was capable of inducing an antiviral state, the impact on virus protein production was not as drastic as previously observed for influenza A virus in IFN-treated A549 cells. This suggested that perhaps MxA was incapable of producing this second mechanism of antiviral activity in MDCK cells. However, it is not possible to conclude that MxA is incapable of blocking the translocation of influenza B virus genome prior to primary transcription. Firstly, unlike in A549 cells, the MDCK cells were not treated with purified IFN at a determined concentration, but with UV-inactivated conditioned media, which did contain IFN, but at an unknown concentration. If the level of IFN was lower then the response was likely to be less robust, therefore causing MxA to be unable to block nuclear translocation. Secondly, the genes that will be up-regulated in response to canine IFN is likely to be different to the genes up-regulated in response to human IFN in A549 cells, therefore it is possible that MDCK cells do not express the same co-factor, that the canine homologue of the IFN-induced co-factor may preferentially bind to canine Mx1 or does not interact with human MxA to allow for this antiviral function to occur.

Interestingly, the impact of C.M treatment prior to a virus growth experiment did not lead to a large synergistic effect alongside the over-expression of MxA as the impact of C.M treatment reduced the titre to only slightly lower than the reduction caused by MxA-expression alone. Again, as described above, this may have been down to a less

than optimal antiviral response. Yet, these results appear to corroborate the results reported by Frensing et al, (2011) who showed that the induction of an antiviral state in MDCKs had a minimal effect on influenza B virus replication, whilst showing in a mini-replicon assay that canine Mx1 has no antiviral activity against influenza B virus. This shows that the impact observed in the studies shown above was through the action of human MxA and other ISGs. Following sequence alignment (data not shown) the lack of activity of canine Mx1 appears to be due to a lack of conservation throughout the L4 loop which has previously been shown to be highly important to MxA's antiviral activity against orthomyxoviruses (Patzina, Haller, and Kochs 2014).

A number of MxA resistance mutations have been identified recently for influenza A virus NP, which have been shown to confer resistance both in a mini-replicon assay and *in vivo* (Riegger et al. 2015; Mänz et al. 2013). NP is one of the most highly conserved proteins between influenza A and B viruses, sharing up to 38% amino acid conservation. However, one clear difference between the NP of these viruses is that influenza B virus NP encodes for an N-terminal extension, in which the first 69 residues show no homology to those of influenza A virus NP. Also, the N-terminus of influenza B virus NP contains an evolutionarily conserved 50-amino-acid extension that is absent in influenza A virus NP (Sherry et al. 2014). Therefore due to differences in the length of influenza A and influenza B virus NP it was necessary to align the two protein structurally to ascertain which amino acids in influenza B virus NP correspond to the resistance clusters in influenza A NP. This analysis concluded that although not all the resistance mutations were present, some of the important resistance mutations, such as at positions 100 and 313, are also encoded in influenza B virus NP. Despite these resistance mutations influenza B virus still shows

susceptibility to MxA, which suggests that there could be other regions of influenza B virus NP that contain residues conferring MxA resistance. Recently, the N-terminal extension of influenza B NP has been shown to be required for efficient nuclear import of recombinant NP protein (Wanitchang, Narkpuk, and Jongkaewwattana 2013). In the context of whole virus it was shown not only to be important for nuclear localization but that this extension was essential for virus viability and played a clear role in mRNA transcription and genome replication (Sherry et al. 2014). It is possible that the N-terminal extension may also play a role in the ability of MxA to inhibit influenza B virus as this highly flexible region may be altering the accessibility of NP to MxA if a direct interaction takes place.

To determine the ability of influenza B virus to become resistant to the antiviral effect of MxA, the virus was blind passaged through MDCK-MxA cells at an approximate MOI of 0.001. Following titration the MOI for each passage was seen to be between 0.001 and 0.01, ensuring a low enough multiplicity to avoid the production of high levels of defective particles. There was a step-wise increase in plaque number when each passaged virus was plaqued on MDCK-MxA cells compared to naïve MDCK cells. By passage P6 the virus produced approximately equal numbers of plaques on both cell types. The NP gene of the P9 virus was then sequenced and compared to that of the starting virus to screen for adaptive mutations. Unfortunately the sequencing did not reveal any adaptive mutations with in the NP of influenza B virus, which is surprising as NP proteins of many viruses are thought to be the viral target for MxA. However, as this sequence analysis only considers NP, it is possible that other mutations may have arisen in other gene segments, such as within the polymerase

subunits, which would have allowed for a replicative advantage in the MDCK-MxA cells.

# Chapter 7 - General Discussion

## 7.1 The impact of IFN and MxA on influenza A virus

Xiao et al. (2013) had previously described the IFN-induced block on influenza virus genome nuclear translocation using a viral input assay. In Fig 3.4, this same assay was used and the nature of this IFN-induced block was investigated using TEM. The electron micrograph images showed a number of multi-membranous structures (MS) in the perinuclear region of the cytoplasm in all experimental conditions. Higher magnification images of IFN-treated, WSN-infected A549 cells suggested that these structures may contain virions. These structures were then determined to be more prevalent in both IFN-treated cells and IFN-treated, WSN-infected cells (Fig 3.7). This suggested that the increase in the MS structures might be an innate immune response, where the cell is responding to incoming endosomes as a potential pathogen.

The literature did not give a clear indication of what these structures might be as the structures fit the description of late endosomes becoming lysosomes or endolysosomes (Huotari and Helenius. 2011), whilst also appearing to fit the description of multi-lamellar autophagosomes (Lai et al. 2008 & Hernandez et al. 2003). Following the recent research suggesting that type I IFN is capable of inducing autophagy (Ambjon et al. 2013, Schmeisser et al. 2013) it is possible that IFN induces non-canonical autophagy of endosomes as a host defence against incoming pathogens. However, to determine whether these structures are related to either the lysosomal or autophagy pathways these structures need further characterisation as to the protein components involved as well as determining whether the virion-like structures observed in these MS structures are in fact viruses. One way of answering these

questions is to use immune-gold labeling following cryogenic sectioning of the samples. This uses antibodies specific to your structures of interest, such as the highly abundant influenza virus NP or M1 proteins, labeled with gold nanoparticles. These gold nanoparticles can differ in size, which allows for co-localisation studies using antibodies specific to different antigens. This would be particularly interesting in relation to the localization of MxA in these MS structures. The IFN-induced block described by Xiao et al. (2013) was shown to be dependent on MxA, therefore if these structures are the organelles that are restricting the nuclear translocation of the viral genome then it is possible that MxA localises to these structures.

The impact of MxA on influenza A virus replication was assessed in both the absence and presence of IFN (Section 3.5 & 3.6) and showed that the over-expression of MxA alone had a small impact on the level of influenza virus protein production. However, the importance of MxA to the IFN response against influenza A virus was highlighted through the use of A549-ΔMxA cells. In the presence of IFN, these cells produced 10-fold more virus than in IFN-treated naïve A549 cells. This suggested that MxA might have two different mechanisms of antiviral activity, one that is IFN-independent and one that is IFN-dependent as described in Fig 7.1. It has previously been suggested that MxA forms large oligomeric ring structures, which could wrap around the influenza vRNP (Gao et al. 2011). However, this hypothesis was based on the fact that that diameter of these ring structures was of a sufficient size to wrap around the vRNPs. This hypothesis was also put forth prior to the current knowledge that MxA restricts influenza virus genome import into the nucleus during viral entry, therefore at the time the hypothesis for the antiviral mechanism of MxA was that it was able to prevent nuclear entry post primary transcription. However a flaw in this model is that most of the experimental data was generated using minireplicon assays in the absence

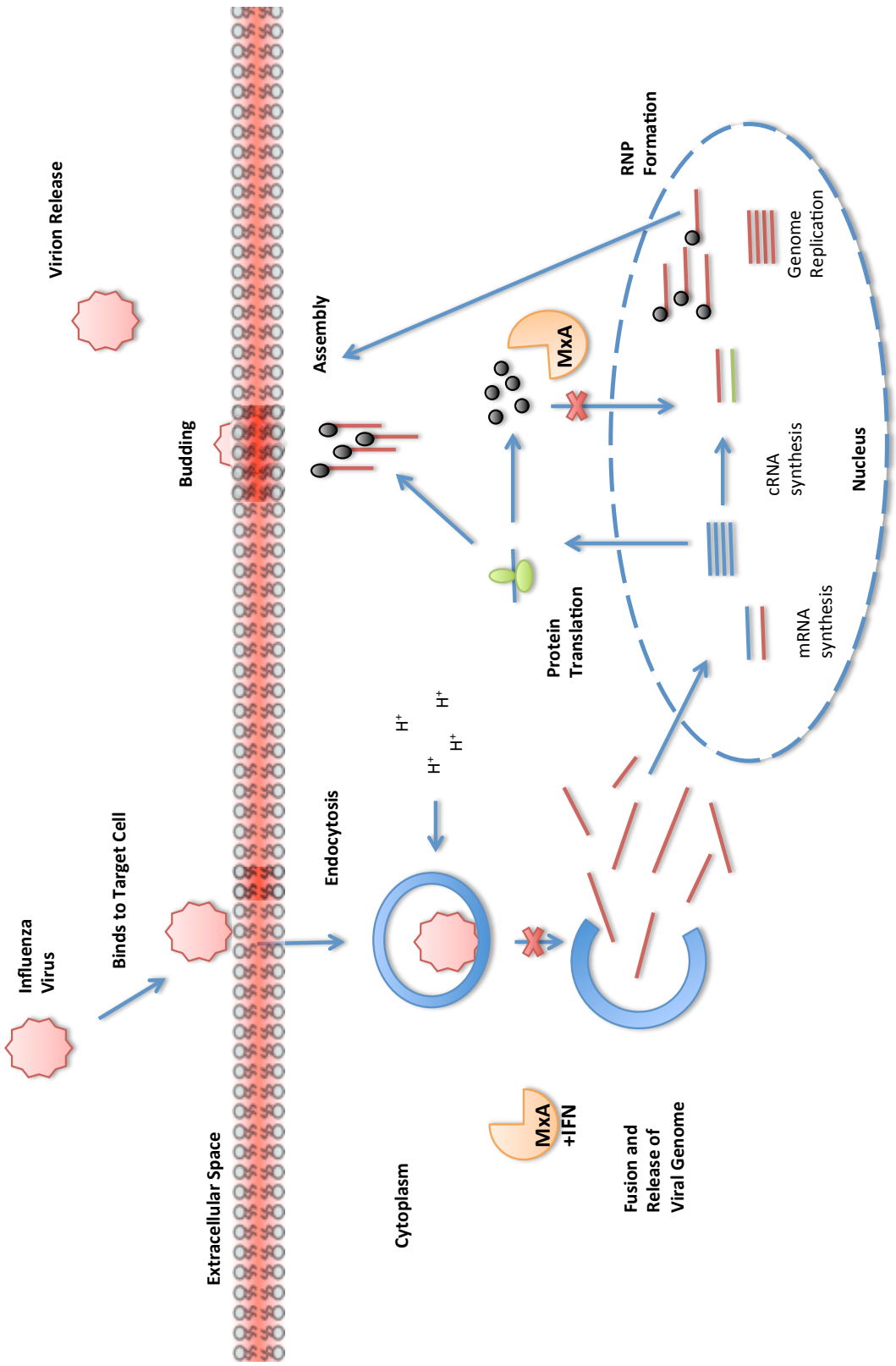


**Figure 7.1. MxA inhibits influenza replication at two distinct stages.** The schematic shows a simplified replication cycle for influenza A virus. Over-expression of MxA can inhibit influenza replication following primary transcription, potentially through the inhibition of nascent NP nuclear translocation. MxA is also capable of inhibiting vRNP nuclear translocation prior to primary transcription in the presence of IFN. This effect could be due to either a conformational change in MxA induced by IFN or through the synergistic effect of an IFN-induced co-factor.

of the viral nuclear export protein (NEP), therefore vRNPs would be entirely nuclear and unavailable for interaction with the exclusively cytoplasmic MxA. It is more likely that after primary transcription MxA is able to bind to newly synthesised NP in the cytoplasm thereby preventing its nuclear entry and subsequent genome replication. Free monomeric NP is a different size and in a different conformation to NP in vRNPs, therefore the predicted model of the antiviral activity of MxA on the post-primary transcription stage of influenza A virus replication is likely incorrect. However as it is now known that MxA is able to block the nuclear entry of vRNPs it is possible that the mechanism of antiviral activity suggested by Gao et al. (2011) is likely to occur at the viral entry stage. Therefore although the mechanism behind the antiviral activity of MxA may have been accurately predicted by Gao et al. (2011), it was postulated to act at the incorrect stage of viral replication. The MxA oligomeric structures observed by Gao et al. (2011) may therefore represent the active conformation of MxA during viral entry, however the conformation of MxA at the point of its post-primary transcription activity may be very different. However confirmation of this requires further work.

Due to the large increase in virus protein and virion production in the absence of MxA in IFN-treated cells and the minor differences observed when MxA is over-expressed in the absence of IFN, the results in this thesis suggests that the IFN-dependent mechanism of antiviral activity of MxA (during viral entry) is likely to be more important to the host defence against influenza A viruses. However, this mechanism appears to be similar to that employed by IFITM3 to block incoming influenza viruses. IFITM3 has been shown to have a wide antiviral spectrum and has been shown to block cellular entry of a number of different viruses including influenza A

virus, HIV, flaviviruses and rhabdoviruses (Bailey et al. 2014). IFITM3 has been shown to block influenza virus entry through the inhibition of fusion pore formation between the virus and the endosome (Desai et al. 2014) and is shown to interact directly with clathrin-mediated endosomes through an interaction with the AP2 μ2 subunit (R. Jia et al. 2014). It is perhaps surprising that MxA and IFITM3 may have duplicated roles in the innate immune response against a number of different viruses. However it appears that they may also have a different range of target viruses, as MxA is capable of inhibiting RNA viruses that are not inhibited by IFITM3 such as Crimean-Congo haemorrhagic fever virus (Andersson et al. 2004). Also, there does not appear to be any evidence for IFITM3 inhibiting DNA virus infection, whereas MxA has been shown to have antiviral activity against viruses like Hepatitis B virus and African Swine Fever virus (N. Li et al. 2012; Netherton et al. 2009). Although both MxA and IFITM3 demonstrate antiviral activity at a similar stage of influenza A virus entry, the mechanism behind the action of MxA is still unknown. It is possible that it has a very different mechanism to that of IFITM3 and therefore represents an alternative line of defence against any viruses that manage to bypass the IFITM3-mediated block. It is also possible that as IFITM3 is found primarily in clathrin-containing endosomes that MxA provides an antiviral defence against viruses that enter cells through non-clathrin-mediated endocytosis. If this is the case it would not be surprising that influenza A viruses are inhibited by both MxA and IFITM3 as these viruses use both clathrin-mediated and non-clathrin-mediated endocytosis mechanisms to enter cells. Further work to uncover the exact mechanism behind the antiviral activity of MxA will shed light on the roles that MxA and IFITM3 play in inhibiting viral infection.

MxA has previously been determined to bind to and tubulate liposomes in vitro (von der Malsburg et al. 2011). Section 3.7 investigated the impact of MxA on overall cellular lipid composition by comparing the lipid profiles of naïve A549 cells and A549-ΔMxA cells. Surprisingly, depleting cells of MxA appeared to have a large impact on the lipid profile of the cell. Firstly, this suggests that although MxA is under tight regulation by type I and type III IFN, there is still a small amount of constitutive expression that may play a role in the lipid metabolism of cells. This was supported by transcriptomic data presented by Benitez et al. (2015), which indicated there were approximately 40 mRNA transcripts of MxA available in naïve uninfected cells. Intriguingly, the two major changes in overall lipid profile suggested an increase in PE whilst also suggesting a reduction in PS, two lipids that could have implications for virus infection. However, these results do not offer quantification on the differences between the A549 and A549-ΔMxA cells, nor does this indicate in which membrane these changes are occurring. To fully characterise the impact of MxA on the cellular lipid profile separation of specific lipid membranes would be required whilst using an internal standard to determine lipid concentrations.

The changes observed in the lipid profile coupled with the increase in virus production from cells lacking MxA could suggest that MxA has a third potential mechanism of antiviral activity. By manipulating cellular lipid metabolism MxA could potentially alter the lipid species available to the virus during the assembly stage, which could have a significant impact on the fluidity of the viral envelope. The virus envelope requires a certain level of fluidity and movement to be able to undergo efficient fusion in the next cell. With an altered lipid profile resulting in decreased fluidity of the virion envelope the virus would still likely be capable of binding to the

cell and initiating receptor-mediated endocyotisis, however the efficiency of fusion could be significantly decreased due to biophysical restrictions imposed by the curvature of the lipid membrane. This would likely result in an increased number of infecting virus particles unable to efficiently deliver their genome into the cell and subsequently undergoing lysosomal degradation.

To determine whether MxA is having this affect on the viral lipid membrane it will be necessary to purify virions that have been produced from both naïve A549 cells and A549-ΔMxA cells in the absence and presence of IFN and analyse the lipid content of the virus envelope. To ascertain whether any identified differences have an impact on virus infectivity would require live cell imaging analysis of cells infected with viruses produced from MxA-expressing cells in which a lipid dye has been inserted into the viral membrane that fluoresces upon viral-endosomal membrane fusion. The effiency of fusion could be determined through fluorescent kinetic analysis alongside assessing virus production following infection with viruses produced in IFN-treated cells.

## 7.2 Investigating the structural and functional characteristics of the antiviral activity of MxA

Section 4.2 set out to investigate the impact of a number of mutations on MxA, some of these had been previously characterised as to there impact on influenza A virus replication, however some of these mutations had yet to be studied in the context of antiviral activity. Two SNPs had been identified within the coding region of MxA (Duc et al. 2012). These led to the two mutations G255E and V268M, which were initially introduced into the wMxA background. Although these mutations showed attenuated antiviral activity compared to wt MxA in a mini-replicon assay, they were

still able to have an effect on the replication of a viral-like RNA. The identification of polymorphisms within ISGs is becoming increasingly important in our understanding of human genetic determinants of disease susceptibility. An SNP identified in the N-terminal region of IFITM3 has been shown to be critically important in patient outcome following infection with influenza A virus (Everitt et al. 2012). Therefore determining the impact of polymorphisms on the antiviral activity of MxA may be very important to future vaccination strategy as society moves towards an era of personalized medicines. Also, as MxA has antiviral activity against a wide-range of viruses it is important that these mutations are assessed in the context of other MxA-sensitive viruses to determine the genetic risk of carrying these mutations.

However, during this study, another publication identified the impact of these SNPs on antiviral activity in the context of the endogenous MxA mRNA sequence with their results suggesting that the G255E mutant lacked antiviral activity (Dick et al. 2015a). This is in contrast to the results in this thesis in which this mutation was introduced into the wMxA background, showing that although the antiviral activity was reduced compared to wt MxA, it was still able to exert some degree of antiviral activity. This difference was emphasized by the clear difference in expression phenotype determined by immunofluorescence (Fig 4.5). This was surprising as the amino acid sequence encoded on the two constructs was identical, with the only difference being in the mRNA nucleotide sequence. This suggested that the changes mRNA sequence had influenced the expression phenotype and therefore the antiviral activity of this MxA mutant. A similar difference in antiviral activity and expression phenotype was also observed for the T103A mutant, which had previously been reported as antivirally inactive and used to suggest that GTPase activity is required for

antiviral activity against influenza A virus (Janzen, Kochs, and Haller 2000). However, in the context of wMxA mRNA, T103A is capable of exerting a small antiviral effect, which suggests that GTPase activity may not be essential for antiviral activity. It seems that the literature has been premature in describing the T103A mutant as inactive due to the loss of GTPase activity, as in all likelihood the lack of activity is simply due to the highly aggregated phenotype shown by this mutant. Therefore the lack of antiviral activity cannot be linked to the lack of GTPase activity until the antiviral effects of the wMxA-T103A mutant are determined, as this mutant does not display an aggregated phenotype. Therefore, to determine the impact of wMxA on this functional characteristic of MxA, this mutant should be purified and analysed for its ability to bind and hydrolyse GTP whilst also tested for its ability to produce oligomers to determine whether the changes in RNA sequence have an impact on the functional characteristics of MxA.

RNA structure is currently a topic of debate within the literature, with a number of recent papers tackling the topic *in vivo* (Mortimer, Kidwell, and Doudna 2014; Ding et al. 2014; Rouskin et al. 2014). Interestingly, changes in the mRNA coding regions have been implicated in the localization of nascent RNA, which could be a key factor in the expression phenotype differences observed in (Fig. A.1). Although structures predicted from mFold are capable of suggesting the most stable differences, recent studies have shown that the predicted structures based on *in vitro* RNA structures are very different to the structures adopted by RNA in the physiological cellular environment (Ding et al. 2014; Rouskin et al. 2014). Interestingly, in the context of plant cells, stress-induced genes have been shown to have much less secondary structure than housekeeping genes (Ding et al. 2014). Potentially this is to prioritise

the translation of these proteins for a rapid response to stress. Therefore it would be interesting to determine the impact of mutations on MxA under the control of an ISRE promoter following stimulation with IFN, rather than in the context of an over-expression plasmid with a promoter designed for consistent expression. This would also determine whether the human polymorphism aggregates under physiological conditions rather than in an over-expression system.

Another key factor in the phenotype differences observed in Fig. 4.5, is that the these mutations could also introduce differences in codon frequency which is detailed in Table A.1, where in the case of T103A, G255E and I376D, the mutation leads to an increase in codon frequency. This could increase the pool of available tRNAs for protein translation, thereby potentially speeding up the rate of translation and impacting the rate of folding. To determine whether this is the case, the endogenous mRNA sequence could be mutated such that all codon variations are tested for a particular mutation. Therefore in the case of T103A it would require 4 different mutants, which would each be transfected and then analysed for the expression phenotype by immunofluorescence.

MxA has been hypothesised to exert its antiviral effect by targeting and binding to influenza A virus NP (Dittmann et al. 2008). However, no direct interaction has been observed between MxA and influenza A virus NP without the aid of cross-linking (G Kochs and Haller 1999; Georg Kochs, Janzen, et al. 2002; Turan et al. 2004). Therefore it is possible that the interaction between NP and MxA may be mediated by another viral or cellular protein. Section 4.5 investigates the potential interacting partners of MxA that were identified through MS/MS analysis. This analysis

successfully identified a number of proteins had been identified previously by other precipitation studies such as actin, tubulin, fanconi anemia proteins and HNRNP1 (Horisberger 1992; Reuter et al. 2003; Roy et al. 2014). Not only did this analysis identify a number of known interacting partners but also identified a number of proteins which are involved in nuclear import, specifically with proteins known to be involved in the nuclear import of influenza proteins such as Importin-β-1 and Alpha-actinin 4. Both Importin-β-1 and Alpha-actinin 4 are involved in the nuclear import of influenza A virus NP and PB2 (E. C. Hutchinson and Fodor 2012; Strambio-De-Castillia, Niepel, and Rout 2010; S. Sharma et al. 2014). Intriguingly, both of these proteins were precipitated with wt wMxA and this is particularly interesting as increasing concentrations of NP, and also to a weaker extent PB2, is capable of reducing the antiviral effect of MxA. This coupled with the absence of these factors from precipitations using the T103A wMxA mutant (which displays reduced antiviral activity in comparison to wt wMxA) suggests the potential for an alternative model of MxA antiviral activity. This proposes a potential mechanism whereby MxA binds to the cellular co-factor required by influenza NP and PB2 for nuclear import, therefore inhibiting the nuclear import of vRNPs or newly synthesised influenza proteins.

However, to confirm this hypothesis a number of factors need to be investigated. For example, to determine the effect of these nuclear import proteins, they could be overexpressed in the context of a mini-replicon assay in the presence of MxA to determine the impact on replication efficiency. If overexpression of either Importin-β-1 or Alpha-actinin 4 result in increased viral replication in the presence of MxA then the interaction between these two proteins should be confirmed via immune-precipitation followed by mapping of this potential interaction between MxA and

these nuclear import factors. This would allow a functional model of the antiviral effects of MxA against influenza A viruses to be proposed.

### 7.3 Investigating the antiviral mechanism of MxA using constitutive expressing cell lines

Chapter 5 investigated the impact of mutations on the antiviral activity of MxA in the context of both viral infection and in the presence of IFN using cells constitutively expressing wt and mutant versions of MxA. The impact of these mutations at the different stages of influenza replication is summarized in Table 7.1. Despite differences in protein levels, the impact of these mutations was consistent across both the level of viral protein produced and the impact on plaque development in sections 5.2 and 5.4, particularly in the presence of IFN. These results showed that MxA expressed in A549-wT103A, A549-wV268M and A549-wKEKE cells exhibited a reduced ability to attenuate plaque development in the presence if IFN compared to wt wMxA. This could offer some insight into the functional characteristics of MxA required for the IFN-dependent block on influenza A virus, suggesting that both GTPase activity and lipid-binding are essential for antiviral activity. However, due to the low levels of MxA expressed, as shown in Fig 5.2, it is not possible to make any clear conclusions on the impact of these mutations on the ability of MxA to inhibit influenza A virus replication. Therefore, all cell lines should be created to express similar levels of protein to ascertain the full impact of these mutations.

However, these cell lines did suggest that the human polymorphism V268M did not show any antiviral activity in the presence of IFN. Similar to the antiviral attenuation described in section 4.2, this could have a severe impact on patient outcome in the

| Mutation | Impact on MxA | Reduced antiviral activity post-primary transcription | Reduced antiviral activity pre-primary transcription |
|---|---|---|---|
| **wT103A** | Abolishes GTPase activity | **Yes** | **Yes** |
| **wR640A** | Preferentially Dimeric | **Yes** | **No** |
| **wV268M** | Human Polymorphism | **Yes** | **Yes** |
| **wG255E** | Human Polymorphism | **Yes** | **No** |
| **wF561V** | L4 loop mutation, reduces antiviral activity against influenza virus | **Yes** | **No** |
| **wF602D** | Monomeric | **Yes** | **No** |
| **wL612K** | Monomeric | **Yes** | **No** |
| **wI376D** | Preferentially Dimeric | **Yes** | **No** |
| **wD478A** | Preferentially Dimeric | **Yes** | **No** |
| **wAKAK** | Potentially impacts lipid binding | **Yes** | **No** |
| **wKEKE** | Potentially impacts lipid binding | **Yes** | **Yes** |

**Table 7.1. Impact of mutations on the antiviral activity of MxA against influenza A virus.** The impact on the antiviral activity for each mutant post-primary transcription was assessed against an Mx-sensitive avian NP from A/Thailand/1(Kan-1)/04 and the impact of these mutations in the presence of IFN was assessed via plaque reduction assay.

context of influenza virus infection. Therefore to determine whether these mutations have an impact *in vivo* it may be necessary to introduce this mutation into an animal model. There are currently transgenic mouse models that constitutively express human MxA instead of murine Mx1 (Hefti et al. 1999). The human SNPs described by Duc et al. (2002) could be introduced into the MxA gene of these transgenic mice and following virus challenge the effects of wt and mutant MxA on animal survival could be determined. This can also be assessed in the absence of IFN as MxA-expressing mice have previously been crossed with mice that do not express the IFN-α/β receptor (Hefti et al. 1999). Therefore, it would be possible to determine whether this mutation also causes a disadvantage for the host following post-primary transcription during challenge with influenza A virus.

As described previously, MxA has a wide range of antiviral targets and appears to have different mechanisms of antiviral activity for a number of different viruses, whether it is through a direct interaction such as with THOV RNPs or via sequestering an important part of the virus replication machinery such as the isolation of LACV N away from viral replication centres (G Kochs and Haller 1999; Georg Kochs, Janzen, et al. 2002). More recently a region in the L4 loop of MxA was determined to be necessary for antiviral activity against bunyaviruses (Patzina, Haller, and Kochs 2014). MxA therefore has a variety of antiviral mechanisms to inhibit a wide range of viruses. Therefore it would be interesting to determine which functional characteristics of MxA are required for the antiviral activity against other viruses through infection of constitutive expressing cell lines.

IFN induced MxA expression appears to have a very distinct expression phenotype, co-localising to the perinuclear regions, likely to ER membranes, and to the plasma membrane (Fig 5.7). This suggests that MxA may be positioned at the plasma membrane in order to quickly localise to any incoming endosomes whilst the cell is in an antiviral state. One method well suited to determine the localization and protein dynamics at the plasma membrane is total internal reflection microscopy (TIRF). TIRF allows for the selective illumination of fluorophores, which are close to the plasma membrane whilst being able to reduce the level of background fluorescence emitted from the rest of the cell. TIRF has been used previously to study the distinct dynamics of endosome formation by determining the presence and absence of proteins throughout the vesicle forming process (Mattheyses, Simon, and Rappoport 2010). This suggests that TIRF would be a good candidate to determine whether MxA is being recruited directly to endosomes during vesicle formation or later stages of the endosomal process.

Section 5.5 attempted to determine whether MxA was recruited to the incoming influenza viruses using N-terminally tagged MxA and Rab proteins (Fig 5.11). Unfortunately, it was not possible to determine any clear co-localisation events in the presence of IFN with a high MOI. This may have been due to the nature of GFP-fluorescence which emits light almost 80-fold wider than the actual size of the GFP molecule itself (Grove 2014). Therefore, to determine whether MxA is localizing with incoming endosomes, it may be necessary to use super resolution microscopy. For example stimulated emission depletion (STED) microscopy is a confocal technique that uses a depletion laser to block the fluorescent emission in the specific area around

a discrete spot of 10–100 nm. This block then allows the proteins of interest within this area to be assessed in isolation (Schermelleh, Heintzmann, and Leonhardt 2010).

It may also be possible to use Photo-Activated Localization Microscopy (PALM), which requires the use of switchable fluorescent proteins such as mEOS or Photo-Activated GFP (PA-GFP). These tags can be triggered from a dark 'off' state into a fluorescent 'on' state using a specific short wavelength activation laser. This followed by illumination with an excitation laser then causes the tagged proteins to emit a bright fluorescent signal before a rapid photo-bleaching event. The signals from each probe appear randomly and with a high probability of only appearing once, making it possible to determine not only molecular localization but also molecular stoichiometry (Lee et al. 2012; Puchner et al. 2013). Applying this technology to the study of MxA cellular localization would not only identify whether MxA localises to early or late endosomes but would also allow the number of MxA molecules present to be determined.

### 7.4 Investigating the antiviral activity of MxA against influenza B virus

Sections 6.2 and 6.3 investigate the impact of MxA on both influenza A and B viruses. Fig 6.3 shows that influenza B virus plaques dropped by approximately 75% in the presence of human MxA in comparison to naïve MDCK cells, showing a similar level of reduction to that seen by Xiao et al. (2013) when investigating the impact of MxA on influenza A virus in the context of A549 cells. This suggests that influenza B virus is also susceptible to MxA, like both influenza A and influenza C viruses (Marschall et al. 2000). The extent of plaque reduction is similar to that seen for A/Udorn/72 in A549-MxA cells. A/Udorn/72 is a virus that contains residues in

NP that have been shown to confer a level of MxA resistance compared to the MxA-sensitive avian influenza viruses. The similarity in plaque reduction observed between A/Udorn/72 and influenza B virus in the presence of MxA suggests that although influenza B virus replication is reduced in the presence of MxA, the virus may have some level of natural resistance to MxA. If this is the case it would not be surprising as influenza B viruses are strictly human pathogens that may have evolved resistance to MxA over time, whereas MxA has been shown to be more effective against zoonotic viruses that cross the species barrier from avian species into humans (Zimmermann et al. 2011; Mänz et al. 2013).

However, what was striking was the difference in plaque reduction observed in influenza A virus-infected MDCK cells expressing MxA. A near 2-log reduction was observed in A/Udorn/72 virus-infected MDCK-MxA cells in comparison to naïve MDCK cells, yet only a 75% reduction in plaque number was observed in A549-MxA cells (section 5.4 and Xiao et al. (2013)). This is somewhat surprising as A/Udorn/72 harbours some of the key MxA resistance mutations that were identified by Mänz et al. (2013). Therefore such a large difference in susceptibility of the same virus in two different cell lines transduced with the same lentivirus construct was unexpected. This level of reduction is similar to those observed in MxA-overexpressing murine 3T3 cells and Vero cells (Pavlovic et al. 1990; Matzinger et al. 2013). This suggests that there may be host differences that affect the level of antiviral activity exerted by MxA against influenza A virus. This offers more evidence to suggest that the inhibition caused by MxA is likely down to an indirect interaction with NP, as a direct interaction would likely show similar levels of reduction across a number of different cell lines.

Influenza A and B virus NP were structurally aligned to establish whether influenza B virus NP encoded for any of the resistance mutations previously identified in influenza A virus NP (Fig 6.8). This analysis showed that influenza B virus NP did appear to have some of the resistance mutations which were present in influenza A NP, yet still showed a log-reduction during viral growth kinetics (Fig 6.5 & Fig 6.7) The presence of potential resistance mutations at conserved positions within NP was unsurprising due to the fact that humans are the natural host of influenza B viruses. Due to the susceptibility displayed in the context of viral growth kinetics and plaque reduction assay, influenza B/Yamanashi/98 was passaged through MDCK-MxA cells until the infectious titre of virus released from naïve MDCK cells and MDCK-MxA cells was similar. Following passage 9 the viral NP gene was sequenced to determine whether any compensatory mutations had taken place within the gene, resulting in the enhanced MxA resistance observed. Unfortunately no differences were found, however, resistance mutations may have taken place in another gene segment involved in MxA resistance, such as has been shown for the PB2 gene of influenza A virus (Turan et al. 2004). However, to determine whether a resistance mutation truly conferred resistance to MxA the mutation would need to be individually introduced into the wt virus in the absence of any mutations by reverse genetics, and the virus then compared to wt virus in viral growth kinetics and plaque reduction assays in both naïve MDCK and MDCK-MxA cells. If the mutation was detected in a polymerase gene the functional consequence of the mutation could be determined by introducing the mutation into the protein expression plasmid used in mini-genome assays and assessing differences in polymerase activity in the presence of MxA.

## 7.5 Conclusions

The aim of this thesis was to investigate the mechanism of antiviral activity of MxA against influenza viruses. This study has led to the conclusion that MxA has two different mechanisms of antiviral activity, one that is dependent of IFN, at the virus entry stage, and one that is independent of IFN post-primary transcription of viral mRNAs. The data suggests that the IFN-independent function of MxA may be mediated by an indirect interaction between MxA and the influenza virus NP with this interaction dependent on a host-derived co-factor. Surprisingly, there is also an indication that MxA may have a third mechanism of antiviral activity against enveloped viruses by affecting lipid composition, thereby potentially decreasing viral infectivity. Although it has not been possible to conclude the specific functions and characteristics of MxA required for antiviral activity, it has been possible to determine a number of different factors which may be important for antiviral activity. Interestingly, it appears that oligomerisation of MxA is not required for MxA to exert its antiviral effect post-primary transcription, yet GTPase activity and potentially lipid-binding may be essential to the IFN-dependent mechanism of antiviral activity.

This work also unexpectedly showed the importance of RNA sequence to the translation of MxA. This suggested that previous conclusions in the literature regarding the functions and characteristics of MxA required for exerting antiviral activity, based on the use of mutant MxA proteins, may be incorrect. The effects of mutations in MxA on its antiviral activity reported in these previous studies may not be due to the protein sequence or function being affected by the mutations, but are likely due to protein aggregation determined by the RNA sequence. This opened up a

number of interesting questions about the importance of RNA sequence and structure for protein translation and localization, which may have implications for wider fields than virology and innate immunity.

The results in chapter 5 have also determined that like other influenza viruses, influenza B virus is also susceptible to the antiviral activity of MxA, despite being a human-specific pathogen, whilst also separately evolving some of the MxA resistance mutations observed in human-derived influenza A viruses.

Overall the data in this thesis has shed light on a number of important aspects of MxA's ability to inhibit influenza virus replication. The data has i) further characterised the role of MxA in preventing entry of influenza viruses into the cell; ii) provided insights into the requirements of MxA to perform its antiviral activity, such as GTPase and lipid-binding abilities; iii) identified natural SNPs as genetic determinants of influenza virus susceptibility; iv) identified a role of MxA in altering cellular lipid metabolism, thereby potentially offering a third antiviral mechanism; and v) characterised the effects of MxA against influenza B viruses for the first time. Taken together the data generated during this project has provided new information illustrating how the human MxA protein provides potent antiviral activity against influenza virus infection. Understanding the molecular basis of how the various components of the innate immune system, such as MxA, function against important human pathogens is fundamentally important in our efforts to create better long-term treatment options for all viral diseases. Furthermore the work has shown that naturally occurring defects in MxA may represent genetic determinants of disease. These results could from the basis for future studies that could provide significant advances

in understanding how genetic defects in innate immunity affect human susceptibility not only to influenza viruses, but also to infection by other pathogens. This will have significant impacts not only on our efforts for controlling viral infections in general, but also for shaping future methods of genetic susceptibility screening and vaccination strategies.

## References


1. Ablasser, Andrea, Marion Goldeck, Taner Cavlar, Tobias Deimling, Gregor Witte, Ingo Röhl, Karl-Peter Hopfner, Janos Ludwig, and Veit Hornung. 2013. "cGAS Produces a 2′-5′-Linked Cyclic Dinucleotide Second Messenger That Activates STING." *Nature* 498 (7454): 380–84. doi:10.1038/nature12306.
2. Accola, Molly A, Bing Huang, Azzah Al Masri, and Mark A McNiven. 2002. "The Antiviral Dynamin Family Member, MxA, Tubulates Lipids and Localizes to the Smooth Endoplasmic Reticulum." *The Journal of Biological Chemistry* 277 (24): 21829–35. doi:10.1074/jbc.M201641200.
3. Akarsu, Hatice, Wilhelm P. Burmeister, Carlo Petosa, Isabelle Petit, Christoph W. Müller, Rob W. H. Ruigrok, and Florence Baudin. 2003. "Crystal Structure of the M1 Protein-Binding Domain of the Influenza A Virus Nuclear Export Protein (NEP/NS2)." *The EMBO Journal* 22 (18): 4646–55. doi:10.1093/emboj/cdg449.
4. Alexopoulou, L, A C Holt, R Medzhitov, and R A Flavell. 2001. "Recognition of Double-Stranded RNA and Activation of NF-kappaB by Toll-like Receptor 3." *Nature* 413 (6857): 732–38. doi:10.1038/35099560.
5. Ambjørn, Malene, Patrick Ejlerskov, Yawei Liu, Michael Lees, Marja Jäättelä, and Shohreh Issazadeh-Navikas. 2013. "IFNB1/interferon-β-Induced Autophagy in MCF-7 Breast Cancer Cells Counteracts Its Proapoptotic Function." *Autophagy* 9 (3): 287–302.
6. Amorim, Maria Joao, Emily A. Bruce, Eliot K. C. Read, Agnes Foeglein, Robert Mahen, Amanda D. Stuart, and Paul Digard. 2011. "A Rab11- and Microtubule-Dependent Mechanism for Cytoplasmic Transport of Influenza A Virus Viral RNA." *Journal of Virology* 85 (9): 4143–56. doi:10.1128/JVI.02606-10.
7. Andersson, Ida, Linda Bladh, Mehrdad Mousavi-Jazi, Karl-Eric Magnusson, Ake Lundkvist, Otto Haller, and Ali Mirazimi. 2004. "Human MxA Protein Inhibits the Replication of Crimean-Congo Hemorrhagic Fever Virus." *Journal of Virology* 78 (8): 4323–29.
8. Andrejeva, J, K S Childs, D F Young, T S Carlos, N Stock, S Goodbourn, and R E Randall. 2004. "The V Proteins of Paramyxoviruses Bind the IFN-Inducible RNA Helicase, Mda-5, and Inhibit Its Activation of the IFN-Beta Promoter." *Proceedings of the National Academy of Sciences of the United States of America* 101 (49): 17264–69. doi:10.1073/pnas.0407639101.
9. Arranz, Rocío, Rocío Coloma, Francisco Javier Chichón, José Javier Conesa, José L Carrascosa, José M Valpuesta, Juan Ortín, and Jaime Martín-Benito. 2012. "The Structure of Native Influenza Virion Ribonucleoproteins." *Science (New York, N.Y.)* 338 (6114): 1634–37. doi:10.1126/science.1228172.
10. Atianand, Maninjay K., and Katherine A. Fitzgerald. 2013. "Molecular Basis of DNA Recognition in the Immune System." *The Journal of Immunology* 190 (5): 1911–18. doi:10.4049/jimmunol.1203162.
11. Ayllon, Juan, and Adolfo García-Sastre. 2015. "The NS1 Protein: A Multitasking Virulence Factor." *Current Topics in Microbiology and Immunology* 386: 73–107. doi:10.1007/82_2014_400.

12. Bailey, Charles C., Guocai Zhong, I-Chueh Huang, and Michael Farzan. 2014. “IFITM-Family Proteins: The Cell’s First Line of Antiviral Defense.” *Annual Review of Virology* 1 (November): 261–83. doi:10.1146/annurev-virology-031413-085537.
13. Barclay, W. S., and P. Palese. 1995. “Influenza B Viruses with Site-Specific Mutations Introduced into the HA Gene.” *Journal of Virology* 69 (2): 1275–79.
14. Bazzigher, L., A. Schwarz, and P. Staeheli. 1993. “No Enhanced Influenza Virus Resistance of Murine and Avian Cells Expressing Cloned Duck Mx Protein.” *Virology* 195 (1): 100–112. doi:10.1006/viro.1993.1350.
15. Benitez, Asiel A., Maryline Panis, Jia Xue, Andrew Varble, Jaehee V. Shim, Amy L. Frick, Carolina B. López, David Sachs, and Benjamin R. tenOever. 2015. “In Vivo RNAi Screening Identifies MDA5 as a Significant Contributor to the Cellular Defense against Influenza A Virus.” *Cell Reports* 11 (11): 1714–26. doi:10.1016/j.celrep.2015.05.032.
16. Betakova, T., M. V. Nermut, and A. J. Hay. 1996. “The NB Protein Is an Integral Component of the Membrane of Influenza B Virus.” *Journal of General Virology* 77 (11): 2689–94. doi:10.1099/0022-1317-77-11-2689.
17. Bhat, Numana, and Katherine A. Fitzgerald. 2014. “Recognition of Cytosolic DNA by cGAS and Other STING-Dependent Sensors.” *European Journal of Immunology* 44 (3): 634–40. doi:10.1002/eji.201344127.
18. Biswas, S. K., and D. P. Nayak. 1994. “Mutational Analysis of the Conserved Motifs of Influenza A Virus Polymerase Basic Protein 1.” *Journal of Virology* 68 (3): 1819–26.
19. Blanc, Mathieu, Wei Yuan Hsieh, Kevin A. Robertson, Kai A. Kropp, Thorsten Forster, Guanghou Shui, Paul Lacaze, et al. 2013. “The Transcription Factor STAT-1 Couples Macrophage Synthesis of 25-Hydroxycholesterol to the Interferon Antiviral Response.” *Immunity* 38 (1): 106–18. doi:10.1016/j.immuni.2012.11.004.
20. Bodewes, Rogier, Danny Morick, Gerrie de Mutsert, Nynke Osinga, Theo Bestebroer, Stefan van der Vliet, Saskia L. Smits, et al. 2013. “Recurring Influenza B Virus Infections in Seals.” *Emerging Infectious Diseases* 19 (3): 511–12. doi:10.3201/eid1903.120965.
21. Braam, J., I. Ulmanen, and R. M. Krug. 1983. “Molecular Model of a Eucaryotic Transcription Complex: Functions and Movements of Influenza P Proteins during Capped RNA-Primed Transcription.” *Cell* 34 (2): 609–18.
22. Brantis-de-Carvalho, Carlos Eduardo, Ghizlane Maarifi, Paulo Eduardo Gonçalves Boldrin, Cleslei Fernando Zanelli, Sébastien Nisole, Mounira K. Chelbi-Alix, and Sandro Roberto Valentini. 2015. “MxA Interacts with and Is Modified by the SUMOylation Machinery.” *Experimental Cell Research* 330 (1): 151–63. doi:10.1016/j.yexcr.2014.10.020.
23. Brass, Abraham L, I-Chueh Huang, Yair Benita, Sinu P John, Manoj N Krishnan, Eric M Feeley, Bethany J Ryan, et al. 2009. “The IFITM Proteins Mediate Cellular Resistance to Influenza A H1N1 Virus, West Nile Virus, and Dengue Virus.” *Cell* 139 (7): 1243–54. doi:10.1016/j.cell.2009.12.017.
24. BRASSARD, DIANA L., GEORGE P. LESER, and ROBERT A. LAMB. 1996. “Influenza B Virus NB Glycoprotein Is a Component of the Virion.” *Virology* 220 (2): 350–60. doi:10.1006/viro.1996.0323.

25. Brest, Patrick, Pierre Lapaquette, Mouloud Souidi, Kevin Lebrigand, Annabelle Cesaro, Valérie Vouret-Craviari, Bernard Mari, et al. 2011. "A Synonymous Variant in IRGM Alters a Binding Site for miR-196 and Causes Deregulation of IRGM-Dependent Xenophagy in Crohn's Disease." *Nature Genetics* 43 (3): 242–45. doi:10.1038/ng.762.
26. Bui, M., E. G. Wills, A. Helenius, and G. R. Whittaker. 2000. "Role of the Influenza Virus M1 Protein in Nuclear Export of Viral Ribonucleoproteins." *Journal of Virology* 74 (4): 1781–86.
27. Calder, Lesley J., Sebastian Wasilewski, John A. Berriman, and Peter B. Rosenthal. 2010. "Structural Organization of a Filamentous Influenza A Virus." *Proceedings of the National Academy of Sciences of the United States of America* 107 (23): 10685–90. doi:10.1073/pnas.1002123107.
28. Cao, Wei, and Yong-Jun Liu. 2007. "Innate Immune Functions of Plasmacytoid Dendritic Cells." *Current Opinion in Immunology* 19 (1): 24–30. doi:10.1016/j.coi.2006.11.004.
29. Capobianchi, M R, H Ankel, F Ameglio, R Paganelli, P M Pizzoli, and F Dianzani. 1992. "Recombinant Glycoprotein 120 of Human Immunodeficiency Virus Is a Potent Interferon Inducer." *AIDS Research and Human Retroviruses* 8 (5): 575–79.
30. Carlos, T. S., R. Fearns, and R. E. Randall. 2005. "Interferon-Induced Alterations in the Pattern of Parainfluenza Virus 5 Transcription and Protein Synthesis and the Induction of Virus Inclusion Bodies." *Journal of Virology* 79 (22): 14112–21. doi:10.1128/JVI.79.22.14112-14121.2005.
31. Chan, Robin B., Lukas Tanner, and Markus R. Wenk. 2010. "Implications for Lipids during Replication of Enveloped Viruses." *Chemistry and Physics of Lipids* 163 (6): 449–59. doi:10.1016/j.chemphyslip.2010.03.002.
32. Chan, Wai-Hon, Andy Ka-Leung Ng, Nicole C. Robb, Mandy Ka-Han Lam, Paul Kay-Sheung Chan, Shannon Wing-Ngor Au, Jia-Huai Wang, Ervin Fodor, and Pang-Chui Shaw. 2010. "Functional Analysis of the Influenza Virus H5N1 Nucleoprotein Tail Loop Reveals Amino Acids That Are Crucial for Oligomerization and Ribonucleoprotein Activities." *Journal of Virology* 84 (14): 7337–45. doi:10.1128/JVI.02474-09.
33. Chen, Benjamin J., George P. Leser, David Jackson, and Robert A. Lamb. 2008. "The Influenza Virus M2 Protein Cytoplasmic Tail Interacts with the M1 Protein and Influences Virus Assembly at the Site of Virus Budding." *Journal of Virology* 82 (20): 10059–70. doi:10.1128/JVI.01184-08.
34. Chen, W., P. A. Calvo, D. Malide, J. Gibbs, U. Schubert, I. Bacik, S. Basta, et al. 2001. "A Novel Influenza A Virus Mitochondrial Protein That Induces Cell Death." *Nature Medicine* 7 (12): 1306–12. doi:10.1038/nm1201-1306.
35. Cheung, Joanne C., and Charles M. Deber. 2008. "Misfolding of the Cystic Fibrosis Transmembrane Conductance Regulator and Disease." *Biochemistry* 47 (6): 1465–73. doi:10.1021/bi702209s.
36. Chien, C. Y., R. Tejero, Y. Huang, D. E. Zimmerman, C. B. Ríos, R. M. Krug, and G. T. Montelione. 1997. "A Novel RNA-Binding Motif in Influenza A Virus Non-Structural Protein 1." *Nature Structural Biology* 4 (11): 891–95.
37. Chieux, V, W Chehadeh, J Harvey, O Haller, P Wattré, and D Hober. 2001. "Inhibition of Coxsackievirus B4 Replication in Stably Transfected Cells Expressing Human MxA Protein." *Virology* 283 (1): 84–92. doi:10.1006/viro.2001.0877.

38. Chou, Yi-ying, Nicholas S. Heaton, Qinshan Gao, Peter Palese, Robert H. Singer, Robert Singer, and Timothée Lionnet. 2013. "Colocalization of Different Influenza Viral RNA Segments in the Cytoplasm before Viral Budding as Shown by Single-Molecule Sensitivity FISH Analysis." *PLoS Pathogens* 9 (5): e1003358. doi:10.1371/journal.ppat.1003358.
39. Ciampor, F., P. M. Bayley, M. V. Nermut, E. M. Hirst, R. J. Sugrue, and A. J. Hay. 1992. "Evidence That the Amantadine-Induced, M2-Mediated Conversion of Influenza A Virus Hemagglutinin to the Low pH Conformation Occurs in an Acidic Trans Golgi Compartment." *Virology* 188 (1): 14–24.
40. Clifford, Monica, James Twigg, and Chris Upton. 2009. "Evidence for a Novel Gene Associated with Human Influenza A Viruses." *Virology Journal* 6: 198. doi:10.1186/1743-422X-6-198.
41. Cros, Jerome F, Adolfo García-Sastre, and Peter Palese. 2005. "An Unconventional NLS Is Critical for the Nuclear Import of the Influenza A Virus Nucleoprotein and Ribonucleoprotein." *Traffic (Copenhagen, Denmark)* 6 (3): 205–13. doi:10.1111/j.1600-0854.2005.00263.x.
42. Daumke, Oliver, Song Gao, Alexander von der Malsburg, Otto Haller, and Georg Kochs. 2010. "Structure of the MxA Stalk Elucidates the Assembly of Ring-like Units of an Antiviral Module." *Small GTPases* 1 (1): 62–64. doi:10.4161/sgtp.1.1.12989.
43. De Conto, Flora, Silvia Covan, Maria Cristina Arcangeletti, Guido Orlandini, Rita Gatti, Giuseppe Dettori, and Carlo Chezzi. 2011. "Differential Infectious Entry of Human Influenza A/NWS/33 Virus (H1N1) in Mammalian Kidney Cells." *Virus Research* 155 (1): 221–30. doi:10.1016/j.virusres.2010.10.008.
44. de Graaf, Miranda, and Ron A. M. Fouchier. 2014. "Role of Receptor Binding Specificity in Influenza A Virus Transmission and Pathogenesis." *The EMBO Journal* 33 (8): 823–41. doi:10.1002/embj.201387442.
45. Degrandi, Daniel, Carolin Konermann, Cornelia Beuter-Gunia, Alexandra Kresse, Jan Würthner, Stefanie Kurig, Sandra Beer, and Klaus Pfeffer. 2007. "Extensive Characterization of IFN-Induced GTPases mGBP1 to mGBP10 Involved in Host Defense." *Journal of Immunology (Baltimore, Md.: 1950)* 179 (11): 7729–40.
46. Delaleau, Mildred, and Katherine L. B. Borden. 2015. "Multiple Export Mechanisms for mRNAs." *Cells* 4 (3): 452–73. doi:10.3390/cells4030452.
47. Demirov, Dimiter, Gülsah Gabriel, Carola Schneider, Heinrich Hohenberg, and Stephan Ludwig. 2012. "Interaction of Influenza A Virus Matrix Protein with RACK1 Is Required for Virus Release." *Cellular Microbiology* 14 (5): 774–89. doi:10.1111/j.1462-5822.2012.01759.x.
48. Deng, Tao, Frank T. Vreede, and George G. Brownlee. 2006. "Different De Novo Initiation Strategies Are Used by Influenza Virus RNA Polymerase on Its cRNA and Viral RNA Promoters during Viral RNA Replication." *Journal of Virology* 80 (5): 2337–48. doi:10.1128/JVI.80.5.2337-2348.2006.
49. Desai, Tanay M., Mariana Marin, Christopher R. Chin, George Savidis, Abraham L. Brass, and Gregory B. Melikyan. 2014. "IFITM3 Restricts Influenza A Virus Entry by Blocking the Formation of Fusion Pores

Following Virus-Endosome Hemifusion." *PLoS Pathogens* 10 (4): e1004048. doi:10.1371/journal.ppat.1004048.
50. de Vries, Erik, Donna M. Tscherne, Marleen J. Wienholts, Viviana Cobos-Jiménez, Florine Scholte, Adolfo García-Sastre, Peter J. M. Rottier, and Cornelis A. M. de Haan. 2011. "Dissection of the Influenza A Virus Endocytic Routes Reveals Macropinocytosis as an Alternative Entry Pathway." *PLoS Pathogens* 7 (3): e1001329. doi:10.1371/journal.ppat.1001329.
51. Dias, Alexandre, Denis Bouvier, Thibaut Crépin, Andrew A McCarthy, Darren J Hart, Florence Baudin, Stephen Cusack, and Rob W H Ruigrok. 2009. "The Cap-Snatching Endonuclease of Influenza Virus Polymerase Resides in the PA Subunit." *Nature* 458 (7240): 914–18. doi:10.1038/nature07745.
52. Dick, Alexej, Laura Graf, Daniel Olal, Alexander von der Malsburg, Song Gao, Georg Kochs, and Oliver Daumke. 2015a. "Role of Nucleotide Binding and GTPase Domain Dimerization in Dynamin-like Myxovirus Resistance Protein A for GTPase Activation and Antiviral Activity." *The Journal of Biological Chemistry*, March. doi:10.1074/jbc.M115.650325.
53. ———. 2015b. "Role of Nucleotide Binding and GTPase Domain Dimerization in Dynamin-like Myxovirus Resistance Protein A for GTPase Activation and Antiviral Activity." *The Journal of Biological Chemistry* 290 (20): 12779–92. doi:10.1074/jbc.M115.650325.
54. Diebold, Sandra S, Tsuneyasu Kaisho, Hiroaki Hemmi, Shizuo Akira, and Caetano Reis e Sousa. 2004. "Innate Antiviral Responses by Means of TLR7-Mediated Recognition of Single-Stranded RNA." *Science (New York, N.Y.)* 303 (5663): 1529–31. doi:10.1126/science.1093616.
55. Diebold, Sandra S, Catherine Massacrier, Shizuo Akira, Carine Paturel, Yannis Morel, and Caetano Reis e Sousa. 2006. "Nucleic Acid Agonists for Toll-like Receptor 7 Are Defined by the Presence of Uridine Ribonucleotides." *European Journal of Immunology* 36 (12): 3256–67. doi:10.1002/eji.200636617.
56. Ding, Yiliang, Yin Tang, Chun Kit Kwok, Yu Zhang, Philip C. Bevilacqua, and Sarah M. Assmann. 2014. "In Vivo Genome-Wide Profiling of RNA Secondary Structure Reveals Novel Regulatory Features." *Nature* 505 (7485): 696–700. doi:10.1038/nature12756.
57. Dittmann, Jan, Silke Stertz, Daniel Grimm, John Steel, Adolfo García-Sastre, Otto Haller, and Georg Kochs. 2008. "Influenza A Virus Strains Differ in Sensitivity to the Antiviral Action of Mx-GTPase." *Journal of Virology* 82 (7): 3624–31. doi:10.1128/JVI.01753-07.
58. Dong, Xiaonan, and Beth Levine. 2013. "Autophagy and Viruses: Adversaries or Allies?" *Journal of Innate Immunity*, January. doi:10.1159/000346388.
59. Duc, Tam Tran Thi, Frédéric Farnir, Charles Michaux, Daniel Desmecht, and Anne Cornet. 2012. "Detection of New Biallelic Polymorphisms in the Human MxA Gene." *Molecular Biology Reports* 39 (8): 8533–38. doi:10.1007/s11033-012-1708-7.
60. Dudek, Sabine E., Ludmilla Wixler, Carolin Nordhoff, Alexandra Nordmann, Darisuren Anhlan, Viktor Wixler, and Stephan Ludwig. 2011. "The Influenza Virus PB1-F2 Protein Has Interferon Antagonistic

Activity." *Biological Chemistry* 392 (12): 1135–44. doi:10.1515/BC.2011.174.
61. Edelmann, Kurt H, Sarah Richardson-Burns, Lena Alexopoulou, Kenneth L Tyler, Richard A Flavell, and Michael B A Oldstone. 2004. "Does Toll-like Receptor 3 Play a Biological Role in Virus Infections?" *Virology* 322 (2): 231–38. doi:10.1016/j.virol.2004.01.033.
62. Edinger, Thomas O., Marie O. Pohl, and Silke Stertz. 2014. "Entry of Influenza A Virus: Host Factors and Antiviral Targets." *The Journal of General Virology* 95 (Pt 2): 263–77. doi:10.1099/vir.0.059477-0.
63. Eichelberger, Maryna C., and Hongquan Wan. 2015. "Influenza Neuraminidase as a Vaccine Antigen." *Current Topics in Microbiology and Immunology* 386: 275–99. doi:10.1007/82_2014_398.
64. Eisfeld, Amie J., Eiryo Kawakami, Tokiko Watanabe, Gabriele Neumann, and Yoshihiro Kawaoka. 2011. "RAB11A Is Essential for Transport of the Influenza Virus Genome to the Plasma Membrane." *Journal of Virology* 85 (13): 6117–26. doi:10.1128/JVI.00378-11.
65. Eisfeld, Amie J., Gabriele Neumann, and Yoshihiro Kawaoka. 2015. "At the Centre: Influenza A Virus Ribonucleoproteins." *Nature Reviews. Microbiology* 13 (1): 28–41. doi:10.1038/nrmicro3367.
66. Engelhardt, Othmar G, Hüseyin Sirma, Pier-Paolo Pandolfi, and Otto Haller. 2004. "Mx1 GTPase Accumulates in Distinct Nuclear Domains and Inhibits Influenza A Virus in Cells That Lack Promyelocytic Leukaemia Protein Nuclear Bodies." *The Journal of General Virology* 85 (Pt 8): 2315–26. doi:10.1099/vir.0.79795-0.
67. Engelhardt, Othmar G., Matt Smith, and Ervin Fodor. 2005. "Association of the Influenza A Virus RNA-Dependent RNA Polymerase with Cellular RNA Polymerase II." *Journal of Virology* 79 (9): 5812–18. doi:10.1128/JVI.79.9.5812-5818.2005.
68. Essere, Boris, Matthieu Yver, Cyrille Gavazzi, Olivier Terrier, Catherine Isel, Emilie Fournier, Fabienne Giroux, et al. 2013. "Critical Role of Segment-Specific Packaging Signals in Genetic Reassortment of Influenza A Viruses." *Proceedings of the National Academy of Sciences of the United States of America* 110 (40): E3840–48. doi:10.1073/pnas.1308649110.
69. Everitt, Aaron R, Simon Clare, Thomas Pertel, Sinu P John, Rachael S Wash, Sarah E Smith, Christopher R Chin, et al. 2012. "IFITM3 Restricts the Morbidity and Mortality Associated with Influenza." *Nature* 484 (7395): 519–23. doi:10.1038/nature10921.
70. Falcón, Ana M, Ana Fernandez-Sesma, Yurie Nakaya, Thomas M Moran, Juan Ortín, and Adolfo García-Sastre. 2005. "Attenuation and Immunogenicity in Mice of Temperature-Sensitive Influenza Viruses Expressing Truncated NS1 Proteins." *The Journal of General Virology* 86 (Pt 10): 2817–21. doi:10.1099/vir.0.80991-0.
71. Fechter, Pierre, Louise Mingay, Jane Sharps, Anna Chambers, Ervin Fodor, and George G. Brownlee. 2003. "Two Aromatic Residues in the PB2 Subunit of Influenza A RNA Polymerase Are Crucial for Cap Binding." *The Journal of Biological Chemistry* 278 (22): 20381–88. doi:10.1074/jbc.M300130200.
72. Feeley, Eric M, Jennifer S Sims, Sinu P John, Christopher R Chin, Thomas Pertel, Li-Mei Chen, Gaurav D Gaiha, et al. 2011. "IFITM3 Inhibits

Influenza A Virus Infection by Preventing Cytosolic Entry." *PLoS Pathogens* 7 (10): e1002337. doi:10.1371/journal.ppat.1002337.
73. Ferguson, Shawn M, and Pietro De Camilli. 2012. "Dynamin, a Membrane-Remodelling GTPase." *Nature Reviews. Molecular Cell Biology* 13 (2): 75–88. doi:10.1038/nrm3266.
74. Firth, Andrew E., and Ian Brierley. 2012. "Non-Canonical Translation in RNA Viruses." *The Journal of General Virology* 93 (Pt 7): 1385–1409. doi:10.1099/vir.0.042499-0.
75. Fitzgerald, Katherine A. 2011. "The Interferon Inducible Gene: Viperin." *Journal of Interferon & Cytokine Research: The Official Journal of the International Society for Interferon and Cytokine Research* 31 (1): 131–35. doi:10.1089/jir.2010.0127.
76. Fodor, E. 2013. "The RNA Polymerase of Influenza a Virus: Mechanisms of Viral Transcription and Replication." *Acta Virologica* 57 (2): 113–22.
77. Fouchier, Ron A. M., Vincent Munster, Anders Wallensten, Theo M. Bestebroer, Sander Herfst, Derek Smith, Guus F. Rimmelzwaan, Björn Olsen, and Albert D. M. E. Osterhaus. 2005. "Characterization of a Novel Influenza A Virus Hemagglutinin Subtype (H16) Obtained from Black-Headed Gulls." *Journal of Virology* 79 (5): 2814–22. doi:10.1128/JVI.79.5.2814-2822.2005.
78. Fredericksen, Brenda L., Brian C. Keller, Jamie Fornek, Michael G. Katze, and Michael Gale. 2008. "Establishment and Maintenance of the Innate Antiviral Response to West Nile Virus Involves Both RIG-I and MDA5 Signaling through IPS-1." *Journal of Virology* 82 (2): 609–16. doi:10.1128/JVI.01305-07.
79. Frensing, Timo, Claudius Seitz, Bjoern Heynisch, Corinna Patzina, Georg Kochs, and Udo Reichl. 2011. "Efficient Influenza B Virus Propagation due to Deficient Interferon-Induced Antiviral Activity in MDCK Cells." *Vaccine*, Vaccine Technology III: Advances in Vaccine Technology, 29 (41): 7125–29. doi:10.1016/j.vaccine.2011.05.069.
80. Frese, M., G. Kochs, U. Meier-Dieter, J. Siebler, and O. Haller. 1995. "Human MxA Protein Inhibits Tick-Borne Thogoto Virus but Not Dhori Virus." *Journal of Virology* 69 (6): 3904–9.
81. Fricke, Thomas, Tommy E. White, Bianca Schulte, Daniel A. de Souza Aranha Vieira, Adarsh Dharan, Edward M. Campbell, Alberto Brandariz-Nuñez, and Felipe Diaz-Griffero. 2014. "MxB Binds to the HIV-1 Core and Prevents the Uncoating Process of HIV-1." *Retrovirology* 11: 68. doi:10.1186/PREACCEPT-6453674081373986.
82. Gabriel, Gülsah, Astrid Herwig, and Hans-Dieter Klenk. 2008. "Interaction of Polymerase Subunit PB2 and NP with Importin alpha1 Is a Determinant of Host Range of Influenza A Virus." *PLoS Pathogens* 4 (2): e11. doi:10.1371/journal.ppat.0040011.
83. Gabriel, Gülsah, Karin Klingel, Anna Otte, Swantje Thiele, Ben Hudjetz, Gökhan Arman-Kalcek, Martina Sauter, et al. 2011. "Differential Use of Importin-α Isoforms Governs Cell Tropism and Host Adaptation of Influenza Virus." *Nature Communications* 2 (January): 156. doi:10.1038/ncomms1158.
84. Gao, Pu, Manuel Ascano, Yang Wu, Winfried Barchet, Barbara L. Gaffney, Thomas Zillinger, Artem A. Serganov, et al. 2013. "Cyclic

[G(2′,5′)pA(3′,5′)p] Is the Metazoan Second Messenger Produced by DNA-Activated Cyclic GMP-AMP Synthase." *Cell* 153 (5): 1094–1107. doi:10.1016/j.cell.2013.04.046.

85. Gao, Song, Alexander von der Malsburg, Alexej Dick, Katja Faelber, Gunnar F Schröder, Otto Haller, Georg Kochs, and Oliver Daumke. 2011. "Structure of Myxovirus Resistance Protein a Reveals Intra- and Intermolecular Domain Interactions Required for the Antiviral Function." *Immunity* 35 (4): 514–25. doi:10.1016/j.immuni.2011.07.012.
86. Gao, Song, Alexander von der Malsburg, Susann Paeschke, Joachim Behlke, Otto Haller, Georg Kochs, and Oliver Daumke. 2010. "Structural Basis of Oligomerization in the Stalk Region of Dynamin-like MxA." *Nature* 465 (7297): 502–6. doi:10.1038/nature08972.
87. García-Sastre, A, A Egorov, D Matassov, S Brandt, D E Levy, J E Durbin, P Palese, and T Muster. 1998. "Influenza A Virus Lacking the NS1 Gene Replicates in Interferon-Deficient Systems." *Virology* 252 (2): 324–30.
88. Gastaminza, Pablo, Beatriz Perales, Ana M. Falcón, and Juan Ortín. 2003. "Mutations in the N-Terminal Region of Influenza Virus PB2 Protein Affect Virus RNA Replication but Not Transcription." *Journal of Virology* 77 (9): 5098–5108.
89. Gavazzi, Cyrille, Matthieu Yver, Catherine Isel, Redmond P. Smyth, Manuel Rosa-Calatrava, Bruno Lina, Vincent Moulès, and Roland Marquet. 2013. "A Functional Sequence-Specific Interaction between Influenza A Virus Genomic RNA Segments." *Proceedings of the National Academy of Sciences of the United States of America* 110 (41): 16604–9. doi:10.1073/pnas.1314419110.
90. Gerber, Marie, Catherine Isel, Vincent Moules, and Roland Marquet. 2014. "Selective Packaging of the Influenza A Genome and Consequences for Genetic Reassortment." *Trends in Microbiology* 22 (8): 446–55. doi:10.1016/j.tim.2014.04.001.
91. Gerlier, Denis, and Douglas S Lyles. 2011. "Interplay between Innate Immunity and Negative-Strand RNA Viruses: Towards a Rational Model." *Microbiology and Molecular Biology Reviews: MMBR* 75 (3): 468–90, second page of table of contents. doi:10.1128/MMBR.00007-11.
92. Getie-Kebtie, Melkamu, Ishrat Sultana, Maryna Eichelberger, and Michail Alterman. 2013. "Label-Free Mass Spectrometry-Based Quantification of Hemagglutinin and Neuraminidase in Influenza Virus Preparations and Vaccines." *Influenza and Other Respiratory Viruses* 7 (4): 521–30. doi:10.1111/irv.12001.
93. Gitlin, Leonid, Winfried Barchet, Susan Gilfillan, Marina Cella, Bruce Beutler, Richard A Flavell, Michael S Diamond, and Marco Colonna. 2006. "Essential Role of Mda-5 in Type I IFN Responses to Polyriboinosinic:polyribocytidylic Acid and Encephalomyocarditis Picornavirus." *Proceedings of the National Academy of Sciences of the United States of America* 103 (22): 8459–64. doi:10.1073/pnas.0603082103.
94. Gómez-Puertas, P., C. Albo, E. Pérez-Pastrana, A. Vivo, and A. Portela. 2000. "Influenza Virus Matrix Protein Is the Major Driving Force in Virus Budding." *Journal of Virology* 74 (24): 11538–47.

95. González, S., and J. Ortín. 1999a. “Characterization of Influenza Virus PB1 Protein Binding to Viral RNA: Two Separate Regions of the Protein Contribute to the Interaction Domain.” *Journal of Virology* 73 (1): 631–37.
96. ———. 1999b. “Distinct Regions of Influenza Virus PB1 Polymerase Subunit Recognize vRNA and cRNA Templates.” *The EMBO Journal* 18 (13): 3767–75. doi:10.1093/emboj/18.13.3767.
97. González, S., T. Zürcher, and J. Ortín. 1996. “Identification of Two Separate Domains in the Influenza Virus PB1 Protein Involved in the Interaction with the PB2 and PA Subunits: A Model for the Viral RNA Polymerase Structure.” *Nucleic Acids Research* 24 (22): 4456–63.
98. Goodbourn, S., L. Didcock, and R. E. Randall. 2000. “Interferons: Cell Signalling, Immune Modulation, Antiviral Response and Virus Countermeasures.” *Journal of General Virology* 81 (10): 2341–64.
99. Gorai, Takeo, Hideo Goto, Takeshi Noda, Tokiko Watanabe, Hiroko Kozuka-Hata, Masaaki Oyama, Ryo Takano, Gabriele Neumann, Shinji Watanabe, and Yoshihiro Kawaoka. 2012. “F1Fo-ATPase, F-Type Proton-Translocating ATPase, at the Plasma Membrane Is Critical for Efficient Influenza Virus Budding.” *Proceedings of the National Academy of Sciences of the United States of America* 109 (12): 4615–20. doi:10.1073/pnas.1114728109.
100. Gordien, E, O Rosmorduc, C Peltekian, F Garreau, C Bréchot, and D Kremsdorf. 2001. “Inhibition of Hepatitis B Virus Replication by the Interferon-Inducible MxA Protein.” *Journal of Virology* 75 (6): 2684–91. doi:10.1128/JVI.75.6.2684-2691.2001.
101. Goujon, Caroline, Olivier Moncorgé, Hélène Bauby, Tomas Doyle, Wendy S. Barclay, and Michael H. Malim. 2014. “Transfer of the Amino-Terminal Nuclear Envelope Targeting Domain of Human MX2 Converts MX1 into an HIV-1 Resistance Factor.” *Journal of Virology* 88 (16): 9017–26. doi:10.1128/JVI.01269-14.
102. Goujon, Caroline, Olivier Moncorgé, Hélène Bauby, Tomas Doyle, Christopher C. Ward, Torsten Schaller, Stéphane Hué, Wendy S. Barclay, Reiner Schulz, and Michael H. Malim. 2013. “Human MX2 Is an Interferon-Induced Post-Entry Inhibitor of HIV-1 Infection.” *Nature* 502 (7472): 559–62. doi:10.1038/nature12542.
103. Graef, Katy M, Frank T Vreede, Yuk-Fai Lau, Amber W McCall, Simon M Carr, Kanta Subbarao, and Ervin Fodor. 2010. “The PB2 Subunit of the Influenza Virus RNA Polymerase Affects Virulence by Interacting with the Mitochondrial Antiviral Signaling Protein and Inhibiting Expression of Beta Interferon.” *Journal of Virology* 84 (17): 8433–45. doi:10.1128/JVI.00879-10.
104. Grove, Joe. 2014. “Super-Resolution Microscopy: A Virus’ Eye View of the Cell.” *Viruses* 6 (3): 1365–78. doi:10.3390/v6031365.
105. Hale, Benjamin G, Randy A Albrecht, and Adolfo García-Sastre. 2010. “Innate Immune Evasion Strategies of Influenza Viruses.” *Future Microbiology* 5 (1): 23–41. doi:10.2217/fmb.09.108.
106. Hale, Benjamin G, Richard E Randall, Juan Ortín, and David Jackson. 2008. “The Multifunctional NS1 Protein of Influenza A Viruses.” *The Journal of General Virology* 89 (Pt 10): 2359–76. doi:10.1099/vir.0.2008/004606-0.

107. Haller, O, M Frese, D Rost, P A Nuttall, and G Kochs. 1995. "Tick-Borne Thogoto Virus Infection in Mice Is Inhibited by the Orthomyxovirus Resistance Gene Product Mx1." *Journal of Virology* 69 (4): 2596–2601.
108. Haller, Otto, Song Gao, Alexander von der Malsburg, Oliver Daumke, and Georg Kochs. 2010. "Dynamin-like MxA GTPase: Structural Insights into Oligomerization and Implications for Antiviral Activity." *The Journal of Biological Chemistry* 285 (37): 28419–24. doi:10.1074/jbc.R110.145839.
109. Haller, Otto, Silke Stertz, and Georg Kochs. 2007. "The Mx GTPase Family of Interferon-Induced Antiviral Proteins." *Microbes and Infection* 9 (14–15): 1636–43. doi:10.1016/j.micinf.2007.09.010.
110. Hamano, Emi, Minako Hijikata, Satoru Itoyama, Tran Quy, Nguyen Chi Phi, Hoang Thuy Long, Le Dang Ha, et al. 2005. "Polymorphisms of Interferon-Inducible Genes OAS-1 and MxA Associated with SARS in the Vietnamese Population." *Biochemical and Biophysical Research Communications* 329 (4): 1234–39. doi:10.1016/j.bbrc.2005.02.101.
111. Hamasaki, Maho, Nobumichi Furuta, Atsushi Matsuda, Akiko Nezu, Akitsugu Yamamoto, Naonobu Fujita, Hiroko Oomori, et al. 2013. "Autophagosomes Form at ER-Mitochondria Contact Sites." *Nature* 495 (7441): 389–93. doi:10.1038/nature11910.
112. Hara, Koyu, Florian I. Schmidt, Mandy Crow, and George G. Brownlee. 2006. "Amino Acid Residues in the N-Terminal Region of the PA Subunit of Influenza A Virus RNA Polymerase Play a Critical Role in Protein Stability, Endonuclease Activity, Cap Binding, and Virion RNA Promoter Binding." *Journal of Virology* 80 (16): 7789–98. doi:10.1128/JVI.00600-06.
113. Harris, Audray, Giovanni Cardone, Dennis C. Winkler, J. Bernard Heymann, Matthew Brecher, Judith M. White, and Alasdair C. Steven. 2006. "Influenza Virus Pleiomorphy Characterized by Cryoelectron Tomography." *Proceedings of the National Academy of Sciences of the United States of America* 103 (50): 19123–27. doi:10.1073/pnas.0607614103.
114. Hatta, Masato, Yasuko Hatta, Jin Hyun Kim, Shinji Watanabe, Kyoko Shinya, Tung Nguyen, Phuong Song Lien, Quynh Mai Le, and Yoshihiro Kawaoka. 2007. "Growth of H5N1 Influenza A Viruses in the Upper Respiratory Tracts of Mice." *PLoS Pathogens* 3 (10): 1374–79. doi:10.1371/journal.ppat.0030133.
115. Hatta, Masato, and Yoshihiro Kawaoka. 2003. "The NB Protein of Influenza B Virus Is Not Necessary for Virus Replication In Vitro." *Journal of Virology* 77 (10): 6050–54. doi:10.1128/JVI.77.10.6050-6054.2003.
116. Hefti, H. P., M. Frese, H. Landis, C. Di Paolo, A. Aguzzi, O. Haller, and J. Pavlovic. 1999. "Human MxA Protein Protects Mice Lacking a Functional Alpha/beta Interferon System against La Crosse Virus and Other Lethal Viral Infections." *Journal of Virology* 73 (8): 6984–91.
117. Heil, Florian, Hiroaki Hemmi, Hubertus Hochrein, Franziska Ampenberger, Carsten Kirschning, Shizuo Akira, Grayson Lipford, Hermann Wagner, and Stefan Bauer. 2004. "Species-Specific Recognition of Single-Stranded RNA via Toll-like Receptor 7 and 8." *Science (New York, N.Y.)* 303 (5663): 1526–29. doi:10.1126/science.1093620.

118. Hemerka, Joseph N., Dan Wang, Yuejin Weng, Wuxun Lu, Radhey S. Kaushik, Jing Jin, Aaron F. Harmon, and Feng Li. 2009. "Detection and Characterization of Influenza A Virus PA-PB2 Interaction through a Bimolecular Fluorescence Complementation Assay." *Journal of Virology* 83 (8): 3944–55. doi:10.1128/JVI.02300-08.
119. Herfst, Sander, Eefje J A Schrauwen, Martin Linster, Salin Chutinimitkul, Emmie de Wit, Vincent J Munster, Erin M Sorrell, et al. 2012. "Airborne Transmission of Influenza A/H5N1 Virus between Ferrets." *Science (New York, N.Y.)* 336 (6088): 1534–41. doi:10.1126/science.1213362.
120. Hermansson, Martin, Kati Hokynar, and Pentti Somerharju. 2011. "Mechanisms of Glycerophospholipid Homeostasis in Mammalian Cells." *Progress in Lipid Research* 50 (3): 240–57. doi:10.1016/j.plipres.2011.02.004.
121. Hernandez, Lorraine D., Marc Pypaert, Richard A. Flavell, and Jorge E. Galán. 2003. "A Salmonella Protein Causes Macrophage Cell Death by Inducing Autophagy." *The Journal of Cell Biology* 163 (5): 1123–31. doi:10.1083/jcb.200309161.
122. Hoenen, Antje, Leah Gillespie, Garry Morgan, Peter van der Heide, Alexander Khromykh, and Jason Mackenzie. 2014. "The West Nile Virus Assembly Process Evades the Conserved Antiviral Mechanism of the Interferon-Induced MxA Protein." *Virology* 448 (January): 104–16. doi:10.1016/j.virol.2013.10.005.
123. Hoff, Florian, Christoph Greb, Christina Hollmann, Ellena Hönig, and Ralf Jacob. 2014. "The Large GTPase Mx1 Is Involved in Apical Transport in MDCK Cells." *Traffic (Copenhagen, Denmark)* 15 (9): 983–96. doi:10.1111/tra.12186.
124. Holzinger, Dirk, Carl Jorns, Silke Stertz, Stéphanie Boisson-Dupuis, Robert Thimme, Manfred Weidmann, Jean-Laurent Casanova, Otto Haller, and Georg Kochs. 2007. "Induction of MxA Gene Expression by Influenza A Virus Requires Type I or Type III Interferon Signaling." *Journal of Virology* 81 (14): 7776–85. doi:10.1128/JVI.00546-06.
125. Horisberger, M A. 1992. "Interferon-Induced Human Protein MxA Is a GTPase Which Binds Transiently to Cellular Proteins." *Journal of Virology* 66 (8): 4705–9.
126. Horisberger, M A, M Wathelet, J Szpirer, C Szpirer, Q Islam, G Levan, G Huez, and J Content. 1988. "cDNA Cloning and Assignment to Chromosome 21 of IFI-78K Gene, the Human Equivalent of Murine Mx Gene." *Somatic Cell and Molecular Genetics* 14 (2): 123–31.
127. Hornung, Veit, Andrea Ablasser, Marie Charrel-Dennis, Franz Bauernfeind, Gabor Horvath, Daniel R. Caffrey, Eicke Latz, and Katherine A. Fitzgerald. 2009. "AIM2 Recognizes Cytosolic dsDNA and Forms a Caspase-1-Activating Inflammasome with ASC." *Nature* 458 (7237): 514–18. doi:10.1038/nature07725.
128. Hornung, Veit, Jana Ellegast, Sarah Kim, Krzysztof Brzózka, Andreas Jung, Hiroki Kato, Hendrik Poeck, et al. 2006. "5'-Triphosphate RNA Is the Ligand for RIG-I." *Science (New York, N.Y.)* 314 (5801): 994–97. doi:10.1126/science.1132505.

129. Hsiang, Tien-Ying, Ligang Zhou, and Robert M. Krug. 2012. "Roles of the Phosphorylation of Specific Serines and Threonines in the NS1 Protein of Human Influenza A Viruses." *Journal of Virology* 86 (19): 10370–76. doi:10.1128/JVI.00732-12.
130. Huang, R. T., B. Lichtenberg, and O. Rick. 1996. "Involvement of Annexin V in the Entry of Influenza Viruses and Role of Phospholipids in Infection." *FEBS Letters* 392 (1): 59–62.
131. Huang, Shengping, Jingjing Chen, Quanjiao Chen, Huadong Wang, Yanfeng Yao, Jianjun Chen, and Ze Chen. 2013. "A Second CRM1-Dependent Nuclear Export Signal in the Influenza A Virus NS2 Protein Contributes to the Nuclear Export of Viral Ribonucleoproteins." *Journal of Virology* 87 (2): 767–78. doi:10.1128/JVI.06519-11.
132. Huang, T, J Pavlovic, P Staeheli, and M Krystal. 1992. "Overexpression of the Influenza Virus Polymerase Can Titrate out Inhibition by the Murine Mx1 Protein." *Journal of Virology* 66 (7): 4154–60.
133. Huarte, Maite, Ana Falcón, Yuri Nakaya, Juan Ortín, Adolfo García-Sastre, and Amelia Nieto. 2003. "Threonine 157 of Influenza Virus PA Polymerase Subunit Modulates RNA Replication in Infectious Viruses." *Journal of Virology* 77 (10): 6007–13.
134. Hug, H, M Costas, P Staeheli, M Aebi, and C Weissmann. 1988. "Organization of the Murine Mx Gene and Characterization of Its Interferon- and Virus-Inducible Promoter." *Molecular and Cellular Biology* 8 (8): 3065–79.
135. Hughey, P. G., P. C. Roberts, L. J. Holsinger, S. L. Zebedee, R. A. Lamb, and R. W. Compans. 1995. "Effects of Antibody to the Influenza A Virus M2 Protein on M2 Surface Expression and Virus Assembly." *Virology* 212 (2): 411–21. doi:10.1006/viro.1995.1498.
136. Hu, Jiao, and Xiufan Liu. 2015. "Crucial Role of PA in Virus Life Cycle and Host Adaptation of Influenza A Virus." *Medical Microbiology and Immunology* 204 (2): 137–49. doi:10.1007/s00430-014-0349-y.
137. Huotari, Jatta, and Ari Helenius. 2011. "Endosome Maturation." *The EMBO Journal* 30 (17): 3481–3500. doi:10.1038/emboj.2011.286.
138. Hutchinson, E. C., and E. Fodor. 2012. "Nuclear Import of the Influenza A Virus Transcriptional Machinery." *Vaccine*, Fourth ESWI Influenza Conference, 30 (51): 7353–58. doi:10.1016/j.vaccine.2012.04.085.
139. Hutchinson, Edward C., Philip D. Charles, Svenja S. Hester, Benjamin Thomas, David Trudgian, Mónica Martínez-Alonso, and Ervin Fodor. 2014. "Conserved and Host-Specific Features of Influenza Virion Architecture." *Nature Communications* 5: 4816. doi:10.1038/ncomms5816.
140. "ICTV Virus Taxonomy 2014." 2015. Accessed July 1. http://www.ictvonline.org/virusTaxonomy.asp.
141. Imai, Yumiko, Keiji Kuba, G Greg Neely, Rubina Yaghubian-Malhami, Thomas Perkmann, Geert van Loo, Maria Ermolaeva, et al. 2008. "Identification of Oxidative Stress and Toll-like Receptor 4 Signaling as a Key Pathway of Acute Lung Injury." *Cell* 133 (2): 235–49. doi:10.1016/j.cell.2008.02.043.

142. Ito, T, M Yang, and W S May. 1999. "RAX, a Cellular Activator for Double-Stranded RNA-Dependent Protein Kinase during Stress Signaling." *The Journal of Biological Chemistry* 274 (22): 15427–32.
143. Ivanova, Pavlina T., David S. Myers, Stephen B. Milne, Jennifer L. McClaren, Paul G. Thomas, and H. Alex Brown. 2015. "Lipid Composition of the Viral Envelope of Three Strains of Influenza Virus—Not All Viruses Are Created Equal." *ACS Infectious Diseases*, June. doi:10.1021/acsinfecdis.5b00040.
144. Jackson, D., R. A. Elderfield, and W. S. Barclay. 2011. "Molecular Studies of Influenza B Virus in the Reverse Genetics Era." *Journal of General Virology* 92 (1): 1–17. doi:10.1099/vir.0.026187-0.
145. Jackson, Lauren P. 2014. "Structure and Mechanism of COPI Vesicle Biogenesis." *Current Opinion in Cell Biology* 29 (August): 67–73. doi:10.1016/j.ceb.2014.04.009.
146. Jagger, B W, H M Wise, J C Kash, K-A Walters, N M Wills, Y-L Xiao, R L Dunfee, et al. 2012. "An Overlapping Protein-Coding Region in Influenza A Virus Segment 3 Modulates the Host Response." *Science (New York, N.Y.)* 337 (6091): 199–204. doi:10.1126/science.1222213.
147. Janzen, C, G Kochs, and O Haller. 2000. "A Monomeric GTPase-Negative MxA Mutant with Antiviral Activity." *Journal of Virology* 74 (17): 8202–6.
148. Jaru-ampornpan, Peera, Jaraspim Narkpuk, Asawin Wanitchang, and Anan Jongkaewwattana. 2014. "Nucleoprotein of Influenza B Virus Binds to Its Type A Counterpart and Disrupts Influenza A Viral Polymerase Complex Formation." *Biochemical and Biophysical Research Communications* 443 (1): 296–300. doi:10.1016/j.bbrc.2013.11.100.
149. Jensen, Ingvill, Artur Albuquerque, Ann-Inger Sommer, and Børre Robertsen. 2002. "Effect of Poly I:C on the Expression of Mx Proteins and Resistance against Infection by Infectious Salmon Anaemia Virus in Atlantic Salmon." *Fish & Shellfish Immunology* 13 (4): 311–26.
150. Jia, Rui, Qinghua Pan, Shilei Ding, Liwei Rong, Shan-Lu Liu, Yunqi Geng, Wentao Qiao, and Chen Liang. 2012. "The N-Terminal Region of IFITM3 Modulates Its Antiviral Activity by Regulating IFITM3 Cellular Localization." *Journal of Virology* 86 (24): 13697–707. doi:10.1128/JVI.01828-12.
151. Jia, Rui, Fengwen Xu, Jin Qian, Yunfang Yao, Chunhui Miao, Yi-Min Zheng, Shan-Lu Liu, et al. 2014. "Identification of an Endocytic Signal Essential for the Antiviral Action of IFITM3." *Cellular Microbiology* 16 (7): 1080–93. doi:10.1111/cmi.12262.
152. Jia, Xiaofei, Qi Zhao, and Yong Xiong. 2015. "HIV Suppression by Host Restriction Factors and Viral Immune Evasion." *Current Opinion in Structural Biology* 31 (April): 106–14. doi:10.1016/j.sbi.2015.04.004.
153. Jin, H. K., A. Takada, Y. Kon, O. Haller, and T. Watanabe. 1999. "Identification of the Murine Mx2 Gene: Interferon-Induced Expression of the Mx2 Protein from the Feral Mouse Gene Confers Resistance to Vesicular Stomatitis Virus." *Journal of Virology* 73 (6): 4925–30.
154. Jin, H. K., K. Yoshimatsu, A. Takada, M. Ogino, A. Asano, J. Arikawa, and T. Watanabe. 2001. "Mouse Mx2 Protein Inhibits Hantavirus but Not Influenza Virus Replication." *Archives of Virology* 146 (1): 41–49.

155. Kane, Melissa, Shalini S. Yadav, Julia Bitzegeio, Sebla B. Kutluay, Trinity Zang, Sam J. Wilson, John W. Schoggins, et al. 2013. "MX2 Is an Interferon-Induced Inhibitor of HIV-1 Infection." *Nature* 502 (7472): 563–66. doi:10.1038/nature12653.
156. Kanneganti, Thirumala-Devi, Mathilde Body-Malapel, Amal Amer, Jong-Hwan Park, Joel Whitfield, Luigi Franchi, Zenobia F Taraporewala, et al. 2006. "Critical Role for Cryopyrin/Nalp3 in Activation of Caspase-1 in Response to Viral Infection and Double-Stranded RNA." *The Journal of Biological Chemistry* 281 (48): 36560–68. doi:10.1074/jbc.M607594200.
157. Kato, Hiroki, Osamu Takeuchi, Eriko Mikamo-Satoh, Reiko Hirai, Tomoji Kawai, Kazufumi Matsushita, Akane Hiiragi, Terence S. Dermody, Takashi Fujita, and Shizuo Akira. 2008. "Length-Dependent Recognition of Double-Stranded Ribonucleic Acids by Retinoic Acid-Inducible Gene-I and Melanoma Differentiation-Associated Gene 5." *The Journal of Experimental Medicine* 205 (7): 1601–10. doi:10.1084/jem.20080091.
158. Kato, Hiroki, Osamu Takeuchi, Shintaro Sato, Mitsutoshi Yoneyama, Masahiro Yamamoto, Kosuke Matsui, Satoshi Uematsu, et al. 2006. "Differential Roles of MDA5 and RIG-I Helicases in the Recognition of RNA Viruses." *Nature* 441 (7089): 101–5. doi:10.1038/nature04734.
159. Katz, Garrett, Younes Benkarroum, Hui Wei, William J. Rice, Doris Bucher, Alexandra Alimova, Al Katz, Joanna Klukowska, Gabor T. Herman, and Paul Gottlieb. 2014. "Morphology of Influenza B/Lee/40 Determined by Cryo-Electron Microscopy." *PLoS ONE* 9 (2): e88288. doi:10.1371/journal.pone.0088288.
160. Kilbourne, E. D., W. G. Laver, J. L. Schulman, and R. G. Webster. 1968. "Antiviral Activity of Antiserum Specific for an Influenza Virus Neuraminidase." *Journal of Virology* 2 (4): 281–88.
161. Kim, Bae-Hoon, Avinash R Shenoy, Pradeep Kumar, Clinton J Bradfield, and John D MacMicking. 2012. "IFN-Inducible GTPases in Host Cell Defense." *Cell Host & Microbe* 12 (4): 432–44. doi:10.1016/j.chom.2012.09.007.
162. Kim, Bae-Hoon, Avinash R Shenoy, Pradeep Kumar, Rituparna Das, Sangeeta Tiwari, and John D MacMicking. 2011. "A Family of IFN-γ-Inducible 65-kD GTPases Protects against Bacterial Infection." *Science (New York, N.Y.)* 332 (6030): 717–21. doi:10.1126/science.1201711.
163. Kimchi-Sarfaty, Chava, Jung Mi Oh, In-Wha Kim, Zuben E. Sauna, Anna Maria Calcagno, Suresh V. Ambudkar, and Michael M. Gottesman. 2007. "A 'Silent' Polymorphism in the MDR1 Gene Changes Substrate Specificity." *Science (New York, N.Y.)* 315 (5811): 525–28. doi:10.1126/science.1135308.
164. King, Megan C, Graça Raposo, and Mark A Lemmon. 2004. "Inhibition of Nuclear Import and Cell-Cycle Progression by Mutated Forms of the Dynamin-like GTPase MxB." *Proceedings of the National Academy of Sciences of the United States of America* 101 (24): 8957–62. doi:10.1073/pnas.0403167101.
165. Kochs, Georg, Markus Haener, Ueli Aebi, and Otto Haller. 2002. "Self-Assembly of Human MxA GTPase into Highly Ordered Dynamin-like Oligomers." *The Journal of Biological Chemistry* 277 (16): 14172–76. doi:10.1074/jbc.M200244200.

166. Kochs, Georg, Christian Janzen, Heinz Hohenberg, and Otto Haller. 2002. "Antivirally Active MxA Protein Sequesters La Crosse Virus Nucleocapsid Protein into Perinuclear Complexes." *Proceedings of the National Academy of Sciences of the United States of America* 99 (5): 3153–58. doi:10.1073/pnas.052430399.
167. Kochs, G, and O Haller. 1999. "Interferon-Induced Human MxA GTPase Blocks Nuclear Import of Thogoto Virus Nucleocapsids." *Proceedings of the National Academy of Sciences of the United States of America* 96 (5): 2082–86.
168. Komuro, Akihiko, and Curt M. Horvath. 2006. "RNA- and Virus-Independent Inhibition of Antiviral Signaling by RNA Helicase LGP2." *Journal of Virology* 80 (24): 12332–42. doi:10.1128/JVI.01325-06.
169. Kresse, Alexandra, Carolin Konermann, Daniel Degrandi, Cornelia Beuter-Gunia, Jan Wuerthner, Klaus Pfeffer, and Sandra Beer. 2008. "Analyses of Murine GBP Homology Clusters Based on in Silico, in Vitro and in Vivo Studies." *BMC Genomics* 9: 158. doi:10.1186/1471-2164-9-158.
170. Krug, Robert M., and Adolfo García-Sastre. 2013. "The NS1 Protein: A Master Regulator of Host and Viral Functions." In *Textbook of Influenza*, edited by Robert G. Webster FRS, Arnold S. Monto MD, Thomas J. Braciale MD, and Robert A. Lamb ScD, 114–32. John Wiley & Sons, Ltd. http://onlinelibrary.wiley.com/doi/10.1002/9781118636817.ch7/summary.
171. Krumbholz, Andi, Anja Philipps, Hartmut Oehring, Katja Schwarzer, Annett Eitner, Peter Wutzler, and Roland Zell. 2011. "Current Knowledge on PB1-F2 of Influenza A Viruses." *Medical Microbiology and Immunology* 200 (2): 69–75. doi:10.1007/s00430-010-0176-8.
172. Lai, Yichen, Robert W. Hickey, Yaming Chen, Hülya Bay|[inodot]|r, Mara L. Sullivan, Charleen T. Chu, Patrick M. Kochanek, et al. 2007. "Autophagy Is Increased after Traumatic Brain Injury in Mice and Is Partially Inhibited by the Antioxidant γ-Glutamylcysteinyl Ethyl Ester." *Journal of Cerebral Blood Flow & Metabolism* 28 (3): 540–50. doi:10.1038/sj.jcbfm.9600551.
173. Lakdawala, Seema S., Elaine W. Lamirande, Amorsolo L. Suguitan, Weijia Wang, Celia P. Santos, Leatrice Vogel, Yumiko Matsuoka, William G. Lindsley, Hong Jin, and Kanta Subbarao. 2011. "Eurasian-Origin Gene Segments Contribute to the Transmissibility, Aerosol Release, and Morphology of the 2009 Pandemic H1N1 Influenza Virus." *PLoS Pathogens* 7 (12): e1002443. doi:10.1371/journal.ppat.1002443.
174. Lakdawala, Seema S., Yicong Wu, Peter Wawrzusin, Juraj Kabat, Andrew J. Broadbent, Elaine W. Lamirande, Ervin Fodor, Nihal Altan-Bonnet, Hari Shroff, and Kanta Subbarao. 2014. "Influenza a Virus Assembly Intermediates Fuse in the Cytoplasm." *PLoS Pathogens* 10 (3): e1003971. doi:10.1371/journal.ppat.1003971.
175. Lamb, R. A., and C. J. Lai. 1980. "Sequence of Interrupted and Uninterrupted mRNAs and Cloned DNA Coding for the Two Overlapping Nonstructural Proteins of Influenza Virus." *Cell* 21 (2): 475–85.
176. Landeras-Bueno, Sara, Núria Jorba, Maite Pérez-Cidoncha, and Juan Ortín. 2011. "The Splicing Factor Proline-Glutamine Rich (SFPQ/PSF)

Is Involved in Influenza Virus Transcription." *PLoS Pathogens* 7 (11): e1002397. doi:10.1371/journal.ppat.1002397.

177. Larsen, Rannveig, Torunn P. Røkenes, and Børre Robertsen. 2004. "Inhibition of Infectious Pancreatic Necrosis Virus Replication by Atlantic Salmon Mx1 Protein." *Journal of Virology* 78 (15): 7938–44. doi:10.1128/JVI.78.15.7938-7944.2004.

178. Latham, T., and J. M. Galarza. 2001. "Formation of Wild-Type and Chimeric Influenza Virus-like Particles Following Simultaneous Expression of Only Four Structural Proteins." *Journal of Virology* 75 (13): 6154–65. doi:10.1128/JVI.75.13.6154-6165.2001.

179. Lee, Sang-Hyuk, Jae Yen Shin, Antony Lee, and Carlos Bustamante. 2012. "Counting Single Photoactivatable Fluorescent Molecules by Photoactivated Localization Microscopy (PALM)." *Proceedings of the National Academy of Sciences* 109 (43): 17436–41. doi:10.1073/pnas.1215175109.

180. Lenschow, Deborah J, Caroline Lai, Natalia Frias-Staheli, Nadia V Giannakopoulos, Andrew Lutz, Thorsten Wolff, Anna Osiak, et al. 2007. "IFN-Stimulated Gene 15 Functions as a Critical Antiviral Molecule against Influenza, Herpes, and Sindbis Viruses." *Proceedings of the National Academy of Sciences of the United States of America* 104 (4): 1371–76. doi:10.1073/pnas.0607038104.

181. Li, Guang, Juyong Zhang, Yi Sun, Hua Wang, and Yiquan Wang. 2009. "The Evolutionarily Dynamic IFN-Inducible GTPase Proteins Play Conserved Immune Functions in Vertebrates and Cephalochordates." *Molecular Biology and Evolution* 26 (7): 1619–30. doi:10.1093/molbev/msp074.

182. Li, Kui, Eileen Foy, Josephine C Ferreon, Mitsuyasu Nakamura, Allan C M Ferreon, Masanori Ikeda, Stuart C Ray, Michael Gale Jr, and Stanley M Lemon. 2005. "Immune Evasion by Hepatitis C Virus NS3/4A Protease-Mediated Cleavage of the Toll-like Receptor 3 Adaptor Protein TRIF." *Proceedings of the National Academy of Sciences of the United States of America* 102 (8): 2992–97. doi:10.1073/pnas.0408824102.

183. Li, Ning, Lei Zhang, Liangwei Chen, Wenfeng Feng, Yinfeng Xu, Feng Chen, Xiaohong Liu, Zhi Chen, and Wei Liu. 2012. "MxA Inhibits Hepatitis B Virus Replication by Interaction with Hepatitis B Core Antigen." *Hepatology (Baltimore, Md.)* 56 (3): 803–11. doi:10.1002/hep.25608.

184. Lin, Ren-Jye, Bi-Lan Chang, Han-Pang Yu, Ching-Len Liao, and Yi-Ling Lin. 2006. "Blocking of Interferon-Induced Jak-Stat Signaling by Japanese Encephalitis Virus NS5 through a Protein Tyrosine Phosphatase-Mediated Mechanism." *Journal of Virology* 80 (12): 5908–18. doi:10.1128/JVI.02714-05.

185. Lin, Ren-Jye, Ching-Len Liao, Elong Lin, and Yi-Ling Lin. 2004. "Blocking of the Alpha Interferon-Induced Jak-Stat Signaling Pathway by Japanese Encephalitis Virus Infection." *Journal of Virology* 78 (17): 9285–94. doi:10.1128/JVI.78.17.9285-9294.2004.

186. Lin, Y. P., V. Gregory, M. Bennett, and A. Hay. 2004. "Recent Changes among Human Influenza Viruses." *Virus Research* 103 (1-2): 47–52. doi:10.1016/j.virusres.2004.02.011.

187. Li, Peiyuan, Qiang Du, Zongxian Cao, Zhong Guo, John Evankovich, Wei Yan, Ying Chang, et al. 2012. "Interferon-Gamma Induces Autophagy with Growth Inhibition and Cell Death in Human Hepatocellular Carcinoma (HCC) Cells through Interferon-Regulatory Factor-1 (IRF-1)." *Cancer Letters* 314 (2): 213–22. doi:10.1016/j.canlet.2011.09.031.
188. Li, Shoudong, Ji-Young Min, Robert M Krug, and Ganes C Sen. 2006. "Binding of the Influenza A Virus NS1 Protein to PKR Mediates the Inhibition of Its Activation by Either PACT or Double-Stranded RNA." *Virology* 349 (1): 13–21. doi:10.1016/j.virol.2006.01.005.
189. Liu, Su-Yang, Roghiyh Aliyari, Kelechi Chikere, Guangming Li, Matthew D. Marsden, Jennifer K. Smith, Olivier Pernet, et al. 2013. "Interferon-Inducible Cholesterol-25-Hydroxylase Broadly Inhibits Viral Entry by Production of 25-Hydroxycholesterol." *Immunity* 38 (1): 92–105. doi:10.1016/j.immuni.2012.11.005.
190. Liu, Zhenlong, Qinghua Pan, Shilei Ding, Jin Qian, Fengwen Xu, Jinming Zhou, Shan Cen, Fei Guo, and Chen Liang. 2013. "The Interferon-Inducible MxB Protein Inhibits HIV-1 Infection." *Cell Host & Microbe* 14 (4): 398–410. doi:10.1016/j.chom.2013.08.015.
191. Llompart, C. M., A. Nieto, and A. Rodriguez-Frandsen. 2014. "Specific Residues of PB2 and PA Influenza Virus Polymerase Subunits Confer the Ability for RNA Polymerase II Degradation and Virus Pathogenicity in Mice." *Journal of Virology* 88 (6): 3455–63. doi:10.1128/JVI.02263-13.
192. Londrigan, Sarah L., Stuart G. Turville, Michelle D. Tate, Yi-Mo Deng, Andrew G. Brooks, and Patrick C. Reading. 2011. "N-Linked Glycosylation Facilitates Sialic Acid-Independent Attachment and Entry of Influenza A Viruses into Cells Expressing DC-SIGN or L-SIGN." *Journal of Virology* 85 (6): 2990–3000. doi:10.1128/JVI.01705-10.
193. Loo, Yueh-Ming, David M. Owen, Kui Li, Andrea K. Erickson, Cynthia L. Johnson, Penny M. Fish, D. Spencer Carney, et al. 2006. "Viral and Therapeutic Control of IFN-Beta Promoter Stimulator 1 during Hepatitis C Virus Infection." *Proceedings of the National Academy of Sciences of the United States of America* 103 (15): 6001–6. doi:10.1073/pnas.0601523103.
194. Lucocq, John Milton, and Christian Hacker. 2013. "Cutting a Fine Figure: On the Use of Thin Sections in Electron Microscopy to Quantify Autophagy." *Autophagy* 9 (9): 1443–48. doi:10.4161/auto.25570.
195. Lund, Jennifer M, Lena Alexopoulou, Ayuko Sato, Margaret Karow, Niels C Adams, Nicholas W Gale, Akiko Iwasaki, and Richard A Flavell. 2004. "Recognition of Single-Stranded RNA Viruses by Toll-like Receptor 7." *Proceedings of the National Academy of Sciences of the United States of America* 101 (15): 5598–5603. doi:10.1073/pnas.0400937101.
196. MacDonald, Leslie, Shilpa Aggarwal, Kendra A. Bussey, Emily A. Desmet, Baek Kim, and Toru Takimoto. 2012. "Molecular Interactions and Trafficking of Influenza A Virus Polymerase Proteins Analyzed by Specific Monoclonal Antibodies." *Virology* 426 (1): 51–59. doi:10.1016/j.virol.2012.01.015.

197. MacMicking, John D. 2012. “Interferon-Inducible Effector Mechanisms in Cell-Autonomous Immunity.” *Nature Reviews. Immunology* 12 (5): 367–82. doi:10.1038/nri3210.
198. Mahanonda, Rangsini, Noppadol Sa-Ard-Iam, Pimprapa Rerkyen, Arunee Thitithanyanont, Keskanya Subbalekha, and Sathit Pichyangkul. 2012. “MxA Expression Induced by α-Defensin in Healthy Human Periodontal Tissue.” *European Journal of Immunology* 42 (4): 946–56. doi:10.1002/eji.201141657.
199. Maier, Helena J., Takahito Kashiwagi, Koyu Hara, and George G. Brownlee. 2008. “Differential Role of the Influenza A Virus Polymerase PA Subunit for vRNA and cRNA Promoter Binding.” *Virology* 370 (1): 194–204. doi:10.1016/j.virol.2007.08.029.
200. Malathi, Krishnamurthy, Beihua Dong, Michael Gale Jr, and Robert H Silverman. 2007. “Small Self-RNA Generated by RNase L Amplifies Antiviral Innate Immunity.” *Nature* 448 (7155): 816–19. doi:10.1038/nature06042.
201. Mänz, Benjamin, Linda Brunotte, Peter Reuther, and Martin Schwemmle. 2012. “Adaptive Mutations in NEP Compensate for Defective H5N1 RNA Replication in Cultured Human Cells.” *Nature Communications* 3: 802. doi:10.1038/ncomms1804.
202. Mänz, Benjamin, Dominik Dornfeld, Veronika Götz, Roland Zell, Petra Zimmermann, Otto Haller, Georg Kochs, and Martin Schwemmle. 2013. “Pandemic Influenza A Viruses Escape from Restriction by Human MxA through Adaptive Mutations in the Nucleoprotein.” *PLoS Pathogens* 9 (3): e1003279. doi:10.1371/journal.ppat.1003279.
203. Mark, G. E., J. M. Taylor, B. Broni, and R. M. Krug. 1979. “Nuclear Accumulation of Influenza Viral RNA Transcripts and the Effects of Cycloheximide, Actinomycin D, and Alpha-Amanitin.” *Journal of Virology* 29 (2): 744–52.
204. Marschall, M, A Zach, A Hechtfischer, G Foerst, H Meier-Ewert, and O Haller. 2000. “Inhibition of Influenza C Viruses by Human MxA Protein.” *Virus Research* 67 (2): 179–88.
205. Martens, Sascha, and Jonathan Howard. 2006. “The Interferon-Inducible GTPases.” *Annual Review of Cell and Developmental Biology* 22: 559–89. doi:10.1146/annurev.cellbio.22.010305.104619.
206. Martin, K., and A. Helenius. 1991. “Nuclear Transport of Influenza Virus Ribonucleoproteins: The Viral Matrix Protein (M1) Promotes Export and Inhibits Import.” *Cell* 67 (1): 117–30.
207. Martyna, Agnieszka, and Jeremy Rossman. 2014. “Alterations of Membrane Curvature during Influenza Virus Budding.” *Biochemical Society Transactions* 42 (5): 1425–28. doi:10.1042/BST20140136.
208. Matlin, K S, H Reggio, A Helenius, and K Simons. 1981. “Infectious Entry Pathway of Influenza Virus in a Canine Kidney Cell Line.” *The Journal of Cell Biology* 91 (3 Pt 1): 601–13.
209. Matrosovich, Mikhail N., Tatyana Y. Matrosovich, Thomas Gray, Noel A. Roberts, and Hans-Dieter Klenk. 2004. “Neuraminidase Is Important for the Initiation of Influenza Virus Infection in Human Airway Epithelium.” *Journal of Virology* 78 (22): 12665–67. doi:10.1128/JVI.78.22.12665-12667.2004.

210. Matsuzawa, Takeshi, Bae-Hoon Kim, Avinash R Shenoy, Shigeki Kamitani, Masami Miyake, and John D Macmicking. 2012. "IFN-γ Elicits Macrophage Autophagy via the p38 MAPK Signaling Pathway." *Journal of Immunology (Baltimore, Md.: 1950)* 189 (2): 813–18. doi:10.4049/jimmunol.1102041.
211. Mattheyses, Alexa L., Sanford M. Simon, and Joshua Z. Rappoport. 2010. "Imaging with Total Internal Reflection Fluorescence Microscopy for the Cell Biologist." *Journal of Cell Science* 123 (21): 3621–28. doi:10.1242/jcs.056218.
212. Matzinger, Shannon R, Timothy D Carroll, Joseph C Dutra, Zhong-Min Ma, and Christopher J Miller. 2013. "Myxovirus Resistance Gene A (MxA) Expression Suppresses Influenza A Virus Replication in Alpha Interferon-Treated Primate Cells." *Journal of Virology* 87 (2): 1150–58. doi:10.1128/JVI.02271-12.
213. McCartney, Stephen A., Larissa B. Thackray, Leonid Gitlin, Susan Gilfillan, Herbert W. Virgin, Herbert W. Virgin Iv, and Marco Colonna. 2008. "MDA-5 Recognition of a Murine Norovirus." *PLoS Pathogens* 4 (7): e1000108. doi:10.1371/journal.ppat.1000108.
214. McCown, Matthew F., and Andrew Pekosz. 2005. "The Influenza A Virus M2 Cytoplasmic Tail Is Required for Infectious Virus Production and Efficient Genome Packaging." *Journal of Virology* 79 (6): 3595–3605. doi:10.1128/JVI.79.6.3595-3605.2005.
215. McMahon, Harvey T., and Emmanuel Boucrot. 2015. "Membrane Curvature at a Glance." *Journal of Cell Science* 128 (6): 1065–70. doi:10.1242/jcs.114454.
216. Meager, Anthony, Kumuthini Visvalingam, Paula Dilger, Donna Bryan, and Meenu Wadhwa. 2005. "Biological Activity of Interleukins-28 and -29: Comparison with Type I Interferons." *Cytokine* 31 (2): 109–18. doi:10.1016/j.cyto.2005.04.003.
217. Mehle, Andrew, Vivien G. Dugan, Jeffery K. Taubenberger, and Jennifer A. Doudna. 2012. "Reassortment and Mutation of the Avian Influenza Virus Polymerase PA Subunit Overcome Species Barriers." *Journal of Virology* 86 (3): 1750–57. doi:10.1128/JVI.06203-11.
218. Melén, Krister, Päivi Keskinen, Tapani Ronni, Timo Sareneva, Kari Lounatmaa, and Ilkka Julkunen. 1996. "Human MxB Protein, an Interferon-α-Inducible GTPase, Contains a Nuclear Targeting Signal and Is Localized in the Heterochromatin Region beneath the Nuclear Envelope." *Journal of Biological Chemistry* 271 (38): 23478–86. doi:10.1074/jbc.271.38.23478.
219. Mibayashi, Masaki, Luis Martínez-Sobrido, Yueh-Ming Loo, Washington B Cárdenas, Michael Gale Jr, and Adolfo García-Sastre. 2007. "Inhibition of Retinoic Acid-Inducible Gene I-Mediated Induction of Beta Interferon by the NS1 Protein of Influenza A Virus." *Journal of Virology* 81 (2): 514–24. doi:10.1128/JVI.01265-06.
220. Min, Ji-Young, and Robert M Krug. 2006. "The Primary Function of RNA Binding by the Influenza A Virus NS1 Protein in Infected Cells: Inhibiting the 2'-5' Oligo (A) synthetase/RNase L Pathway." *Proceedings of the National Academy of Sciences of the United States of America* 103 (18): 7100–7105. doi:10.1073/pnas.0602184103.

221. Min, Ji-Young, Shoudong Li, Ganes C Sen, and Robert M Krug. 2007. "A Site on the Influenza A Virus NS1 Protein Mediates Both Inhibition of PKR Activation and Temporal Regulation of Viral RNA Synthesis." *Virology* 363 (1): 236–43. doi:10.1016/j.virol.2007.01.038.
222. Mitchell, Patrick S, Corinna Patzina, Michael Emerman, Otto Haller, Harmit S Malik, and Georg Kochs. 2012. "Evolution-Guided Identification of Antiviral Specificity Determinants in the Broadly Acting Interferon-Induced Innate Immunity Factor MxA." *Cell Host & Microbe* 12 (4): 598–604. doi:10.1016/j.chom.2012.09.005.
223. Moeller, Arne, Robert N Kirchdoerfer, Clinton S Potter, Bridget Carragher, and Ian A Wilson. 2012. "Organization of the Influenza Virus Replication Machinery." *Science (New York, N.Y.)* 338 (6114): 1631–34. doi:10.1126/science.1227270.
224. Momose, Fumitaka, Yuji Kikuchi, Katsuhiro Komase, and Yuko Morikawa. 2007. "Visualization of Microtubule-Mediated Transport of Influenza Viral Progeny Ribonucleoprotein." *Microbes and Infection / Institut Pasteur* 9 (12-13): 1422–33. doi:10.1016/j.micinf.2007.07.007.
225. Momose, Fumitaka, Tetsuya Sekimoto, Takashi Ohkura, Shuichi Jo, Atsushi Kawaguchi, Kyosuke Nagata, and Yuko Morikawa. 2011. "Apical Transport of Influenza A Virus Ribonucleoprotein Requires Rab11-Positive Recycling Endosome." *PloS One* 6 (6): e21123. doi:10.1371/journal.pone.0021123.
226. Mondal, Arindam, Gregory K. Potts, Anthony R. Dawson, Joshua J. Coon, and Andrew Mehle. 2015. "Phosphorylation at the Homotypic Interface Regulates Nucleoprotein Oligomerization and Assembly of the Influenza Virus Replication Machinery." *PLoS Pathogens* 11 (4): e1004826. doi:10.1371/journal.ppat.1004826.
227. Mortimer, Stefanie A., Mary Anne Kidwell, and Jennifer A. Doudna. 2014. "Insights into RNA Structure and Function from Genome-Wide Studies." *Nature Reviews Genetics* 15 (7): 469–79. doi:10.1038/nrg3681.
228. Mossman, K L, P F Macgregor, J J Rozmus, A B Goryachev, A M Edwards, and J R Smiley. 2001. "Herpes Simplex Virus Triggers and Then Disarms a Host Antiviral Response." *Journal of Virology* 75 (2): 750–58. doi:10.1128/JVI.75.2.750-758.2001.
229. Mould, Jorgen A., Reay G. Paterson, Makoto Takeda, Yuki Ohigashi, Padma Venkataraman, Robert A. Lamb, and Lawrence H. Pinto. 2003. "Influenza B Virus BM2 Protein Has Ion Channel Activity That Conducts Protons across Membranes." *Developmental Cell* 5 (1): 175–84.
230. Muramoto, Yukiko, Takeshi Noda, Eiryo Kawakami, Ramesh Akkina, and Yoshihiro Kawaoka. 2013. "Identification of Novel Influenza A Virus Proteins Translated from PA mRNA." *Journal of Virology* 87 (5): 2455–62. doi:10.1128/JVI.02656-12.
231. Naito, Tadasuke, Fumitaka Momose, Atsushi Kawaguchi, and Kyosuke Nagata. 2007. "Involvement of Hsp90 in Assembly and Nuclear Import of Influenza Virus RNA Polymerase Subunits." *Journal of Virology* 81 (3): 1339–49. doi:10.1128/JVI.01917-06.
232. Neil, Stuart J D, Trinity Zang, and Paul D Bieniasz. 2008. "Tetherin Inhibits Retrovirus Release and Is Antagonized by HIV-1 Vpu." *Nature* 451 (7177): 425–30. doi:10.1038/nature06553.

233. Nemeroff, M E, S M Barabino, Y Li, W Keller, and R M Krug. 1998. "Influenza Virus NS1 Protein Interacts with the Cellular 30 kDa Subunit of CPSF and Inhibits 3'end Formation of Cellular Pre-mRNAs." *Molecular Cell* 1 (7): 991–1000.
234. Netherton, Christopher L, Jennifer Simpson, Otto Haller, Thomas E Wileman, Haru-Hisa Takamatsu, Paul Monaghan, and Geraldine Taylor. 2009. "Inhibition of a Large Double-Stranded DNA Virus by MxA Protein." *Journal of Virology* 83 (5): 2310–20. doi:10.1128/JVI.00781-08.
235. Neumann, Gabriele, Mark T. Hughes, and Yoshihiro Kawaoka. 2000. "Influenza A Virus NS2 Protein Mediates vRNP Nuclear Export through NES-Independent Interaction with hCRM1." *The EMBO Journal* 19 (24): 6751–58. doi:10.1093/emboj/19.24.6751.
236. Neumann, Gabriele, and Yoshihiro Kawaoka. 2015. "Transmission of Influenza A Viruses." *Virology*, 60th Anniversary Issue, 479–480 (May): 234–46. doi:10.1016/j.virol.2015.03.009.
237. Ng, Andy Ka-Leung, Mandy Ka-Han Lam, Hongmin Zhang, Jinhuan Liu, Shannon Wing-Ngor Au, Paul Kay-Sheung Chan, Jiahuai Wang, and Pang-Chui Shaw. 2012. "Structural Basis for RNA Binding and Homo-Oligomer Formation by Influenza B Virus Nucleoprotein." *Journal of Virology* 86 (12): 6758–67. doi:10.1128/JVI.00073-12.
238. Ng, Andy Ka-Leung, Hongmin Zhang, Kemin Tan, Zongli Li, Jin-huan Liu, Paul Kay-Sheung Chan, Sui-Mui Li, et al. 2008. "Structure of the Influenza Virus A H5N1 Nucleoprotein: Implications for RNA Binding, Oligomerization, and Vaccine Design." *FASEB Journal: Official Publication of the Federation of American Societies for Experimental Biology* 22 (10): 3638–47. doi:10.1096/fj.08-112110.
239. Noda, Takeshi, Hiroshi Sagara, Albert Yen, Ayato Takada, Hiroshi Kida, R. Holland Cheng, and Yoshihiro Kawaoka. 2006. "Architecture of Ribonucleoprotein Complexes in Influenza A Virus Particles." *Nature* 439 (7075): 490–92. doi:10.1038/nature04378.
240. Noton, Sarah L., Elizabeth Medcalf, Dawn Fisher, Anne E. Mullin, Debra Elton, and Paul Digard. 2007. "Identification of the Domains of the Influenza A Virus M1 Matrix Protein Required for NP Binding, Oligomerization and Incorporation into Virions." *The Journal of General Virology* 88 (Pt 8): 2280–90. doi:10.1099/vir.0.82809-0.
241. O'Neill, R. E., R. Jaskunas, G. Blobel, P. Palese, and J. Moroianu. 1995. "Nuclear Import of Influenza Virus RNA Can Be Mediated by Viral Nucleoprotein and Transport Factors Required for Protein Import." *The Journal of Biological Chemistry* 270 (39): 22701–4.
242. O'Neill, R. E., J. Talon, and P. Palese. 1998. "The Influenza Virus NEP (NS2 Protein) Mediates the Nuclear Export of Viral Ribonucleoproteins." *The EMBO Journal* 17 (1): 288–96. doi:10.1093/emboj/17.1.288.
243. Orvedahl, Anthony, Sarah MacPherson, Rhea Sumpter Jr, Zsolt Tallóczy, Zhongju Zou, and Beth Levine. 2010. "Autophagy Protects against Sindbis Virus Infection of the Central Nervous System." *Cell Host & Microbe* 7 (2): 115–27. doi:10.1016/j.chom.2010.01.007.
244. Osterhaus, A. D. M. E., G. F. Rimmelzwaan, B. E. E. Martina, T. M. Bestebroer, and R. a. M. Fouchier. 2000. "Influenza B Virus in Seals." *Science* 288 (5468): 1051–53. doi:10.1126/science.288.5468.1051.

245. Patel, C V, I Handy, T Goldsmith, and R C Patel. 2000. "PACT, a Stress-Modulated Cellular Activator of Interferon-Induced Double-Stranded RNA-Activated Protein Kinase, PKR." *The Journal of Biological Chemistry* 275 (48): 37993–98. doi:10.1074/jbc.M004762200.
246. Paterson, Reay G., Makoto Takeda, Yuki Ohigashi, Lawrence H. Pinto, and Robert A. Lamb. 2003. "Influenza B Virus BM2 Protein Is an Oligomeric Integral Membrane Protein Expressed at the Cell Surface." *Virology* 306 (1): 7–17.
247. Patzina, Corinna, Otto Haller, and Georg Kochs. 2014. "Structural Requirements for the Antiviral Activity of the Human MxA Protein against Thogoto and Influenza A Virus." *The Journal of Biological Chemistry* 289 (9): 6020–27. doi:10.1074/jbc.M113.543892.
248. Paul Glezen, W., Jordana K. Schmier, Carrie M. Kuehn, Kellie J. Ryan, and John Oxford. 2013. "The Burden of Influenza B: A Structured Literature Review." *American Journal of Public Health* 103 (3): e43–51. doi:10.2105/AJPH.2012.301137.
249. Pauli, Eva-K, Mirco Schmolke, Thorsten Wolff, Dorothee Viemann, Johannes Roth, Johannes G Bode, and Stephan Ludwig. 2008. "Influenza A Virus Inhibits Type I IFN Signaling via NF-kappaB-Dependent Induction of SOCS-3 Expression." *PLoS Pathogens* 4 (11): e1000196. doi:10.1371/journal.ppat.1000196.
250. Pavlovic, J., T. Zürcher, O. Haller, and P. Staeheli. 1990. "Resistance to Influenza Virus and Vesicular Stomatitis Virus Conferred by Expression of Human MxA Protein." *Journal of Virology* 64 (7): 3370–75.
251. Perez Bay, Andres E., Ryan Schreiner, and Enrique Rodriguez-Boulan. 2015. "Chapter 17 - Structural and Functional Analysis of Endosomal Compartments in Epithelial Cells." In *Methods in Cell Biology*, edited by Wei Guo, 130:271–88. Sorting and Recycling Endosomes. Academic Press. http://www.sciencedirect.com/science/article/pii/S0091679X15001594.
252. Pérez, L., and L. Carrasco. 1994. "Involvement of the Vacuolar H(+)-ATPase in Animal Virus Entry." *The Journal of General Virology* 75 ( Pt 10) (October): 2595–2606.
253. Pflug, Alexander, Delphine Guilligay, Stefan Reich, and Stephen Cusack. 2014. "Structure of Influenza A Polymerase Bound to the Viral RNA Promoter." *Nature* 516 (7531): 355–60. doi:10.1038/nature14008.
254. Pichlmair, Andreas, Oliver Schulz, Choon Ping Tan, Tanja I Näslund, Peter Liljeström, Friedemann Weber, and Caetano Reis e Sousa. 2006. "RIG-I-Mediated Antiviral Responses to Single-Stranded RNA Bearing 5'-Phosphates." *Science (New York, N.Y.)* 314 (5801): 997–1001. doi:10.1126/science.1132998.
255. Pichlmair, Andreas, Oliver Schulz, Choon-Ping Tan, Jan Rehwinkel, Hiroki Kato, Osamu Takeuchi, Shizuo Akira, Michael Way, Giampietro Schiavo, and Caetano Reis e Sousa. 2009. "Activation of MDA5 Requires Higher-Order RNA Structures Generated during Virus Infection." *Journal of Virology* 83 (20): 10761–69. doi:10.1128/JVI.00770-09.
256. Plotch, S. J., M. Bouloy, and R. M. Krug. 1979. "Transfer of 5'-Terminal Cap of Globin mRNA to Influenza Viral Complementary RNA

during Transcription in Vitro." *Proceedings of the National Academy of Sciences of the United States of America* 76 (4): 1618–22.
257. Ponten, A., C. Sick, M. Weeber, O. Haller, and G. Kochs. 1997. "Dominant-Negative Mutants of Human MxA Protein: Domains in the Carboxy-Terminal Moiety Are Important for Oligomerization and Antiviral Activity." *Journal of Virology* 71 (4): 2591–99.
258. Poon, L. L., D. C. Pritlove, E. Fodor, and G. G. Brownlee. 1999. "Direct Evidence That the poly(A) Tail of Influenza A Virus mRNA Is Synthesized by Reiterative Copying of a U Track in the Virion RNA Template." *Journal of Virology* 73 (4): 3473–76.
259. Pothlichet, Julien, Michel Chignard, and Mustapha Si-Tahar. 2008. "Cutting Edge: Innate Immune Response Triggered by Influenza A Virus Is Negatively Regulated by SOCS1 and SOCS3 through a RIG-I/IFNAR1-Dependent Pathway." *Journal of Immunology (Baltimore, Md.: 1950)* 180 (4): 2034–38.
260. Preston, Chris M., Andrew N. Harman, and Mary Jane Nicholl. 2001. "Activation of Interferon Response Factor-3 in Human Cells Infected with Herpes Simplex Virus Type 1 or Human Cytomegalovirus." *Journal of Virology* 75 (19): 8909–16. doi:10.1128/JVI.75.19.8909-8916.2001.
261. Puchner, Elias M., Jessica M. Walter, Robert Kasper, Bo Huang, and Wendell A. Lim. 2013. "Counting Molecules in Single Organelles with Superresolution Microscopy Allows Tracking of the Endosome Maturation Trajectory." *Proceedings of the National Academy of Sciences* 110 (40): 16015–20. doi:10.1073/pnas.1309676110.
262. Randall, Richard E, and Stephen Goodbourn. 2008. "Interferons and Viruses: An Interplay between Induction, Signalling, Antiviral Responses and Virus Countermeasures." *The Journal of General Virology* 89 (Pt 1): 1–47. doi:10.1099/vir.0.83391-0.
263. Ran, Zhiguang, Huigang Shen, Yuekun Lang, Elizabeth A. Kolb, Nuri Turan, Laihua Zhu, Jingjiao Ma, et al. 2015. "Domestic Pigs Are Susceptible to Infection with Influenza B Viruses." *Journal of Virology* 89 (9): 4818–26. doi:10.1128/JVI.00059-15.
264. Reeves, R H, B F O'Hara, W J Pavan, J D Gearhart, and O Haller. 1988. "Genetic Mapping of the Mx Influenza Virus Resistance Gene within the Region of Mouse Chromosome 16 That Is Homologous to Human Chromosome 21." *Journal of Virology* 62 (11): 4372–75.
265. Reich, Stefan, Delphine Guilligay, Alexander Pflug, Hélène Malet, Imre Berger, Thibaut Crépin, Darren Hart, et al. 2014. "Structural Insight into Cap-Snatching and RNA Synthesis by Influenza Polymerase." *Nature* 516 (7531): 361–66. doi:10.1038/nature14009.
266. Reuter, Tanja Y., Annette L. Medhurst, Quinten Waisfisz, Yu Zhi, Sabine Herterich, Holger Hoehn, Hans J. Gross, et al. 2003. "Yeast Two-Hybrid Screens Imply Involvement of Fanconi Anemia Proteins in Transcription Regulation, Cell Signaling, Oxidative Metabolism, and Cellular Transport." *Experimental Cell Research* 289 (2): 211–21.
267. Richardson, J. C., and R. K. Akkina. 1991. "NS2 Protein of Influenza Virus Is Found in Purified Virus and Phosphorylated in Infected Cells." *Archives of Virology* 116 (1-4): 69–80.

268. Riegger, David, Rong Hai, Dominik Dornfeld, Benjamin Mänz, Victor Leyva-Grado, Maria T. Sánchez-Aparicio, Randy A. Albrecht, et al. 2015. "The Nucleoprotein of Newly Emerged H7N9 Influenza A Virus Harbors a Unique Motif Conferring Resistance to Antiviral Human MxA." *Journal of Virology* 89 (4): 2241–52. doi:10.1128/JVI.02406-14.
269. Robb, Nicole C., Matt Smith, Frank T. Vreede, and Ervin Fodor. 2009. "NS2/NEP Protein Regulates Transcription and Replication of the Influenza Virus RNA Genome." *The Journal of General Virology* 90 (Pt 6): 1398–1407. doi:10.1099/vir.0.009639-0.
270. Roberts, P. C., R. A. Lamb, and R. W. Compans. 1998. "The M1 and M2 Proteins of Influenza A Virus Are Important Determinants in Filamentous Particle Formation." *Virology* 240 (1): 127–37. doi:10.1006/viro.1997.8916.
271. Rodriguez, Kenny R., Annie M. Bruns, and Curt M. Horvath. 2014. "MDA5 and LGP2: Accomplices and Antagonists of Antiviral Signal Transduction." *Journal of Virology* 88 (15): 8194–8200. doi:10.1128/JVI.00640-14.
272. Rossman, Jeremy S., Xianghong Jing, George P. Leser, and Robert A. Lamb. 2010. "Influenza Virus M2 Protein Mediates ESCRT-Independent Membrane Scission." *Cell* 142 (6): 902–13. doi:10.1016/j.cell.2010.08.029.
273. Rossman, Jeremy S., and Robert A. Lamb. 2011. "Influenza Virus Assembly and Budding." *Virology* 411 (2): 229–36. doi:10.1016/j.virol.2010.12.003.
274. Rossman, Jeremy S., George P. Leser, and Robert A. Lamb. 2012. "Filamentous Influenza Virus Enters Cells via Macropinocytosis." *Journal of Virology* 86 (20): 10950–60. doi:10.1128/JVI.05992-11.
275. Rota, P. A., T. R. Wallis, M. W. Harmon, J. S. Rota, A. P. Kendal, and K. Nerome. 1990. "Cocirculation of Two Distinct Evolutionary Lineages of Influenza Type B Virus since 1983." *Virology* 175 (1): 59–68.
276. Rouskin, Silvi, Meghan Zubradt, Stefan Washietl, Manolis Kellis, and Jonathan S. Weissman. 2014. "Genome-Wide Probing of RNA Structure Reveals Active Unfolding of mRNA Structures in Vivo." *Nature* 505 (7485): 701–5. doi:10.1038/nature12894.
277. Roy, Rajat, Danielle Durie, Hui Li, Bing-Qian Liu, John Mark Skehel, Francesco Mauri, Lucia Veronica Cuorvo, et al. 2014. "hnRNPA1 Couples Nuclear Export and Translation of Specific mRNAs Downstream of FGF-2/S6K2 Signalling." *Nucleic Acids Research* 42 (20): 12483–97. doi:10.1093/nar/gku953.
278. Russell, Rupert J., Lesley F. Haire, David J. Stevens, Patrick J. Collins, Yi Pu Lin, G. Michael Blackburn, Alan J. Hay, Steven J. Gamblin, and John J. Skehel. 2006. "The Structure of H5N1 Avian Influenza Neuraminidase Suggests New Opportunities for Drug Design." *Nature* 443 (7107): 45–49. doi:10.1038/nature05114.
279. Sadler, Anthony J, and Bryan R G Williams. 2008. "Interferon-Inducible Antiviral Effectors." *Nature Reviews. Immunology* 8 (7): 559–68. doi:10.1038/nri2314.
280. ———. 2011. "Dynamiting Viruses with MxA." *Immunity* 35 (4): 491–93. doi:10.1016/j.immuni.2011.10.005.

281. Sakaguchi, Atsushi, Etsuko Hirayama, Akihiro Hiraki, Y. o-ichi Ishida, and Jeman Kim. 2003. "Nuclear Export of Influenza Viral Ribonucleoprotein Is Temperature-Dependently Inhibited by Dissociation of Viral Matrix Protein." *Virology* 306 (2): 244–53. doi:10.1016/S0042-6822(02)00013-2.
282. Santos, Andres, Sangita Pal, Jason Chacón, Katherine Meraz, Jeanette Gonzalez, Karla Prieto, and Germán Rosas-Acosta. 2013. "SUMOylation Affects the Interferon Blocking Activity of the Influenza A Nonstructural Protein NS1 without Affecting Its Stability or Cellular Localization." *Journal of Virology* 87 (10): 5602–20. doi:10.1128/JVI.02063-12.
283. Sasaki, Keisuke, Akihiro Yoneda, Akinori Ninomiya, Manabu Kawahara, and Tomomasa Watanabe. 2013. "Both Antiviral Activity and Intracellular Localization of Chicken Mx Protein Depend on a Polymorphism at Amino Acid Position 631." *Biochemical and Biophysical Research Communications* 430 (1): 161–66. doi:10.1016/j.bbrc.2012.11.053.
284. Satoh, Takashi, Hiroki Kato, Yutaro Kumagai, Mitsutoshi Yoneyama, Shintaro Sato, Kazufumi Matsushita, Tohru Tsujimura, Takashi Fujita, Shizuo Akira, and Osamu Takeuchi. 2010. "LGP2 Is a Positive Regulator of RIG-I- and MDA5-Mediated Antiviral Responses." *Proceedings of the National Academy of Sciences of the United States of America* 107 (4): 1512–17. doi:10.1073/pnas.0912986107.
285. Satterly, Neal, Pei-Ling Tsai, Jan van Deursen, Daniel R Nussenzveig, Yaming Wang, Paula A Faria, Agata Levay, David E Levy, and Beatriz M A Fontoura. 2007. "Influenza Virus Targets the mRNA Export Machinery and the Nuclear Pore Complex." *Proceedings of the National Academy of Sciences of the United States of America* 104 (6): 1853–58. doi:10.1073/pnas.0610977104.
286. Schermelleh, Lothar, Rainer Heintzmann, and Heinrich Leonhardt. 2010. "A Guide to Super-Resolution Fluorescence Microscopy." *The Journal of Cell Biology* 190 (2): 165–75. doi:10.1083/jcb.201002018.
287. Schmeisser, Hana, Samuel B Fey, Julie Horowitz, Elizabeth R Fischer, Corey A Balinsky, Kotaro Miyake, Joseph Bekisz, Andrew L Snow, and Kathryn C Zoon. 2013. "Type I Interferons Induce Autophagy in Certain Human Cancer Cell Lines." *Autophagy* 9 (5): 683–96. doi:10.4161/auto.23921.
288. Schoggins, John W., Donna A. MacDuff, Naoko Imanaka, Maria D. Gainey, Bimmi Shrestha, Jennifer L. Eitson, Katrina B. Mar, et al. 2014. "Pan-Viral Specificity of IFN-Induced Genes Reveals New Roles for cGAS in Innate Immunity." *Nature* 505 (7485): 691–95. doi:10.1038/nature12862.
289. Schroeder, Cornelia, Harald Heider, Elisabeth Möncke-Buchner, and Tse-I. Lin. 2005. "The Influenza Virus Ion Channel and Maturation Cofactor M2 Is a Cholesterol-Binding Protein." *European Biophysics Journal: EBJ* 34 (1): 52–66. doi:10.1007/s00249-004-0424-1.
290. Schulte, Bianca, Cindy Buffone, Silvana Opp, Francesca Di Nunzio, Daniel Augusto De Souza Aranha Vieira, Alberto Brandariz-Nuñez, and Felipe Diaz-Griffero. 2015. "Restriction of HIV-1 Requires the N-Terminal

Region of MxB/Mx2 as a Capsid-Binding Motif but Not as a Nuclear Localization Signal." *Journal of Virology*, June, JVI.00753–15. doi:10.1128/JVI.00753-15.

291. Sediri, Hanna, Folker Schwalm, Gülsah Gabriel, and Hans-Dieter Klenk. 2015. "Adaptive Mutation PB2 D701N Promotes Nuclear Import of Influenza vRNPs in Mammalian Cells." *European Journal of Cell Biology*, June. doi:10.1016/j.ejcb.2015.05.012.
292. Segawa, Katsumori, Sachiko Kurata, Yuichi Yanagihashi, Thijn R. Brummelkamp, Fumihiko Matsuda, and Shigekazu Nagata. 2014. "Caspase-Mediated Cleavage of Phospholipid Flippase for Apoptotic Phosphatidylserine Exposure." *Science (New York, N.Y.)* 344 (6188): 1164–68. doi:10.1126/science.1252809.
293. Selman, Mohammed, Samar K. Dankar, Nicole E. Forbes, Jian-Jun Jia, and Earl G. Brown. 2012. "Adaptive Mutation in Influenza A Virus Non-Structural Gene Is Linked to Host Switching and Induces a Novel Protein by Alternative Splicing." *Emerging Microbes & Infections* 1 (11): e42. doi:10.1038/emi.2012.38.
294. Shaker, Olfat G., Mohamed T. Abdel-Rahim, and Salma T. Bayoumi. 2015. "Gene Polymorphisms of IL-10 and MxA in Responders and Non-Responders to Interferon Therapy in HCV Egyptian Patients Genotype 4." *Cell Biochemistry and Biophysics* 71 (2): 617–25. doi:10.1007/s12013-014-0241-9.
295. Shanmuganatham, Karthik, Mohammed M. Feeroz, Lisa Jones-Engel, David Walker, SmRabiul Alam, Mkamrul Hasan, Pamela McKenzie, Scott Krauss, Richard J. Webby, and Robert G. Webster. 2014. "Genesis of Avian Influenza H9N2 in Bangladesh." *Emerging Microbes & Infections* 3 (12): e88. doi:10.1038/emi.2014.84.
296. Sharma, Kulbhushan, Shashank Tripathi, Priya Ranjan, Purnima Kumar, Rebecca Garten, Varough Deyde, Jacqueline M Katz, et al. 2011. "Influenza A Virus Nucleoprotein Exploits Hsp40 to Inhibit PKR Activation." *PloS One* 6 (6): e20215. doi:10.1371/journal.pone.0020215.
297. Sharma, Shipra, Adarsh K. Mayank, Himani Nailwal, Shashank Tripathi, Jenish R. Patel, John B. Bowzard, Pratibha Gaur, et al. 2014. "Influenza A Viral Nucleoprotein Interacts with Cytoskeleton Scaffolding Protein α-Actinin-4 for Viral Replication." *The FEBS Journal* 281 (13): 2899–2914. doi:10.1111/febs.12828.
298. Shaw, Megan L., Kathryn L. Stone, Christopher M. Colangelo, Erol E. Gulcicek, and Peter Palese. 2008. "Cellular Proteins in Influenza Virus Particles." *PLoS Pathogens* 4 (6): e1000085. doi:10.1371/journal.ppat.1000085.
299. Sherry, Lee, Matt Smith, Sophie Davidson, and David Jackson. 2014. "The N Terminus of the Influenza B Virus Nucleoprotein Is Essential for Virus Viability, Nuclear Localization, and Optimal Transcription and Replication of the Viral Genome." *Journal of Virology* 88 (21): 12326–38. doi:10.1128/JVI.01542-14.
300. Shimizu, Teppei, Naoki Takizawa, Ken Watanabe, Kyosuke Nagata, and Nobuyuki Kobayashi. 2011. "Crucial Role of the Influenza Virus NS2 (NEP) C-Terminal Domain in M1 Binding and Nuclear Export of vRNP." *FEBS Letters* 585 (1): 41–46. doi:10.1016/j.febslet.2010.11.017.

301. Shi, Weifeng, Yi Shi, Ying Wu, Di Liu, and George F. Gao. 2013. "Origin and Molecular Characterization of the Human-Infecting H6N1 Influenza Virus in Taiwan." *Protein & Cell* 4 (11): 846–53. doi:10.1007/s13238-013-3083-0.
302. Shtyrya, Y.A., L.V. Mochalova, and N.V. Bovin. 2009. "Influenza Virus Neuraminidase: Structure and Function." *Acta Naturae* 1 (2): 26–32.
303. Shuck, Kevin, Robert A. Lamb, and Lawrence H. Pinto. 2000. "Analysis of the Pore Structure of the Influenza A Virus M2 Ion Channel by the Substituted-Cysteine Accessibility Method." *Journal of Virology* 74 (17): 7755–61.
304. Sieczkarski, Sara B., and Gary R. Whittaker. 2002. "Influenza Virus Can Enter and Infect Cells in the Absence of Clathrin-Mediated Endocytosis." *Journal of Virology* 76 (20): 10455–64.
305. Smith, Derek J, Alan S Lapedes, Jan C de Jong, Theo M Bestebroer, Guus F Rimmelzwaan, Albert D M E Osterhaus, and Ron A M Fouchier. 2004. "Mapping the Antigenic and Genetic Evolution of Influenza Virus." *Science (New York, N.Y.)* 305 (5682): 371–76. doi:10.1126/science.1097211.
306. Staeheli, P, R Grob, E Meier, J G Sutcliffe, and O Haller. 1988. "Influenza Virus-Susceptible Mice Carry Mx Genes with a Large Deletion or a Nonsense Mutation." *Molecular and Cellular Biology* 8 (10): 4518–23.
307. Stertz, Silke, Jan Dittmann, Jorge C. G. Blanco, Lioubov M. Pletneva, Otto Haller, and Georg Kochs. 2007. "The Antiviral Potential of Interferon-Induced Cotton Rat Mx Proteins against Orthomyxovirus (influenza), Rhabdovirus, and Bunyavirus." *Journal of Interferon & Cytokine Research: The Official Journal of the International Society for Interferon and Cytokine Research* 27 (10): 847–55. doi:10.1089/jir.2006.0176.
308. Stoeckle, M. Y., M. W. Shaw, and P. W. Choppin. 1987. "Segment-Specific and Common Nucleotide Sequences in the Noncoding Regions of Influenza B Virus Genome RNAs." *Proceedings of the National Academy of Sciences* 84 (9): 2703–7.
309. Strambio-De-Castillia, Caterina, Mario Niepel, and Michael P. Rout. 2010. "The Nuclear Pore Complex: Bridging Nuclear Transport and Gene Regulation." *Nature Reviews Molecular Cell Biology* 11 (7): 490–501. doi:10.1038/nrm2928.
310. Stranden, A M, P Staeheli, and J Pavlovic. 1993. "Function of the Mouse Mx1 Protein Is Inhibited by Overexpression of the PB2 Protein of Influenza Virus." *Virology* 197 (2): 642–51. doi:10.1006/viro.1993.1639.
311. Sugiyama, Kanako, Eiji Obayashi, Atsushi Kawaguchi, Yukari Suzuki, Jeremy R H Tame, Kyosuke Nagata, and Sam-Yong Park. 2009. "Structural Insight into the Essential PB1-PB2 Subunit Contact of the Influenza Virus RNA Polymerase." *The EMBO Journal* 28 (12): 1803–11. doi:10.1038/emboj.2009.138.
312. Suthar, Mehul S., Hilario J. Ramos, Margaret M. Brassil, Jason Netland, Craig P. Chappell, Gabriele Blahnik, Aimee McMillan, et al. 2012. "The RIG-I-like Receptor LGP2 Controls CD8(+) T Cell Survival and Fitness." *Immunity* 37 (2): 235–48. doi:10.1016/j.immuni.2012.07.004.
313. Su, Wen-Chi, Yung-Chia Chen, Chung-Hsin Tseng, Paul Wei-Che Hsu, Kuo-Feng Tung, King-Song Jeng, and Michael M. C. Lai. 2013. "Pooled

RNAi Screen Identifies Ubiquitin Ligase Itch as Crucial for Influenza A Virus Release from the Endosome during Virus Entry." *Proceedings of the National Academy of Sciences of the United States of America* 110 (43): 17516–21. doi:10.1073/pnas.1312374110.

314. Tabeta, Koichi, Philippe Georgel, Edith Janssen, Xin Du, Kasper Hoebe, Karine Crozat, Suzanne Mudd, et al. 2004. "Toll-like Receptors 9 and 3 as Essential Components of Innate Immune Defense against Mouse Cytomegalovirus Infection." *Proceedings of the National Academy of Sciences of the United States of America* 101 (10): 3516–21. doi:10.1073/pnas.0400525101.
315. Takeda, Makoto, Andrew Pekosz, Kevin Shuck, Lawrence H. Pinto, and Robert A. Lamb. 2002. "Influenza A Virus M2 Ion Channel Activity Is Essential for Efficient Replication in Tissue Culture." *Journal of Virology* 76 (3): 1391–99. doi:10.1128/JVI.76.3.1391-1399.2002.
316. Takeuchi, Osamu, and Shizuo Akira. 2009. "Innate Immunity to Virus Infection." *Immunological Reviews* 227 (1): 75–86. doi:10.1111/j.1600-065X.2008.00737.x.
317. Tallóczy, Zsolt, Wenxia Jiang, Herbert W Virgin 4th, David A Leib, Donalyn Scheuner, Randal J Kaufman, Eeva-Liisa Eskelinen, and Beth Levine. 2002. "Regulation of Starvation- and Virus-Induced Autophagy by the eIF2alpha Kinase Signaling Pathway." *Proceedings of the National Academy of Sciences of the United States of America* 99 (1): 190–95. doi:10.1073/pnas.012485299.
318. Tang, YuJie, Gongxun Zhong, Lianhui Zhu, Xing Liu, Yufei Shan, Huapeng Feng, ZhiGao Bu, Hualan Chen, and Chen Wang. 2010. "Herc5 Attenuates Influenza A Virus by Catalyzing ISGylation of Viral NS1 Protein." *Journal of Immunology (Baltimore, Md.: 1950)* 184 (10): 5777–90. doi:10.4049/jimmunol.0903588.
319. Taubenberger, Jeffery K. 1998. "Influenza Virus Hemagglutinin Cleavage into HA1, HA2: No Laughing Matter." *Proceedings of the National Academy of Sciences* 95 (17): 9713–15. doi:10.1073/pnas.95.17.9713.
320. tenOever, Benjamin R, Marc J Servant, Nathalie Grandvaux, Rongtuan Lin, and John Hiscott. 2002. "Recognition of the Measles Virus Nucleocapsid as a Mechanism of IRF-3 Activation." *Journal of Virology* 76 (8): 3659–69.
321. Tong, Suxiang, Yan Li, Pierre Rivailler, Christina Conrardy, Danilo A Alvarez Castillo, Li-Mei Chen, Sergio Recuenco, et al. 2012. "A Distinct Lineage of Influenza A Virus from Bats." *Proceedings of the National Academy of Sciences of the United States of America* 109 (11): 4269–74. doi:10.1073/pnas.1116200109.
322. Tong, Suxiang, Xueyong Zhu, Yan Li, Mang Shi, Jing Zhang, Melissa Bourgeois, Hua Yang, et al. 2013. "New World Bats Harbor Diverse Influenza A Viruses." *PLoS Pathogens* 9 (10): e1003657. doi:10.1371/journal.ppat.1003657.
323. Tripal, Philipp, Michael Bauer, Elisabeth Naschberger, Thomas Mörtinger, Christine Hohenadl, Emmanuelle Cornali, Mathias Thurau, and Michael Stürzl. 2007. "Unique Features of Different Members of the Human Guanylate-Binding Protein Family." *Journal of Interferon & Cytokine Research: The Official Journal of the International Society for*

*Interferon and Cytokine Research* 27 (1): 44–52. doi:10.1089/jir.2007.0086.

324. Turan, Kadir, Masaki Mibayashi, Kenji Sugiyama, Shoko Saito, Akiko Numajiri, and Kyosuke Nagata. 2004. "Nuclear MxA Proteins Form a Complex with Influenza Virus NP and Inhibit the Transcription of the Engineered Influenza Virus Genome." *Nucleic Acids Research* 32 (2): 643–52. doi:10.1093/nar/gkh192.
325. Turrell, Lauren, Edward C. Hutchinson, Frank T. Vreede, and Ervin Fodor. 2015. "Regulation of Influenza A Virus Nucleoprotein Oligomerization by Phosphorylation." *Journal of Virology* 89 (2): 1452–55. doi:10.1128/JVI.02332-14.
326. Turrell, Lauren, Jon W. Lyall, Laurence S. Tiley, Ervin Fodor, and Frank T. Vreede. 2013. "The Role and Assembly Mechanism of Nucleoprotein in Influenza A Virus Ribonucleoprotein Complexes." *Nature Communications* 4: 1591. doi:10.1038/ncomms2589.
327. Ulmanen, I., B. A. Broni, and R. M. Krug. 1981. "Role of Two of the Influenza Virus Core P Proteins in Recognizing Cap 1 Structures (m7GpppNm) on RNAs and in Initiating Viral RNA Transcription." *Proceedings of the National Academy of Sciences of the United States of America* 78 (12): 7355–59.
328. Uzé, Gilles, and Danièle Monneron. 2007. "IL-28 and IL-29: Newcomers to the Interferon Family." *Biochimie* 89 (6-7): 729–34. doi:10.1016/j.biochi.2007.01.008.
329. van de Sandt, Carolien E, Joost H C M Kreijtz, and Guus F Rimmelzwaan. 2012. "Evasion of Influenza a Viruses from Innate and Adaptive Immune Responses." *Viruses* 4 (9): 1438–76. doi:10.3390/v4091438.
330. van Meer, Gerrit, Dennis R. Voelker, and Gerald W. Feigenson. 2008. "Membrane Lipids: Where They Are and How They Behave." *Nature Reviews Molecular Cell Biology* 9 (2): 112–24. doi:10.1038/nrm2330.
331. Varga, Zsuzsanna T, Irene Ramos, Rong Hai, Mirco Schmolke, Adolfo García-Sastre, Ana Fernandez-Sesma, and Peter Palese. 2011. "The Influenza Virus Protein PB1-F2 Inhibits the Induction of Type I Interferon at the Level of the MAVS Adaptor Protein." *PLoS Pathogens* 7 (6): e1002067. doi:10.1371/journal.ppat.1002067.
332. Vasin, A. V., O. A. Temkina, V. V. Egorov, S. A. Klotchenko, M. A. Plotnikova, and O. I. Kiselev. 2014. "Molecular Mechanisms Enhancing the Proteome of Influenza A Viruses: An Overview of Recently Discovered Proteins." *Virus Research* 185 (June): 53–63. doi:10.1016/j.virusres.2014.03.015.
333. Venkataraman, Thiagarajan, Maikel Valdes, Rachel Elsby, Shigeru Kakuta, Gisela Caceres, Shinobu Saijo, Yoichiro Iwakura, and Glen N. Barber. 2007. "Loss of DExD/H Box RNA Helicase LGP2 Manifests Disparate Antiviral Responses." *Journal of Immunology (Baltimore, Md.: 1950)* 178 (10): 6444–55.
334. von der Malsburg, Alexander, Inbal Abutbul-Ionita, Otto Haller, Georg Kochs, and Dganit Danino. 2011. "Stalk Domain of the Dynamin-like MxA GTPase Protein Mediates Membrane Binding and Liposome

Tubulation via the Unstructured L4 Loop." *The Journal of Biological Chemistry* 286 (43): 37858–65. doi:10.1074/jbc.M111.249037.

335. Vreede, Frank T., Annie Y. Chan, Jane Sharps, and Ervin Fodor. 2010. "Mechanisms and Functional Implications of the Degradation of Host RNA Polymerase II in Influenza Virus Infected Cells." *Virology* 396 (1): 125–34. doi:10.1016/j.virol.2009.10.003.
336. Vreede, Frank T., Hugh Gifford, and George G. Brownlee. 2008. "Role of Initiating Nucleoside Triphosphate Concentrations in the Regulation of Influenza Virus Replication and Transcription." *Journal of Virology* 82 (14): 6902–10. doi:10.1128/JVI.00627-08.
337. Wang, Xiuyan, Ella R Hinson, and Peter Cresswell. 2007. "The Interferon-Inducible Protein Viperin Inhibits Influenza Virus Release by Perturbing Lipid Rafts." *Cell Host & Microbe* 2 (2): 96–105. doi:10.1016/j.chom.2007.06.009.
338. Wanitchang, Asawin, Jaraspim Narkpuk, and Anan Jongkaewwattana. 2013. "Nuclear Import of Influenza B Virus Nucleoprotein: Involvement of an N-Terminal Nuclear Localization Signal and a Cleavage-Protection Motif." *Virology* 443 (1): 59–68. doi:10.1016/j.virol.2013.04.025.
339. Watanabe, Rie, George P Leser, and Robert A Lamb. 2011. "Influenza Virus Is Not Restricted by Tetherin Whereas Influenza VLP Production Is Restricted by Tetherin." *Virology* 417 (1): 50–56. doi:10.1016/j.virol.2011.05.006.
340. Wilkins, Courtney, and Michael Gale. 2013. "Sterol-Izing Innate." *Immunity* 38 (1): 3–5. doi:10.1016/j.immuni.2013.01.002.
341. Williams, M. A., and R. A. Lamb. 1986. "Determination of the Orientation of an Integral Membrane Protein and Sites of Glycosylation by Oligonucleotide-Directed Mutagenesis: Influenza B Virus NB Glycoprotein Lacks a Cleavable Signal Sequence and Has an Extracellular NH2-Terminal Region." *Molecular and Cellular Biology* 6 (12): 4317–28. doi:10.1128/MCB.6.12.4317.
342. Wise, Helen M, Agnes Foeglein, Jiechao Sun, Rosa Maria Dalton, Sheetal Patel, Wendy Howard, Emma C Anderson, Wendy S Barclay, and Paul Digard. 2009. "A Complicated Message: Identification of a Novel PB1-Related Protein Translated from Influenza A Virus Segment 2 mRNA." *Journal of Virology* 83 (16): 8021–31. doi:10.1128/JVI.00826-09.
343. Wise, Helen M., Edward C. Hutchinson, Brett W. Jagger, Amanda D. Stuart, Zi H. Kang, Nicole Robb, Louis M. Schwartzman, et al. 2012. "Identification of a Novel Splice Variant Form of the Influenza A Virus M2 Ion Channel with an Antigenically Distinct Ectodomain." *PLoS Pathogens* 8 (11): e1002998. doi:10.1371/journal.ppat.1002998.
344. Wisskirchen, Christian, Thomas H. Ludersdorfer, Dominik A. Müller, Eva Moritz, and Jovan Pavlovic. 2011. "Interferon-Induced Antiviral Protein MxA Interacts with the Cellular RNA Helicases UAP56 and URH49." *The Journal of Biological Chemistry* 286 (40): 34743–51. doi:10.1074/jbc.M111.251843.
345. Xiao, Han, Marian J. Killip, Peter Staeheli, Richard E. Randall, and David Jackson. 2013. "The Human Interferon-Induced MxA Protein Inhibits Early Stages of Influenza A Virus Infection by Retaining the

Incoming Viral Genome in the Cytoplasm." *Journal of Virology* 87 (23): 13053–58. doi:10.1128/JVI.02220-13.

346. Yamanaka, K., A. Ishihama, and K. Nagata. 1990. "Reconstitution of Influenza Virus RNA-Nucleoprotein Complexes Structurally Resembling Native Viral Ribonucleoprotein Cores." *The Journal of Biological Chemistry* 265 (19): 11151–55.
347. Yasuda, J., S. Nakada, A. Kato, T. Toyoda, and A. Ishihama. 1993. "Molecular Assembly of Influenza Virus: Association of the NS2 Protein with Virion Matrix." *Virology* 196 (1): 249–55. doi:10.1006/viro.1993.1473.
348. Yen, Hui-Ling, Chi-Hui Liang, Chung-Yi Wu, Heather L. Forrest, Angela Ferguson, Ka-Tim Choy, Jeremy Jones, et al. 2011. "Hemagglutinin-Neuraminidase Balance Confers Respiratory-Droplet Transmissibility of the Pandemic H1N1 Influenza Virus in Ferrets." *Proceedings of the National Academy of Sciences of the United States of America* 108 (34): 14264–69. doi:10.1073/pnas.1111000108.
349. Ye, Qiaozhen, Robert M Krug, and Yizhi Jane Tao. 2006. "The Mechanism by Which Influenza A Virus Nucleoprotein Forms Oligomers and Binds RNA." *Nature* 444 (7122): 1078–82. doi:10.1038/nature05379.
350. Yewdell, Jonathan W., and William L. Ince. 2012. "Virology. Frameshifting to PA-X Influenza." *Science (New York, N.Y.)* 337 (6091): 164–65. doi:10.1126/science.1225539.
351. Yondola, Mark A, Fiona Fernandes, Alan Belicha-Villanueva, Melissa Uccelini, Qinshan Gao, Carol Carter, and Peter Palese. 2011. "Budding Capability of the Influenza Virus Neuraminidase Can Be Modulated by Tetherin." *Journal of Virology* 85 (6): 2480–91. doi:10.1128/JVI.02188-10.
352. Yount, Jacob S, Leonid Gitlin, Thomas M Moran, and Carolina B López. 2008. "MDA5 Participates in the Detection of Paramyxovirus Infection and Is Essential for the Early Activation of Dendritic Cells in Response to Sendai Virus Defective Interfering Particles." *Journal of Immunology (Baltimore, Md.: 1950)* 180 (7): 4910–18.
353. Yuan, Puwei, Mark Bartlam, Zhiyong Lou, Shoudeng Chen, Jie Zhou, Xiaojing He, Zongyang Lv, et al. 2009. "Crystal Structure of an Avian Influenza Polymerase PA(N) Reveals an Endonuclease Active Site." *Nature* 458 (7240): 909–13. doi:10.1038/nature07720.
354. Zebedee, S L, and R A Lamb. 1988. "Influenza A Virus M2 Protein: Monoclonal Antibody Restriction of Virus Growth and Detection of M2 in Virions." *Journal of Virology* 62 (8): 2762–72.
355. Zhang, Tao, Yuhai Bi, Huaiyu Tian, Xiaowen Li, Di Liu, Ying Wu, Tao Jin, et al. 2014. "Human Infection with Influenza Virus A(H10N8) from Live Poultry Markets, China, 2014." *Emerging Infectious Diseases* 20 (12). doi:10.3201/eid2012.140911.
356. Zhang, Xiaoai, Hongmei Xu, Xiaodan Chen, Xiujun Li, Xianjun Wang, Shujun Ding, Renli Zhang, et al. 2014. "Association of Functional Polymorphisms in the MxA Gene with Susceptibility to Enterovirus 71 Infection." *Human Genetics* 133 (2): 187–97. doi:10.1007/s00439-013-1367-3.

357. Zhang, Ying, Qianyi Zhang, Huihui Kong, Yongping Jiang, Yuwei Gao, Guohua Deng, Jianzhong Shi, et al. 2013. "H5N1 Hybrid Viruses Bearing 2009/H1N1 Virus Genes Transmit in Guinea Pigs by Respiratory Droplet." *Science (New York, N.Y.)* 340 (6139): 1459–63. doi:10.1126/science.1229455.
358. Zhao, Chen, Carilee Denison, Jon M Huibregtse, Steven Gygi, and Robert M Krug. 2005a. "Human ISG15 Conjugation Targets Both IFN-Induced and Constitutively Expressed Proteins Functioning in Diverse Cellular Pathways." *Proceedings of the National Academy of Sciences of the United States of America* 102 (29): 10200–205. doi:10.1073/pnas.0504754102.
359. Zhao, Chen, Carilee Denison, Jon M. Huibregtse, Steven Gygi, and Robert M. Krug. 2005b. "Human ISG15 Conjugation Targets Both IFN-Induced and Constitutively Expressed Proteins Functioning in Diverse Cellular Pathways." *Proceedings of the National Academy of Sciences of the United States of America* 102 (29): 10200–205. doi:10.1073/pnas.0504754102.
360. Zhao, Chen, Tien-Ying Hsiang, Rei-Lin Kuo, and Robert M. Krug. 2010. "ISG15 Conjugation System Targets the Viral NS1 Protein in Influenza A Virus-Infected Cells." *Proceedings of the National Academy of Sciences of the United States of America* 107 (5): 2253–58. doi:10.1073/pnas.0909144107.
361. Zhao, Zijiang, Blima Fux, Megan Goodwin, Ildiko R. Dunay, David Strong, Brian C. Miller, Ken Cadwell, et al. 2008. "Autophagosome-Independent Essential Function for the Autophagy Protein Atg5 in Cellular Immunity to Intracellular Pathogens." *Cell Host & Microbe* 4 (5): 458–69. doi:10.1016/j.chom.2008.10.003.
362. Zhirnov, O. P. 1990. "Solubilization of Matrix Protein M1/M from Virions Occurs at Different pH for Orthomyxo- and Paramyxoviruses." *Virology* 176 (1): 274–79.
363. Zhou, Zhangle, Ole J Hamming, Nina Ank, Søren R Paludan, Anders L Nielsen, and Rune Hartmann. 2007. "Type III Interferon (IFN) Induces a Type I IFN-like Response in a Restricted Subset of Cells through Signaling Pathways Involving Both the Jak-STAT Pathway and the Mitogen-Activated Protein Kinases." *Journal of Virology* 81 (14): 7749–58. doi:10.1128/JVI.02438-06.
364. Zimmermann, Petra, Benjamin Mänz, Otto Haller, Martin Schwemmle, and Georg Kochs. 2011. "The Viral Nucleoprotein Determines Mx Sensitivity of Influenza A Viruses." *Journal of Virology* 85 (16): 8133–40. doi:10.1128/JVI.00712-11.
365. Zürcher, T, J Pavlovic, and P Staeheli. 1992. "Nuclear Localization of Mouse Mx1 Protein Is Necessary for Inhibition of Influenza Virus." *Journal of Virology* 66 (8): 5059–66.

# Appendix.

## Appendix A. Impact of mutations on RNA structure

During the last decade a number of studies have indicated the importance of RNA sequence and structure to the ability of a protein to be both functional and correctly folded. One of the first studies to shed light on this subject showed that a synonymous single nucleotide polymorphism (SNP) altered the specificity and conformation of MDR1 (Kimchi-Sarfaty et al. 2007). They hypothesized that this SNP introduced a rare codon into the mRNA and altered the timing of translation, therefore impacting the overall conformation of the protein. Intriguingly, another study showed that a synonymous mutation in the coding region of immunity-related GTPase M, altered a mircoRNA binding site leading to the constitutive activation of the gene during inflammation and explaining the relationship between this mutation and the incidence of Crohn's disease (Brest et al. 2011). More recently, RNA structure within the coding region has been shown to be involved in the rate of translation, which can vary by several orders of magnitude across a single mRNA transcript as well as having control over the localization of the nascent RNA (Mortimer, Kidwell, and Doudna 2014).

The differences in phenotype and functionality of MxA as a result of different mRNA backgrounds could be due to the mRNA sequence influencing the ability of the mutated protein to be efficiently translated or targeted to the correct location. Therefore to assess the impact of these mutations on the wt mRNA, the sequences were analysed using mFold to identify any major differences in the predicted mRNA secondary structures. Fig. 4.7 shows the predicted mRNA structures and Gibbs free energy for each of the phenotype altering mutations.

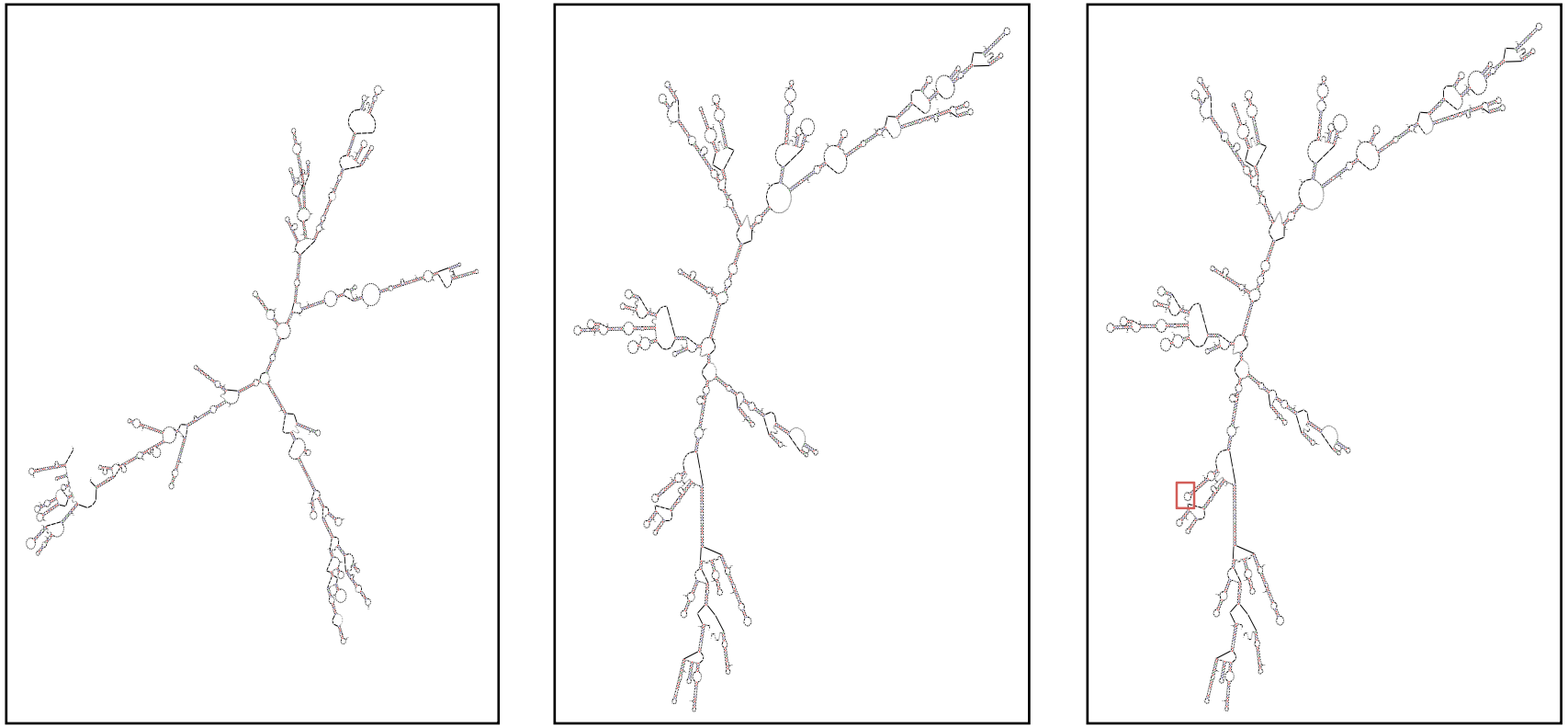

**Wt wMxA**
**ΔG= -573.41**

**Wt MxA**
**ΔG= -597.05**

**T103A MxA**
**ΔG= -597.05**

**Figure A.1 Predicted mRNA structures. A.** The RNA sequences for wt wMxA, wt MxA, and T103A MxA were predicted through the online RNA structure prediction tool, mFold. The images show the most stable RNA structure for each mutant and details the Gibbs Free Energy (ΔG). The location of the mutations is indicated by the red box.

**G255E MxA**
**ΔG= -596.95**

**I376D MxA**
**ΔG= -591.57**

**D478A MxA**
**ΔG= -599.35**

**Figure A.1 Predicted mRNA structures. B.** The RNA sequences for G255E MxA, D478A MxA and I376D MxA were predicted through the online RNA structure prediction tool, mFold. The images show the most stable RNA structure for each mutant and details the Gibbs Free Energy (ΔG). The location of the mutations is indicated by the red box.

The predicted mRNA secondary structures for wt MxA and wt wMxA show extremely different structures that differ in the Gibbs free energy required to produce the most stable structure. This is to be expected as shown in Fig. 4.1 there are 678 nucleotide changes in the wobble mRNA construct, therefore it is highly unlikely that these two sequences would share similar secondary structure. The RNA structure for the wt MxA mRNA containing the T103A mutation was identical to the wt secondary structure possessing the exact same Gibbs free energy. The only difference was a single nucleotide change at nucleotide position 307 from adenosine to guanine which as shown in Fig. 4.7 occurs at the top of a stem loop, therefore not impacting any secondary structure within the mRNA sequence. Similarly, G255E is encoded by a point mutation at nucleotide position 764 exchanging a guanine for an adenosine. Although this mutation resulted in a small change in Gibbs free energy required to produce the most stable structure requiring 0.1 $\Delta G$ more than wt MxA, this mutation had no impact on the overall structure of the RNA as this mutation takes place within an asymmetric loop prior to two stem loops, which is unlikely to have an impact on the overall structure.

However, both I376D and D478A mutations introduce nucleotide changes that have an impact on the predicted secondary structure of the MxA mRNA. The introduction of aspartic acid in place of isoleucine changed a whole codon beginning at nucleotide position 1126, where ATA became GAC, which not only increased the required Gibbs free energy but also altered the overall secondary structure of the mRNA. As highlighted in Fig. 4.7 the introduction of GAC completely changes the secondary structure from nucleotide position 996 through to 1136 compared to the wt mRNA

structure. This large change in predicted mRNA secondary structure suggests this may play a role in the altered distribution phenotype observed for MxA containing the I376D mutation.

The change in mRNA secondary structure for D478A was less drastic as the aspartic acid to alanine mutation only required a single nucleotide mutation, swapping adenosine for cytosine at nucleotide position 1433. The introduction of this mutation actually lowered the Gibbs free energy required to produce this structure and also had a small impact on the predicted mRNA secondary structure. This suggests that the change in overall RNA structure could be responsible for the atypical localization of D478A MxA.

The prediction of the full-length mRNA structures for each mutant revealed that both I376D and D478A mutations have an impact on the overall secondary structure in comparison to wt MxA. However, this analysis also showed that the two mutants that showed an aggregation phenotype, T103A and G255E, had no impact on the global secondary structure. To further investigate the impact of these mutations on mRNA structure, smaller 400-nucleotide windows, starting approximately 200 nucleotides away from the mutation were analysed through mFold and compared to the same window in wt MxA. Fig. 4.8 shows the initial 400-nucleotide window and the subsequent images achieved through systematically moving 50 nucleotides towards the introduced mutation to determine the predicted impact on localised mRNA structure in comparison to wt MxA. In three of the five windows (100-500 nt, 200-600 nt and 250-650 nt) there was no difference in localised secondary structure or Gibbs free energy when comparing wt MxA to T103A mRNA. In all three of these structures, as in the full-length mRNA structure, the mutation occurred in the loop

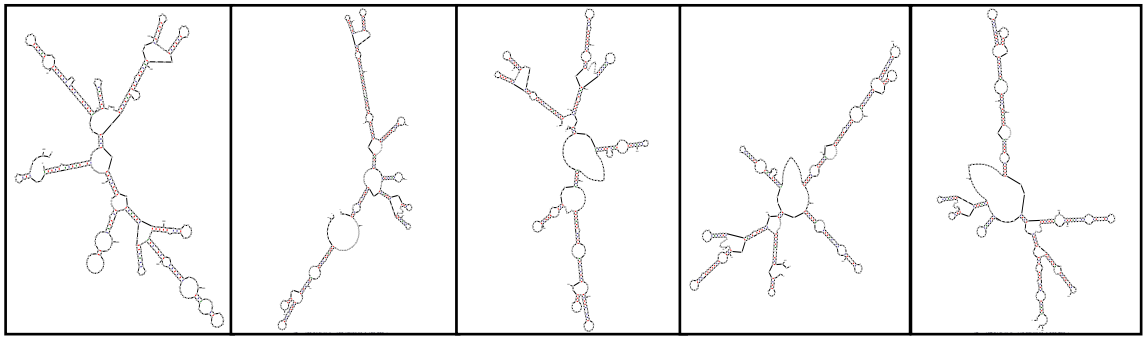

| WT MxA 100-500 nt ΔG= - 125.27 | WT MxA 150-550 nt ΔG= -120.04 | WT MxA 200-600 nt ΔG= -120.24 | WT MxA 250-650 nt ΔG= -115.08 | WT MxA 300-700 nt ΔG= -107.81 |
|---|---|---|---|---|

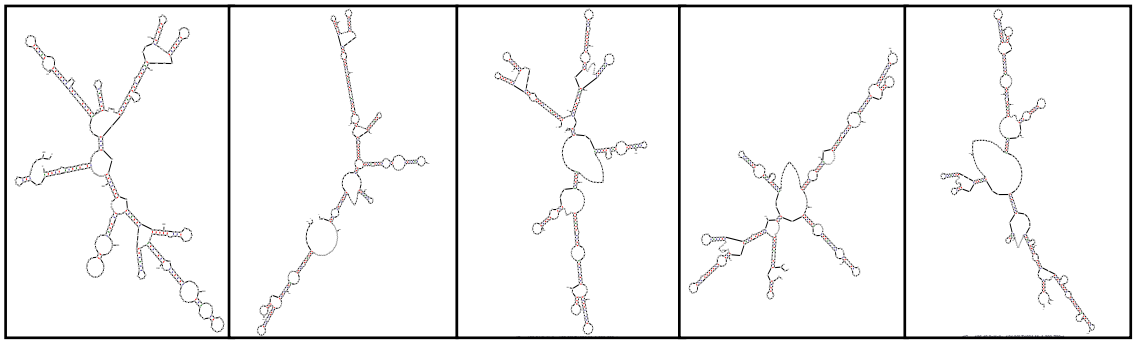

| T103A MxA 100-500 nt ΔG= -125.27 | T103A MxA 150-550 nt ΔG= -119.77 | T103A MxA 200-600 nt ΔG= -120.24 | T103A MxA 250-650 nt ΔG= -115.08 | T103A MxA 300-700 nt ΔG= -106.49 |
|---|---|---|---|---|

**Figure A.2. A. Predicted localised mRNA structures.** The RNA secondary structures for wt MxA and T103A MxA were predicted through the online RNA structure prediction tool, mFold. The sequences were analysed in 400 nt windows for the sequence between 100-700nt. The images show the most stable RNA structure for each mutant and indicate the Gibbs Free Energy (ΔG).

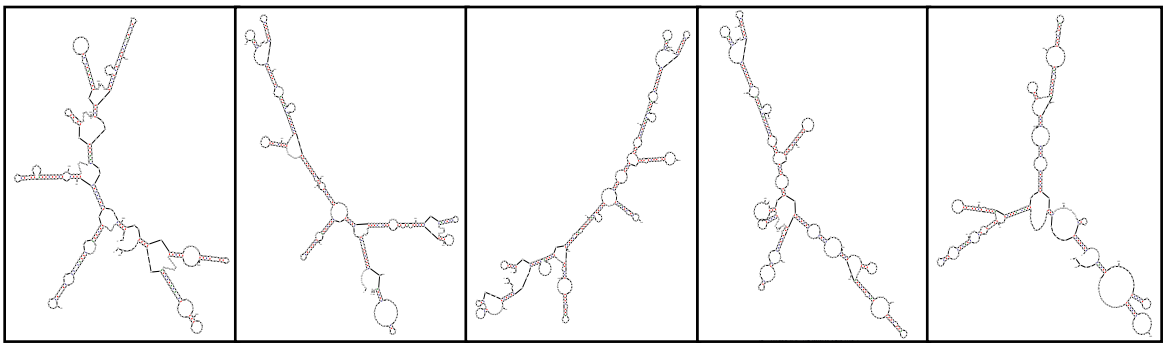

**WT MxA 560-960 nt ΔG= -118.31** | **WT MxA 610-1010 nt ΔG= -129.69** | **WT MxA 660-1060 nt ΔG= -111.42** | **WT MxA 710-1110 nt ΔG= -111.22** | **WT MxA 750-1150 nt ΔG= -94.27**

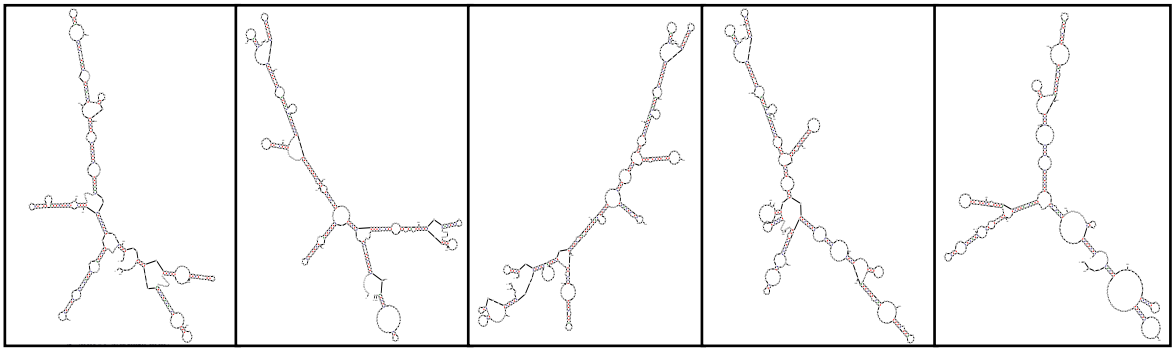

**G255E MxA 560-960 nt ΔG= -120.96** | **G255E MxA 610-1010 nt ΔG= -129.59** | **G255E MxA 660-1060 nt ΔG= -111.32** | **G255E MxA 710-1110 nt ΔG= -111.12** | **G255E MxA 750-1150 nt ΔG= -93.66**

**Figure A.2. B. Predicted localised mRNA structures.** The RNA secondary structures for wt MxA and G255E MxA were predicted through the online RNA structure prediction tool, mFold. The sequences were analysed in 400 nt windows for the sequence between 560-1150nt. The images show the most stable RNA structure for each mutant and indicate the Gibbs Free Energy (ΔG).

region of a hairpin, therefore having no impact on complementarity. However, the A to G nucleotide mutation was predicted to impact the RNA structure in the windows depicting nucleotides 150-550 and 300-700. In the RNA structure for nucleotides 150-550 (in each image the starting nucleotide is numbered as 1 i.e position 1 = nucleotide 150 in overall sequence), the mutation was found at position 157 and led to an extensive change in secondary structure between nucleotide position 134 and 263 in comparison to the predicted wt mRNA structure. In the predicted 300-700 nucleotide structure the mutation occured very early in the sequence at position 7 which had a large impact on the overall predicted structure. Using this systematic approach to increase proximity to the mutations allowed an insight into the potential structures the RNA might take during translation. Therefore based on these predicted structures it appears that T103A may have more of an impact on the localised mRNA structures than on the global structure, which could in turn impact the rate of translation resulting in the aggregated distribution phenotype exhibited by this mutant.

Similarly to T103A, three of the windows in the case of G255E show identical predicted structure to wt RNA. In the windows showing 610-1010 nt, 660-1060 nt and 710-1110 nt the mutation occured in an asymmetric loop prior to two hairpin loop structures, therefore being unlikely to have an impact on the predicted secondary structure. However, the G255E window 560-960 nt shows a markedly different structure to wt MxA mRNA between nucleotides 138 and 260 as the guanine to adenosine mutation increased the complementarity of the RNA which increased the stability and therefore reduced the required Gibbs free energy to produce this structure. The change in secondary structure for the window depicting the nucleotide window 750-1150 shows the mutation occurred at position 15, and shows a much

more subtle change in secondary structure compared to the predicted wt mRNA. The mutation led to a reduction in the asymmetric loop, which in turn reduced the size of the following bulge in comparison to the predicted wt mRNA structure. Therefore this suggests that this single nucleotide change may have an increased impact on localised RNA secondary structure, which could be important to the rate of translation or the ability to bind or be recognised by RNA binding proteins.

Another potential impact of these mutations is the effects they have on codon frequency and subsequent tRNA availability. Kimchi-Sarfaty et al. (2007) suggested that an SNP led to the introduction of a rare codon in the mRNA of MDR1 that in turn altered the rate in translation causing an altered conformation and specificity for substrates and inhibitors. Table 4.2 summarises the changes in codon frequency for the mutations leading to atypical expression patterns of MxA. The table shows the codon frequency per 1000 codons within a human cell showing some intriguing differences. Firstly, the codon change for T103A leads to an increase in codon frequency, with approximately 9 more alanine codons available per 1000 than threonine. This suggests that the corresponding transfer RNA (tRNA) could be recruited to the ribosome quicker leading to an increased rate in translation and therefore could impact the rate at which the protein folds leading to aggregation at the site of translation. We see a similar increase in codon frequency for G255E as the GAA codon appears just over 10 times more frequently per 1000 codons the original GGA suggesting that the aggregation phenotype seen for G255E may also be determined by an increased tRNA availability disrupting the rate at which the translating protein folds.

| Mutation | Original Codon Frequency (/1000) | Mutated Codon Frequency (/1000) |
|---|---|---|
| **T103A** | ACC = 19.2 | GCC = 28.5 |
| **G255E** | GGA = 18.6 | GAA = 29.0 |
| **I376D** | ATA = 7.1 | GAC = 26.0 |
| **D478A** | GAT = 22.3 | GCT = 18.6 |

**Table A.1. Codon Frequencies of MxA mutations producing atypical expression phenotypes.** The codon frequencies for each of the mutations were determined using the genscript online codon frequency usage for *Homo sapiens*. The codon frequencies are expressed as number of codons found per 1000 codons.

Interestingly, the I376D mutation has the largest difference in codon frequency from a rare codon encoding isoleucine with only 7 ATA codons per 1000 to a relatively frequent codon appearing 26 times per 1000 codons. This could have an impact on the rate of translation, however the distribution phenotype is not indicative of aggregation but a potentially aberrant localization that could be induced by the predicted change in RNA structure. Alternatively, this codon does infer a slight conformational change to the protein, which leads to large oligomeric structures being formed within the cytoplasm. The introduction of alanine at position 478 in place of aspartic acid is the only mutation that leads to a decrease in codon availability reducing the number available by approximately 4 per 1000 codons. Although this is a less drastic change this could also play a role in the phenotype described for D478A as slowing the rate of translation can also have an impact on the conformation of MxA leading to atypical localization.

**Discussion**

For the two mutants showing aggregated phenotypes, T103A and G255E, the nucleotide changes were predicted to take place on the end of hairpin loop structures (Fig. A.1), and therefore suggesting that these changes are unlikely to impact the overall structure of the mRNA, making it unlikely to be the cause of the aggregation. Whereas the mutations that introduced the I376D and D478A changes did appear to have an impact on the overall mRNA structure. Interestingly, mRNA coding regions have been suggested to be highly important for the localization of nascent RNA and therefore these changes in RNA secondary structure may lead to these proteins being trafficked to different cellular organelles, leading to the expression phenotypes observed here (Mortimer, Kidwell, and Doudna 2014).

However, although the nucleotide mutations for T103A and G255E may not have impacted overall RNA structure it is possible that these mutations could have had an impact on localised mRNA structure, as the structure is likely to change throughout translation while the mRNA is processed through the ribosome. The structures predicted by mFold suggest that this could be the case. The caveat of this analysis is that the predicted structures are determined based on the free energies of the RNA sequence being able to fold into it's most stable structure. This is unlike the cellular environment which is a highly packed with a number of RNA interacting factors such as other RNA molecules and mRNA binding proteins like NXF1 and CRM1, which could alter the overall structure of the mRNA (Delaleau and Borden 2015). In fact, a number of recent studies have attempted to determine the accuracy of *in vitro* RNA structure predictions in comparison to RNA structure within cells. Studies in plant, yeast and human cells have all suggested that the RNA folds present inside the cell are very different to those formed under artificial conditions (Ding et al. 2014; Rouskin et al. 2014). Therefore, suggesting that although this analysis can offer an insight as to the impact of nucleotide changes on RNA structure, it is should only be used as a starting point for future studies in a more relevant context.

Although these small changes in nucleotide sequence do not appear to have a huge impact on RNA structure, it is possible that these changes do impact the speed of translation through changes in codon frequency. The coding region is well documented to have an impact both on the localization of nascent RNA as well as the rate of translation (Mortimer, Kidwell, and Doudna 2014). Table A.1 shows the changes in codon frequency associated with each of the mutations. For the two

mutants that exhibit aggregated phenotypes and the I376D mutant, the codon frequency increases, which suggests that the rate of translation may change and impact the ability of the protein to fold correctly. This has been described for a number of different proteins, such as MDR1, where a synonymous mutation caused the protein to have increased affinities for different substrates due to a conformational change in the active site despite having the same primary amino acid sequence (Kimchi-Sarfaty et al. 2007). A more severe example is displayed in Cystic Fibrosis, where the CFTR gene misfolds due to a codon deletion at position 508, changing the rate of translation and causing the protein to be trafficked to the proteasome for degradation (Cheung and Deber 2008). However, to determine if codon frequency and subsequent tRNA availability is the cause of the aberrant protein folding in these MxA mutants, further work is required.

## Appendix B - Pulldown Raw Data

| Biological sample name | Protein name | Protein ident | Exclusive uni | % sequence coverage |
|---|---|---|---|---|
| Tap Control | Chain A, The Structure Of An Antitumor Ch2-Domain-Deleted Humanized Antibody | 100.00% | 2 | 54.10% |
| Tap Control | glutamyl-prolyl-tRNA synthetase, isoform CRA_a [Homo sapiens] | 96.60% | 1 | 0.53% |
| Tap Control | Chain H, Crystal Structure Of Anti-ngf Antibody Cnto7309 | 100.00% | 2 | 0.00% |
| Tap Control | RecName: Full=Ig heavy chain V-III region BUT | 100.00% | 2 | 35.70% |
| Tap Control | Unknown (protein for IMAGE:3544292), partial [Homo sapiens] | 99.10% | 1 | 5.37% |
| Tap Control | immunoglobulin kappa light chain variable region, partial [Homo sapiens] | 100.00% | 2 | 0.00% |
| Tap Control | Chain A, Crystal Structure Of The Novel Complex Formed Between Zinc 2-Glycoprotein (Zag) And Prolactin Inducible Protein (Pip) From Human Seminal Plasma | 99.90% | 1 | 3.60% |
| Tap Control | immunoglobulin lambda 1 light chain [Homo sapiens] | 99.10% | 1 | 37.00% |
| Tap Control | unnamed protein product [Homo sapiens] | 100.00% | 2 | 4.47% |
| Tap Control | immunoglobulin kappa light chain VLJ region [Homo sapiens] | 100.00% | 2 | 56.50% |
| Tap Control | keratin, type I cytoskeletal 13 isoform a [Homo sapiens] | 100.00% | 4 | 18.10% |
| Tap Control | Chain A, Human Serum Albumin Complexed With Myristate And Aspirin | 100.00% | 18 | 32.50% |
| Tap Control | immunoglobulin gamma heavy chain [Homo sapiens] | 100.00% | 2 | 30.20% |
| Tap Control | ATP synthase, H+ transporting, mitochondrial F1 complex, gamma polypeptide 1 [Homo sapiens] | 95.20% | 1 | 3.69% |
| Tap Control | ATP synthase subunit alpha, mitochondrial isoform a precursor [Homo sapiens] | 100.00% | 6 | 15.70% |
| Tap Control | keratin, type II cytoskeletal 2 epidermal [Homo sapiens] | 100.00% | 30 | 68.50% |
| Tap Control | SSA1 [Homo sapiens] | 100.00% | 5 | 10.90% |
| Tap Control | immunoglobulin light chain variable region, partial [Homo sapiens] | 100.00% | 2 | 0.00% |
| Tap Control | ADP/ATP translocase 3 [Homo sapiens] | 58.10% | 0 | 17.80% |
| Tap Control | ribosomal protein S4, X-linked, isoform CRA_a [Homo sapiens] | 94.90% | 1 | 3.38% |
| Tap Control | ribosomal protein S5, isoform CRA_b [Homo sapiens] | 99.10% | 1 | 7.50% |
| Tap Control | keratin, type I cuticular Ha1 [Homo sapiens] | 99.10% | 1 | 7.21% |
| Tap Control | unnamed protein product [Homo sapiens] | 100.00% | 9 | 41.50% |
| Tap Control | keratin 10 (epidermolytic hyperkeratosis; keratosis palmaris et plantaris), isoform CRA_b [Homo sapiens] | 100.00% | 35 | 58.30% |
| Tap Control | Chain A, Human Heart L-Lactate Dehydrogenase H Chain, Ternary Complex With Nadh And Oxamate | 99.10% | 1 | 3.60% |
| Tap Control | immunoglobulin heavy chain variable region [Homo sapiens] | 100.00% | 2 | 42.70% |
| Tap Control | coatomer subunit beta [Homo sapiens] | 99.10% | 1 | 1.15% |
| Tap Control | transmembrane protein 33 [Homo sapiens] | 98.80% | 1 | 4.86% |
| Tap Control | immunoglobin heavy chain [Homo sapiens] | 100.00% | 2 | 40.30% |
| Tap Control | protein S100-A7 [Homo sapiens] | 100.00% | 2 | 19.80% |
| Tap Control | Chain A, Semi-Extended Solution Structure Of Human Myeloma Immunoglobulin D Determined By Constrained X-Ray Scattering | 98.90% | 1 | 54.70% |
| Tap Control | unnamed protein product [Homo sapiens] | 99.10% | 1 | 5.19% |
| Tap Control | immunoglobulin heavy chain variable region [Homo sapiens] | 98.20% | 1 | 27.20% |
| Tap Control | immunoglobulin kappa light chain variable region [Homo sapiens] | 100.00% | 3 | 61.80% |
| Tap Control | monoclonal IgM antibody light chain [Homo sapiens] | 99.10% | 1 | 53.80% |
| Tap Control | coatomer subunit gamma-1 [Homo sapiens] | 99.10% | 1 | 1.95% |
| Tap Control | immunoglobulin gamma 2 heavy chain variable region [Homo sapiens] | 100.00% | 2 | 39.20% |
| Tap Control | unnamed protein product [Homo sapiens] | 100.00% | 4 | 42.10% |
| Tap Control | Chain A, Refined Solution Structure Of Human Cystatin A | 99.10% | 1 | 7.14% |

| | | | | |
|---|---|---|---|---|
| Tap Control | exportin-2 isoform 1 [Homo sapiens] | 100.00% | 10 | 17.00% |
| Tap Control | immunoglobulin light chain [Homo sapiens] | 100.00% | 2 | 54.50% |
| Tap Control | immunoglobulin A heavy chain variable region, partial [Homo sapiens] | 100.00% | 2 | 0.00% |
| Tap Control | immunoglobulin variable region [Homo sapiens] | 100.00% | 9 | 25.40% |
| Tap Control | tubulin beta-2B chain [Mus musculus] | 100.00% | 2 | 51.50% |
| Tap Control | Chain L, Crystal Structure Of Broadly Neutralizing Antibody Cr8020 Bound To The Influenza A H3 Hemagglutinin | 100.00% | 4 | 58.80% |
| Tap Control | polypyrimidine tract binding protein 1, isoform CRA_b [Homo sapiens] | 99.10% | 1 | 4.36% |
| Tap Control | immunoglobulin light chain variable region [Homo sapiens] | 100.00% | 2 | 52.10% |
| Tap Control | actin, beta, partial [Homo sapiens] | 100.00% | 6 | 18.50% |
| Tap Control | Keratin 14 [Homo sapiens] | 100.00% | 18 | 50.80% |
| Tap Control | immunoglobulin kappa chain variable region [Homo sapiens] | 100.00% | 1 | 27.90% |
| Tap Control | immunoglobulin kappa chain variable region [Homo sapiens] | 100.00% | 2 | 49.50% |
| Tap Control | exportin-1 [Homo sapiens] | 100.00% | 11 | 15.20% |
| Tap Control | RAN binding protein 5, isoform CRA_b [Homo sapiens] | 100.00% | 1 | 1.79% |
| Tap Control | elongation factor 1-alpha 1 [Homo sapiens] | 100.00% | 9 | 31.00% |
| Tap Control | Ig lambda chain - human | 100.00% | 2 | 51.50% |
| Tap Control | immunoglobulin kappa heavy chain [Homo sapiens] | 100.00% | 2 | 51.00% |
| Tap Control | IGH@ protein [Homo sapiens] | 100.00% | 3 | 52.50% |
| Tap Control | immunoglobulin kappa light chain VLJ region [Homo sapiens] | 100.00% | 3 | 40.60% |
| Tap Control | unnamed protein product [Homo sapiens] | 100.00% | 8 | 40.90% |
| Tap Control | Chain L, Crystal Structure Of Ectodomain 3 Of The Il-13 Receptor Alpha1 In Complex With A Human Neutralizing Monoclonal Antibody Fragment | 100.00% | 2 | 0.00% |
| Tap Control | keratin 1 [Homo sapiens] | 100.00% | 42 | 65.50% |
| Tap Control | lupus La protein [Homo sapiens] | 100.00% | 5 | 14.50% |
| Tap Control | Chain B, Crystal Structure Of The Human Notch1 Negative Regulatory Re Bound To The Fab Fragment Of An Antagonist Antibody | 99.10% | 1 | 24.70% |
| Tap Control | immunoglobulin A heavy chain variable region, partial [Homo sapiens] | 99.10% | 1 | 0.00% |
| Tap Control | ribosomal protein S7, isoform CRA_a [Homo sapiens] | 99.90% | 1 | 12.90% |
| Tap Control | RuvB-like 1 [Homo sapiens] | 100.00% | 4 | 13.80% |
| Tap Control | immunoglobulin kappa light chain VLJ region [Homo sapiens] | 100.00% | 2 | 43.50% |
| Tap Control | epididymis luminal protein 214 [Homo sapiens] | 100.00% | 7 | 0.00% |
| Tap Control | Chain C, Solution Structure Of Human Immunoglobulin M | 100.00% | 7 | 45.10% |
| Tap Control | Chain H, Mechanisms Of Neutralization Of A Human Anti-alpha Toxin Antibody | 100.00% | 2 | 0.00% |
| Tap Control | Chain L, Her3 Extracellular Domain In Complex With Fab Fragment Of Mor09825 | 100.00% | 2 | 0.00% |
| Tap Control | anti-SARS-CoV S protein immunoglobulin kappa light chain [Homo sapiens] | 100.00% | 2 | 62.10% |
| Tap Control | Chain C, Crystal Structure Of Mj5 Fab, A Germline Antibody Variant Of Anti-Human Cytomegalovirus Antibody 8f9 | 100.00% | 4 | 80.10% |
| Tap Control | Chain B, Crystal Structure Of The Novel Complex Formed Between Zinc 2-Glycoprotein (Zag) And Prolactin Inducible Protein (Pip) From Human Seminal Plasma | 100.00% | 3 | 35.60% |
| Tap Control | Ig lambda chain - human (fragment) | 99.90% | 1 | 46.50% |
| Tap Control | Chain H, Crystal Structure Of Rv144-elicited Antibody Ch59 In Complex With V2 Peptide | 100.00% | 2 | 0.00% |
| Tap Control | Chain A, Hepcidin-Fab Complex | 100.00% | 3 | 64.40% |
| Tap Control | nucleophosmin isoform 1 [Homo sapiens] | 99.10% | 1 | 3.06% |
| Tap Control | immunoglobulin variable region [Homo sapiens] | 100.00% | 3 | 9.49% |

| | | | | |
|---|---|---|---|---|
| Tap Control | immunoglobulin heavy-chain subgroup VIII V-D-J region, partial [Homo sapiens] | 100.00% | 2 | 33.30% |
| Tap Control | immunoglobulin heavy chain variable region [Homo sapiens] | 100.00% | 2 | 48.70% |
| Tap Control | immunoglobulin kappa light chain variable region [Homo sapiens] | 100.00% | 2 | 44.40% |
| Tap Control | B cell antibody heavy chain variable region [Homo sapiens] | 99.10% | 1 | 9.32% |
| Tap Control | immunoglobulin kappa light chain [Homo sapiens] | 100.00% | 2 | 42.70% |
| Tap Control | anti-tetanus toxoid immunoglobulin light chain variable region [Homo sapiens] | 100.00% | 3 | 59.80% |
| Tap Control | Chain L, Crystal Structure Of Hiv-1 Neutralizing Antibody Ch04 | 100.00% | 3 | 61.40% |
| Tap Control | immunoglobulin lambda light chain VLJ region [Homo sapiens] | 100.00% | 2 | 54.80% |
| Tap Control | unnamed protein product [Homo sapiens] | 100.00% | 4 | 7.14% |
| Tap Control | hCG2016250, isoform CRA_c [Homo sapiens] | 100.00% | 2 | 8.86% |
| Tap Control | ATP-dependent RNA helicase A [Homo sapiens] | 99.10% | 1 | 0.95% |
| Tap Control | immunoglobulin G heavy chain variable region [Homo sapiens] | 100.00% | 2 | 26.00% |
| Tap Control | Chain A, Crystal Structure Of The Broadly Hiv-1 Neutralizing Fab X5 At 1.90 Angstrom Resolution | 100.00% | 2 | 49.30% |
| Tap Control | immunoglobulin heavy chain [Homo sapiens] | 100.00% | 2 | 43.20% |
| Tap Control | tubulin alpha-1B chain [Mus musculus] | 100.00% | 21 | 66.50% |
| Tap Control | This CDS feature is included to show the translation of the corresponding V_region. Presently translation qualifiers on V_region features are illegal, partial [Homo sapiens] | 100.00% | 2 | 32.30% |
| Tap Control | Tubulin, beta 2C [Homo sapiens] | 100.00% | 5 | 70.10% |
| Tap Control | heat shock 70 kDa protein 1A/1B [Homo sapiens] | 100.00% | 19 | 46.60% |
| Tap Control | heterogeneous nuclear ribonucleoprotein H1 (H), isoform CRA_b [Homo sapiens] | 92.70% | 1 | 4.07% |
| Tap Control | Chain A, Unusual Twinning In Crystals Of The Cits Binding Antibody Fab Fragment F3p4 | 100.00% | 2 | 65.60% |
| Tap Control | Keratin, hair, basic, 1 [Homo sapiens] | 99.10% | 1 | 3.76% |
| Tap Control | ribosomal protein S18, isoform CRA_c [Homo sapiens] | 99.70% | 1 | 6.25% |
| Tap Control | unnamed protein product [Homo sapiens] | 100.00% | 7 | 42.10% |
| Tap Control | PREDICTED: ruvB-like 2 isoform X1 [Homo sapiens] | 98.60% | 1 | 0.00% |
| Tap Control | Chain L, Crystal Structure Of Fab Dx-2930 In Complex With Human Plasma Kallikrein At 2.4 Angstrom Resolution | 100.00% | 4 | 0.00% |
| Tap Control | immunoglobulin light chain [Homo sapiens] | 98.10% | 1 | 51.90% |
| Tap Control | immunoglobulin variable region VL kappa domain [Homo sapiens] | 100.00% | 2 | 39.40% |
| Tap Control | IGL@ protein [Homo sapiens] | 98.40% | 1 | 43.80% |
| Tap Control | immunoglobulin VH_3c kappa chain [Homo sapiens] | 100.00% | 1 | 35.50% |
| Tap Control | immunoglobulin A heavy chain variable region, partial [Homo sapiens] | 100.00% | 2 | 0.00% |
| Tap Control | immunoglobulin heavy chain variable region [Homo sapiens] | 100.00% | 2 | 41.00% |
| Tap Control | D-3-phosphoglycerate dehydrogenase [Homo sapiens] | 100.00% | 10 | 23.80% |
| Tap Control | isoleucine-tRNA synthetase, isoform CRA_b [Homo sapiens] | 98.70% | 1 | 0.63% |
| Tap Control | immunoglobulin variable region [Homo sapiens] | 100.00% | 2 | 22.00% |
| Tap Control | HRV Fab 025-VL [Homo sapiens] | 100.00% | 2 | 55.80% |
| Tap Control | immunoglobulin kappa light chain variable region, partial [Homo sapiens] | 100.00% | 3 | 0.00% |
| Tap Control | immunoglobulin heavy chain variable region [Homo sapiens] | 100.00% | 2 | 44.20% |
| Tap Control | JUP protein [Homo sapiens] | 100.00% | 2 | 5.10% |
| Tap Control | immunoglobulin kappa chain variable region [Homo sapiens] | 100.00% | 3 | 25.30% |
| Tap Control | immunoglobulin kappa chain variable region [Homo sapiens] | 100.00% | 2 | 29.50% |

| | | | | |
|---|---|---|---|---|
| Tap Control | Chain L, Crystal Structure Of The Therapeutical Antibody Fragment Of Canakinumab In Its Unbound State | 100.00% | 4 | 0.00% |
| Tap Control | immunoglobulin G heavy chain variable region, partial [Homo sapiens] | 100.00% | 2 | 0.00% |
| Tap Control | 60S ribosomal protein L13 isoform 1 [Homo sapiens] | 99.10% | 1 | 5.21% |
| Tap Control | immunoglobulin variable region [Homo sapiens] | 99.10% | 1 | 58.70% |
| Tap Control | unnamed protein product [Homo sapiens] | 97.40% | 1 | 2.04% |
| Tap Control | immunoglobulin lambda 1 light chain [Homo sapiens] | 100.00% | 2 | 47.50% |
| Tap Control | anti-tetanus toxoid immunoglobulin light chain variable region [Homo sapiens] | 100.00% | 2 | 84.30% |
| Tap Control | CLTC protein [Homo sapiens] | 97.10% | 0 | 0.00% |
| Tap Control | dermcidin preproprotein [Homo sapiens] | 99.10% | 1 | 10.00% |
| Tap Control | desmoglein-1 preproprotein [Homo sapiens] | 100.00% | 3 | 4.39% |
| Tap Control | squamous cell carcinoma antigen-1 isoform SCCA-PD [Homo sapiens] | 100.00% | 3 | 7.95% |
| Tap Control | immunoglobulin heavy chain variable region [Homo sapiens] | 99.10% | 1 | 39.80% |
| Tap Control | immunoglobulin light chain [Homo sapiens] | 100.00% | 2 | 86.50% |
| Tap Control | PREDICTED: keratin, type II cytoskeletal 6A [Pan troglodytes] | 100.00% | 17 | 51.60% |
| Tap Control | Chain A, Crystal Structure Of Abt-007 Fab Fragment With The Soluble Domain Of Epo Receptor | 100.00% | 3 | 57.50% |
| Tap Control | 78 kDa glucose-regulated protein precursor [Homo sapiens] | 99.90% | 1 | 3.52% |
| Tap Control | Chain K, Crystal Structure Of Fab 2g1 In Complex With A H2n2 Influenza Virus Hemagglutinin | 100.00% | 2 | 0.00% |
| Tap Control | immunoglobulin lambda light chain variable region, partial [Homo sapiens] | 100.00% | 2 | 22.60% |
| Tap Control | anti-HIV-1 immunoglobulin cap256-048-050815 chain variable region, partial [Homo sapiens] | 100.00% | 2 | 0.00% |
| Tap Control | calcium-binding mitochondrial carrier protein Aralar2 isoform 1 [Homo sapiens] | 84.00% | 1 | 2.51% |
| Tap Control | immunoglobulin lambda-1 variable region [Homo sapiens] | 100.00% | 2 | 26.60% |
| Tap Control | Chain A, Human Pyruvate Dehydrogenase S264e Variant | 100.00% | 2 | 6.30% |
| Tap Control | immunoglobulin variable region [Homo sapiens] | 100.00% | 2 | 44.30% |
| Tap Control | RecName: Full=Ig kappa chain V-I region CAR | 100.00% | 2 | 31.80% |
| Tap Control | OMM protein (Ig gamma3) heavy chain [Homo sapiens] | 99.90% | 2 | 38.00% |
| Tap Control | Keratin 77 [Homo sapiens] | 62.10% | 0 | 4.67% |
| Tap Control | unnamed protein product [Homo sapiens] | 100.00% | 3 | 3.91% |
| Tap Control | Chain L, Crystal Structure Of Recombinant A.17 Antibody Fab Fragment | 100.00% | 4 | 64.80% |
| Tap Control | ADP/ATP translocase 2 [Macaca mulatta] | 100.00% | 6 | 22.10% |
| Tap Control | Similar to ribosomal protein L23, partial [Homo sapiens] | 100.00% | 2 | 26.10% |
| Tap Control | 40S ribosomal protein S14 [Homo sapiens] | 99.10% | 1 | 7.28% |
| Tap Control | Chain B, Crystal Structures Of Native And Inhibited Forms Of Human Cathepsin D: Implications For Lysosomal Targeting And Drug Design | 99.10% | 1 | 0.00% |
| Tap Control | Ig G1 H Nie | 100.00% | 4 | 44.00% |
| Tap Control | hypothetical protein [Homo sapiens] | 100.00% | 2 | 53.60% |
| Tap Control | unnamed protein product [Homo sapiens] | 100.00% | 2 | 48.70% |
| Tap Control | immunoglobulin kappa chain variable region [Homo sapiens] | 100.00% | 2 | 43.00% |
| Tap Control | tubulin alpha-1A chain isoform 2 [Homo sapiens] | 98.70% | 1 | 68.80% |
| Tap Control | keratin, type II cytoskeletal 5 [Homo sapiens] | 100.00% | 24 | 49.00% |
| Tap Control | immunoglobulin heavy chain, partial [Homo sapiens] | 100.00% | 20 | 0.00% |
| Tap Control | immunoglobulin lambda light chain VLJ region [Homo sapiens] | 100.00% | 2 | 32.00% |

| | | | | |
|---|---|---|---|---|
| Tap Control | immunoglobulin kappa light chain variable region [Homo sapiens] | 100.00% | 2 | 32.40% |
| Tap Control | type I keratin 16 [Homo sapiens] | 100.00% | 10 | 54.50% |
| Tap Control | unnamed protein product [Homo sapiens] | 100.00% | 3 | 49.80% |
| Tap Control | immunoglobulin kappa light chain variable region [Homo sapiens] | 100.00% | 2 | 44.70% |
| Tap Control | immunoglobulin light chain variable region, partial [Homo sapiens] | 100.00% | 2 | 0.00% |
| Tap Control | Chain H, Cryo-em Structure Of Dengue Virus Serotype 1 Complexed With Fab Fragments Of Human Antibody 1f4 | 99.10% | 1 | 0.00% |
| Tap Control | exportin 5, isoform CRA_a [Homo sapiens] | 99.10% | 1 | 0.83% |
| Tap Control | glyceraldehyde-3-phosphate dehydrogenase, isoform CRA_a [Homo sapiens] | 99.90% | 1 | 2.44% |
| Tap Control | keratin, type I cytoskeletal 9 [Homo sapiens] | 100.00% | 30 | 74.20% |
| Tap Control | Chain L, Crystal Structure Of Broadly And Potently Neutralizing Antibody Vrc- Ch31 In Complex With Hiv-1 Clade A/e Gp120 93th057 With Loop D And Loop V5 From Clade A Strain 3415_v1_c1 | 100.00% | 2 | 0.00% |
| Tap Control | IgG L chain [Homo sapiens] | 100.00% | 2 | 0.00% |
| Tap Control | immunoglobulin variable region [Homo sapiens] | 100.00% | 1 | 36.30% |
| Tap Control | anti-tetanus toxoid immunoglobulin light chain variable region [Homo sapiens] | 100.00% | 2 | 84.30% |
| Tap Control | unnamed protein product [Homo sapiens] | 100.00% | 2 | 36.40% |
| Tap Control | Ig A1 Bur | 100.00% | 3 | 7.87% |
| Tap Control | anti-tetanus toxoid immunoglobulin light chain variable region [Homo sapiens] | 100.00% | 2 | 27.10% |
| Tap Control | heat shock protein beta-1 [Homo sapiens] | 99.10% | 1 | 7.80% |
| Tap Control | Chain A, Crystal Structure Of Human Lnkh2b-h2a.z-anp32e | 99.10% | 1 | 0.00% |
| Tap Control | 60 kDa SS-A/Ro ribonucleoprotein isoform 1 [Homo sapiens] | 100.00% | 9 | 19.00% |
| Tap Control | Chain H, Crystal Structure Of Hiv-Gp120 Core In Complex With Cd4-Binding Site Antibody B13, Space Group C222 | 100.00% | 2 | 29.40% |
| Tap Control | immunoglobulin light chain variable region kappa, partial [Homo sapiens] | 100.00% | 2 | 0.00% |
| Tap Control | protein kinase, DNA-activated, catalytic polypeptide, isoform CRA_c [Homo sapiens] | 38.70% | 0 | 0.00% |
| Tap Control | immunoglobulin light chain variable region, partial [Homo sapiens] | 100.00% | 1 | 0.00% |
| Tap Control | immunoglobulin light chain kappa, partial [Homo sapiens] | 100.00% | 2 | 0.00% |
| Tap Control | leucine--tRNA ligase, cytoplasmic [Homo sapiens] | 99.80% | 1 | 1.02% |
| Tap Control | immunoglobulin G heavy chain variable region, partial [Homo sapiens] | 100.00% | 2 | 0.00% |
| Tap Control | unnamed protein product [Homo sapiens] | 100.00% | 5 | 33.30% |
| Tap Control | protein Len,Bence-Jones | 100.00% | 7 | 57.30% |
| Tap Control | protein Rei,Bence-Jones | 100.00% | 4 | 42.10% |
| Tap Control | Ribosomal protein, large, P0 [Homo sapiens] | 100.00% | 1 | 9.78% |
| Tap Control | immunoglobulin kappa chain variable region [Homo sapiens] | 100.00% | 2 | 31.20% |
| Tap Control | transferrin receptor (p90, CD71), isoform CRA_b [Homo sapiens] | 100.00% | 4 | 5.97% |
| Tap Control | tubulin beta-5 chain [Mus musculus] | 100.00% | 20 | 70.30% |
| Tap Control | heat shock cognate 71 kDa protein isoform 1 [Homo sapiens] | 100.00% | 11 | 26.90% |
| Tap Control | dnaJ homolog subfamily A member 2 [Homo sapiens] | 100.00% | 2 | 5.58% |
| Tap Control | Chain C, An Antibody Against The C-terminal Domain Of Pcsk9 Lowers Ldl Cholesterol Levels In Vivo | 100.00% | 2 | 0.00% |
| Tap Control | IgG kappa chain [Homo sapiens] | 100.00% | 4 | 76.60% |
| Tap Control | unnamed protein product [Homo sapiens] | 100.00% | 3 | 34.10% |
| Tap Control | Chain A, Crystal Structure Of Human Ed-4f2hc | 99.10% | 1 | 2.83% |
| Tap Control | protein S100-A8 [Homo sapiens] | 100.00% | 3 | 28.00% |

| | | | | |
|---|---|---|---|---|
| Tap Control | immunoglobulin kappa light chain variable region [Homo sapiens] | 100.00% | 2 | 38.90% |
| Tap Control | hCG1984476, isoform CRA_b [Homo sapiens] | 100.00% | 2 | 15.30% |
| Tap Control | Heat shock 70kDa protein 9 (mortalin) [Homo sapiens] | 100.00% | 2 | 3.39% |
| Tap Control | hCG19195 [Homo sapiens] | 97.40% | 1 | 9.64% |
| Tap Control | Chain C, Crystal Structure Of Mt-Sp1 In Complex With Fab Inhibitor E2 | 100.00% | 3 | 68.70% |
| Tap Control | Chain H, Crystal Structure Of Human Germline Antibody 5-51/o12 | 100.00% | 3 | 0.00% |
| Tap Control | keratin 4 [Homo sapiens] | 99.10% | 1 | 6.41% |
| Tap Control | anti-HBsAg immunoglobulin Fab kappa chain [Homo sapiens] | 100.00% | 3 | 64.00% |
| Tap Control | Chain L, Crystal Structure Of A Chimeric Fab' Fragment Of An Antibody Binding Tumour Cells | 100.00% | 2 | 43.60% |
| wt MxA | glutamyl-prolyl-tRNA synthetase, isoform CRA_a [Homo sapiens] | 100.00% | 6 | 6.35% |
| wt MxA | Chain H, Crystal Structure Of Anti-ngf Antibody Cnto7309 | 98.10% | 1 | 0.00% |
| wt MxA | Translocase of inner mitochondrial membrane 50 homolog (S. cerevisiae) [Homo sapiens] | 99.90% | 1 | 2.19% |
| wt MxA | arginyl-tRNA synthetase [Homo sapiens] | 100.00% | 2 | 3.48% |
| wt MxA | Unknown (protein for IMAGE:3544292), partial [Homo sapiens] | 100.00% | 9 | 44.60% |
| wt MxA | Chain A, Crystal Structure Of The Novel Complex Formed Between Zinc 2-Glycoprotein (Zag) And Prolactin Inducible Protein (Pip) From Human Seminal Plasma | 100.00% | 2 | 8.63% |
| wt MxA | unnamed protein product [Homo sapiens] | 100.00% | 3 | 5.19% |
| wt MxA | immunoglobulin kappa light chain VLJ region [Homo sapiens] | 63.70% | 0 | 16.70% |
| wt MxA | keratin, type I cytoskeletal 13 isoform a [Homo sapiens] | 100.00% | 5 | 19.20% |
| wt MxA | HNRPF protein [Homo sapiens] | 100.00% | 1 | 4.10% |
| wt MxA | Chain A, Human Serum Albumin Complexed With Myristate And Aspirin | 100.00% | 18 | 31.30% |
| wt MxA | ATP synthase, H+ transporting, mitochondrial F1 complex, gamma polypeptide 1 [Homo sapiens] | 100.00% | 4 | 15.10% |
| wt MxA | ATP synthase subunit alpha, mitochondrial isoform a precursor [Homo sapiens] | 100.00% | 13 | 31.30% |
| wt MxA | keratin, type II cytoskeletal 2 epidermal [Homo sapiens] | 100.00% | 31 | 65.70% |
| wt MxA | actinin, alpha 4, isoform CRA_c [Homo sapiens] | 99.80% | 2 | 2.43% |
| wt MxA | Heterogeneous nuclear ribonucleoprotein A1 [Homo sapiens] | 100.00% | 2 | 9.69% |
| wt MxA | immunoglobulin light chain variable region, partial [Homo sapiens] | 98.10% | 1 | 0.00% |
| wt MxA | ADP/ATP translocase 3 [Homo sapiens] | 100.00% | 2 | 46.00% |
| wt MxA | ribosomal protein S5, isoform CRA_b [Homo sapiens] | 100.00% | 2 | 14.00% |
| wt MxA | apoptosis-inducing factor 1, mitochondrial isoform 2 precursor [Homo sapiens] | 100.00% | 11 | 23.30% |
| wt MxA | keratin, type I cuticular Ha1 [Homo sapiens] | 100.00% | 2 | 6.25% |
| wt MxA | unnamed protein product [Homo sapiens] | 100.00% | 13 | 54.50% |
| wt MxA | unnamed protein product [Homo sapiens] | 100.00% | 2 | 4.56% |
| wt MxA | DEAH (Asp-Glu-Ala-His) box polypeptide 15, isoform CRA_d [Homo sapiens] | 100.00% | 2 | 3.69% |
| wt MxA | heat shock 70 kDa protein 1A/1B [Homo sapiens] | 100.00% | 34 | 64.00% |
| wt MxA | exportin 7, isoform CRA_a [Homo sapiens] | 100.00% | 2 | 2.21% |
| wt MxA | Chain A, Human Heart L-Lactate Dehydrogenase H Chain, Ternary Complex With Nadh And Oxamate | 100.00% | 3 | 8.71% |
| wt MxA | immunoglobulin heavy chain variable region [Homo sapiens] | 98.10% | 1 | 24.80% |
| wt MxA | unnamed protein product [Homo sapiens] | 100.00% | 2 | 3.90% |
| wt MxA | IGL@ protein [Homo sapiens] | 80.40% | 1 | 36.20% |
| wt MxA | coatomer subunit beta [Homo sapiens] | 100.00% | 22 | 31.50% |

| | | | | |
|---|---|---|---|---|
| wt MxA | transmembrane protein 33 [Homo sapiens] | 100.00% | 2 | 8.91% |
| wt MxA | immunoglobin heavy chain [Homo sapiens] | 98.10% | 1 | 24.20% |
| wt MxA | protein S100-A7 [Homo sapiens] | 100.00% | 3 | 33.70% |
| wt MxA | N-ethylmaleimide-sensitive factor [Homo sapiens] | 100.00% | 2 | 2.96% |
| wt MxA | unnamed protein product [Homo sapiens] | 100.00% | 9 | 21.30% |
| wt MxA | PREDICTED: ADP-ribosylation factor-like protein 1-like isoform 2 [Nomascus leucogenys] | 100.00% | 5 | 30.50% |
| wt MxA | anti-HBsAg immunoglobulin Fab kappa chain [Homo sapiens] | 100.00% | 1 | 48.60% |
| wt MxA | coatomer subunit gamma-1 [Homo sapiens] | 100.00% | 11 | 16.50% |
| wt MxA | unnamed protein product [Homo sapiens] | 100.00% | 4 | 42.10% |
| wt MxA | ADP-ribosylation factor 4 [Homo sapiens] | 100.00% | 4 | 23.90% |
| wt MxA | Chain A, Refined Solution Structure Of Human Cystatin A | 100.00% | 3 | 40.80% |
| wt MxA | immunoglobulin variable region [Homo sapiens] | 75.00% | 1 | 25.40% |
| wt MxA | heat shock protein HSP 90-alpha isoform 1 [Homo sapiens] | 100.00% | 13 | 34.70% |
| wt MxA | polyubiquitin [Homo sapiens] | 100.00% | 3 | 5.58% |
| wt MxA | heterogeneous nuclear ribonucleoproteins C1/C2 isoform a [Homo sapiens] | 99.90% | 1 | 2.94% |
| wt MxA | Ig heavy chain VH3 region [Homo sapiens] | 98.10% | 1 | 25.00% |
| wt MxA | unnamed protein product [Homo sapiens] | 100.00% | 2 | 4.55% |
| wt MxA | Eukaryotic translation elongation factor 1 gamma [Homo sapiens] | 100.00% | 5 | 12.60% |
| wt MxA | coatomer subunit delta isoform 1 [Homo sapiens] | 100.00% | 3 | 6.46% |
| wt MxA | unnamed protein product [Homo sapiens] | 100.00% | 9 | 16.10% |
| wt MxA | Chain B, Three Dimensional Structure Of Broadly Neutralizing Human Anti - Hepatitis C Virus (hcv) Glycoprotein E2 Fab Fragment Hc84-1 | 98.10% | 1 | 0.00% |
| wt MxA | pyrroline-5-carboxylate reductase-like, isoform CRA_b [Homo sapiens] | 100.00% | 3 | 15.00% |
| wt MxA | KIAA1794, isoform CRA_c [Homo sapiens] | 100.00% | 6 | 5.79% |
| wt MxA | ATPase, Ca++ transporting, cardiac muscle, slow twitch 2, isoform CRA_a [Homo sapiens] | 100.00% | 4 | 5.45% |
| wt MxA | dihydrolipoamide S-acetyltransferase (E2 component of pyruvate dehydrogenase complex), isoform CRA_a [Homo sapiens] | 100.00% | 7 | 16.20% |
| wt MxA | Similar to ribophorin I, partial [Homo sapiens] | 100.00% | 11 | 23.60% |
| wt MxA | ATPase family, AAA domain containing 3A, isoform CRA_c [Homo sapiens] | 100.00% | 7 | 10.80% |
| wt MxA | hypothetical protein [Homo sapiens] | 98.10% | 1 | 40.40% |
| wt MxA | heterogeneous nuclear ribonucleoprotein U (scaffold attachment factor A), isoform CRA_b [Homo sapiens] | 100.00% | 2 | 3.96% |
| wt MxA | SSA1 [Homo sapiens] | 100.00% | 10 | 24.20% |
| wt MxA | hCG33299, isoform CRA_a [Homo sapiens] | 100.00% | 3 | 15.20% |
| wt MxA | anti-rabies SOJA immunoglobulin heavy chain [Homo sapiens] | 98.10% | 1 | 45.40% |
| wt MxA | Chain A, Human Factor Viii C2 Domain Complexed To Human Monoclonal Bo2c11 Fab | 94.70% | 1 | 52.60% |
| wt MxA | mitochondrial heat shock 60kD protein 1 variant 1 [Homo sapiens] | 100.00% | 8 | 19.90% |
| wt MxA | Ribosomal protein, large, P0 [Homo sapiens] | 100.00% | 6 | 26.50% |
| wt MxA | unnamed protein product [Homo sapiens] | 100.00% | 5 | 33.10% |
| wt MxA | RecName: Full=Elongation factor Tu, mitochondrial; Short=EF-Tu; AltName: Full=P43; Flags: Precursor | 100.00% | 12 | 34.50% |
| wt MxA | immunoglobulin variable region [Homo sapiens] | 27.50% | 0 | 24.80% |
| wt MxA | immunoglobulin light chain [Homo sapiens] | 100.00% | 9 | 52.60% |
| wt MxA | NADH dehydrogenase [ubiquinone] iron-sulfur protein 3, mitochondrial precursor [Homo sapiens] | 100.00% | 2 | 9.09% |

| | | | | |
|---|---|---|---|---|
| wt MxA | Chain A, Crystal Structure Of Human Nmprtase As Free-Form | 100.00% | 2 | 8.02% |
| wt MxA | immunoglobulin G heavy chain variable region, partial [Homo sapiens] | 98.10% | 1 | 0.00% |
| wt MxA | ENO1 protein, partial [Homo sapiens] | 100.00% | 2 | 8.09% |
| wt MxA | unnamed protein product [Homo sapiens] | 100.00% | 14 | 18.20% |
| wt MxA | Chain L, Crystal Structure Of The Anti-human Ngf Fab Ape1531 | 100.00% | 2 | 0.00% |
| wt MxA | interferon-induced Mx protein [Homo sapiens] | 100.00% | 52 | 82.20% |
| wt MxA | immunoglobulin light chain [Homo sapiens] | 100.00% | 2 | 56.20% |
| wt MxA | aldehyde dehydrogenase 3 family, member A2, isoform CRA_c [Homo sapiens] | 100.00% | 2 | 8.56% |
| wt MxA | t-complex 1, isoform CRA_b [Homo sapiens] | 100.00% | 2 | 10.20% |
| wt MxA | serpin B12 [Homo sapiens] | 100.00% | 2 | 5.93% |
| wt MxA | interleukin enhancer-binding factor 2 [Mus musculus] | 100.00% | 5 | 18.50% |
| wt MxA | exportin-2 isoform 1 [Homo sapiens] | 100.00% | 18 | 24.90% |
| wt MxA | immunoglobulin A heavy chain variable region, partial [Homo sapiens] | 98.10% | 1 | 0.00% |
| wt MxA | desmoglein-1 preproprotein [Homo sapiens] | 100.00% | 2 | 2.86% |
| wt MxA | YWHAE/FAM22A fusion protein, partial [Homo sapiens] | 100.00% | 3 | 9.64% |
| wt MxA | immunoglobulin variable region [Homo sapiens] | 98.10% | 1 | 24.60% |
| wt MxA | pachytene checkpoint protein 2 homolog isoform 1 [Homo sapiens] | 95.10% | 1 | 2.31% |
| wt MxA | tubulin beta-2B chain [Mus musculus] | 100.00% | 4 | 62.90% |
| wt MxA | polypyrimidine tract binding protein 1, isoform CRA_b [Homo sapiens] | 100.00% | 2 | 5.31% |
| wt MxA | unnamed protein product [Homo sapiens] | 100.00% | 3 | 5.12% |
| wt MxA | general transcription factor II-I isoform 1 [Homo sapiens] | 100.00% | 4 | 5.71% |
| wt MxA | unnamed protein product [Homo sapiens] | 100.00% | 2 | 4.49% |
| wt MxA | actin, beta, partial [Homo sapiens] | 100.00% | 10 | 39.70% |
| wt MxA | pancreatic adenocarcinoma upregulated factor [Homo sapiens] | 100.00% | 2 | 9.69% |
| wt MxA | Keratin 14 [Homo sapiens] | 100.00% | 23 | 60.80% |
| wt MxA | X-ray repair cross-complementing protein 5 [Homo sapiens] | 100.00% | 5 | 12.00% |
| wt MxA | exportin-1 [Homo sapiens] | 100.00% | 26 | 32.90% |
| wt MxA | RAN binding protein 5, isoform CRA_b [Homo sapiens] | 100.00% | 2 | 2.87% |
| wt MxA | elongation factor 1-alpha 1 [Homo sapiens] | 100.00% | 15 | 50.60% |
| wt MxA | coatomer protein complex, subunit alpha, isoform CRA_b [Homo sapiens] | 100.00% | 4 | 3.72% |
| wt MxA | eukaryotic translation initiation factor 4 gamma, 1, isoform CRA_c [Homo sapiens] | 100.00% | 2 | 1.31% |
| wt MxA | IGH@ protein [Homo sapiens] | 100.00% | 2 | 47.30% |
| wt MxA | chaperonin containing TCP1, subunit 4 (delta), isoform CRA_a [Homo sapiens] | 99.90% | 2 | 3.30% |
| wt MxA | keratin 1 [Homo sapiens] | 100.00% | 42 | 52.30% |
| wt MxA | importin 4, isoform CRA_d [Homo sapiens] | 100.00% | 4 | 4.89% |
| wt MxA | lupus La protein [Homo sapiens] | 100.00% | 12 | 32.10% |
| wt MxA | Chain B, Crystal Structure Of The Human Notch1 Negative Regulatory Re Bound To The Fab Fragment Of An Antagonist Antibody | 98.10% | 1 | 24.70% |
| wt MxA | immunoglobulin A heavy chain variable region, partial [Homo sapiens] | 98.10% | 1 | 0.00% |
| wt MxA | tripartite motif-containing 28, isoform CRA_a [Homo sapiens] | 100.00% | 2 | 2.57% |
| wt MxA | RuvB-like 1 [Homo sapiens] | 100.00% | 13 | 39.90% |

| | | | | |
|---|---|---|---|---|
| wt MxA | unnamed protein product [Homo sapiens] | 100.00% | 2 | 7.24% |
| wt MxA | ubiquitin-protein ligase E3C [Homo sapiens] | 100.00% | 2 | 1.75% |
| wt MxA | immunoglobulin kappa light chain VLJ region [Homo sapiens] | 63.70% | 0 | 32.00% |
| wt MxA | epididymis luminal protein 214 [Homo sapiens] | 100.00% | 5 | 0.00% |
| wt MxA | Chain C, Solution Structure Of Human Immunoglobulin M | 100.00% | 5 | 39.40% |
| wt MxA | Chain H, Mechanisms Of Neutralization Of A Human Anti-alpha Toxin Antibody | 98.10% | 1 | 0.00% |
| wt MxA | Chain B, Crystal Structure Of The Novel Complex Formed Between Zinc 2-Glycoprotein (Zag) And Prolactin Inducible Protein (Pip) From Human Seminal Plasma | 100.00% | 6 | 68.60% |
| wt MxA | dnaJ homolog subfamily A member 2 [Homo sapiens] | 100.00% | 6 | 20.90% |
| wt MxA | Chain A, Human Mutsalpha (Msh2MSH6) BOUND TO A G T MISPAIR, WITH Adp Bound To Msh2 Only | 100.00% | 3 | 3.64% |
| wt MxA | Chain A, Hepcidin-Fab Complex | 94.40% | 1 | 44.00% |
| wt MxA | heat shock 105kDa/110kDa protein 1, isoform CRA_d [Homo sapiens] | 100.00% | 3 | 6.85% |
| wt MxA | nucleophosmin isoform 1 [Homo sapiens] | 100.00% | 2 | 10.20% |
| wt MxA | Chain C, Crystal Structure Of Mt-Sp1 In Complex With Fab Inhibitor E2 | 98.10% | 1 | 47.70% |
| wt MxA | immunoglobulin kappa light chain [Homo sapiens] | 98.10% | 1 | 42.70% |
| wt MxA | calcium-binding mitochondrial carrier protein Aralar2 isoform 1 [Homo sapiens] | 100.00% | 6 | 12.70% |
| wt MxA | unnamed protein product [Homo sapiens] | 100.00% | 32 | 50.10% |
| wt MxA | hCG2016250, isoform CRA_c [Homo sapiens] | 100.00% | 3 | 15.10% |
| wt MxA | ATP-dependent RNA helicase A [Homo sapiens] | 100.00% | 2 | 1.73% |
| wt MxA | prohibitin 2 [Homo sapiens] | 100.00% | 3 | 14.20% |
| wt MxA | tubulin alpha-1B chain [Mus musculus] | 100.00% | 22 | 62.50% |
| wt MxA | This CDS feature is included to show the translation of the corresponding V_region. Presently translation qualifiers on V_region features are illegal, partial [Homo sapiens] | 98.10% | 1 | 23.60% |
| wt MxA | Tubulin, beta 2C [Homo sapiens] | 100.00% | 5 | 72.10% |
| wt MxA | unnamed protein product [Homo sapiens] | 100.00% | 7 | 25.30% |
| wt MxA | heterogeneous nuclear ribonucleoprotein H1 (H), isoform CRA_b [Homo sapiens] | 100.00% | 3 | 11.20% |
| wt MxA | insulin receptor substrate 4 [Homo sapiens] | 100.00% | 7 | 6.84% |
| wt MxA | ribosomal protein S18, isoform CRA_c [Homo sapiens] | 100.00% | 3 | 25.00% |
| wt MxA | unnamed protein product [Homo sapiens] | 100.00% | 6 | 32.00% |
| wt MxA | serine palmitoyltransferase 1 isoform a [Homo sapiens] | 100.00% | 3 | 9.73% |
| wt MxA | Chain L, Crystal Structure Of Fab Dx-2930 In Complex With Human Plasma Kallikrein At 2.4 Angstrom Resolution | 98.10% | 1 | 0.00% |
| wt MxA | mitochondrial citrate transport protein [Homo sapiens] | 100.00% | 3 | 11.30% |
| wt MxA | Chain C, Crystal Structure Of Mj5 Fab, A Germline Antibody Variant Of Anti-Human Cytomegalovirus Antibody 8f9 | 98.10% | 1 | 44.00% |
| wt MxA | Unknown (protein for MGC:32654) [Homo sapiens] | 98.10% | 1 | 42.40% |
| wt MxA | immunoglobulin VH_3c kappa chain [Homo sapiens] | 98.10% | 1 | 31.30% |
| wt MxA | immunoglobulin A heavy chain variable region, partial [Homo sapiens] | 98.10% | 1 | 0.00% |
| wt MxA | D-3-phosphoglycerate dehydrogenase [Homo sapiens] | 100.00% | 13 | 32.60% |
| wt MxA | Chain A, Crystal Structure Of Human Pyrroline-5-Carboxylate Reductase | 100.00% | 3 | 13.00% |
| wt MxA | nucleoporin 205kDa, isoform CRA_b [Homo sapiens] | 100.00% | 2 | 0.89% |
| wt MxA | matrin-3 isoform a [Homo sapiens] | 100.00% | 5 | 10.50% |
| wt MxA | carboxy terminus of Hsp70-interacting protein [Homo sapiens] | 100.00% | 4 | 15.80% |
| wt MxA | importin 9, isoform CRA_a [Homo sapiens] | 100.00% | 2 | 2.21% |

| | | | | |
|---|---|---|---|---|
| wt MxA | JUP protein [Homo sapiens] | 100.00% | 3 | 8.05% |
| wt MxA | 60S ribosomal protein L13 isoform 1 [Homo sapiens] | 100.00% | 2 | 9.00% |
| wt MxA | unnamed protein product [Homo sapiens] | 100.00% | 5 | 12.20% |
| wt MxA | lamin-B1 isoform 1 [Homo sapiens] | 100.00% | 19 | 42.50% |
| wt MxA | CLTC protein [Homo sapiens] | 100.00% | 25 | 21.70% |
| wt MxA | dermcidin preproprotein [Homo sapiens] | 100.00% | 2 | 20.00% |
| wt MxA | squamous cell carcinoma antigen-1 isoform SCCA-PD [Homo sapiens] | 100.00% | 6 | 17.20% |
| wt MxA | DnaJ (Hsp40) homolog, subfamily A, member 1, isoform CRA_d [Homo sapiens] | 100.00% | 3 | 15.40% |
| wt MxA | pyrroline-5-carboxylate reductase family, member 2, isoform CRA_c [Homo sapiens] | 100.00% | 2 | 11.30% |
| wt MxA | Solute carrier family 1 (neutral amino acid transporter), member 5 [Homo sapiens] | 100.00% | 3 | 6.84% |
| wt MxA | immunoglobulin lambda-1 variable region [Homo sapiens] | 98.10% | 1 | 19.30% |
| wt MxA | PREDICTED: keratin, type II cytoskeletal 6A [Pan troglodytes] | 100.00% | 14 | 48.90% |
| wt MxA | signal recognition particle receptor subunit beta [Homo sapiens] | 100.00% | 2 | 10.30% |
| wt MxA | 78 kDa glucose-regulated protein precursor [Homo sapiens] | 100.00% | 9 | 20.80% |
| wt MxA | coatomer subunit gamma-2 [Homo sapiens] | 100.00% | 5 | 13.10% |
| wt MxA | 40S ribosomal protein S13 [Homo sapiens] | 100.00% | 3 | 24.50% |
| wt MxA | unnamed protein product [Homo sapiens] | 100.00% | 2 | 4.21% |
| wt MxA | Chain A, Human Pyruvate Dehydrogenase S264e Variant | 100.00% | 2 | 5.48% |
| wt MxA | hemoglobin alpha-1 globin chain [Homo sapiens] | 100.00% | 4 | 36.60% |
| wt MxA | isoleucine-tRNA synthetase, isoform CRA_b [Homo sapiens] | 100.00% | 24 | 24.50% |
| wt MxA | 60S ribosomal protein L38 [Homo sapiens] | 100.00% | 3 | 50.00% |
| wt MxA | Keratin 77 [Homo sapiens] | 100.00% | 5 | 16.30% |
| wt MxA | unnamed protein product [Homo sapiens] | 100.00% | 9 | 11.90% |
| wt MxA | Chain L, Crystal Structure Of Recombinant A.17 Antibody Fab Fragment | 98.00% | 1 | 43.50% |
| wt MxA | ADP/ATP translocase 2 [Macaca mulatta] | 100.00% | 14 | 50.00% |
| wt MxA | ribosomal protein S7, isoform CRA_a [Homo sapiens] | 100.00% | 3 | 26.50% |
| wt MxA | 40S ribosomal protein S14 [Homo sapiens] | 100.00% | 2 | 15.90% |
| wt MxA | ribosomal protein L22, isoform CRA_c [Homo sapiens] | 100.00% | 2 | 23.80% |
| wt MxA | Chain B, Crystal Structures Of Native And Inhibited Forms Of Human Cathepsin D: Implications For Lysosomal Targeting And Drug Design | 100.00% | 3 | 0.00% |
| wt MxA | Chaperonin containing TCP1, subunit 3 (gamma) [Homo sapiens] | 100.00% | 4 | 8.27% |
| wt MxA | Ig G1 H Nie | 100.00% | 3 | 40.40% |
| wt MxA | Similar to ribosomal protein L23, partial [Homo sapiens] | 100.00% | 4 | 38.10% |
| wt MxA | PREDICTED: ruvB-like 2 isoform X1 [Homo sapiens] | 100.00% | 12 | 0.00% |
| wt MxA | unnamed protein product [Homo sapiens] | 36.30% | 0 | 43.20% |
| wt MxA | RANBP8 [Homo sapiens] | 100.00% | 2 | 2.22% |
| wt MxA | tubulin alpha-1A chain isoform 2 [Homo sapiens] | 100.00% | 2 | 67.80% |
| wt MxA | Chain L, Crystal Structure Of Igf-Ii Antibody Complex | 98.10% | 1 | 40.00% |
| wt MxA | keratin 10 (epidermolytic hyperkeratosis; keratosis palmaris et plantaris), isoform CRA_b [Homo sapiens] | 100.00% | 34 | 58.30% |
| wt MxA | keratin, type II cytoskeletal 5 [Homo sapiens] | 100.00% | 21 | 44.70% |
| wt MxA | immunoglobulin heavy chain, partial [Homo sapiens] | 100.00% | 12 | 0.00% |

| | | | | |
|---|---|---|---|---|
| wt MxA | type I keratin 16 [Homo sapiens] | 100.00% | 14 | 60.90% |
| wt MxA | unnamed protein product [Homo sapiens] | 98.10% | 1 | 41.20% |
| wt MxA | spliceosomal protein SAP 155 [Homo sapiens] | 100.00% | 2 | 2.15% |
| wt MxA | dolichyl-phosphate mannosyltransferase polypeptide 1, catalytic subunit, isoform CRA_b [Homo sapiens] | 100.00% | 3 | 8.57% |
| wt MxA | heterogeneous nuclear ribonucleoproteins A2/B1 isoform B1 [Homo sapiens] | 100.00% | 2 | 5.10% |
| wt MxA | unnamed protein product [Homo sapiens] | 100.00% | 2 | 6.29% |
| wt MxA | heat shock 70kDa protein 4, isoform CRA_b [Homo sapiens] | 100.00% | 5 | 9.10% |
| wt MxA | exportin 5, isoform CRA_a [Homo sapiens] | 100.00% | 4 | 4.07% |
| wt MxA | unnamed protein product [Homo sapiens] | 100.00% | 6 | 28.90% |
| wt MxA | unnamed protein product [Homo sapiens] | 100.00% | 2 | 4.74% |
| wt MxA | Chain A, Human Annexin A2 With Heparin Tetrasaccharide Bound | 100.00% | 2 | 8.77% |
| wt MxA | glyceraldehyde-3-phosphate dehydrogenase, isoform CRA_a [Homo sapiens] | 100.00% | 3 | 18.00% |
| wt MxA | keratin, type I cytoskeletal 9 [Homo sapiens] | 100.00% | 31 | 75.60% |
| wt MxA | IgG L chain [Homo sapiens] | 94.80% | 1 | 0.00% |
| wt MxA | immunoglobulin variable region [Homo sapiens] | 100.00% | 2 | 9.59% |
| wt MxA | hCG41114, isoform CRA_b [Homo sapiens] | 100.00% | 2 | 18.40% |
| wt MxA | Ig A1 Bur | 100.00% | 2 | 3.79% |
| wt MxA | heat shock protein beta-1 [Homo sapiens] | 100.00% | 3 | 17.60% |
| wt MxA | Chain A, Crystal Structure Of Human Lnkh2b-h2a.z-anp32e | 98.10% | 1 | 0.00% |
| wt MxA | Chain A, Structural Changes Of The Active Site Cleft And Different Saccharide Binding Modes In Human Lysozyme Co-Crystallized With Hexa-N-Acetyl-Chitohexaose At Ph 4.0 | 100.00% | 4 | 46.20% |
| wt MxA | 60 kDa SS-A/Ro ribonucleoprotein isoform 1 [Homo sapiens] | 100.00% | 12 | 29.90% |
| wt MxA | Chain H, Crystal Structure Of Hiv-Gp120 Core In Complex With Cd4-Binding Site Antibody B13, Space Group C222 | 52.70% | 0 | 20.80% |
| wt MxA | unnamed protein product [Homo sapiens] | 100.00% | 2 | 4.24% |
| wt MxA | Chain B, Structure Of Appbp1-Uba3~nedd8-Nedd8-Mgatp-Ubc12(C111a), A Trapped Ubiquitin-Like Protein Activation Complex | 100.00% | 6 | 10.60% |
| wt MxA | protein kinase, DNA-activated, catalytic polypeptide, isoform CRA_c [Homo sapiens] | 100.00% | 2 | 0.53% |
| wt MxA | leucine--tRNA ligase, cytoplasmic [Homo sapiens] | 100.00% | 13 | 16.00% |
| wt MxA | Keratin, hair, basic, 1 [Homo sapiens] | 100.00% | 3 | 7.33% |
| wt MxA | NADH dehydrogenase [ubiquinone] 1 alpha subcomplex subunit 4 [Homo sapiens] | 99.90% | 2 | 27.20% |
| wt MxA | unnamed protein product [Homo sapiens] | 100.00% | 3 | 29.80% |
| wt MxA | protein Len,Bence-Jones | 98.10% | 1 | 26.40% |
| wt MxA | protein Rei,Bence-Jones | 100.00% | 3 | 30.40% |
| wt MxA | tubulin alpha-1C chain [Homo sapiens] | 100.00% | 2 | 58.10% |
| wt MxA | ZW10 protein [Homo sapiens] | 100.00% | 3 | 7.14% |
| wt MxA | transferrin receptor (p90, CD71), isoform CRA_b [Homo sapiens] | 100.00% | 12 | 18.50% |
| wt MxA | tubulin beta-5 chain [Mus musculus] | 100.00% | 21 | 72.30% |
| wt MxA | heat shock cognate 71 kDa protein isoform 1 [Homo sapiens] | 100.00% | 26 | 52.90% |
| wt MxA | unnamed protein product [Homo sapiens] | 100.00% | 4 | 23.10% |
| wt MxA | hCG1784554, isoform CRA_a [Homo sapiens] | 100.00% | 2 | 7.53% |
| wt MxA | eukaryotic translation initiation factor 3, subunit 9 eta, 116kDa, isoform CRA_c [Homo sapiens] | 100.00% | 2 | 2.69% |
| wt MxA | IgG kappa chain [Homo sapiens] | 100.00% | 2 | 56.10% |

| | | | | |
|---|---|---|---|---|
| wt MxA | mitochondrial 2-oxoglutarate/malate carrier protein isoform 1 [Homo sapiens] | 100.00% | 5 | 21.30% |
| wt MxA | mutant beta-globin [Homo sapiens] | 100.00% | 4 | 34.70% |
| wt MxA | Chain A, Crystal Structure Of Human Ed-4f2hc | 100.00% | 5 | 17.90% |
| wt MxA | protein S100-A8 [Homo sapiens] | 100.00% | 5 | 47.30% |
| wt MxA | hCG1984476, isoform CRA_b [Homo sapiens] | 98.10% | 1 | 6.87% |
| wt MxA | Heat shock 70kDa protein 9 (mortalin) [Homo sapiens] | 100.00% | 16 | 30.80% |
| wt MxA | unnamed protein product [Homo sapiens] | 100.00% | 2 | 2.69% |
| wt MxA | unnamed protein product [Homo sapiens] | 100.00% | 2 | 3.20% |
| wt MxA | hCG19195 [Homo sapiens] | 100.00% | 2 | 25.30% |
| wt MxA | Chain B, Human Pyruvate Dehydrogenase S264e Variant | 100.00% | 3 | 12.60% |
| wt MxA | Chain H, Crystal Structure Of Human Germline Antibody 5-51/o12 | 98.10% | 1 | 0.00% |
| wt MxA | Fanconi anemia group D2 protein isoform a [Homo sapiens] | 100.00% | 3 | 2.31% |
| wt MxA | unnamed protein product [Homo sapiens] | 100.00% | 6 | 5.09% |
| wt MxA | unnamed protein product [Homo sapiens] | 100.00% | 9 | 25.10% |
| wt MxA | keratin 4 [Homo sapiens] | 100.00% | 5 | 17.10% |
| wt MxA | ribosomal protein S4, X-linked, isoform CRA_a [Homo sapiens] | 100.00% | 3 | 9.35% |
| wt MxA | Chain L, Crystal Structure Of A Chimeric Fab' Fragment Of An Antibody Binding Tumour Cells | 96.30% | 1 | 40.80% |
| T103A wMxA | Chain A, The Structure Of An Antitumor Ch2-Domain-Deleted Humanized Antibody | 90.40% | 1 | 47.30% |
| T103A wMxA | Chain H, Crystal Structure Of Anti-ngf Antibody Cnto7309 | 100.00% | 2 | 0.00% |
| T103A wMxA | Translocase of inner mitochondrial membrane 50 homolog (S. cerevisiae) [Homo sapiens] | 100.00% | 2 | 5.92% |
| T103A wMxA | Unknown (protein for IMAGE:3544292), partial [Homo sapiens] | 100.00% | 7 | 33.10% |
| T103A wMxA | Chain A, Crystal Structure Of The Novel Complex Formed Between Zinc 2-Glycoprotein (Zag) And Prolactin Inducible Protein (Pip) From Human Seminal Plasma | 96.20% | 1 | 3.60% |
| T103A wMxA | ribosomal protein S18, isoform CRA_c [Homo sapiens] | 100.00% | 3 | 22.70% |
| T103A wMxA | unnamed protein product [Homo sapiens] | 98.50% | 1 | 1.88% |
| T103A wMxA | immunoglobulin kappa light chain VLJ region [Homo sapiens] | 100.00% | 2 | 56.50% |
| T103A wMxA | keratin, type I cytoskeletal 13 isoform a [Homo sapiens] | 51.20% | 0 | 9.17% |
| T103A wMxA | HNRPF protein [Homo sapiens] | 100.00% | 3 | 16.40% |
| T103A wMxA | ribosomal protein S5, isoform CRA_b [Homo sapiens] | 98.50% | 1 | 7.50% |
| T103A wMxA | Chain A, Human Serum Albumin Complexed With Myristate And Aspirin | 100.00% | 14 | 22.40% |
| T103A wMxA | immunoglobulin gamma heavy chain [Homo sapiens] | 100.00% | 2 | 30.20% |
| T103A wMxA | ATP synthase, H+ transporting, mitochondrial F1 complex, gamma polypeptide 1 [Homo sapiens] | 100.00% | 3 | 12.10% |
| T103A wMxA | ATP synthase subunit alpha, mitochondrial isoform a precursor [Homo sapiens] | 100.00% | 10 | 25.90% |
| T103A wMxA | keratin, type II cytoskeletal 2 epidermal [Homo sapiens] | 100.00% | 30 | 63.80% |
| T103A wMxA | SSA1 [Homo sapiens] | 100.00% | 7 | 15.60% |
| T103A wMxA | immunoglobulin light chain variable region, partial [Homo sapiens] | 100.00% | 2 | 0.00% |
| T103A wMxA | ADP/ATP translocase 3 [Homo sapiens] | 100.00% | 1 | 19.10% |
| T103A wMxA | apoptosis-inducing factor 1, mitochondrial isoform 2 precursor [Homo sapiens] | 100.00% | 3 | 6.08% |
| T103A wMxA | keratin, type I cuticular Ha1 [Homo sapiens] | 38.00% | 0 | 1.68% |
| T103A wMxA | unnamed protein product [Homo sapiens] | 100.00% | 10 | 44.40% |
| T103A wMxA | heterogeneous nuclear ribonucleoproteins C1/C2 isoform a [Homo sapiens] | 100.00% | 2 | 7.52% |

| | | | | |
|---|---|---|---|---|
| T103A wMxA | Chain A, Human Heart L-Lactate Dehydrogenase H Chain, Ternary Complex With Nadh And Oxamate | 98.50% | 1 | 3.60% |
| T103A wMxA | immunoglobulin heavy chain variable region [Homo sapiens] | 98.50% | 1 | 7.63% |
| T103A wMxA | coatomer subunit beta [Homo sapiens] | 100.00% | 11 | 16.60% |
| T103A wMxA | unnamed protein product [Homo sapiens] | 100.00% | 3 | 6.07% |
| T103A wMxA | immunoglobin heavy chain [Homo sapiens] | 98.50% | 1 | 29.80% |
| T103A wMxA | protein S100-A7 [Homo sapiens] | 95.00% | 1 | 10.90% |
| T103A wMxA | unnamed protein product [Homo sapiens] | 98.50% | 1 | 5.19% |
| T103A wMxA | immunoglobulin heavy chain variable region [Homo sapiens] | 100.00% | 2 | 35.80% |
| T103A wMxA | immunoglobulin kappa light chain variable region [Homo sapiens] | 100.00% | 2 | 35.30% |
| T103A wMxA | PREDICTED: ADP-ribosylation factor-like protein 1-like isoform 2 [Nomascus leucogenys] | 100.00% | 5 | 44.50% |
| T103A wMxA | monoclonal IgM antibody light chain [Homo sapiens] | 100.00% | 2 | 66.10% |
| T103A wMxA | coatomer subunit gamma-1 [Homo sapiens] | 100.00% | 4 | 6.75% |
| T103A wMxA | unnamed protein product [Homo sapiens] | 100.00% | 3 | 37.70% |
| T103A wMxA | Chain A, Semi-Extended Solution Structure Of Human Myeloma Immunoglobulin D Determined By Constrained X-Ray Scattering | 100.00% | 2 | 59.80% |
| T103A wMxA | ADP-ribosylation factor 4 [Homo sapiens] | 100.00% | 3 | 15.60% |
| T103A wMxA | Chain A, Refined Solution Structure Of Human Cystatin A | 100.00% | 3 | 46.90% |
| T103A wMxA | immunoglobulin variable region [Homo sapiens] | 100.00% | 1 | 37.30% |
| T103A wMxA | heat shock protein HSP 90-alpha isoform 1 [Homo sapiens] | 100.00% | 4 | 18.10% |
| T103A wMxA | polyubiquitin [Homo sapiens] | 100.00% | 3 | 5.58% |
| T103A wMxA | mitochondrial 2-oxoglutarate/malate carrier protein isoform 1 [Homo sapiens] | 100.00% | 3 | 8.60% |
| T103A wMxA | Ig heavy chain VH3 region [Homo sapiens] | 100.00% | 2 | 40.00% |
| T103A wMxA | unnamed protein product [Homo sapiens] | 96.70% | 1 | 2.18% |
| T103A wMxA | Eukaryotic translation elongation factor 1 gamma [Homo sapiens] | 100.00% | 3 | 7.32% |
| T103A wMxA | unnamed protein product [Homo sapiens] | 100.00% | 5 | 7.31% |
| T103A wMxA | Chain B, Three Dimensional Structure Of Broadly Neutralizing Human Anti - Hepatitis C Virus (hcv) Glycoprotein E2 Fab Fragment Hc84-1 | 100.00% | 2 | 0.00% |
| T103A wMxA | KIAA1794, isoform CRA_c [Homo sapiens] | 21.20% | 0 | 0.00% |
| T103A wMxA | Chain B, Structure Of Hepatitis C Virus Envelope Glycoprotein E2 Core Bound To Broadly Neutralizing Antibody Ar3c | 98.50% | 1 | 0.00% |
| T103A wMxA | dihydrolipoamide S-acetyltransferase (E2 component of pyruvate dehydrogenase complex), isoform CRA_a [Homo sapiens] | 100.00% | 3 | 8.81% |
| T103A wMxA | Similar to ribophorin I, partial [Homo sapiens] | 99.50% | 1 | 2.64% |
| T103A wMxA | ATPase family, AAA domain containing 3A, isoform CRA_c [Homo sapiens] | 100.00% | 7 | 11.80% |
| T103A wMxA | immunoglobulin kappa light chain variable region [Homo sapiens] | 100.00% | 2 | 55.00% |
| T103A wMxA | hypothetical protein [Homo sapiens] | 100.00% | 2 | 47.60% |
| T103A wMxA | heterogeneous nuclear ribonucleoprotein U (scaffold attachment factor A), isoform CRA_b [Homo sapiens] | 98.50% | 1 | 2.16% |
| T103A wMxA | tubulin alpha-1C chain [Homo sapiens] | 100.00% | 2 | 65.00% |
| T103A wMxA | hCG33299, isoform CRA_a [Homo sapiens] | 100.00% | 3 | 11.70% |
| T103A wMxA | anti-rabies SOJA immunoglobulin heavy chain [Homo sapiens] | 100.00% | 3 | 49.60% |
| T103A wMxA | Chain A, Human Factor Viii C2 Domain Complexed To Human Monoclonal Bo2c11 Fab | 98.50% | 1 | 53.60% |
| T103A wMxA | mitochondrial heat shock 60kD protein 1 variant 1 [Homo sapiens] | 26.70% | 0 | 0.00% |
| T103A wMxA | immunoglobulin heavy chain gamma-3 variant [Homo sapiens] | 89.80% | 1 | 0.00% |
| T103A wMxA | Ribosomal protein, large, P0 [Homo sapiens] | 100.00% | 5 | 22.10% |

| | | | | |
|---|---|---|---|---|
| T103A wMxA | Unknown (protein for MGC:32654) [Homo sapiens] | 100.00% | 2 | 49.60% |
| T103A wMxA | Chain L, Crystal Structure Of Igf-Ii Antibody Complex | 100.00% | 3 | 60.00% |
| T103A wMxA | RecName: Full=Elongation factor Tu, mitochondrial; Short=EF-Tu; AltName: Full=P43; Flags: Precursor | 100.00% | 13 | 41.80% |
| T103A wMxA | immunoglobulin heavy chain variable region, partial [Homo sapiens] | 98.50% | 1 | 25.00% |
| T103A wMxA | immunoglobulin variable region [Homo sapiens] | 100.00% | 2 | 38.30% |
| T103A wMxA | immunoglobulin kappa light chain [Homo sapiens] | 100.00% | 1 | 44.40% |
| T103A wMxA | Chain B, Structure Of Appbp1-Uba3~nedd8-Nedd8-Mgatp-Ubc12(C111a), A Trapped Ubiquitin-Like Protein Activation Complex | 100.00% | 4 | 6.83% |
| T103A wMxA | recombinant IgG4 heavy chain [Homo sapiens] | 99.40% | 1 | 32.10% |
| T103A wMxA | Chain A, Crystal Structure Of Human Nmprtase As Free-Form | 100.00% | 1 | 4.01% |
| T103A wMxA | immunoglobulin heavy chain variable region [Homo sapiens] | 99.90% | 1 | 33.90% |
| T103A wMxA | immunoglobulin G heavy chain variable region, partial [Homo sapiens] | 100.00% | 2 | 0.00% |
| T103A wMxA | unnamed protein product [Homo sapiens] | 100.00% | 3 | 4.05% |
| T103A wMxA | Chain L, Crystal Structure Of The Anti-human Ngf Fab Ape1531 | 100.00% | 3 | 0.00% |
| T103A wMxA | interferon-induced Mx protein [Homo sapiens] | 100.00% | 51 | 81.10% |
| T103A wMxA | immunoglobulin light chain [Homo sapiens] | 100.00% | 2 | 60.30% |
| T103A wMxA | Chain H, Antibody 2g12 Recognizes Di-Mannose Equivalently In Domain- And Non- Domain-Exchanged Forms, But Only Binds The Hiv-1 Glycan Shield If Domain-Exchanged | 100.00% | 2 | 22.20% |
| T103A wMxA | t-complex 1, isoform CRA_b [Homo sapiens] | 41.60% | 0 | 0.00% |
| T103A wMxA | hypothetical protein [Homo sapiens] | 100.00% | 2 | 44.00% |
| T103A wMxA | immunoglobulin light chain variable region, partial [Homo sapiens] | 49.00% | 0 | 0.00% |
| T103A wMxA | serpin B12 [Homo sapiens] | 99.70% | 1 | 1.98% |
| T103A wMxA | immunoglobulin G heavy chain variable region [Homo sapiens] | 100.00% | 2 | 42.70% |
| T103A wMxA | interleukin enhancer-binding factor 2 [Mus musculus] | 100.00% | 3 | 10.50% |
| T103A wMxA | exportin-2 isoform 1 [Homo sapiens] | 100.00% | 7 | 6.90% |
| T103A wMxA | immunoglobulin light chain [Homo sapiens] | 100.00% | 2 | 54.50% |
| T103A wMxA | immunoglobulin A heavy chain variable region, partial [Homo sapiens] | 98.50% | 1 | 0.00% |
| T103A wMxA | desmoglein-1 preproprotein [Homo sapiens] | 100.00% | 2 | 3.34% |
| T103A wMxA | YWHAE/FAM22A fusion protein, partial [Homo sapiens] | 100.00% | 3 | 7.81% |
| T103A wMxA | immunoglobulin variable region [Homo sapiens] | 100.00% | 4 | 24.60% |
| T103A wMxA | pachytene checkpoint protein 2 homolog isoform 1 [Homo sapiens] | 100.00% | 2 | 4.17% |
| T103A wMxA | tubulin beta-2B chain [Mus musculus] | 100.00% | 4 | 60.70% |
| T103A wMxA | Chain L, Crystal Structure Of Broadly Neutralizing Antibody Cr8020 Bound To The Influenza A H3 Hemagglutinin | 100.00% | 2 | 55.10% |
| T103A wMxA | polypyrimidine tract binding protein 1, isoform CRA_b [Homo sapiens] | 98.50% | 1 | 1.52% |
| T103A wMxA | immunoglobulin light chain variable region [Homo sapiens] | 99.90% | 1 | 32.20% |
| T103A wMxA | actin, beta, partial [Homo sapiens] | 100.00% | 11 | 43.20% |
| T103A wMxA | Chain L, Crystal Structure Of Ectodomain 3 Of The Il-13 Receptor Alpha1 In Complex With A Human Neutralizing Monoclonal Antibody Fragment | 98.50% | 1 | 0.00% |
| T103A wMxA | Keratin 14 [Homo sapiens] | 100.00% | 18 | 52.30% |
| T103A wMxA | immunoglobulin kappa chain variable region [Homo sapiens] | 100.00% | 2 | 44.20% |
| T103A wMxA | exportin-1 [Homo sapiens] | 100.00% | 16 | 21.80% |
| T103A wMxA | elongation factor 1-alpha 1 [Homo sapiens] | 100.00% | 11 | 40.00% |
| T103A wMxA | Ig lambda chain - human | 98.50% | 1 | 48.10% |

| | | | | |
|---|---|---|---|---|
| T103A wMxA | immunoglobulin kappa heavy chain [Homo sapiens] | 99.90% | 1 | 47.80% |
| T103A wMxA | IGH@ protein [Homo sapiens] | 100.00% | 3 | 50.80% |
| T103A wMxA | immunoglobulin kappa light chain VLJ region [Homo sapiens] | 100.00% | 1 | 32.50% |
| T103A wMxA | unnamed protein product [Homo sapiens] | 100.00% | 9 | 37.00% |
| T103A wMxA | keratin 1 [Homo sapiens] | 100.00% | 38 | 59.20% |
| T103A wMxA | lupus La protein [Homo sapiens] | 100.00% | 11 | 31.60% |
| T103A wMxA | Chain B, Crystal Structure Of The Human Notch1 Negative Regulatory Re Bound To The Fab Fragment Of An Antagonist Antibody | 100.00% | 2 | 27.80% |
| T103A wMxA | immunoglobulin A heavy chain variable region, partial [Homo sapiens] | 100.00% | 2 | 0.00% |
| T103A wMxA | ribosomal protein S7, isoform CRA_a [Homo sapiens] | 100.00% | 3 | 26.50% |
| T103A wMxA | RuvB-like 1 [Homo sapiens] | 100.00% | 9 | 27.40% |
| T103A wMxA | unnamed protein product [Homo sapiens] | 98.50% | 1 | 5.43% |
| T103A wMxA | immunoglobulin kappa light chain VLJ region [Homo sapiens] | 100.00% | 2 | 42.00% |
| T103A wMxA | epididymis luminal protein 214 [Homo sapiens] | 100.00% | 6 | 0.00% |
| T103A wMxA | Chain C, Solution Structure Of Human Immunoglobulin M | 100.00% | 7 | 44.40% |
| T103A wMxA | Chain H, Mechanisms Of Neutralization Of A Human Anti-alpha Toxin Antibody | 100.00% | 2 | 0.00% |
| T103A wMxA | anti-SARS-CoV S protein immunoglobulin kappa light chain [Homo sapiens] | 98.50% | 1 | 48.10% |
| T103A wMxA | immunoglobulin VH_3c kappa chain [Homo sapiens] | 100.00% | 2 | 39.70% |
| T103A wMxA | Chain B, Crystal Structure Of The Novel Complex Formed Between Zinc 2-Glycoprotein (Zag) And Prolactin Inducible Protein (Pip) From Human Seminal Plasma | 100.00% | 6 | 68.60% |
| T103A wMxA | dnaJ homolog subfamily A member 2 [Homo sapiens] | 100.00% | 3 | 11.70% |
| T103A wMxA | Chain L, Her3 Extracellular Domain In Complex With Fab Fragment Of Mor09825 | 98.50% | 1 | 0.00% |
| T103A wMxA | Ig lambda chain - human (fragment) | 100.00% | 2 | 50.00% |
| T103A wMxA | Chain A, Hepcidin-Fab Complex | 100.00% | 3 | 64.40% |
| T103A wMxA | nucleophosmin isoform 1 [Homo sapiens] | 98.50% | 1 | 7.14% |
| T103A wMxA | immunoglobulin variable region [Homo sapiens] | 100.00% | 2 | 9.49% |
| T103A wMxA | B cell antibody heavy chain variable region [Homo sapiens] | 100.00% | 2 | 26.30% |
| T103A wMxA | immunoglobulin kappa light chain [Homo sapiens] | 98.50% | 1 | 42.70% |
| T103A wMxA | unnamed protein product [Homo sapiens] | 98.50% | 1 | 33.50% |
| T103A wMxA | anti-tetanus toxoid immunoglobulin light chain variable region [Homo sapiens] | 98.50% | 1 | 31.80% |
| T103A wMxA | Chain L, Crystal Structure Of Hiv-1 Neutralizing Antibody Ch04 | 99.90% | 2 | 53.00% |
| T103A wMxA | calcium-binding mitochondrial carrier protein Aralar2 isoform 1 [Homo sapiens] | 100.00% | 5 | 10.50% |
| T103A wMxA | unnamed protein product [Homo sapiens] | 100.00% | 21 | 35.40% |
| T103A wMxA | hCG2016250, isoform CRA_c [Homo sapiens] | 98.50% | 1 | 4.80% |
| T103A wMxA | prohibitin 2 [Homo sapiens] | 98.50% | 1 | 5.88% |
| T103A wMxA | immunoglobulin G heavy chain variable region [Homo sapiens] | 98.50% | 1 | 9.16% |
| T103A wMxA | Chain A, Crystal Structure Of Human Pyrroline-5-Carboxylate Reductase | 100.00% | 3 | 13.00% |
| T103A wMxA | Chain A, Crystal Structure Of The Broadly Hiv-1 Neutralizing Fab X5 At 1.90 Angstrom Resolution | 100.00% | 2 | 49.30% |
| T103A wMxA | immunoglobulin heavy chain [Homo sapiens] | 98.50% | 1 | 31.40% |
| T103A wMxA | tubulin alpha-1B chain [Mus musculus] | 100.00% | 23 | 69.60% |
| T103A wMxA | This CDS feature is included to show the translation of the corresponding V_region. Presently translation qualifiers on V_region features are illegal, partial [Homo sapiens] | 98.50% | 1 | 32.30% |
| T103A wMxA | Tubulin, beta 2C [Homo sapiens] | 100.00% | 5 | 70.80% |

| | | | | |
|---|---|---|---|---|
| T103A wMxA | unnamed protein product [Homo sapiens] | 100.00% | 5 | 17.40% |
| T103A wMxA | heat shock 70 kDa protein 1A/1B [Homo sapiens] | 100.00% | 33 | 64.40% |
| T103A wMxA | heterogeneous nuclear ribonucleoprotein H1 (H), isoform CRA_b [Homo sapiens] | 100.00% | 4 | 15.30% |
| T103A wMxA | insulin receptor substrate 4 [Homo sapiens] | 77.00% | 1 | 0.64% |
| T103A wMxA | unnamed protein product [Homo sapiens] | 100.00% | 8 | 39.50% |
| T103A wMxA | Chain H, Crystal Structure Of Rv144-elicited Antibody Ch59 In Complex With V2 Peptide | 98.30% | 1 | 0.00% |
| T103A wMxA | PREDICTED: ruvB-like 2 isoform X1 [Homo sapiens] | 100.00% | 8 | 0.00% |
| T103A wMxA | Chain L, Crystal Structure Of Fab Dx-2930 In Complex With Human Plasma Kallikrein At 2.4 Angstrom Resolution | 100.00% | 3 | 0.00% |
| T103A wMxA | mitochondrial citrate transport protein [Homo sapiens] | 100.00% | 3 | 11.00% |
| T103A wMxA | immunoglobulin light chain [Homo sapiens] | 100.00% | 2 | 56.00% |
| T103A wMxA | immunoglobulin variable region VL kappa domain [Homo sapiens] | 96.60% | 1 | 31.20% |
| T103A wMxA | Chain C, Crystal Structure Of Mj5 Fab, A Germline Antibody Variant Of Anti-Human Cytomegalovirus Antibody 8f9 | 100.00% | 4 | 80.10% |
| T103A wMxA | immunoglobulin A heavy chain variable region, partial [Homo sapiens] | 98.50% | 1 | 0.00% |
| T103A wMxA | immunoglobulin heavy chain variable region [Homo sapiens] | 98.50% | 1 | 33.60% |
| T103A wMxA | D-3-phosphoglycerate dehydrogenase [Homo sapiens] | 100.00% | 13 | 29.80% |
| T103A wMxA | isoleucine-tRNA synthetase, isoform CRA_b [Homo sapiens] | 100.00% | 3 | 3.15% |
| T103A wMxA | immunoglobulin variable region [Homo sapiens] | 100.00% | 2 | 22.00% |
| T103A wMxA | HRV Fab 025-VL [Homo sapiens] | 98.50% | 1 | 38.90% |
| T103A wMxA | matrin-3 isoform a [Homo sapiens] | 100.00% | 2 | 4.13% |
| T103A wMxA | carboxy terminus of Hsp70-interacting protein [Homo sapiens] | 100.00% | 3 | 11.90% |
| T103A wMxA | immunoglobulin heavy chain variable region [Homo sapiens] | 99.90% | 1 | 31.80% |
| T103A wMxA | JUP protein [Homo sapiens] | 99.80% | 1 | 1.74% |
| T103A wMxA | immunoglobulin kappa chain variable region [Homo sapiens] | 100.00% | 2 | 29.50% |
| T103A wMxA | Chain L, Crystal Structure Of The Therapeutical Antibody Fragment Of Canakinumab In Its Unbound State | 100.00% | 2 | 0.00% |
| T103A wMxA | immunoglobulin G heavy chain variable region, partial [Homo sapiens] | 98.50% | 1 | 0.00% |
| T103A wMxA | Chain B, Crystal Structure Of Pertuzumab Clambda Fab With Variable And Constant Domain Redesigns (vrd2 And Crd2) At 1.6a | 100.00% | 2 | 0.00% |
| T103A wMxA | immunoglobulin variable region [Homo sapiens] | 100.00% | 2 | 58.10% |
| T103A wMxA | unnamed protein product [Homo sapiens] | 100.00% | 2 | 4.82% |
| T103A wMxA | immunoglobulin lambda 1 light chain [Homo sapiens] | 98.50% | 1 | 43.80% |
| T103A wMxA | lamin-B1 isoform 1 [Homo sapiens] | 100.00% | 10 | 18.30% |
| T103A wMxA | CLTC protein [Homo sapiens] | 98.50% | 1 | 0.55% |
| T103A wMxA | dermcidin preproprotein [Homo sapiens] | 98.50% | 1 | 10.00% |
| T103A wMxA | squamous cell carcinoma antigen-1 isoform SCCA-PD [Homo sapiens] | 100.00% | 4 | 13.10% |
| T103A wMxA | DnaJ (Hsp40) homolog, subfamily A, member 1, isoform CRA_d [Homo sapiens] | 100.00% | 4 | 15.70% |
| T103A wMxA | immunoglobulin heavy chain variable region [Homo sapiens] | 100.00% | 2 | 55.10% |
| T103A wMxA | DEAH (Asp-Glu-Ala-His) box polypeptide 15, isoform CRA_d [Homo sapiens] | 98.50% | 1 | 1.85% |
| T103A wMxA | pyrroline-5-carboxylate reductase family, member 2, isoform CRA_c [Homo sapiens] | 100.00% | 2 | 11.30% |
| T103A wMxA | immunoglobulin light chain [Homo sapiens] | 96.60% | 1 | 74.40% |
| T103A wMxA | PREDICTED: keratin, type II cytoskeletal 6A [Pan troglodytes] | 100.00% | 13 | 44.10% |
| T103A wMxA | signal recognition particle receptor subunit beta [Homo sapiens] | 100.00% | 2 | 12.90% |

| | | | | |
|---|---|---|---|---|
| T103A wMxA | Chain A, Crystal Structure Of Abt-007 Fab Fragment With The Soluble Domain Of Epo Receptor | 100.00% | 3 | 65.40% |
| T103A wMxA | 78 kDa glucose-regulated protein precursor [Homo sapiens] | 100.00% | 4 | 10.90% |
| T103A wMxA | coatomer subunit gamma-2 [Homo sapiens] | 94.80% | 1 | 4.25% |
| T103A wMxA | anti-HIV-1 immunoglobulin cap256-048-050815 chain variable region, partial [Homo sapiens] | 80.40% | 1 | 0.00% |
| T103A wMxA | Chain K, Crystal Structure Of Fab 2g1 In Complex With A H2n2 Influenza Virus Hemagglutinin | 99.90% | 1 | 0.00% |
| T103A wMxA | IGL@ protein [Homo sapiens] | 100.00% | 2 | 47.20% |
| T103A wMxA | immunoglobulin lambda-1 variable region [Homo sapiens] | 100.00% | 2 | 26.60% |
| T103A wMxA | Chain A, Human Pyruvate Dehydrogenase S264e Variant | 100.00% | 3 | 8.77% |
| T103A wMxA | immunoglobulin variable region [Homo sapiens] | 98.50% | 1 | 27.40% |
| T103A wMxA | 60S ribosomal protein L38 [Homo sapiens] | 72.10% | 0 | 0.00% |
| T103A wMxA | Keratin 77 [Homo sapiens] | 100.00% | 2 | 8.30% |
| T103A wMxA | unnamed protein product [Homo sapiens] | 100.00% | 2 | 2.35% |
| T103A wMxA | Chain L, Crystal Structure Of Recombinant A.17 Antibody Fab Fragment | 100.00% | 2 | 51.40% |
| T103A wMxA | ADP/ATP translocase 2 [Macaca mulatta] | 100.00% | 7 | 22.80% |
| T103A wMxA | 40S ribosomal protein S13 [Homo sapiens] | 100.00% | 2 | 17.90% |
| T103A wMxA | 40S ribosomal protein S14 [Homo sapiens] | 100.00% | 1 | 7.28% |
| T103A wMxA | aldehyde dehydrogenase 3 family, member A2, isoform CRA_c [Homo sapiens] | 70.00% | 0 | 0.00% |
| T103A wMxA | Chain B, Crystal Structures Of Native And Inhibited Forms Of Human Cathepsin D: Implications For Lysosomal Targeting And Drug Design | 100.00% | 3 | 0.00% |
| T103A wMxA | Ig G1 H Nie | 100.00% | 5 | 43.10% |
| T103A wMxA | Similar to ribosomal protein L23, partial [Homo sapiens] | 100.00% | 4 | 38.10% |
| T103A wMxA | hypothetical protein [Homo sapiens] | 98.50% | 1 | 47.90% |
| T103A wMxA | unnamed protein product [Homo sapiens] | 100.00% | 2 | 48.30% |
| T103A wMxA | immunoglobulin kappa chain variable region [Homo sapiens] | 98.20% | 1 | 20.30% |
| T103A wMxA | tubulin alpha-1A chain isoform 2 [Homo sapiens] | 100.00% | 2 | 75.20% |
| T103A wMxA | Chain L, Crystal Structure Of Broadly And Potently Neutralizing Antibody Vrc- Ch31 In Complex With Hiv-1 Clade A/e Gp120 93th057 With Loop D And Loop V5 From Clade A Strain 3415_v1_c1 | 100.00% | 2 | 0.00% |
| T103A wMxA | keratin 10 (epidermolytic hyperkeratosis; keratosis palmaris et plantaris), isoform CRA_b [Homo sapiens] | 100.00% | 34 | 58.30% |
| T103A wMxA | keratin, type II cytoskeletal 5 [Homo sapiens] | 100.00% | 21 | 44.90% |
| T103A wMxA | immunoglobulin light chain [Homo sapiens] | 100.00% | 14 | 86.50% |
| T103A wMxA | immunoglobulin heavy chain, partial [Homo sapiens] | 100.00% | 16 | 0.00% |
| T103A wMxA | immunoglobulin lambda light chain VLJ region [Homo sapiens] | 98.50% | 1 | 28.70% |
| T103A wMxA | immunoglobulin kappa light chain variable region [Homo sapiens] | 100.00% | 2 | 32.40% |
| T103A wMxA | type I keratin 16 [Homo sapiens] | 100.00% | 11 | 55.20% |
| T103A wMxA | unnamed protein product [Homo sapiens] | 100.00% | 3 | 49.60% |
| T103A wMxA | immunoglobulin kappa light chain variable region [Homo sapiens] | 100.00% | 2 | 44.70% |
| T103A wMxA | Chain H, Cryo-em Structure Of Dengue Virus Serotype 1 Complexed With Fab Fragments Of Human Antibody 1f4 | 100.00% | 2 | 0.00% |
| T103A wMxA | dolichyl-phosphate mannosyltransferase polypeptide 1, catalytic subunit, isoform CRA_b [Homo sapiens] | 100.00% | 3 | 9.52% |
| T103A wMxA | unnamed protein product [Homo sapiens] | 98.50% | 1 | 2.25% |
| T103A wMxA | exportin 5, isoform CRA_a [Homo sapiens] | 100.00% | 2 | 1.66% |
| T103A wMxA | glyceraldehyde-3-phosphate dehydrogenase, isoform CRA_a [Homo sapiens] | 95.50% | 1 | 4.27% |
| T103A wMxA | keratin, type I cytoskeletal 9 [Homo sapiens] | 100.00% | 29 | 74.20% |

| | | | | |
|---|---|---|---|---|
| T103A wMxA | IgG L chain [Homo sapiens] | 98.50% | 1 | 0.00% |
| T103A wMxA | immunoglobulin variable region [Homo sapiens] | 100.00% | 3 | 28.80% |
| T103A wMxA | anti-tetanus toxoid immunoglobulin light chain variable region [Homo sapiens] | 96.60% | 1 | 84.30% |
| T103A wMxA | hCG41114, isoform CRA_b [Homo sapiens] | 21.50% | 0 | 0.00% |
| T103A wMxA | Ig A1 Bur | 100.00% | 2 | 4.37% |
| T103A wMxA | anti-tetanus toxoid immunoglobulin light chain variable region [Homo sapiens] | 31.10% | 0 | 10.30% |
| T103A wMxA | heat shock protein beta-1 [Homo sapiens] | 100.00% | 3 | 17.60% |
| T103A wMxA | Chain A, Crystal Structure Of Human Lnkh2b-h2a.z-anp32e | 100.00% | 3 | 0.00% |
| T103A wMxA | Chain A, Structural Changes Of The Active Site Cleft And Different Saccharide Binding Modes In Human Lysozyme Co-Crystallized With Hexa-N-Acetyl-Chitohexaose At Ph 4.0 | 100.00% | 1 | 21.50% |
| T103A wMxA | 60 kDa SS-A/Ro ribonucleoprotein isoform 1 [Homo sapiens] | 100.00% | 13 | 34.70% |
| T103A wMxA | Chain H, Crystal Structure Of Hiv-Gp120 Core In Complex With Cd4-Binding Site Antibody B13, Space Group C222 | 91.90% | 1 | 28.60% |
| T103A wMxA | anti-HBsAg immunoglobulin Fab kappa chain [Homo sapiens] | 100.00% | 2 | 57.00% |
| T103A wMxA | unnamed protein product [Homo sapiens] | 98.50% | 1 | 2.39% |
| T103A wMxA | unnamed protein product [Homo sapiens] | 100.00% | 4 | 16.60% |
| T103A wMxA | immunoglobulin light chain variable region kappa, partial [Homo sapiens] | 62.70% | 0 | 0.00% |
| T103A wMxA | immunoglobulin lambda 1 light chain [Homo sapiens] | 100.00% | 2 | 41.70% |
| T103A wMxA | immunoglobulin light chain variable region, partial [Homo sapiens] | 100.00% | 2 | 0.00% |
| T103A wMxA | immunoglobulin light chain kappa, partial [Homo sapiens] | 50.30% | 0 | 0.00% |
| T103A wMxA | immunoglobulin kappa light chain variable region [Homo sapiens] | 87.70% | 1 | 27.40% |
| T103A wMxA | leucine--tRNA ligase, cytoplasmic [Homo sapiens] | 100.00% | 3 | 4.34% |
| T103A wMxA | NADH dehydrogenase [ubiquinone] 1 alpha subcomplex subunit 4 [Homo sapiens] | 71.30% | 0 | 0.00% |
| T103A wMxA | unnamed protein product [Homo sapiens] | 100.00% | 5 | 32.70% |
| T103A wMxA | protein Len,Bence-Jones | 100.00% | 3 | 37.30% |
| T103A wMxA | protein Rei,Bence-Jones | 100.00% | 4 | 42.10% |
| T103A wMxA | immunoglobulin kappa chain variable region [Homo sapiens] | 98.50% | 1 | 31.20% |
| T103A wMxA | transferrin receptor (p90, CD71), isoform CRA_b [Homo sapiens] | 100.00% | 7 | 9.45% |
| T103A wMxA | tubulin beta-5 chain [Mus musculus] | 100.00% | 22 | 70.90% |
| T103A wMxA | heat shock cognate 71 kDa protein isoform 1 [Homo sapiens] | 100.00% | 26 | 53.10% |
| T103A wMxA | unnamed protein product [Homo sapiens] | 100.00% | 2 | 13.40% |
| T103A wMxA | hCG1784554, isoform CRA_a [Homo sapiens] | 100.00% | 2 | 8.60% |
| T103A wMxA | eukaryotic translation initiation factor 3, subunit 9 eta, 116kDa, isoform CRA_c [Homo sapiens] | 98.40% | 1 | 1.10% |
| T103A wMxA | Chain C, An Antibody Against The C-terminal Domain Of Pcsk9 Lowers Ldl Cholesterol Levels In Vivo | 100.00% | 2 | 0.00% |
| T103A wMxA | IgG kappa chain [Homo sapiens] | 100.00% | 2 | 60.30% |
| T103A wMxA | unnamed protein product [Homo sapiens] | 100.00% | 2 | 29.30% |
| T103A wMxA | Chain A, Crystal Structure Of Human Ed-4f2hc | 99.90% | 1 | 2.83% |
| T103A wMxA | protein S100-A8 [Homo sapiens] | 100.00% | 2 | 20.40% |
| T103A wMxA | hCG1984476, isoform CRA_b [Homo sapiens] | 98.50% | 1 | 6.87% |
| T103A wMxA | Heat shock 70kDa protein 9 (mortalin) [Homo sapiens] | 100.00% | 12 | 22.70% |
| T103A wMxA | unnamed protein product [Homo sapiens] | 100.00% | 2 | 3.20% |
| T103A wMxA | hCG19195 [Homo sapiens] | 100.00% | 2 | 25.30% |

| | | | | |
|---|---|---|---|---|
| T103A wMxA | Chain B, Human Pyruvate Dehydrogenase S264e Variant | 100.00% | 1 | 3.23% |
| T103A wMxA | Chain C, Crystal Structure Of Mt-Sp1 In Complex With Fab Inhibitor E2 | 100.00% | 2 | 60.30% |
| T103A wMxA | Chain H, Crystal Structure Of Human Germline Antibody 5-51/o12 | 100.00% | 3 | 0.00% |
| T103A wMxA | unnamed protein product [Homo sapiens] | 98.50% | 1 | 1.00% |
| T103A wMxA | unnamed protein product [Homo sapiens] | 100.00% | 4 | 11.00% |
| T103A wMxA | keratin 4 [Homo sapiens] | 98.10% | 1 | 6.41% |
| T103A wMxA | ribosomal protein S4, X-linked, isoform CRA_a [Homo sapiens] | 100.00% | 2 | 4.94% |
| T103A wMxA | Chain L, Crystal Structure Of A Chimeric Fab' Fragment Of An Antibody Binding Tumour Cells | 88.20% | 1 | 41.20% |